



日中笹川医学奨学金制度
第42期（学位取得コース）

中間報告書

2020年4月～2021年3月

公益財団法人 日中医学協会

目 次

No.	氏名	所属機関	研究先	指導責任者	頁数
G1	趙 景敏 チョウ ケイミン (論文博士)	吉林大学中日聯誼医院 主治医師	福島県立医科大学 放射線医学講座	伊藤 浩 教授	……P1
研究テーマ：脳神経画像を用いた虚血性脳血管障害の治療効果・予後評価の研究					
G2	焦 丹丹 ショウ タンタン (課程博士)	河南科技大学第一附属医院 主管護師	筑波大学大学院人間総合科学研究科 国際発達ケア：エンパワメント科学研究室	安梅 勅江 教授	……P14
研究テーマ：国際発達ケア：エンパワメント科学研究					
G3	張 碧航 チョウ ヘキョウ (課程博士)	中南大学湘雅医院 大学院生	自治医科大学 外科学講座	吉村 浩太郎 教授	……P26
研究テーマ：幹細胞培養上清成分を用いた再生医療の開発					
G4	劉 霄 リュウ ショウ (課程博士)	慶應義塾大学医学部 大学院生	慶應義塾大学医学部・医学研究科 眼科学教室	坪田 一男 教授	……P32
研究テーマ：東アジア人におけるABCA4関連網膜症の臨床的・分子遺伝学的調査					
G5	孟 華川 モウ カン (課程博士)	中日友好医院院 通訳（日本プロジェクト担当）	国際医療福祉大学大学院 医療福祉経営専攻 医療経営管理分野 医学研究科 医学専攻	島崎 謙治教授 桐生 茂教授	……P106
研究テーマ：ICTを活用した遠隔医療の導入効果及び推進方策					
G6	翟 達 テイ タツ (課程博士)	長崎大学大学院 大学院生	長崎大学原爆後障害医療研究所 幹細胞生物学研究分野	李 桃生 教授	……P113
研究テーマ：メカノストレスが癌細胞に与える影響と機序					

日中笹川医学奨学金制度(学位取得コース)中間評価書

論文博士：指導教官用



第 42 期 研究者番号： G4201

作成日：2021年3月6日

氏名	趙景敏	Zhao Jingmin	性別	M	生年月日	1987. 02. 25
所属機関(役職)	吉林大学中日聯誼医院神経内科(主治医師)					
研究先(指導教官)	福島県立医科大学放射線医学講座(伊藤 浩)					
研究テーマ	脳神経画像を用いた虚血性脳血管障害の治療効果・予後評価の研究 Investigation of pathophysiology of ischemic cerebrovascular diseases using neuroimaging techniques					
専攻種別	<input checked="" type="checkbox"/> 論文博士			<input type="checkbox"/> 課程博士		

研究者評価(指導教官記入欄)

成績状況	優 良 可 不可	取得単位数
		取得単位数/取得すべき単位数総数
学生本人が行った研究の概要	優	
総合評価		
学位取得見込		

1) 核医学的分子イメージングを用いた脳神経機能損傷の評価法の開発
びまん性軸索損傷(DAI)ラットモデルにおいて、¹⁸F-FDG PETを用いて、脳損傷前後の脳糖代謝の変化を評価し、病理組織学的所見と比較検討を行った。その結果、¹⁸F-FDG PETの脳画像解析では、脳損傷後24時間での脳糖代謝が低下した。DAIラットの脳病理組織において、脳損傷のバイオマーカーのAmyloid precursor protein (APP)の陽性所見が認められた。

2) 若齢マウスと高齢マウスの全身及び脳局所における糖代謝の比較及び高齢マウスの脳局所の糖代謝における漢方薬の効果評価
若齢と高齢マウスの全身及び脳局所における糖代謝と高齢マウスの脳代謝に対する漢方薬の効果について、糖代謝のバイオマーカーである¹⁸F-FDGの体内分布と¹⁸F-FDGのオートラジオグラフィ(ARG)法を用いて評価した。その結果、高齢マウスの各臓器と脳局所の糖代謝が低下したが、漢方薬の治療により脳の糖代謝の潜在力が改善されたことが認められた。

【良かった点】
1) 核医学的分子イメージングを用いた脳神経機能損傷の評価法の開発の課題について、DAIラットモデルの作成に大きいな進展があり、短い期間で¹⁸F-FDG PETまで実施し、またDAIの病理検討まで進めたこと。
2) 若齢マウスと高齢マウスの全身及び脳局所における糖代謝の比較及び高齢マウスの脳局所の糖代謝における漢方薬の効果評価について、短い期間で研究成果を2篇の論文にまとめて投稿したこと(現在査読者からのコメントに対して回答・再投稿中)。

【改善すべき点】
DAIラットモデル作成において、DAIモデルの成功率と質を上げるためには、DAIモデル作成装置の改善が必要であると思う。しかしこれには高いコストがかかる。またDAIラットモデルにおいて、¹⁸F-FDG PET画像解析と病理学的陽性所見にはバラつきが大きいので、画像評価方法と病理染色項目の選択に工夫が必要であると思う。

【今後の展望】
DAIラットモデルにおいて、骨髄間質細胞(BMSC)の移植治療により、脳糖代謝の改善とともにDAIによる高次脳機能障害の改善が¹⁸F-FDG PETで実証されることが期待される。

現在すでに症例報告をまとめた英文論文を英文雑誌に掲載している。またここで行った研究成果について英文論文にまとめて、インパクトファクターが3を超えた英文雑誌に2篇を投稿して、査読者からのコメントに対する回答と修正した論文を再投稿し、編集長からの最終的な決定を待っている。さらに本学の論文博士に係る学識認定試験(外国語)にも合格しているので、学位取得の見込みは十分可能だと思う。

評価者 伊藤 浩



日中笹川医学奨学金制度(学位取得コース)中間報告書 研究者用



第42期

研究者番号: G4201

作成日: 2021年3月1日

氏名	Zhao Jingmin	趙 景敏	性別	M	生年月日 1987. 02. 25
所属機関(役職)	吉林大学中日聯誼医院神経内科(主治医師)				
研究先(指導教官)	福島県立医科大学放射線医学講座(伊藤 浩教授)				
研究テーマ	脳神経画像を用いた虚血性脳血管障害の治療効果・予後評価の研究 Investigation of pathophysiology of ischemic cerebrovascular diseases using neuroimaging techniques				
専攻種別	論文博士	<input checked="" type="checkbox"/>	課程博士	<input type="checkbox"/>	
1. 研究概要(1)					
1) 目的(Goal) Exploring changes of glucose metabolism by ¹⁸ F-FDG PET in diffuse axonal injury (DAI) rat model					
2) 戦略(Approach)					
① Make the rat DAI model					
② Perform the ¹⁸ F-FDG PET imaging					
③ Perform the neurological assessments					
④ Perform the immunohistochemical analysis					
3) 材料と方法(Materials and methods)					
We used Marmarou's weight drop model for this study. In this model, the energy of impact is applied via a 500g steel block that falls freely from a designated height through a Plexiglas tube. The rat skull is exposed by a midline incision. A stainless steel disc is mounted on the skull midline between the lambda and the bregma to prevent skull fracture. The rats are then placed on a foam bed and subjected to the impact by dropping the steel block onto the stainless steel disc. After palinesthesia, neurological severity score (NSS) is determined. We used the modified Morris Water Maze (MWM) test in a blind manner to investigate learning and memory processes in rats. Then ¹⁸ F-FDG PET was carried out before and 24h after making DAI model. The blood glucose level measured every time before ¹⁸ F-FDG PET. After the last scan, the rats were sacrificed 90min after ¹⁸ F-FDG injection. The brains were removed, stored in 10% paraformaldehyde for 1 day, then chaged into the 1% paraformaldehyde for several days. Coranal sections were prepared for immunohistochemical analysis. Each section was treated with antibodies against β -APP.					
4) 実験結果(Results)					
Compared with before the injury, the weight of rat dropped significantly after the injury. ¹⁸ F-FDG PET images showed that glucose metabolism was reduced in animals with DAI after 24h. The overall curve shows a downward trend. Neurological severity score (NSS) was reduced in animals with DAI after 24h. APP positive injured axons were found in DAI rat model.					
5) 考察(Discussion)					
The tracer used in microPET, 2-[¹⁸ F]-fluoro-2-deoxy-D-glucose (¹⁸ F-FDG), is a well-known radiotracer that has frequently been used as a marker of brain glucose metabolism. Because the glucose is the primary fuel source under normal conditions in the adult, the level of glucose utilization correlates with the degree of neuronal activity. We found that ¹⁸ F-FDG PET images showed that glucose metabolism was reduced in APP positive DAI rat model and neurological severity score (NSS) was reduced in animals with DAI after 24h. These results demonstrate that injury-induced hypometabolism in the brain at the acute stage of DAI were correlated with neural dysfunctions. We need to further study and expand the sample size to confirm this result.					
6) 参考文献(References)					
[1] J. Li, L. Gu, D.F. Feng, F. Ding, G. Zhu, and J. Rong. Exploring temporospatial changes in glucose metabolic disorder, learning, and memory dysfunction in a rat model of diffuse axonal injury. J Neurotrauma 2012;29:2635-2646.					
[2] M.M. van Eijck, G.G. Schoonman, J. van der Naalt, J. de Vries, and G. Roks. Diffuse axonal injury after traumatic brain injury is a prognostic factor for functional outcome: a systematic review and meta-analysis. Brain Inj 2018;32:39					
[3] W. Zheng, C. Ma, L. Kong, X. Chen, and W. Fan. Detecting diffuse axonal injury in rat brainstems by diffusion tensor imaging and AQP4 expression. Biomed Mater Eng 2015;26(Suppl 1):S1169-1175.					
[4] V.E. Johnson, W. Stewart, M.T. Weber, D.K. Cullen, R. Siman, and D.H. Smith. SNTF immunostaining reveals previously undetected axonal pathology in traumatic brain injury. Acta Neuropathol 2016;131:115-135.					

1. 研究概要(2)

1) 目的(Goal)

The aim of this study is to evaluate the effect of Ninjin'yoeito (NYT) on regional brain glucose metabolism in aged wild-type mice.

2) 戦略(Approach)

- ① Evaluate organ glucose metabolism by ^{18}F -FDG accumulation with insulin loading in aged mice compared with young normal mice.
- ② Evaluate the regional brain glucose metabolism by ^{18}F -FDG accumulation with insulin loading in aged mice compared with young normal mice.
- ③ Evaluate the effect of Ninjin'yoeito (NYT) on regional brain glucose metabolism by ^{18}F -FDG autoradiography with insulin loading in aged mice.

3) 材料と方法(Materials and methods)

In the first step, each animal was initially anesthetized with 4% isoflurane in air and maintained via spontaneous ventilation with 2% isoflurane in air. ^{18}F -FDG (11.5 MBq/0.1 ml) was injected into the tail vein. Ninety minutes later, the animals were sacrificed and their organs were excised. The radioactivity of organs (muscle, heart, lungs, spleen, pancreas, white adipose tissue (superior pole of epididymis), testes, stomach, small intestine, large intestine, kidneys, liver, brown adipose tissue (between the shoulder blades), and brain) were determined with a gamma counter. In the second step, eight-week-old and 96-week-old male mice ($n = 6$, each group) were assigned to the control and insulin-loaded groups, then perform the ^{18}F -FDG autoradiography. In the third step, after 12 weeks of feeding NYT, mice were assigned to the control and insulin-loaded groups and received an intraperitoneal injection of human insulin (2 U/kg body weight) 30 min prior to ^{18}F -FDG injection. Ninety minutes after the injection, brain autoradiography was performed.

4) 実験結果(Results)

In the untreated groups, the levels of ^{18}F -FDG accumulation in the blood, plasma, muscle, lungs, spleen, pancreas, testes, stomach, small intestine, kidneys, liver, brain, and brain regions, namely, the cortex, striatum, thalamus, and hippocampus, were all significantly higher in the aged mice. The treated group showed lower ^{18}F -FDG accumulation levels in the pancreas and kidneys, as well as in the cortex, striatum, thalamus, and hippocampus in the aged mice than the untreated groups, whereas higher ^{18}F -FDG accumulation levels were observed in those in the young mice. After insulin loading, the ^{18}F -FDG accumulation showed negative changes in the cortex, striatum, thalamus, and hippocampus in the control group, whereas positive changes were observed in the NYT-treated group.

5) 考察(Discussion)

These results demonstrate that insulin loading decreases effect on ^{18}F -FDG accumulation levels in some organs of the aged mice. In the young mice group, the levels of ^{18}F -FDG accumulation in the cortex, striatum, and hippocampus significantly increased after insulin loading. Compared with the young group, the levels of ^{18}F -FDG accumulation in the striatum, thalamus and hippocampus in the aged group did not markedly change after insulin loading. In contrast, the level of ^{18}F -FDG accumulation in the cortex significantly decreased after insulin loading in the aged group. Aging is associated with reductions in the levels of both insulin and its receptor in the brain, which may even cause the brain to be in the state of insulin resistance. Ninjin'yoeito could improve the glucose metabolism dysfunction in brain regions in aged mice. Ninjin'yoeito may potentially reduce insulin resistance in the brain regions in aged mice, thereby preventing age-related brain diseases.

6) 参考文献(References)

- [1] C. Kudoh, R. Arita, M. Honda, T. Kishi, Y. Komatsu, H. Asou, and M. Mimura. Effect of ninjin'yoeito, a Kampo (traditional Japanese) medicine, on cognitive impairment and depression in patients with Alzheimer's disease: 2 years of observation. *Psychogeriatrics* 2016;16:85-92.
- [2] S. Suzuki, F. Aihara, M. Shibahara, and K. Sakai. Safety and Effectiveness of Ninjin'yoeito: A Utilization Study in Elderly Patients. *Front Nutr* 2019;6:14.
- [3] G.M. Martin, The biology of aging: 1985-2010 and beyond. *Faseb J* 2011;25: 3756-3762.
- [4] J. Xiao, J. Weng, L. Ji, W. Jia, J. Lu, Z. Shan, J. Liu, H. Tian, Q. Ji, Z. Yang, and W. Yang. Worse pancreatic β -cell function and better insulin sensitivity in older Chinese without diabetes. *J Gerontol A Biol Sci Med Sci* 2014;69:463-170.
- [5] B. Cholerton, L.D. Baker, and S. Craft. Insulin resistance and pathological brain ageing. *Diabet Med* 2011;28:1463-1475.
- [6] W.A. Banks, J.B. Jaspan, and A.J. Kastin, Effect of diabetes mellitus on the permeability of the blood-brain barrier to insulin. *Peptides* 18 (1997) 1577-84.
- [7] G.J. Biessels, L.P. van der Heide, A. Kamal, R.L. Bleys, and W.H. Gispen. Ageing and diabetes: implications for brain function. *Eur J Pharmacol* 2002;441:1-14.
- [8] H.N. Frazier, K.L. Anderson, S. Maimaiti, A.O. Ghoweri, S.D. Kraner, G.J. Popa, K.K. Hampton, M.D. Mendenhall, C.M. Norris, R.J. Craven, and O. Thibault. Expression of a Constitutively Active Human Insulin Receptor in Hippocampal Neurons Does Not Alter VGCC Currents. *Neurochem Res* 2019;44:269-280.
- [9] E.M. Rhea, and W.A. Banks, Role of the Blood-Brain Barrier in Central Nervous System Insulin Resistance. *Front Neurosci* 2019;13:521.
- [10] L.M. Voipio-Pulkki, P. Nuutila, M.J. Knuuti, U. Ruotsalainen, M. Haaparanta, M. Teräs, U. Wegelius, and V.A. Koivisto. Heart and skeletal muscle glucose disposal in type 2 diabetic patients as determined by positron emission tomography. *J Nucl Med* 1993;34:2064-2067.

2. 執筆論文 Publication of thesis ※記載した論文を添付してください。Attach all of the papers listed below.

論文名 1 Title	Bilateral Medial Medullary Infarction Accompanied by Cerebral Watershed Infarction: A case report					
掲載誌名 Published journal	Journal of Radiology Case Reports					
	2020 年 4 月	14 (4) 巻(号)	1 頁 ~	7 頁	言語 Language	English
第1著者名 First author	Jingmin Zhao	第2著者名 Second author	Guangxian Nan		第3著者名 Third author	Guangxun Shen
その他著者名 Other authors	Songji Zhao; Hiroshi Ito					
論文名 2 Title						
掲載誌名 Published journal						
	年 月	巻(号)	頁 ~	頁	言語 Language	
第1著者名 First author		第2著者名 Second author			第3著者名 Third author	
その他著者名 Other authors						
論文名 3 Title						
掲載誌名 Published journal						
	年 月	巻(号)	頁 ~	頁	言語 Language	
第1著者名 First author		第2著者名 Second author			第3著者名 Third author	
その他著者名 Other authors						
論文名 4 Title						
掲載誌名 Published journal						
	年 月	巻(号)	頁 ~	頁	言語 Language	
第1著者名 First author		第2著者名 Second author			第3著者名 Third author	
その他著者名 Other authors						
論文名 5 Title						
掲載誌名 Published journal						
	年 月	巻(号)	頁 ~	頁	言語 Language	
第1著者名 First author		第2著者名 Second author			第3著者名 Third author	
その他著者名 Other authors						

3. 学会発表 Conference presentation ※筆頭演者として総会・国際学会を含む主な学会で発表したものを記載してください。

※Describe your presentation as the principal presenter in major academic meetings including general meetings or international meeting

学会名 Conference					
演題 Topic					
開催日 date	年	月	日	開催地 venue	
形式 method	<input type="checkbox"/> 口頭発表 Oral	<input type="checkbox"/> ポスター発表 Poster	言語 Language	<input type="checkbox"/> 日本語	<input type="checkbox"/> 英語 <input type="checkbox"/> 中国語
共同演者名 Co-presenter					
学会名 Conference					
演題 Topic					
開催日 date	年	月	日	開催地 venue	
形式 method	<input type="checkbox"/> 口頭発表 Oral	<input type="checkbox"/> ポスター発表 Poster	言語 Language	<input type="checkbox"/> 日本語	<input type="checkbox"/> 英語 <input type="checkbox"/> 中国語
共同演者名 Co-presenter					
学会名 Conference					
演題 Topic					
開催日 date	年	月	日	開催地 venue	
形式 method	<input type="checkbox"/> 口頭発表 Oral	<input type="checkbox"/> ポスター発表 Poster	言語 Language	<input type="checkbox"/> 日本語	<input type="checkbox"/> 英語 <input type="checkbox"/> 中国語
共同演者名 Co-presenter					
学会名 Conference					
演題 Topic					
開催日 date	年	月	日	開催地 venue	
形式 method	<input type="checkbox"/> 口頭発表 Oral	<input type="checkbox"/> ポスター発表 Poster	言語 Language	<input type="checkbox"/> 日本語	<input type="checkbox"/> 英語 <input type="checkbox"/> 中国語
共同演者名 Co-presenter					

4. 受賞(研究業績) Award (Research achievement)

名称 Award name	国名 Country		受賞年 Year of award	年	月
	国名 Country		受賞年 Year of award	年	月

5. 本研究テーマに関わる他の研究助成金受給 Other research grants concerned with your research theme

受給実績 Receipt record	<input type="checkbox"/> 有 <input type="checkbox"/> 無
助成機関名称 Funding agency	
助成金名称 Grant name	
受給期間 Supported period	年 月 ~ 年 月
受給額 Amount received	円
受給実績 Receipt record	<input type="checkbox"/> 有 <input type="checkbox"/> 無
助成機関名称 Funding agency	
助成金名称 Grant name	
受給期間 Supported period	年 月 ~ 年 月
受給額 Amount received	円

6. 他の奨学金受給 Another awarded scholarship

受給実績 Receipt record	<input type="checkbox"/> 有 <input type="checkbox"/> 無
助成機関名称 Funding agency	
奨学金名称 Scholarship name	
受給期間 Supported period	年 月 ~ 年 月
受給額 Amount received	円

7. 研究活動に関する報道発表 Press release concerned with your research activities

※記載した記事を添付してください。Attach a copy of the article described below

報道発表 Press release	<input type="checkbox"/> 有 <input type="checkbox"/> 無	発表年月日 Date of release	
発表機関 Released medium			
発表形式 Release method	・新聞 ・雑誌 ・Web site ・記者発表 ・その他()		
発表タイトル Released title			

8. 本研究テーマに関する特許出願予定 Patent application concerned with your research theme

出願予定 Scheduled	<input type="checkbox"/> 有 <input type="checkbox"/> 無	出願国 Application	
出願内容(概要) Application contents			

9. その他 Others

--

指導責任者(署名) 伊藤 浩



Bilateral Medial Medullary Infarction Accompanied by Cerebral Watershed Infarction: A case report

Jingmin Zhao^{1,2}, Guangxian Nan^{1*}, Guangxun Shen¹, Songji Zhao^{3,4}, Hiroshi Ito^{2,3}

1. Department of Neurology, China-Japan Union Hospital of Jilin University, Changchun, China

2. Department of Radiology and Nuclear Medicine, Fukushima Medical University, Fukushima, Japan

3. Advanced Clinical Research Center, Fukushima Global Medical Science Center, Fukushima Medical University, Fukushima, Japan

4. Basic Medical College of Jilin University, Changchun, China

* **Correspondence:** Guangxian Nan, MD, PhD, Department of Neurology, China-Japan Union Hospital of Jilin University, 126 XianTai Street, Changchun, 130031, Jilin, China
(✉ nanguangxian@hotmail.com)

Radiology Case. 2020 Apr; 14(4):1-7 :: DOI: 10.3941/jrcr.v14i4.3905

ABSTRACT

Bilateral medial medullary infarction is a rare stroke subtype, and its diagnosis has become possible by brain magnetic resonance imaging. In this report, we describe a case in which acute bilateral medial medullary infarction accompanied by cerebral watershed infarction was clearly identified by diffusion-weighted imaging, and we discuss the mechanisms of bilateral medial medullary infarction accompanied by cerebral watershed infarction.

CASE REPORT

CASE REPORT

A 50-year-old man was admitted to our hospital with sensory dysfunction and pain in the four limbs, which began 2 hours before admission. The patient's condition, however, worsened into a rapidly progressive tetraparesis with slurred speech and dysphagia within 3 hours after admission. He had a history of hypertension, cigarette smoking, and myocardial infarction. Neurologic examination revealed breathing difficulty, dysarthria, hyporeflexia, quadriplegia, diminished pain sensation, and a muscle power of grade 4 for his four limbs. His National Institutes of Health Stroke Scale score was 12/42. Brain magnetic resonance imaging (MRI) performed 11 hours after admission showed the 'heart appearance' sign detected as a hyperintense signal in the bilateral anteromedial medullae (Fig. 1A), cortical watershed infarction (CWI) (Fig. 1B), and internal watershed infarction (IWI) (Fig. 1C) of the right cerebral hemisphere shown by diffusion-weighted

imaging (DWI), respectively. He then underwent a brain digital subtraction angiography (DSA), which showed mild stenosis in the basilar artery (BA) (Fig. 2A), plaque formation in the right internal carotid artery (ICA) without obvious stenosis (Fig. 2B), mild stenosis in the right middle cerebral artery (MCA) (Fig. 2C), and a normal right vertebral artery (VA) (Fig. 2D), which appeared more dominant than the left in the extracranial portion (Fig. 2E). The left VA was occluded at the distal intracranial portion (Fig. 2F). Two days after admission, the patient required an endotracheal intubation because of respiratory distress with disorder of consciousness (Glasgow Coma Scale score, 3/15) and a tracheotomy mask on day 3 of hospitalization. On day 10 of hospitalization, his consciousness improved (Glasgow Coma Scale score, 2+2+T/15) and his respiratory distress significantly improved; however, his four limbs remained weak. The patient had a modified Rankin Scale score of 5/6 at the time of his discharge without further treatment.

DISCUSSION

Etiology & Demographics:

Medial medullary infarction (MMI) is a rare stroke subtype, accounting for only 0.5—1.5% of all strokes [1,2], and bilateral MMI is even rarer [3]. Clinicopathologic studies have demonstrated that MMI is a rare condition, and in a series of 700 patients who died of cerebrovascular disease and were autopsied, only four were found to have ischemic damage in the medial medullae [4]. Bilateral MMI is even more rarely reported, and it is speculated that it may be related to an unpaired anterior spinal artery as an anatomical variation [5,6]. The etiological classifications of infarctions are large-artery atherosclerosis (LA), small-vessel disease (SV), arterial dissection (DI), cardiac embolism (CE), and stroke of undetermined etiology. Risk factors for cerebral infarction include atrial fibrillation, hypertension, smoking habit, diabetes mellitus, ischemic heart disease, and dyslipidemia. According to previous magnetic resonance angiography findings, bilateral MMI might be related to artery stenosis or occlusion, including VA atherosclerosis (38.5%), VA occlusion (15.4%), basilar artery atherosclerosis (19.2%), dissection (7.7%), anterior spinal artery (ASA) occlusion (3.8%; an autopsy case), and no abnormalities (38.5%) [3]. In patients with normal vascular imaging findings, the stroke mechanism was likely atheromatous branch occlusion or ASA occlusion, which could not be demonstrated by DSA [3].

Clinical & Imaging Findings:

The diagnosis of bilateral MMI was previously possible only at autopsy; however, its diagnosis has recently become possible by diffusion-weighted brain MRI, which shows the characteristic “heart appearance” sign. Previous case reports of bilateral MMI described the same heart appearance sign on axial MR images [4,5]. It is considered that blood is supplied to these areas by the vertebral and anterior spinal arteries, but it is often difficult to identify the occluded blood vessel because of the vastly complex network formed by these vessels. The heart appearance sign is considered to appear when the infarct occurs in the anteromedial territory and anterolateral territory [7].

Treatment & Prognosis:

It is difficult to diagnose bilateral MMI in its early stages. However, when properly diagnosed, its treatment is the same as that of cerebral infarction, including endotracheal intubation when respiratory distress occurs. A systematic review (38 patients, from 1992 to 2011) reported that bilateral MMI was present with quadriplegia in 24% of patients, dysarthria in 18%, and hypoglossal palsy in 9% [3]. Furthermore, approximately 9—24% of patients with bilateral MMI may develop respiratory failure, which is more prevalent in bilateral MMI than in unilateral MMI [3]. In contrast to unilateral MMI, the clinical outcome of bilateral MMI is usually poor [6]. However, no comparative studies have been reported to date.

Differential Diagnoses:

Bilateral MMI with respiratory failure can be frequently misdiagnosed as Guillain-Barre syndrome (GBS), particularly when the initial symptoms develop into flaccid quadriplegia [8]. Indeed, the patient’s medical history is very important. Brain MRI and DWI are also helpful, as they can show the classical heart or V/Y appearance at the ventral medulla in patients with bilateral MMI [7,8]. Of note, the abnormal MRI or DWI signal may be a small dot or a linear shape at the midline of the medulla in the early stages of bilateral MMI [9]. GBS can also be confirmed on the basis of the cerebrospinal finding of an elevated protein level without pleocytosis at slightly later stages. A key point to differentiate between these syndromes is the evolution of clinical presentation: GBS has a subacute evolution, whereas bilateral MMI has a more acute presentation [8].

Case Discussion:

To the best of our knowledge, bilateral MMI accompanied by cerebral watershed infarction (WSI) confirmed by DWI has not yet been reported. In this report, we first described a case in which acute bilateral MMI accompanied by WSI was identified by DWI. Below we discuss the causes of MMI and the possible mechanism of WSI.

In the current case, DWI showed bilateral MMI accompanied by WSI. WSI, that is, ischemic lesions between two non-anastomosing main arterial territories, can be classified as either CWI or IWI, which can be further divided into subtypes. CWI is further divided into anterior watershed infarction (AWI, between the anterior cerebral artery and the middle cerebral artery), posterior watershed infarction (PWI, between the middle cerebral artery and the posterior cerebral artery), and mixed-type infarction (AWI plus PWI). IWI is also further divided into partial IWI (P-IWI, a single lesion or chainlike, the so-called “rosary-like” pattern in the centrum semiovale) and confluent IWI (C-IWI, large cigar-shaped infarction alongside the lateral ventricle). The simultaneous occurrence of CWI and IWI is identified as mixed-type infarction [10]. In our case, apart from MMI, the hyperintense “heart appearance” sign in the bilateral anteromedial medullae (Fig. 1A), PWI, in the right cerebral hemisphere (Fig. 1B), and P-IWI in the right cerebral hemisphere (Fig. 1C) were detected by DWI. Most IWIs are accompanied by CWIs. To the best of our knowledge, the simultaneous occurrence of bilateral MMI and WSI has yet to be reported, and the mechanism of WSI is not yet fully understood. Traditionally, HDI has been widely accepted as a cause of WSI [11]. From the clinicians’ viewpoint, each case of IWI could be linked to a hemodynamic impairment. Previous studies demonstrated an association between IWI and critical stenosis of ICA. This finding supported the theory that HDI may be the main cause of IWI [10,12]. The relationship between CWI and HDI appears more complicated, with a previous report stating that artery-to-artery embolism might play an important role in isolated CWI [13]. The susceptibility of the internal border-zone area to HDI is probably due to low perfusion pressure in the perforating medullary arteries, the most distal branches of the ICA with insufficient collateral

supply of deep perforating lenticulostriate arteries [10]. Previous studies [10,13] revealed that the rosary-like infarction in the centrum semiovale, which was identified as P-IWI in those studies, appears to be associated with HDI. However, Moustafa et al. [14] found that in addition to HDI, microemboli might also play a role in the pathogenesis of the rosary-like infarction. If there is no blood flow reduction, an embolic mechanism can be considered. Few studies have thoroughly compared the difference between C-IWI and P-IWI. One study showed that critical ICA stenosis was more common in P-IWI patients than in C-IWI patients [10]. In our case, brain MRI showed PWI in the right cerebral hemisphere (Fig. 1B) and P-IWI in the right cerebral hemisphere (Fig. 1C) on DWI images. Furthermore, brain DSA showed mild stenosis in the BA (Fig. 2A), plaque formation in the right ICA without obvious stenosis (Fig. 2B), and mild stenosis in the right MCA (Fig. 2C). Therefore, it is considered that bilateral MMI might be associated with basilar artery atherosclerosis. However, there is no evidence to conclude that bilateral MMI might be associated with HDI or microemboli, which might cause the CWI.

Maybe there is another mechanism; in the current case, brain DSA showed that the right VA was more dominant than the left VA in the extracranial portion, and the left VA was occluded at the distal intracranial portion (Figs. 2A, E, and F). The anatomic variability of the left perforator branches, which supply the bilateral anteromedial arterial or ASAs originating from the left VA, might explain the bilateral MMI with unilateral VA occlusion [15].

TEACHING POINT

MRI shows the classical heart appearance or V/Y sign at the ventral medulla in patients with bilateral medial medullary infarction. Hemodynamic impairment and microemboli are both the causes of cortical watershed infarction.

REFERENCES

1. Toyoda K, Imamura T, Saku Y, Oita J, Ibayashi S, Minematsu K, Yamaguchi T, Fujishima M. Medial medullary infarction: analyses of eleven patients. *Neurology*. 1996;47(5):1141-1147. PMID: 8909419
2. Shono Y, Koga M, Toyoda K, et al. Medial medullary infarction identified by diffusion-weighted magnetic resonance imaging. *Cerebrovasc Dis* 2010;30:519-524. PMID: 20861624
3. Pongmoragot J, Parthasarathy S, Selchen D, et al. Bilateral medial medullary infarction: a systematic review. *J Stroke Cerebrovasc Dis* 2013;22:775-780. PMID: 22541608

4. Maeda M, Shimono T, Tsukahara H, Maier SE, Takeda K. Acute bilateral medial medullary infarction: a unique "Heart Appearance" sign by diffusion-weighted imaging. *Eur Neurol*. 2004;51(4):236-237. PMID: 15159607
5. Thijs RD, Wijman CA, van Dijk GW, van Gijn J. A case of bilateral medial medullary infarction demonstrated by magnetic resonance imaging with diffusion-weighted imaging. *J Neurol*. 2001;248:339-340. PMID: 11374104
6. Kumral E, Afsar N, Kirbas D, Balkir K, Ozdemirkiran T. Spectrum of medial medullary infarction: clinical and magnetic resonance imaging findings. *J Neurol*. 2002;249:85-93. PMID: 11954873
7. Parsi K, Itgampalli RK, Suryanarayana A, et al. Bilateral medial medullary infarction: heart appearance. *Neurol India* 2013;61:84-85. PMID: 23466852
8. Ma L, Deng Y, Wang J, et al. Bilateral medial medullary infarction presenting as Guillain-Barre-like syndrome. *Clin Neurol Neurosurg* 2011;113:589-591. PMID: 21397385
9. Torabi AM. Bilateral medial medullary stroke: a challenge in early diagnosis. *Case Rep Neurol Med* 2013;2013:274373. PMID: 24198988
10. Li Y, Li M, Zhang X, et al. Clinical features and the degree of cerebrovascular stenosis in different types and subtypes of cerebral watershed infarction. *BMC Neurology*. 2017;17:166. PMID: 28851301
11. Hoffman SJ, Yee AH, Slusser JP, et al. Neuroimaging patterns of ischemic stroke after percutaneous coronary intervention. *Catheter Cardiovasc Interv*. 2015;85(6):1033-1040. PMID: 25256948
12. Del Sette M, Eliasziw M, Streifler JY, Hachinski VC, Fox AJ, Barnett HJ. Internal borderzone infarction: a marker for severe stenosis in patients with symptomatic internal carotid artery disease. For the North American Symptomatic Carotid Endarterectomy (NASCET) Group. *Stroke*. 2000;31:631-636. PMID: 10700496
13. Derdeyn CP, Khosla A, Videen TO, et al. Severe hemodynamic impairment and border zone--region infarction. *Radiology*. 2001;220:195-201. PMID: 11425997
14. Moustafa RR, Momjian-Mayor I, Jones PS, et al. Microembolism versus hemodynamic impairment in rosary-like deep watershed infarcts: a combined positron emission tomography and transcranial Doppler study. *Stroke*. 2011;42:3138-3143. PMID: 21852602
15. Gillilan LA. The correlation of the blood supply to the human brain stem with clinical brain stem lesions. *J Neuropathol Exp Neurol* 1964;23:78-108. PMID: 14105311

FIGURES

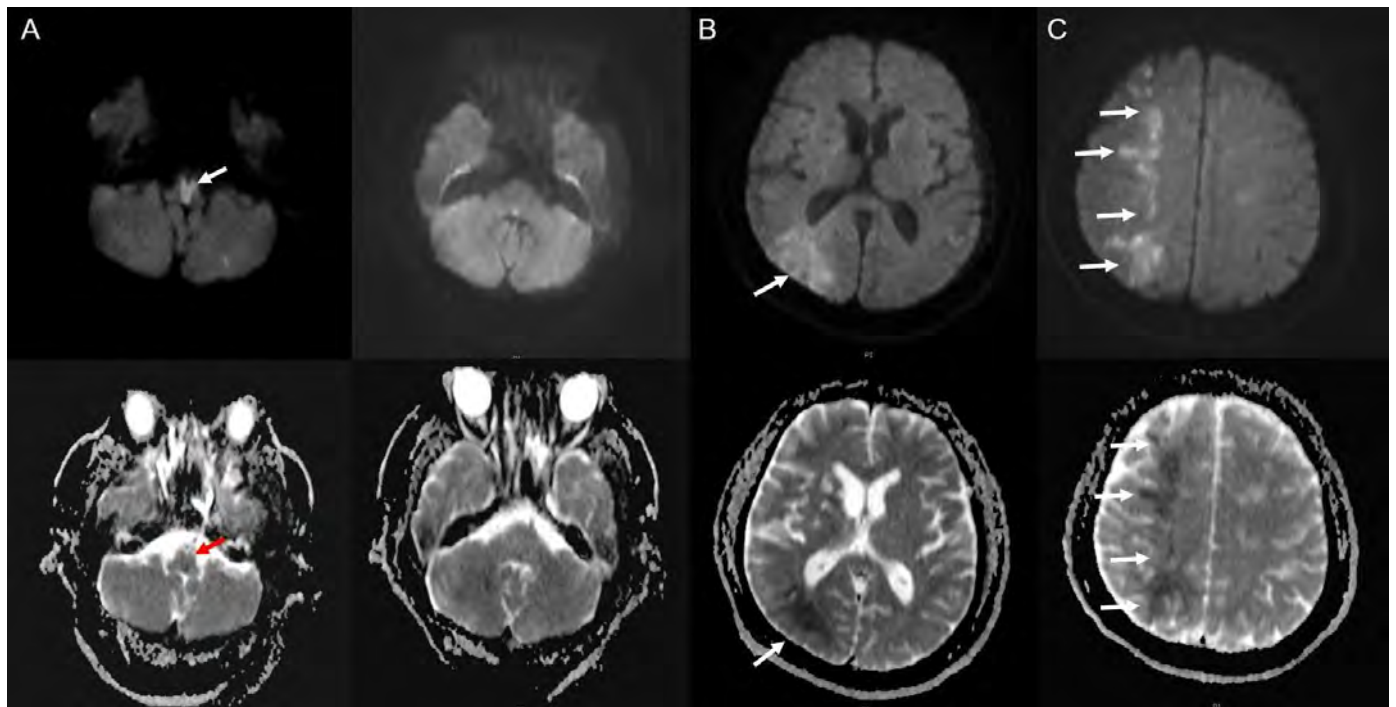


Figure 1: 50-year-old male with medial medullary infarction accompanied by cerebral watershed infarction.

Findings: MRI showed a hyperintense "heart appearance" signal in the bilateral anteromedial medullae on DWI images (top) with corresponding axial apparent diffusion coefficient (ADC) maps (bottom) (Fig. 1A), cortical watershed infarction in the right cerebral hemisphere on DWI images (top) with corresponding ADC maps (bottom) (Fig. 1B) and internal watershed infarction in the right cerebral hemisphere on DWI images (top) with corresponding ADC maps (bottom) (Fig. 1C).

TECHNIQUE: Axial diffusion-weighted 1.5T-MRI of the head.

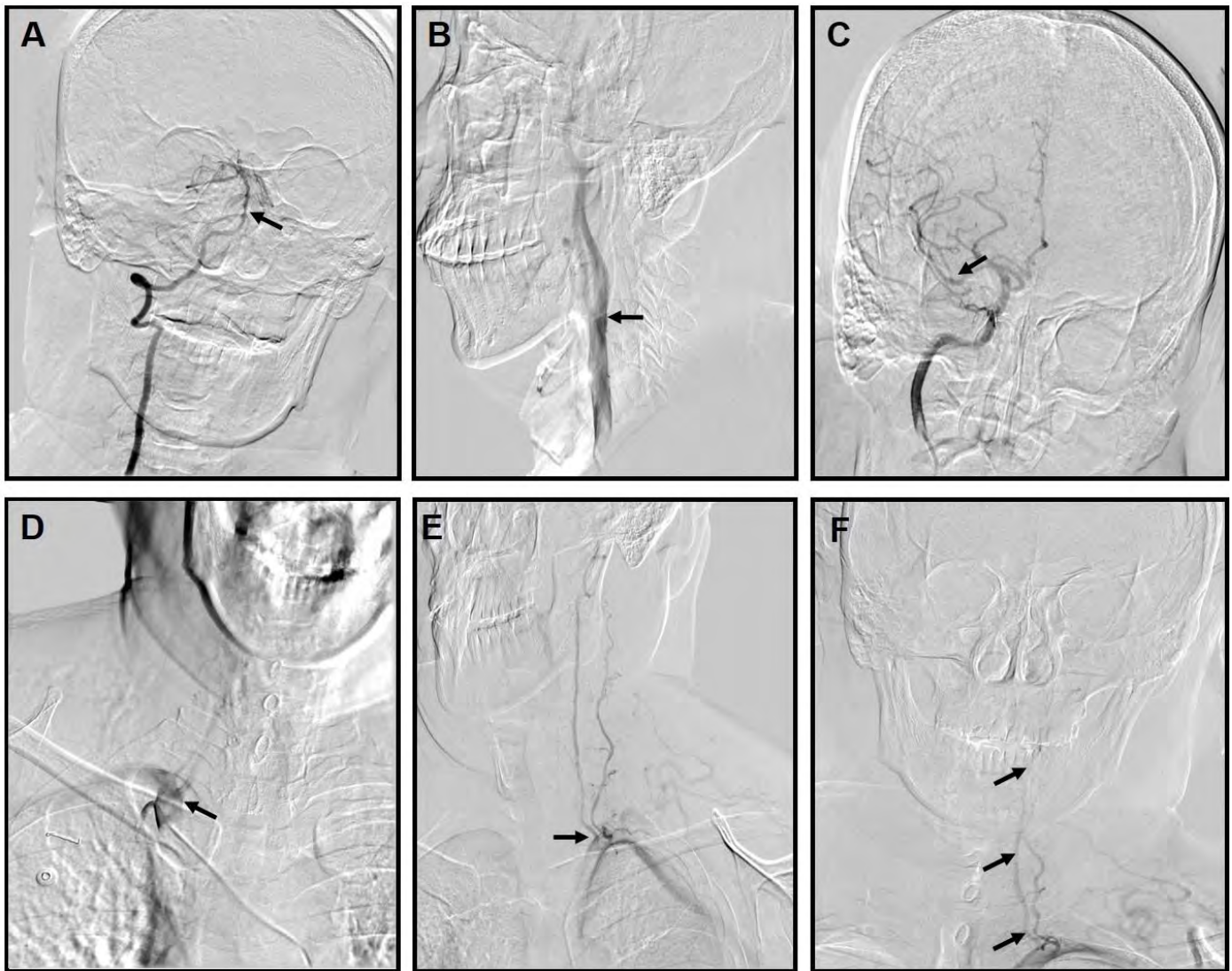


Figure 2: 50-year-old male with medial medullary infarction accompanied by cerebral watershed infarction.

Findings: Brain digital subtraction angiography (DSA) showed mild stenosis in the basilar artery (BA) (Fig. 2A), plaque formation in the right internal carotid artery (ICA) without obvious stenosis (Fig. 2B), mild stenosis in the right middle cerebral artery (MCA) (Fig. 2C), and normal right vertebral artery (VA) (Fig. 2D), which appeared more dominant than the left in the extracranial portion (Fig. 2E). The left VA was occluded at the distal intracranial portion (Fig. 2F).

TECHNIQUE: DSA projections following vertebral (4ml/s Omnipaque 240 contrast), left SCA (8ml/s Omnipaque 240 contrast), right SCA (8ml/s Omnipaque 240 contrast), and right ICA injections (6ml/s Omnipaque 240 contrast).
Figure 2-2 (magnification of figure 2-1)

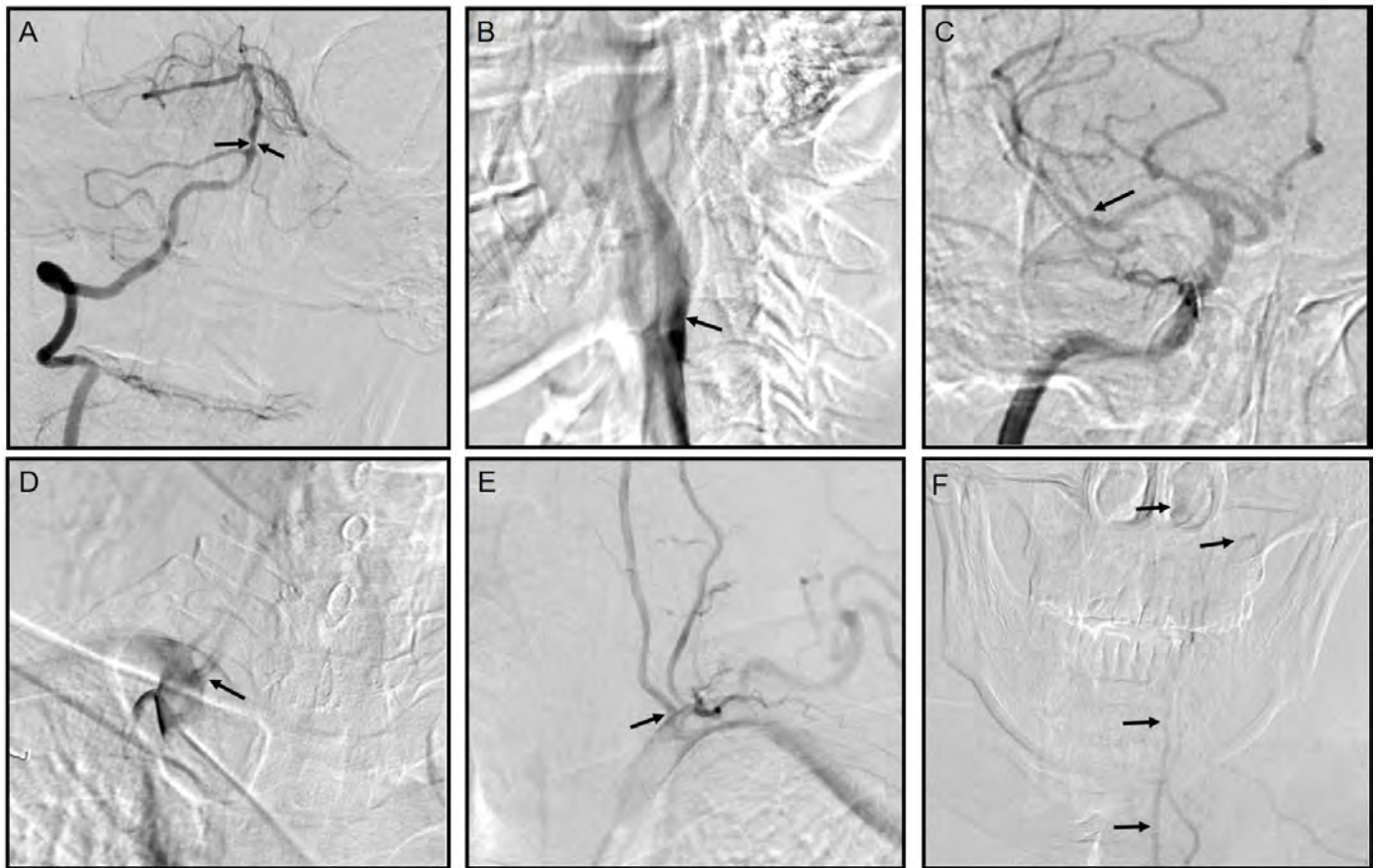


Figure 3: 50-year-old male with medial medullary infarction accompanied by cerebral watershed infarction. (magnification of figure 2)

Findings: Brain digital subtraction angiography (DSA) showed mild stenosis in the basilar artery (BA) (Fig. 2A), plaque formation in the right internal carotid artery (ICA) without obvious stenosis (Fig. 2B), mild stenosis in the right middle cerebral artery (MCA) (Fig. 2C), and normal right vertebral artery (VA) (Fig. 2D), which appeared more dominant than the left in the extracranial portion (Fig. 2E). The left VA was occluded at the distal intracranial portion (Fig. 2F).

TECHNIQUE: DSA projections following vertebral (4ml/s Omnipaque 240 contrast), left SCA (8ml/s Omnipaque 240 contrast), right SCA (8ml/s Omnipaque 240 contrast), and right ICA injections (6ml/s Omnipaque 240 contrast).

Etiology	The etiological classifications of infarctions are large-artery atherosclerosis (LA), small-vessel disease (SV), arterial dissection (DI), cardiac embolism (CE), and stroke of un- determined etiology.
Incidence	Medial medullary infarction (MMI) is a rare stroke subtype, accounting for only 0.5—1.5% of all strokes [1,2], and bilateral MMI is even rarer [3].
Risk factors	Atrial fibrillation, hypertension, smoking habits, diabetes mellitus, ischemic heart disease, and dyslipidemia
Treatment	The same as cerebral infarction treatment, and to perform endotracheal intubation when respiratory distress occurs.
Symptoms	They include quadriplegia, dysarthria, hypoglossal palsy, respiratory failure, and so on.
prognosis	The clinical outcome of bilateral MMI is usually poor [6].
Imaging findings	Brain magnetic resonance imaging (MRI) shows a hyperintense “heart appearance” signal in the bilateral anteromedial medullae.

Table 1: Summary table for Bilateral Medial Medullary Infarction

Diagnosis	X-Ray	CT	MRI	Key point
Bilateral Medial Medullary Infarction	Not mentioned	Not mentioned	MRI shows the classical “heart” or “V/Y” appearance at the ventral medulla in patients with bilateral MMI [7, 8]	A key point to differentiate between syndromes is the evolution of the clinical presentation; BMMI has a more acute presentation [8].
Guillain-Barre syndrome	Not mentioned	Not mentioned	No abnormalities found.	GBS has subacute evolution of clinical presentation [8].

Table 2: Differential diagnosis table for Bilateral Medial Medullary Infarction

ABBREVIATIONS

ADC = Apparent diffusion coefficient
 ASA = Anterior spinal artery
 AWI = Anterior watershed infarction
 BA = Basilar artery
 C-IWI = Confluent internal watershed infarction
 CWI = Cortical watershed infarction
 DSA = Digital subtraction angiography
 DWI = Diffusion-weighted imaging
 HDI = Hemodynamic impairment
 ICA = Internal carotid artery
 IWI = Internal watershed infarction
 MCA = Middle cerebral artery
 MMI = Medial medullary infarction
 MRI = Magnetic resonance imaging
 P-IWI = Partial internal watershed infarction
 PWI = Posterior watershed infarction
 SCA = Subclavian artery
 VA = Vertebral artery
 WSI = Watershed infarction

KEYWORDS

Bilateral medial medullary infarction; Cerebral watershed infarction; Hemodynamic impairment; Diffusion-weighted imaging; Digital subtraction angiography

ACKNOWLEDGEMENTS

We thank the patient and his family for their consent to publish the case report. We also thank Kunjun Wu who helped us during writing of this manuscript.

Online access

This publication is online available at:
www.radiologycases.com/index.php/radiologycases/article/view/3905

Peer discussion

Discuss this manuscript in our protected discussion forum at:
www.radiopolis.com/forums/JRCR

Interactivity

This publication is available as an interactive article with scroll, window/level, magnify and more features.
 Available online at www.RadiologyCases.com

Published by EduRad



www.EduRad.org

日中笹川医学奨学金制度(学位取得コース)中間評価書

課程博士：指導教官用



第 42 期

研究者番号： G4202

作成日： 2021 年 3 月 1 日

氏名	焦丹丹	Jiao Dandan	性別	F	生年月日	1985. 12. 21
所属機関(役職)	河南科技大学第一附属医院心外重症監護室(主管護師)					
研究先(指導教官)	筑波大学大学院人間総合科学研究科 国際発達ケア：エンパワメント科学研究室(安梅 勅江教授)					
研究テーマ	国際発達ケア：エンパワメント科学研究 International community care and life-span development: empowerment sciences					
専攻種別	<input type="checkbox"/> 論文博士			<input checked="" type="checkbox"/> 課程博士		

研究者評価(指導教官記入欄)

成績状況	<input checked="" type="checkbox"/> 優 良 可 不可 学業成績係数=3.2	取得単位数 38
		取得単位数/取得すべき単位数総数 38/30
学生本人が行った研究の概要	エンパワメントの技術を活用し、地域に住む人々の健康増進のための促進因子を明らかにする研究を実施しています。社会とのかかわりは、高齢者の健康状態維持に貢献する要因です。焦丹丹氏は、地域在住高齢者の健康長寿に向けた重要な研究を継続しています。	
総合評価	【良かった点】 1. 高い研究技術を学びました。 2. チームワークの技術を学びました。 3. プロジェクトマネジメントについて習得しました。	
	【改善すべき点】 さらに高度な統計スキルを学ぶ必要があります。	
	【今後の展望】 今後とも研究に真摯に取り組み、卒後プロとして活躍ください。	
学位取得見込	焦丹丹氏は、博士取得見込です。	
評価者(指導教官名) 		

日中笹川医学奨学金制度(学位取得コース)中間報告書

研究者用



第42期 研究者番号： G4202 作成日：2021年3月01日

氏名	Jiao Dandan	焦 丹丹	性別	F	生年月日 1985. 12. 21
所属機関(役職)	河南科技大学第一附属医院心外重症監護室（主管護師）				
研究先（指導教官）	筑波大学大学院人間総合科学研究科国際発達ケア:エンパワメント科学研究室(安梅勅江教授)				
研究テーマ	国際発達ケア：エンパワメント科学研究 International community care and life-span development: empowerment sciences				
専攻種別	論文博士	<input type="checkbox"/>	課程博士	<input checked="" type="checkbox"/>	
<p>1. 研究概要（1）</p> <p>1) 目的（Goal） To examine the role of social relationships on the association between chronic diseases and functional decline among community-dwelling older adults in Japan.</p> <p>2) 戦略（Approach） This three-year longitudinal study used data from a single-center cohort project, the “Community empowerment and care for well-being and healthy longevity: Evidence from a cohort study” [1], which started in 1991. This survey was conducted in a suburban area in central Japan with a population of around 5,000 with the goal of creating a health-promoting program that would maximize quantity and quality of life for residents. Questionnaires were mailed to all residents every three years, and interviews were conducted with people who needed assistance in completing the questionnaires.</p> <p>3) 材料と方法（Materials and methods）</p> <p>a. Participants For the purpose of the present study, we used data collected from individuals aged 65 years and older in 2014 and 2017 as baseline and follow-up, respectively. In 2014, at baseline, 523 individuals with at least one chronic disease (hypertension, stroke, heart disease, diabetes, hyperlipidemia, lung disease, arthritis, cancer, immune disease, depression, eye disease, and ear disease) were initially included. Then, in 2017, a follow up was conducted to assess the incidence of physical function decline among participants.</p> <p>b. Measurements Functional status. Functional status was assessed by instrumental activities of daily living (IADL) using the subscale of the Tokyo Metropolitan Institute of Gerontology Index of Competence, which was used to measure the functional competence of the community older adults [2]. The IADL subscale comprises five items, namely, using public transportation, shopping, preparing meals, paying bills, and individual banking management. For each item, a positive response was coded as 1, and a negative response was coded as 0. The total score ranges from 0 to 5. A score of 5 was considered normal IADL, while a score of 0 - 4 indicated low IADL[3].</p> <p>Social relations. Social relations were evaluated by the Index of Social Interaction (ISI) was used to evaluate social relationships [4]. The ISI includes five subscales and 18 items which is comprised of 5 subscales: 1) Independence, which includes having a motivation to live an active lifestyle, taking an active approach towards one’s life, being motivated to live a healthy life, and having a regular or routine lifestyle; 2) Social curiosity, which comprised reading newspapers, reading books, trying to use new equipment, having a hobby, and having a feeling of importance; 3) Interaction, composed of communication within the family, communication with non-family persons, and interactions with non-family persons; 4) Participation in society, made up of participation in social groups, participation in neighborhood affairs, watching television and having an active role in society; and 5) Feelings of safety, meaning having counsel, and having someone to give support in an emergency .</p> <p>c. Statistical analysis. Logistic regression analysis was employed to investigate the association between total changes in social relationships and physical function decline after adjusting for covariates.</p>					

1. 研究概要 (2)

4) 実験結果 (Results)

Data from 422 individuals were included in the analysis after excluding participants who were lost to follow-up and had missing information in IADL. Of the participants, the majority were women, not living alone, doing exercise, no smoking and drinking. 55.7% had one chronic disease.

The logistic regression results showed that rich social relationships were significantly associated with low incidence of physical function, with the odds ratio = 0.77, 95% confidence interval = 0.64-0.93 after controlling the confounding variables.

5) 考察 (Discussion)

The present study examined the effects of social relationships on functional status and showed that rich social relationships could reduce the physical functional decline among older adults with chronic diseases. Social relationships seem to have adverse effects on functional decline in older adults with chronic disease. This result is in line with a previous study, in which Christian et al. [5] conducted research in six countries and showed that social capital was linked to increased subject well-being regardless of the chronic disease conditions. A systematic review indicated that social relationships play an important role in well-being and mental health among people with disabilities [6]. Social relations affect health outcomes through a reciprocity exchange [7] that social relations might extend resources, including transportation support and caring, which can affect health-related behavior. People with chronic diseases may gain benefits from social relationships, including a high chance of undergoing medical checkups, important health-related information, and confidence in health promotion behaviors, which can delay physical decline. Knowing the effects of social relationships on health outcomes among people with chronic conditions may provide evidence of chronic disease management.

Several limitations exist in this study. First, the disease severity and duration were not examined, which may have affected the results. Second, only one indicator was used to examine the functional status, and combining subjective and objective measurements as functional indicators might strengthen the reliability of results. Third, this study was conducted in one area, which may limit the generalizability of the results. Further studies should be conducted to address these limitations.

Despite these limitations, the present study addresses the association between social relationships and functional status among community-dwelling older adults with chronic conditions. These findings supplement evidence of the role of social relationships, indicating that social relationships contribute to health outcomes for both the general population and able-bodied people.

6) 参考文献 (References)

1. Anme, T. (2015, December 20). Community empowerment and care for well-being and healthy longevity: Evidence from cohort study (abbr. CEC). <http://plaza.umin.ac.jp/~empower/cec/en/>
2. W. Koyano, H. Shibata, K. Nakazato, H. Haga, Y. Suyama, Measurement of competence: reliability and validity of the TMIG Index of Competence, *Arch Gerontol Geriatr.* 13(2) (1991) 103 - 116. doi: 10.1016/0167-4943(91)90053-s
3. T. Ishizaki, I. Kai, Y. Kobayashi, Y. Imanaka, Functional transitions and active life expectancy for older Japanese living in a community, *Arch Gerontol Geriatr.* 35(2) (2002) 107 - 120. doi: 10.1016/s0167-4943(02)00002-x
4. T. Anme, C. Shimada, Social interaction and mortality in a five-year longitudinal study of the elderly, *Jpn. J. Public Health.* 47(2000) 127 - 133.
5. A.K. Christian, O.A. Sanuade, M. A. Okyere, K. Adjaye-Gbewonyo, Social capital is associated with improved subjective well-being of older adults with chronic non-communicable disease in six low- and middle-income countries, *Global Health.* 16(1) (2020) 2. doi: 10.1186/s12992-019-0538-y
6. H. Tough, J. Siegrist, C. Fekete, Social relationships, mental health and wellbeing in physical disability: a systematic review, *BMC Pub Health.* 17(1) (2017) 414. doi: 10.1186/s12889-017-4308-6
7. W.C. Cockerham, B.W. Hamby, G.R. Oates, The .Social Determinants of Chronic Disease, *Am J Prev Med.* 52(1s1) (2017) S5 - s12. doi: 10.1016/j.amepre.2016.09.010

2. 執筆論文 Publication of thesis ※記載した論文を添付してください。Attach all of the papers listed below.

論文名 1 Title	Multimorbidity and functional limitation: the role of social relationships				
掲載誌名 Published journal	Archives of Gerontology and Geriatrics				
	2021 年 1 月	92 巻 (号)	140249 頁 ~	頁	言語 Language English
第 1 著者名 First author	Dandan Jiao	第 2 著者名 Second author	Kumi Watanabe	第 3 著者名 Third author	Yuko Sawada
その他著者名 Other authors	Emiko Tanaka, Taeko Watanabe, Etsuko Tomisaki, Sumio Ito, Rika Okumura, Yuriko Kawasaki, Tokie Anme*				
論文名 2 Title					
掲載誌名 Published journal					
	年 月	巻 (号)	頁 ~	頁	言語 Language
第 1 著者名 First author		第 2 著者名 Second author		第 3 著者名 Third author	
その他著者名 Other authors					
論文名 3 Title					
掲載誌名 Published journal					
	年 月	巻 (号)	頁 ~	頁	言語 Language
第 1 著者名 First author		第 2 著者名 Second author		第 3 著者名 Third author	
その他著者名 Other authors					
論文名 4 Title					
掲載誌名 Published journal					
	年 月	巻 (号)	頁 ~	頁	言語 Language
第 1 著者名 First author		第 2 著者名 Second author		第 3 著者名 Third author	
その他著者名 Other authors					
論文名 5 Title					
掲載誌名 Published journal					
	年 月	巻 (号)	頁 ~	頁	言語 Language
第 1 著者名 First author		第 2 著者名 Second author		第 3 著者名 Third author	
その他著者名 Other authors					

3. 学会発表 Conference presentation ※筆頭演者として総会・国際学会を含む主な学会で発表したものを記載してください。※Describe your presentation as the principal presenter in major academic meetings including general meetings or international meetings.

学会名 Conference	Tsukuba Global Science Week (2020)		
演題 Topic	Multimorbidity and functional limitation: the role of social relationships		
開催日 date	2020 年 9 月 18 日	開催地 venue	Tsukuba,Japan
形式 method	<input type="checkbox"/> 口頭発表 Oral	<input checked="" type="checkbox"/> ポスター発表 Poster	言語 Language <input type="checkbox"/> 日本語 <input checked="" type="checkbox"/> 英語 <input type="checkbox"/> 中国語
共同演者名 Co-presenter	Dandan Jiao, Kumi Watanabe, Yoko Sawada, Emiko Tanaka, Taeko Watanabe,Etsuko Tomisaki,Sumio Ito,Rika Okumura,Yuriko Kawasaki, Tokie Anme*		
学会名 Conference			
演題 Topic			
開催日 date	年 月 日	開催地 venue	
形式 method	<input type="checkbox"/> 口頭発表 Oral	<input type="checkbox"/> ポスター発表 Poster	言語 Language <input type="checkbox"/> 日本語 <input type="checkbox"/> 英語 <input type="checkbox"/> 中国語
共同演者名 Co-presenter			
学会名 Conference			
演題 Topic			
開催日 date	年 月 日	開催地 venue	
形式 method	<input type="checkbox"/> 口頭発表 Oral	<input type="checkbox"/> ポスター発表 Poster	言語 Language <input type="checkbox"/> 日本語 <input type="checkbox"/> 英語 <input type="checkbox"/> 中国語
共同演者名 Co-presenter			
学会名 Conference			
演題 Topic			
開催日 date	年 月 日	開催地 venue	
形式 method	<input type="checkbox"/> 口頭発表 Oral	<input type="checkbox"/> ポスター発表 Poster	言語 Language <input type="checkbox"/> 日本語 <input type="checkbox"/> 英語 <input type="checkbox"/> 中国語
共同演者名 Co-presenter			

4. 受賞 (研究業績) Award (Research achievement)

名称 Award name	国名 Country	受賞年 Year of award	年 月
名称 Award name	国名 Country	受賞年 Year of award	年 月

5. 本研究テーマに関わる他の研究助成金受給 Other research grants concerned with your research theme

受給実績 Receipt record	<input type="checkbox"/> 有 <input checked="" type="checkbox"/> 無
助成機関名称 Funding agency	
助成金名称 Grant name	
受給期間 Supported period	年 月 ~ 年 月
受給額 Amount received	円
受給実績 Receipt record	<input type="checkbox"/> 有 <input checked="" type="checkbox"/> 無
助成機関名称 Funding agency	
助成金名称 Grant name	
受給期間 Supported period	年 月 ~ 年 月
受給額 Amount received	円

6. 他の奨学金受給 Another awarded scholarship

受給実績 Receipt record	<input type="checkbox"/> 有 <input checked="" type="checkbox"/> 無
助成機関名称 Funding agency	
奨学金名称 Scholarship name	
受給期間 Supported period	年 月 ~ 年 月
受給額 Amount received	円

7. 研究活動に関する報道発表 Press release concerned with your research activities

※記載した記事を添付してください。 Attach a copy of the article described below

報道発表 Press release	<input type="checkbox"/> 有 <input checked="" type="checkbox"/> 無	発表年月日 Date of release	
発表機関 Released medium			
発表形式 Release method	・新聞 ・雑誌 ・Web site ・記者発表 ・その他 ()		
発表タイトル Released title			

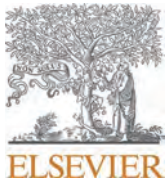
8. 本研究テーマに関する特許出願予定 Patent application concerned with your research theme

出願予定 Scheduled	<input type="checkbox"/> 有 <input checked="" type="checkbox"/> 無	出願国 Application country	
出願内容 (概要) Application contents			

9. その他 Others

None

指導責任者 (署名) 



Contents lists available at ScienceDirect

Archives of Gerontology and Geriatrics

journal homepage: www.elsevier.com/locate/archger

Multimorbidity and functional limitation: the role of social relationships

Dandan Jiao^a, Kumi Watanabe^a, Yuko Sawada^b, Emiko Tanaka^c, Taeko Watanabe^d, Etsuko Tomisaki^e, Sumio Ito^f, Rika Okumura^f, Yuriko Kawasaki^f, Tokie Anne^{g,*}^a Graduate School of Comprehensive Human Sciences, University of Tsukuba, Tsukuba, Ibaraki, 305-8577, Japan^b Medical Sciences, Morinomiya University of Medical Sciences, Osaka, 559-8611, Japan^c Community Nursing, Musashino University, Tokyo, 202-8585, Japan^d College of Nursing and Nutrition, Shukutoku University, Chiba, 260-8703, Japan^e Faculty of Nursing and Medical Care, Keio University, Tokyo, 160-0016, Japan^f Department of Public Welfare, Tobishima, Aichi, 490-1434, Japan^g Faculty of Medicine, University of Tsukuba, 1-1-1 Tennodai, Tsukuba, Ibaraki, 305-8577, Japan

ARTICLE INFO

Keywords:

Older adults
functioning
multimorbidity
prevention
social relationships

ABSTRACT

Objectives: To examine the relationship between multimorbidity and functional limitation, and how social relationships alter that association.**Methods:** This cross-sectional study used data collected by self-reported questionnaires from adults aged 65 years and older living in a rural area in Japan in 2017. This analysis included complete data from 570 residents. Multimorbidity status was defined as having two chronic diseases exist simultaneously in one individual, and the function status was measured by their long-term care needs. Social relationships were assessed by the Index of Social Interaction and divided into high and low levels. Multiple logistic regression analysis was used to examine the association between social relationships and functional limitation and to assess the role of social relationships in this association.**Results:** The logistic regression model indicated that the risk of functional limitation was higher in multimorbidity participants than free-of-multimorbidity participants (OR = 2.55, 95% CI = 1.56–4.16). Compared with participants with no multimorbidity and a high level of social relationships, low level of social relationships increased the risk of functional limitation among participants both with and without multimorbidity, with the OR = 7.71, 95% CI = 3.03–19.69 and OR = 3.28, 95% CI = 1.30–8.27, respectively. However, no significant result was found in participants with multimorbidity and a high level of social relationships ($P = 0.365$).**Conclusions:** Multimorbidity was associated with functional limitations. However, this association could be increased by a low level of social relationships and decreased by a high level of social relationships.

1. Introduction

Healthy Ageing is defined as ‘the process of developing and maintaining the functional ability that enables wellbeing in older age’ (WHO, 2018). Functional ability is of great concern because functional limitations would result in depression (Turvey, Schultz, Beglinger, Klein, 2009), cognitive impairment (Zaninotto, Batty, Allerhand, Deary, 2018), and mortality (Liu et al., 2018), posing a burden on the whole society.

Multimorbidity is defined as the co-occurrence of two chronic conditions in a person (Fortin, Bravo, Hudon, Vanasse, Lapointe, 2005). It has increasingly gained public health attention and causes challenges for

healthcare systems because multimorbidity is linked to low quality of life (Mujica-Mota et al., 2015), impaired mental health, and a high risk of mortality (Kuzuya, 2019). Many studies have proved that multimorbidity is linked to functional limitations (Formiga et al., 2005; Storeng, Vinjerui, Sund, Krokstad, 2020; Wensing, Vingerhoets, Grol, 2001). However, some studies indicated that there was no significant association between multimorbidity and physical functioning (Baker Whitfield, 2006; Parker, Moran, Roberts, Calvert, McCahon, 2014), and a cohort study showed at least 50% of the participants were functionally independent in spite of chronic disorders among older people (Santoni et al., 2017). Although multimorbidity has gained research interest recently, many studies have been conducted in the

* Corresponding author.

E-mail address: tokieanne@gmail.com (T. Anne).<https://doi.org/10.1016/j.archger.2020.104249>

Received 23 June 2020; Received in revised form 16 August 2020; Accepted 18 August 2020

Available online 7 September 2020

0167-4943/© 2020 Elsevier B.V. All rights reserved.

United States (Baker & Whitfield, 2006) and European countries (Storeng et al., 2020; Wensing et al., 2001), but relatively few studies have been conducted in Japan. For example, Ishizaki et al. (2019) reported that both poor objective and subjective physical functioning is related to multimorbidity among people aged 60 years and older. Physiological change, however, differs with aging (Aalami, Fang, Song, & Nacamuli, 2003). Another Japanese study demonstrated that the prevalence of multimorbidity increased with age before approximately the age of 90, but decreased after 90 (Mitsutake, Ishizaki, Teramoto, Shimizu, & Ato, 2019). The effects of multimorbidity on functional status might be different according to age range. Thus, clarifying the effects of multimorbidity on functional limitation status among adults aged 65 years and over may add evidence regarding previously reported mixed results and enrich a tailored knowledge of multimorbidity management among older people in rural areas.

Social relationships positively contributed to a decrease in functional limitations. Having an active social relationship was significantly associated with higher basic activities of daily living, instrumental activities of daily living (Shinkai et al., 2003), and lower mortality (Takahashi et al., 2019). On the other hand, people with greater social relationships experienced a lower risk of multimorbidity (Cantarero-Prieto, Pascual-Saez, & Blazquez-Fernandez, 2018; Singer, Green, Rowe, Ben-Shlomo, & Morrissey, 2019). Social relationships play an important role in reducing/delaying adverse health outcomes among older adults. To date, most studies have focused separately on the association between social relationships and multimorbidity (Cantarero-Prieto et al., 2018; Singer et al., 2019), and functional status (Shinkai et al., 2003). The role of social relationships on the association between multimorbidity and functional limitation among older adults remains underexamined.

To fill in these research gaps, we aimed to investigate (1) the association of multimorbidity with functioning status, and (2) the role of social relationships in this association among older adults. Our hypothesis was that (1) multimorbidity is related to a high risk of functional limitations, and (2) high social relationships might attenuate this relationship; for e.g., rich social relationships could decrease the risk of functional limitations among people with multimorbidity. The results might provide new insights into the management of multimorbidity among older people.

2. Methods

2.1. Study design and participants

This study used data from a longitudinal cohort study, which was a survey of community-dwelling people in a rural area in the central part of Japan. The longitudinal study began in 1991, aiming to assess risk factors associated with well-being and longevity and to improve the quality of life of residents. Questionnaires were distributed to all residents every three years. For participants who needed help with answering the questionnaires, their caregivers completed them on their behalf. For the present cross-sectional study, we extracted data from people aged 65 years and older in 2017. There were 1088 people aged 65 years and older, and 842 participants with no missing data in terms of disease and functional status information were initially included. Next, we excluded participants with missing information on any of the variables, resulting in a total of 570 participants who were retained for the study.

2.2. Measurements

2.2.1. Functioning status

One question was used to assess participants' functional status: 'Do you need care/assistance in your daily life?' A 'yes' response indicated the need for long-term support and 'no' indicated otherwise. In Japan, the long-term care system is widely used and certified by the

government when people need some care support in life. People needing support suggests that their ability to perform activities of daily living is partly or totally dependent on others (Matsuda, Muramatsu, & Hayashida, 2011). Therefore, the 'yes' and 'no' responses indicate the presence or absence of functional limitations, respectively.

2.2.2. Multimorbidity

Multimorbidity was evaluated by using the simple method of counting the number of disease conditions that were self-reported by the participants. These conditions include the following ten chronic diseases: hypertension, stroke, heart disease, diabetes, lung disease, cancer, depression, dementia, Parkinson's disease, and arthritis. Respondents who answered as having any two of these conditions were classified as having multimorbidity; otherwise, they were classified as free of multimorbidity.

2.2.3. Social relationships

The Index of Social Interaction (ISI) was used to assess the social relationship status. The ISI includes 18 items which were developed for evaluating various aspects of social relationships, including independence, social curiosity, feeling of safety, interaction, and participation (Anme & Shimada, 2000). The 18 items are: 'Do you have motivation to live an active lifestyle?' 'Do you take an active approach toward your life?' 'Are you motivated to live a healthy life?' 'Do you have a regular or routine lifestyle?' 'Do you read newspapers regularly?' 'Do you read books or magazines regularly?' 'Do you try to use new equipment like a video?' 'Do you have any hobbies?' 'Do you have a feeling of importance in society?' 'Do you often communicate with your family members?' 'Do you communicate with nonfamily people regularly?' 'Do you interact with non-family people regularly?' 'Do you have a chance to participate in social groups?' 'Do you watch television?' 'Do you have a chance to participate in your neighbourhood affairs?' 'Do you have an active role in society or social affairs?' 'Do you have someone to counsel with in a difficult situation?' 'Do you have someone to support you in an emergency?' Each item was coded 1 for a positive response and 0 for a negative response. The total possible score is 18, with a higher score showing a higher level of social relationships. Due to the skewed distribution of participants, the median value (17.0) of ISI was used to divide participants into high ISI (18.0) and low ISI (≤ 17.0).

2.2.4. Covariates

Based on previous studies (Ishizaki et al., 2019; Singer et al., 2019), age, gender, physical activity, drinking, smoking, and living status were considered. Age was a continuous variable. Physical activity was dichotomized responses as activity if they answered 'usually' and 'sometimes' and inactivity for a 'no' response to the question: 'do you do physical activities?' Participants were identified as 'non-drinker' if they answered 'not drinking' and 'others' if they answered 'everyday' and 'sometimes'. The smoking status was decided based on their choices of one of three answers: 'currently smoking', 'previously smoking but now stopped', and 'never smoke'. Then smoking was trichotomously coded as 'current smoker', 'ex-smoker', and 'non-smoker'. Living status was coded as 'living alone' and 'not alone'.

2.3. Statistical analysis

Median and frequency were used to describe continuous and categorical data, respectively. Chi-square tests and the Mann-Whitney U-test were used for the bivariate analysis to examine the association between participants' characteristics and function status. Next, multiple logistic regression analysis was employed to examine the association between multimorbidity and functional status.

To examine the role of social relationships, we constructed an additional model to evaluate the risk of developing functional limitations among the different four groups: participants with no multimorbidity and low ISI (Group 1), those with multimorbidity and low ISI

(Group 2), those with multimorbidity and high ISI (Group 3), and those with no multimorbidity and high ISI (Group 4). Group 4 was considered the reference group. IBM SPSS 22.0 was used for data analysis.

2.4. Ethical considerations

This study was approved by the Ethics Committee of a University to which the authors are affiliated. The data were anonymized and provided by the municipality via written contracts.

3. Results

In total, 570 participants with completed data information were included in the analysis. For these participants, the mean (SD) for age was 74.1 (7.5) years. Of the participants, over half were women (50.2%), engaged in physical activity (58.1%), current drinkers (63.0%), non-smokers (61.6%), and not living alone (94.7%). The proportion of participants with multimorbidity was 28.6% and of participants reporting high level of social relationships was 31.2% (Table 1).

Of ten chronic diseases, hypertension has the highest prevalence (55.8%), followed by diabetes (15.8%), and arthritis (10.2%). The prevalence of stroke and lung disease is around 5%, while depression and Parkinson’s disease (0.9%) has the lowest percentage (Table 2).

The bivariate analysis indicated that age, physical activity, drinking status, smoking status, and multimorbidity were significantly associated with functional status (Table 3). When these significant variables were analysed by multivariate analysis, we found that age (OR = 1.14, 95% CI = 1.10–1.17), and multimorbidity (OR = 2.55, 95% CI = 1.56–4.16) were significantly associated with functional limitation (Table 4).

Regarding the role of social relationships, the risks of functional limitation were similar in Groups 1 and 2. Compared to participants with no multimorbidity and high ISI (Group 4), the risks for functional limitation increased for individuals with no multimorbidity and low ISI

Table 1 Characteristics of participants.

Variables	Category	n	%
Age (Mean ± SD)		74.1 ± 7.5	
Sex	Men	284	49.8
	Women	286	50.2
Physical activity	Activity	331	58.1
	Inactivity	239	41.9
Drinking	Yes	359	63.0
	No	211	37.0
Smoking	Current smoker	63	11.1
	Ex-smoker	156	27.3
	Non-smoker	351	61.6
Living status	Alone	30	5.3
	Not alone	540	94.7
ISI	High	178	31.2
	Low	392	68.8
Multimorbidity	Yes	163	28.6
	No	407	71.4
Group 1 ^a		265	46.5
Group 2 ^b		127	22.3
Group 3 ^c		36	6.3
Group 4 ^d		142	24.9

ISI = index of social interaction; SD = standard deviation.

- ^a No multimorbidity + low ISI.
- ^b Multimorbidity + low ISI.
- ^c Multimorbidity + high ISI.
- ^d No multimorbidity + high ISI.

Table 2 Percentage of each chronic disease.

N = 570		
Disease	n	%
Hypertension	252	55.8
Diabetes	90	15.8
Arthritis	58	10.2
Heart disease	48	8.4
Stroke	31	5.4
Lung disease	29	5.1
Cancer	23	4.0
Dementia	13	2.3
Depression	5	0.9
Parkinson’s disease	5	0.9

(Groups 1) (OR = 3.28, 95% CI = 1.30–8.27), and such a relationship was greater in participants with multimorbidity and low ISI (Group 2) (OR = 7.71, 95% CI = 3.03–19.69), whereas the relationship was not observed in participants with multimorbidity and high ISI (Group 3) (P = 0.365) (Table 5).

4. Discussion

The present study identified that older persons with multimorbidity have a high risk of functional limitation if they are aged 65 years and older living in a rural area, and social relationships altered the association between multimorbidity and function status.

Our findings suggest that individuals with multimorbidity are more likely to be linked to functional limitation, which is consistent with

Table 3 Participants’ characteristics and functional limitations.

Characteristics	Category	Yes (n = 105) n (%)	No (n = 465) n (%)	χ ² /Z	P
Age				-8.739	<0.001
Sex	Men	47 (16.5)	237 (83.5)	1.320	0.251
	Women	58 (20.3)	228 (79.7)		
Physical activity	Activity	49 (14.8)	282 (85.2)	6.874	0.009
	Inactivity	56 (23.4)	183 (76.6)		
Drinking	Yes	52 (14.5)	307 (85.5)	10.000	0.002
	No	53 (25.1)	158 (74.9)		
Smoking	Current smoker	4 (6.3)	59 (93.7)	7.395	0.025
	Ex-smoker	34 (21.8)	122 (78.2)		
	Non-smoker	67 (19.1)	284 (80.9)		
Living status	Alone	6 (20.0)	24 (80.0)	0.503	0.819
	Not alone	99 (18.3)	441 (81.7)		
ISI	High	9 (5.1)	169 (94.9)	30.764	<0.001
	Low	96 (24.5)	296 (75.5)		
Multimorbidity	Yes	49 (30.1)	114 (69.9)	20.583	<0.001
	No	56 (13.8)	351 (86.2)		
Group 1 ^a		50 (18.9)	215 (81.1)	48.289	<0.001
Group 2 ^b		46 (36.2)	81 (63.8)		
Group 3 ^c		3 (8.3)	33 (91.7)		
Group 4 ^d		6 (4.2)	136 (95.8)		

ISI = index of social interaction.

- ^a No multimorbidity + low ISI.
- ^b Multimorbidity + low ISI.
- ^c Multimorbidity + high ISI.
- ^d No multimorbidity + high ISI.

Table 4
Association between multimorbidity and functional limitations.

Variables	Category	Unadjusted			Adjusted				
		OR	95% CI	P	OR	95% CI	P		
Age		1.14	1.11	1.18	<0.001	1.14	1.10	1.17	<0.001
Physical activity		1.75	1.15	2.70	0.009	1.28	0.78	2.08	0.328
Drinking		0.51	0.33	0.78	0.002	0.62	0.36	1.08	0.092
Smoking	Current smoker	0.29	0.10	0.82	0.020	0.51	0.16	1.59	0.245
	Ex-smoker	1.18	0.74	1.88	0.482	1.66	0.93	2.96	0.090
	Non-smoker	ref							
Multimorbidity		2.69	1.74	4.17	<0.001	2.55	1.56	4.16	<0.001

Table 5
The role of ISI in the association between multimorbidity and functional limitations.

Variables	Category	Unadjusted			Adjusted				
		OR	95% CI	P	OR	95% CI	P		
Age		1.14	1.11	1.18	<0.001	1.12	1.08	1.16	<0.001
Physical activity		1.75	1.15	2.70	0.009	1.07	0.65	1.76	0.806
Drinking		0.51	0.33	0.78	0.002	0.69	0.39	1.21	0.193
Smoking	Current smoker	0.29	0.10	0.82	0.020	0.49	0.16	1.57	0.230
	Ex-smoker	1.18	0.74	1.88	0.482	1.66	0.92	3.01	0.090
	Non-smoker	ref							
Multimorbidity		2.69	1.74	4.17	<0.001				
ISI		0.16	0.08	0.33	<0.001				
Group based on multimorbidity and ISI status									
Group 1 ^a		5.27	2.20	12.63	<0.001	3.28	1.30	8.27	0.012
Group 2 ^b		12.87	5.26	31.46	<0.001	7.71	3.03	19.69	<0.001
Group 3 ^c		2.06	0.49	8.67	0.324	1.99	0.45	8.88	0.365
Group 4 ^d		ref							

ISI = index of social interaction.

^a No multimorbidity + low ISI.

^b Multimorbidity + low ISI.

^c Multimorbidity + high ISI.

^d No multimorbidity + high ISI.

previous studies. A study conducted in the United States showed participants with multimorbidity had a higher level of disability in both activities of daily living and instrumental activities of daily living compared to participants with a single disease in individuals aged 65 years or older (Quinones, Markwardt, & Botoseneanu, 2016). In a review including both cross-sectional studies and cohort studies, Ryan, Wallace, O'Hara, and Smith (2015) reported that people with multimorbidity are also more likely to have poor function status. Furthermore, even when multimorbidity was evaluated using a different counting method (three chronic conditions), the same relationship between multimorbidity and functional limitation was observed (Storeng et al., 2020). Multimorbidity appears to be an important determinant of poor physical functioning among older adults. On the other hand, functional limitation would impact multimorbidity, which will develop a 'vicious circle'. Attention should be paid and measures should be taken to reduce/delay the deterioration of function limitation among older people with multimorbidity.

Social relationships could alter the impact of multimorbidity on function limitations. Comparing with older adults with no multimorbidity and a high level of social relationships, those who experience multimorbidity and high social relationships are less likely to have function limitations. Participants with multimorbidity and low social relationships, however, have the highest risk of developing functional limitations, followed by those without multimorbidity and low social relationships. In other words, high ISI helped to decrease the likelihood of function disabilities in older people with multimorbidity, while low ISI increased the probability of functional limitation status. Similarly, a cohort study examining the moderation effects of social support on the impact of multimorbidity on mortality survival time, suggested supportive social relationships increase the survival opportunities of people

with multimorbidity (Olaya et al., 2017). Mazzella et al. (2010) found that individuals with low social support and multimorbidity presented a high rate of death. Enriching social relationships could be a protective measure against function limitation among older individuals who suffer from multimorbidity. Conversely, lacking social support may affect people's non-adherence to therapies (DiMatteo, 2004), which may accelerate the progression of diseases and cause adverse outcomes, including functional limitation.

The role of social relationships may work mainly through two pathways. First, there is the stress buffering pathway, suggesting social relationships modify personal behaviours by providing resources, including informational and emotional support, when people are experiencing stress (Cohen & Wills, 1985). Comparing participants with only one or no chronic disease, it is plausible that people with multimorbidity experience more stress. High social resources could mitigate the negative effects of stress on health outcomes and therefore modify the effects of multimorbidity on physical limitations. Second, the main direct effects model posits that social relationships have a direct benefit to health regardless of whether people are presenting as experiencing stress (Broadhead et al., 1983). Through social connection, individuals acquire signals of behavioural guidance and the feeling of meaning in life, and then these signals could regulate an individual's neuroendocrine and immunological functions to improve physical functioning (Berkman, Glass, Brissette, & Seeman, 2000).

Our findings show that participants with multimorbidity would gain benefits through rich social relationships, which may provide evidence about how to reduce the burden of their multimorbidity. Since the management of multimorbidity is costly, interventions tailored to improve social relationships such as tele-support services are cost-effective (Findlay, 2003). Promoting social relationships of

participants is likely to improve multimorbidity self-management, maintain independence, and reduce function limitation. Moreover, few studies have been conducted to examine the role of social relationships on the association between multimorbidity and function limitation. Our results conclude that developing and facilitating social relationships might be a promising strategy for multimorbidity management among adults aged 65 years and older. Furthermore, since little research on multimorbidity has been conducted in Asian countries (Kuzuya, 2019), our findings may add evidence to the research topic of multimorbidity among older people. The final strength of our study is the multidimensional evaluation of the ISI, evaluating many aspects of social relationships in the daily lives of older people.

Several limitations of this study should be considered. First, this is a cross-sectional study that cannot deduce the causation relationship between multimorbidity and function limitations. Thus, longitudinal studies are needed to examine the role of high social relationships that can attenuate the relationship between multimorbidity and functional limitations. Further longitudinal studies adjusting for more potential confounders should also be performed to confirm these findings. Second, due to the limited sample size, the confidence interval is wide after being stratified by social relationships. Moreover, the high rate of missing values might reduce the power of the results. We suggest that future studies use a larger sample size to identify the effects of social relationships on altering the association between multimorbidity and function status. Third, although social relationships were found to positively affect the impact of multimorbidity on function disability, the specific aspects of social relationships should be explored in future studies. Fourth, only one functional measure was used. Future studies can use more indicators to measure the functional status, which may strengthen the validity of the results. Fifth, the stress buffering pathway suggests social relationships could modify the effects of multimorbidity on functional limitations. However, we did not assess the specific level of stress. Future studies considering the use of stress measures are expected.

5. Conclusions

The present study supplements existing evidence that multimorbidity poses risks on function disability in older adults aged 65 years and older, and the level of social relationships may alter that association. Our study suggests that the risk of function disability among participants with multimorbidity may be reduced by increasing social relationships. These results suggest a method for health professionals to assess people's social relationship and stimulate social support for older people with multimorbidity.

Funding

This research was supported by the Grants-in-Aid for Scientific Research (JP17H02604).

CRedit authorship contribution statement

Dandan Jiao: Conceptualization, Methodology, Formal analysis, Writing - original draft. **Kumi Watanabe:** Investigation, Formal analysis. **Yuko Sawada:** Investigation. **Emiko Tanaka:** Investigation. **Taeko Watanabe:** Investigation. **Etsuko Tomisaki:** Investigation. **Sumio Ito:** Project administration. **Rika Okumura:** Project administration. **Yuriko Kawasaki:** Project administration. **Tokie Anne:** Conceptualization, Investigation, Writing - review & editing, Project administration, Funding acquisition.

Declaration of Competing Interest

The authors report no declarations of interest.

Acknowledgments

We express our deep gratitude to all study participants and investigators.

References

- Aalami, O. O., Fang, T. D., Song, H. M., & Nacamuli, R. P. (2003). Physiological features of aging persons. *Archives of Surgery*, 138(10), 1068–1076. <https://doi.org/10.1001/archsurg.138.10.1068>.
- Anne, T., & Shimada, C. (2000). Social interaction and mortality in a five year longitudinal study of the elderly. *Japanese Journal of Public Health*, 47(2), 127–133.
- Baker, T. A., & Whitfield, K. E. (2006). Physical functioning in older blacks: An exploratory study identifying psychosocial and clinical predictors. *Journal of the National Medical Association*, 98(7), 1114–1120.
- Berkman, L. F., Glass, T., Brissette, I., & Seeman, T. E. (2000). From social integration to health: Durkheim in the new millennium. *Social Science and Medicine*, 51(6), 843–857. [https://doi.org/10.1016/S0277-9536\(00\)00065-4](https://doi.org/10.1016/S0277-9536(00)00065-4).
- Broadhead, W. E., Kaplan, B. H., James, S. A., Wagner, E. H., Schoenbach, V. J., Grimson, R., & Gehlbach, S. H. (1983). The epidemiologic evidence for a relationship between social support and health. *American Journal of Epidemiology*, 117(5), 521–537. <https://doi.org/10.1093/oxfordjournals.aje.a113575>.
- Cantarero-Prieto, D., Pascual-Saez, M., & Blazquez-Fernandez, C. (2018). Social isolation and multiple chronic diseases after age 50: A European macro-regional analysis. *PLOS ONE*, 13(10), e0205062. <https://doi.org/10.1371/journal.pone.0205062>.
- DiMatteo, M. R., & MR. (2004). Social Support and Patient Adherence to Medical Treatment: A Meta-Analysis. *Health Psychology*, 23(2), 207–218. <https://doi.org/10.1037/0278-6133.23.2.207>.
- Cohen, S., & Wills, T. A. (1985). Stress, social support, and the buffering hypothesis. *Psychological Bulletin*, 98(2), 310–357. <https://doi.org/10.1037/0033-2909.98.2.310>.
- Findlay, R. A. (2003). Interventions to reduce social isolation amongst older people: Where is the evidence? *Ageing and Society*, 23(5), 647–658. <https://doi.org/10.1017/s0144686x03001296>.
- Formiga, F., Pujol, R., Perez-Castejon, J. M., Ferrer, A., Henriquez, E., & De Llobregat, S. F. (2005). Low comorbidity and male sex in nonagenarian community-dwelling people are associated with better functional and cognitive abilities: The NonaSantefeliu study. *Journal of the American Geriatrics Society*, 53(10), 1836–1837. <https://doi.org/10.1111/j.1532-5415.2005.53528.4.x>.
- Fortin, M., Bravo, G., Hudon, C., Vanasse, A., & Lapointe, L. (2005). Prevalence of multimorbidity among adults seen in family practice. *Annals of Family Medicine*, 3(3), 223–228. <https://doi.org/10.1370/afm.272>.
- Ishizaki, T., Kobayashi, E., Fukaya, T., Takahashi, Y., Shinkai, S., & Liang, J. (2019). Association of physical performance and self-rated health with multimorbidity among older adults: Results from a nationwide survey in Japan. *Archives of Gerontology and Geriatrics*, 84, Article 103904. <https://doi.org/10.1016/j.archger.2019.103904>.
- Kuzuya, M. (2019). Era of geriatric medical challenges: Multimorbidity among older patients. *Geriatrics and Gerontology International*, 19(8), 699–704. <https://doi.org/10.1111/ggi.13742>.
- Liu, Z. Y., Wei, Y. Z., Wei, L. Q., Jiang, X. Y., Wang, X. F., Shi, Y., & Hai, H. (2018). Frailty transitions and types of death in Chinese older adults: A population-based cohort study. *Clinical Interventions in Aging*, 13, 947–956. <https://doi.org/10.2147/cia.s157089>.
- Mazzella, F., Cacciatore, F., Galizia, G., Della-Morte, D., Rossetti, M., Abbruzzese, R., & Abete, P. (2010). Social support and long-term mortality in the elderly: role of comorbidity. *Archives of Gerontology and Geriatrics*, 51(3), 323–328. <https://doi.org/10.1016/j.archger.2010.01.011>.
- Matsuda, S., Muramatsu, K., & Hayashida, K. (2011). Eligibility classification logic of the Japanese long term care insurance. *Asian Pacific Journal of Disease Management*, 5(3), 65–74. <https://doi.org/10.7223/apjdm.5.65>.
- Mitsutake, S., Ishizaki, T., Teramoto, C., Shimizu, S., & Ito, H. (2019). Patterns of co-occurrence of chronic disease among older adults in Tokyo, Japan. *Preventing Chronic Disease*, 16, Article 180170. <https://doi.org/10.5888/pcd16.180170>.
- Mujica-Mota, R. E., Roberts, M., Abel, G., Elliott, M., Lyratzopoulos, G., Roland, M., & Campbell, J. (2015). Common patterns of morbidity and multi-morbidity and their impact on health-related quality of life: Evidence from a national survey. *Quality of Life Research*, 24(4), 909–918. <https://doi.org/10.1007/s11136-014-0820-7>.
- Olaya, B., Domenech-Abella, J., Moneta, M. V., Lara, E., Caballero, F. F., Rico-Uribe, L. A., & Haro, J. M. (2017). All-cause mortality and multimorbidity in older adults: The role of social support and loneliness. *Experimental Gerontology*, 99, 120–126. <https://doi.org/10.1016/j.exger.2017.10.001>.
- Parker, L., Moran, G. M., Roberts, L. M., Calvert, M., & McCahon, D. (2014). The burden of common chronic disease on health-related quality of life in an elderly community-dwelling population in the UK. *Family Practice*, 31(5), 557–563. <https://doi.org/10.1093/fampra/cmu035>.
- Quinones, A. R., Markwardt, S., & Botoseneanu, A. (2016). Multimorbidity combinations and disability in older adults. *The Journals of Gerontology: Series A*, 71(6), 823–830. <https://doi.org/10.1093/gerona/glw035>.
- Ryan, A., Wallace, E., O'Hara, P., & Smith, S. M. (2015). Multimorbidity and functional decline in community-dwelling adults: A systematic review. *Health and Quality of Life Outcomes*, 13, 168. <https://doi.org/10.1186/s12955-015-0355-9>.
- Santoni, G., Marengoni, A., Calderón-Larrañaga, A., Angleman, S., Rizzuto, D., Welmer, A. K., & Fratiglioni, L. (2017). Defining health trajectories in older adults

- with five clinical indicators. *The Journals of Gerontology. Series A*, 72(8), 1123–1129. <https://doi.org/10.1093/gerona/glw2>.
- Shinkai, S., Kumagai, S., Fujiwara, Y., Amano, H., Yoshida, Y., Watanabe, S., & Shibata, H. (2003). Predictors for the onset of functional decline among initially non-disabled older people living in a community during a 6-year follow-up. *Geriatrics and Gerontology International*, 3(1), 31–39. <https://doi.org/10.1111/j.1444-0594.2003.00094.x>.
- Singer, L., Green, M., Rowe, F., Ben-Shlomo, Y., & Morrissey, K. (2019). Social determinants of multimorbidity and multiple functional limitations among the ageing population of England, 2002–2015. *SSM Population Health*, 8, Article 100413. <https://doi.org/10.1016/j.ssmph.2019.100413>.
- Storeng, S. H., Vinjerui, K. H., Sund, E. R., & Krokstad, S. (2020). Associations between complex multimorbidity, activities of daily living and mortality among older Norwegians. A prospective cohort study: The HUNT Study, Norway. *BMC Geriatrics*, 20(1), 21. <https://doi.org/10.1186/s12877-020-1425-3>.
- Takahashi, S., Ojima, T., Kondo, K., Shimizu, S., Fukuhara, S., & Yamamoto, Y. (2019). Social participation and the combination of future needs for long-term care and mortality among older Japanese people: A prospective cohort study from the Aichi Gerontological Evaluation Study (AGES). *BMJ Open*, 9(11), e030500. <https://doi.org/10.1136/bmjopen-2019-030500>.
- Turvey, C. L., Schultz, S. K., Beglinger, L., & Klein, D. M. (2009). A longitudinal community-based study of chronic illness, cognitive and physical function, and depression. *The American Journal of Geriatric Psychiatry*, 17(8), 632–641. <https://doi.org/10.1097/JGP.0b013e31819c498c>.
- Wensing, M., Vingerhoets, E., & Grol, R. (2001). Functional status, health problems, age and comorbidity in primary care patients. *Quality of Life Research*, 10(2), 141–148. <https://doi.org/10.1023/a:1016705615207>.
- WHO. (2018). *What is healthy ageing?*. Retrieved from <https://www.who.int/ageing/healthy-ageing/en/>.
- Zaninotto, P., Batty, G. D., Allerhand, M., & Deary, I. J. (2018). Cognitive function trajectories and their determinants in older people: 8 years of follow-up in the English Longitudinal Study of Ageing. *Journal of Epidemiology and Community Health*, 72, 685–694. <https://doi.org/10.1136/jech-2017-210116>.

日中笹川医学奨学金制度(学位取得コース)中間評価書

課程博士：指導教官用



第42期

研究者番号： G4203

作成日： 2021年3月11日

氏名	張 碧航	Zhang Bihang	性別	F	生年月日	1994. 03. 19
所属機関(役職)	中南大学湘雅医院整形重建外科(大学院生)					
研究先(指導教官)	自治医科大学外科学講座(吉村 浩太郎教授)					
研究テーマ	幹細胞培養上清成分を用いた再生医療の開発 The Role of Adipose-derived Stem/Stromal Cell Concentrated Conditioned Medium (ASC-CCM) in Regenerative Medicine					
専攻種別	<input type="checkbox"/> 論文博士			<input checked="" type="checkbox"/> 課程博士		

研究者評価(指導教官記入欄)

成績状況	<input checked="" type="radio"/> 良 可 不可 学業成績係数=	取得単位数
		取得単位数 12 / 取得すべき単位数 12
学生本人が行った研究の概要	来日以降は、一連の研究手技(細胞単離、細胞培養、組織染色など)の習得に努めるとともに、 培養上清の分析や実験動物モデルの作成を行った。	
総合評価	【良かった点】 まじめに勤勉に研究と学習に取り組んでいる。 関連分野の文献検索と解析を行い、投稿するレビュー論文を完成させた。	
	【改善すべき点】 日本語の習得。人間関係作り。	
	【今後の展望】 才能があり、研究成果が期待できる。	
学位取得見込	2024年3月取得見込み。	

評価者(指導教官名)

吉村浩太郎



日中笹川医学奨学金制度(学位取得コース)中間報告書 研究者用



第42期

研究者番号: G4203

作成日: 2021年2月19日

氏名	Zhang Bihang	張 碧航	性別	F	生年月日 1994. 03. 19
所属機関(役職)	中南大学湘雅医院整形重建外科(大学院生)				
研究先(指導教官)	自治医科大学外科学講座(吉村 浩太郎教授)				
研究テーマ	幹細胞培養上清成分を用いた再生医療の開発 The Role of Adipose-derived Stem/Stromal Cell Concentrated Conditioned Medium (ASC-CCM) in Regenerative Medicine				
専攻種別	論文博士	<input type="checkbox"/>	課程博士	<input checked="" type="checkbox"/>	

1. 研究概要(1)

1) 目的(Goal)

1. To investigate an optimum and effective ASCs' culture medium without serum in lower cost. It is expected that the usage of culture medium without xenogeneic serum, which is widely used in ASCs culture, would be more biosafe for clinical use. However, the commercial medium without xenogeneic serum nowadays is sold at a high price, which would cost a lot if the mass production of CM is applied. Thus, an optimum and effective ASCs' culture medium without serum in lower cost is needed.

2. To explore a novel method to purify and concentrate the culture supernatant of ASCs. It is known from our previous experiment that there is not only beneficial bioactive factors such as growth factors in the CM, but also a large amount of metabolic waste from stem cells accumulated in the supernatant which do harm to cells and tissues. Therefore, in order to apply a safer and more effective regenerative medicine therapy, it is necessary to remove these harmful substances before its administration. And till now, as far as I concerned, there is no example of any attempt to purify and concentrate CM before the treatment, and it is a completely new plan.

3. To investigate the effect of purified CCM in vitro and its effects on different chronic wound healing animal models in vivo, and compare its effect with unpurified CM and basic culture medium.

4. To characterize the exact contents and concentrations of the effective factors in culture medium supernatant and in CCM, and try to explain their underlying mechanism in wound healing and tissue regeneration.

5. To make the purified CCM into convenient ready-to-use biological products.

6. The amount of culture supernatant that is discarded daily around the world is enormous. What if the discarded media can be reused and applied into regenerative medicine, the benefits will be numerous. Besides, it can be applied into allograft for no cell substances. Since the production and storage are simple with no need to maintain cell viability, it can be conveniently made into potential ready-to-use biological products and be administrated directly when emergency needs arise. Thus, this is an epoch-making research plan from the viewpoint of ecology and reusing waste.

2) 戦略(Approach)

1. To investigate an optimum and effective ASCs' culture medium without serum in lower cost. The basic culture media of DMEM/F12 of ASCs are supplemented with different effective factors, such as IGF, bFGF and PDGF. And the function of supplemented medium is compared with commercial culture medium by the proliferation assay of ASCs, ELISA of growth factors, and so on.

2. To explore a novel method to purify and concentrate the culture supernatant of ASCs. The novel method of purification and concentration has been explored (sorry there is no details to be disclosed about this new method before it is publicly published). And its effectiveness is evaluated by measuring the concentrations of ammonia and effective growth factors in the CCM.

3. To evaluate the effects of purified CCM in vitro.

The in vitro effects of purified and concentrated CM on wound healing are investigated by the proliferation assay and the migration assay (the scratch assay) of fibroblasts and keratinocytes.

4. To investigate the effects of purified CCM on different chronic wound healing animal models in vivo.

5. To make the purified CCM into convenient ready-to-use biological products.

3) 材料と方法(Materials and methods)

1. The proliferation assay of ASCs:

ASCs are plated on 96-well plates and are cultured in DMEM/F12 with 10% FBS for 24 h. Then the culturing medium is changed to the medium which needs to be investigated, such as the DMEM/F12 supplemented with different effective factors and the commercial medium. The ASCs are cultured for 72 h. Then the proliferation is measured using a CCK-8 kit. Briefly, ASCs are changed to a complex

1. 研究概要(2)

solution of 100 μ L DMEM/F12 with 10% FBS and 10 μ L CCK-8 solution, and incubated for 1.5 h. Then the absorbance is measured at 450 nm using a microplate reader. The OD values of each well are calculated to represent the proliferation of ASCs. All the experiments need to be performed in triplicate.

2. The ELISA testing:

The supernatant of ASCs culturing and the purified CCM of ASCs from this novel method is collected. The concentrations of several growth factors and cytokines are measured using sandwich ELISA kits, such as the vascular endothelial growth factor (VEGF), basic fibroblast growth factor (bFGF), transforming growth factor (TGF)- β 1 and β 2, hepatocyte growth factor (HGF) and platelet-derived growth factor (PDGF), according to the manufacturer's instructions.

3. The evaluation of ammonia's concentrations:

The concentrations of ammonia in unpurified CM and purified CCM are measured by the machine of FujiFILM DRI-CHEN NX10N.

4. The proliferation assay of fibroblasts and keratinocytes:

The fibroblasts and keratinocytes are seeded in 96-well plates respectively and cultured with correspondingly appropriate culture medium. After overnight attachment, the cells are incubated in the medium containing the purified CCM for 72 hours. The cell number is measured by the CCK-8 assay kit. Absorbance is measured at 450nm using a microplate reader. The OD values of each well are measured to represent the proliferation of fibroblasts and keratinocytes. All the experiments need to be performed in triplicate.

5. The migration assay of fibroblasts and keratinocytes:

For the measurement of cell migration, confluent fibroblasts and keratinocytes are wounded with a plastic micropipette tip with a large orifice. After washing, the medium is replaced with the medium containing the purified CCM. Photographs of the wounded area are taken every 24 hours by phase-contrast microscopy. For evaluation of the wound closure, four randomly selected points along each wound are marked, and the horizontal distance of migrating cells from the initial wound is measured.

6. In vivo wound healing models:

Different diseased animal models, such as the heat injury, irradiated mice and diabetic mice, are created or purchased accordingly, wounded with cutaneous defects and treated with purified CCM to investigate its promoted effects in wound healing, tissue regeneration and angiogenesis.

After anesthesia, one circular full-thickness wound of 6 mm diameter is created on the back of each mouse. A silicone ring (9 mm diameter) is then placed around the perimeter of the wound and fixed with 6-0 sutures to prevent wound contraction. The purified CCM of ASCs, unpurified CM, ASCs, basic culture medium are locally injected repeatedly to the wounds according to the randomly divided groups:

7 groups: (n = 6, N = 42 in total)

1. wounds treated with DMEM/F12
2. wounds treated with DMEM/F12 with 10% FBS
3. wounds treated with ASCs in DMEM/F12
4. wounds treated with unpurified and unconcentrated ASC-CM
5. wounds treated with purified ASC-CCM
6. wounds treated with purified ASC-CCM and ASCs
7. Healthy control (non-diseased mice): wounds treated with DMEM/F12

These media are repeated every 3 days till the wounds are healed. Animal behavior, weight and spirit are monitored during the experiment. Wounds are evaluated at 0, 3, 7, 14, 21, 28 days after wounding. Digital pictures are taken to visualize the wounds. Wound healing is quantitatively measured and calculated by the remaining wound area.

7. Histological examinations:

28 days after wounding, these mice are sacrificed and the skin around the wounds are harvested. Skin samples are fixed in 4% formalin, embedded in paraffin, and sectioned. The sections are subjected to Hematoxylin and Eosin (H&E) and Masson Trichrome staining for the analysis of the epithelialization, collagenization, and angiogenesis of wounds. And the immunostaining is also needed to explore the underlying possible mechanism.

8. The purified CCM can be made into the convenient ready-to-use biological products of freeze-dried powders by the freeze-drier machine.

4) 実験結果 (Results)

5) 考察 (Discussion)

Sorry for that the parts of results and discussion are unable to be wrote because I have just arrived Japan for several months for the outbreak of coronavirus.

2. 執筆論文 Publication of thesis ※記載した論文を添付してください。Attach all of the papers listed below.

論文名 1 Title	None					
掲載誌名 Published journal						
	年	月	巻(号)	頁 ~	頁	言語 Language
第1著者名 First author			第2著者名 Second author			第3著者名 Third author
その他著者名 Other authors						
論文名 2 Title						
掲載誌名 Published journal						
	年	月	巻(号)	頁 ~	頁	言語 Language
第1著者名 First author			第2著者名 Second author			第3著者名 Third author
その他著者名 Other authors						
論文名 3 Title						
掲載誌名 Published journal						
	年	月	巻(号)	頁 ~	頁	言語 Language
第1著者名 First author			第2著者名 Second author			第3著者名 Third author
その他著者名 Other authors						
論文名 4 Title						
掲載誌名 Published journal						
	年	月	巻(号)	頁 ~	頁	言語 Language
第1著者名 First author			第2著者名 Second author			第3著者名 Third author
その他著者名 Other authors						
論文名 5 Title						
掲載誌名 Published journal						
	年	月	巻(号)	頁 ~	頁	言語 Language
第1著者名 First author			第2著者名 Second author			第3著者名 Third author
その他著者名 Other authors						

3. 学会発表 Conference presentation ※筆頭演者として総会・国際学会を含む主な学会で発表したものを記載してください。

※Describe your presentation as the principal presenter in major academic meetings including general meetings or international meeting

学会名 Conference	None			
演題 Topic				
開催日 date	年	月	日	開催地 venue
形式 method	<input type="checkbox"/> 口頭発表 Oral	<input type="checkbox"/> ポスター発表 Poster	言語 Language	<input type="checkbox"/> 日本語 <input type="checkbox"/> 英語 <input type="checkbox"/> 中国語
共同演者名 Co-presenter				
学会名 Conference				
演題 Topic				
開催日 date	年	月	日	開催地 venue
形式 method	<input type="checkbox"/> 口頭発表 Oral	<input type="checkbox"/> ポスター発表 Poster	言語 Language	<input type="checkbox"/> 日本語 <input type="checkbox"/> 英語 <input type="checkbox"/> 中国語
共同演者名 Co-presenter				
学会名 Conference				
演題 Topic				
開催日 date	年	月	日	開催地 venue
形式 method	<input type="checkbox"/> 口頭発表 Oral	<input type="checkbox"/> ポスター発表 Poster	言語 Language	<input type="checkbox"/> 日本語 <input type="checkbox"/> 英語 <input type="checkbox"/> 中国語
共同演者名 Co-presenter				
学会名 Conference				
演題 Topic				
開催日 date	年	月	日	開催地 venue
形式 method	<input type="checkbox"/> 口頭発表 Oral	<input type="checkbox"/> ポスター発表 Poster	言語 Language	<input type="checkbox"/> 日本語 <input type="checkbox"/> 英語 <input type="checkbox"/> 中国語
共同演者名 Co-presenter				

4. 受賞(研究業績) Award (Research achievement)

名称 Award name	None			
	国名 Country		受賞年 Year of award	年 月
名称 Award name				
	国名 Country		受賞年 Year of award	年 月

5. 本研究テーマに関わる他の研究助成金受給 Other research grants concerned with your research theme

受給実績 Receipt record	<input type="checkbox"/> 有 <input checked="" type="checkbox"/> 無
助成機関名称 Funding agency	
助成金名称 Grant name	
受給期間 Supported period	年 月 ~ 年 月
受給額 Amount received	円
受給実績 Receipt record	<input type="checkbox"/> 有 <input type="checkbox"/> 無
助成機関名称 Funding agency	
助成金名称 Grant name	
受給期間 Supported period	年 月 ~ 年 月
受給額 Amount received	円

6. 他の奨学金受給 Another awarded scholarship

受給実績 Receipt record	<input type="checkbox"/> 有 <input checked="" type="checkbox"/> 無
助成機関名称 Funding agency	
奨学金名称 Scholarship name	
受給期間 Supported period	年 月 ~ 年 月
受給額 Amount received	円

7. 研究活動に関する報道発表 Press release concerned with your research activities

※記載した記事を添付してください。Attach a copy of the article described below

報道発表 Press release	<input type="checkbox"/> 有 <input checked="" type="checkbox"/> 無	発表年月日 Date of release	
発表機関 Released medium			
発表形式 Release method	・新聞 ・雑誌 ・Web site ・記者発表 ・その他()		
発表タイトル Released title			

8. 本研究テーマに関する特許出願予定 Patent application concerned with your research theme

出願予定 Scheduled	<input type="checkbox"/> 有 <input checked="" type="checkbox"/> 無	出願国 Application	
出願内容(概要) Application contents			

9. その他 Others

None

指導責任者(署名) 吉村浩太郎



日中笹川医学奨学金制度(学位取得コース)中間評価書

課程博士：指導教官用



第 42 期

研究者番号： G4205

作成日： 2021 年 3 月 2 日

氏名	劉 霄	Liu Xiao	性別	F	生年月日	1989. 10. 09
所属機関(役職)	慶應義塾大学医学部眼科(大学院生)					
研究先(指導教官)	慶應義塾大学医学部・医学研究科眼科学教室(坪田 一男教授)					
研究テーマ	東アジア人における ABCA4 関連網膜症の臨床的・分子遺伝学的調査 Clinical and genetic Investigation of ABCA4-associated Retinal Disorder in East Asian population					
専攻種別	論文博士			<input checked="" type="checkbox"/> 課程博士		

研究者評価(指導教官記入欄)

成績状況	<input checked="" type="radio"/> 優 <input type="radio"/> 良 <input type="radio"/> 可 <input type="radio"/> 不可 学業成績係数=優	取得単位数
学生本人が行った研究の概要	東アジア人における ABCA4 関連網膜症の臨床的・分子遺伝学的調査研究において、データベースより中国人・日本人コホートを構築し、視力、視野、網膜画像、電気生理学的検査を含む臨床情報の解析ならびに、同定された ABCA4 バリエントに対する分子遺伝学的解析を行った。さらに、臨床情報と遺伝情報についての関連解析、他民族との比較検討解析を行い、ABCA4 バリエントの世界的な分布を解明した。	
総合評価	【良かった点】 眼科臨床情報、遺伝情報の解析について、主体的に取り組み、他施設の眼科臨床医、遺伝学者、遺伝情報学者と密に連携をとりながら、研究業務を進めました。第一著者として5報の論文を国際雑誌に執筆しており、インパクトのある研究を形として発信できています。	
	【改善すべき点】 中国人・日本人のデータを中心とした解析となっており、韓国人やその他の東アジア人データの集積を行う事で、東アジア内での疾患分布を同定する事が治療導入につながると考えます。	
	【今後の展望】 中国人・日本人コホートに加え、韓国人コホートの調査を行う事で、東アジア人全体での疾患理解を進め、地球規模での病態解明・治療導入の実現が望まれます。	
学位取得見込	2022年3月 学位取得見込	
評価者(指導教官名)  		

日中笹川医学奨学金制度(学位取得コース)中間報告書 研究者用



第42期

研究者番号: G4205

作成日: 2021年02月04日

氏名	Liu Xiao	劉 霄	性別	F	生年月日	1989. 10. 09
所属機関(役職)	慶應義塾大学医学部眼科(大学院生)					
研究先(指導教官)	慶應義塾大学医学部・医学研究科眼科学教室(坪田 一男教授)					
研究テーマ	東アジア人におけるABCA4関連網膜症の臨床的・分子遺伝学的調査 Clinical and genetic Investigation of <i>ABCA4</i> -associated Retinal Disorder in East Asian population					
専攻種別	論文博士	<input type="checkbox"/>	課程博士	<input checked="" type="checkbox"/>		
<p>1. 研究概要(1)</p> <p>1) 目的(Goal)</p> <p>Inherited Retinal Disease (IRD) have become one of the leading causes of blindness in advanced countries and the <i>ABCA4</i>-retinopathy (<i>ABCA4</i>-RD) is thought to be the most common inherited macular dystrophy while the available effective treatments are limited(1-4). The purpose of this study is to intensively investigate the clinical and genetic features in East Asian patients with <i>ABCA4</i>-RD.</p> <p>2) 戦略(Approach)</p> <p>a)Collect the clinical and genetic data of the patients with <i>ABCA4</i>-RD from China and Japan. b)Analyse the phenotype and genotype of the patients with <i>ABCA4</i>-RD. c)Investigate an association between the phenotype and genotype. d)Compare the East Asian features to the Europeans to figure out the similarities/differences.</p> <p>3) 材料と方法(Materials and methods)</p> <p>The patients with multiple pathogenic <i>ABCA4</i> variants or with one <i>ABCA4</i> variant and classical phenotype were recruited. Advanced technologies in retinal imaging capabilities, including fundus autofluorescence (FAF) and spectral-domain optical coherence tomography (SD-OCT), as well as psychophysical testing methods such as microperimetry, electrophysiological examination, etc. were applied, offering new possibilities to identify biomarkers for severity/progression.</p> <p>For the genetic data, genetic screening in the <i>ABCA4</i> gene was performed by utilising whole exome sequencing with target analysis, target enrichment-based exome sequencing, and direct sequencing. Molecular genetic analysis was performed for the detected variants with prediction soft wares and public databases.</p> <p>Comparison analysis of prelatent <i>ABCA4</i> variants was performed among ethnicities utilising the resources of thousands of patients from the other continents, to identify the geographical distribution of pathogenic variants.</p> <p>4) 実験結果(Results)</p> <p>Forty-two unrelated patients with <i>ABCA4</i>-RD mostly originating from Western China were recruited. Comprehensive ophthalmological examinations, including visual acuity measurements, fundus photography, FAF imaging, and full-field electroretinography, were performed. Next-generation sequencing (target/whole exome) and direct sequencing were conducted. Genotype grouping was performed based on the presence of deleterious variants. The median age of onset/age was 10.0 (5-52)/29.5 (12-72) years, and the median visual acuity in the right/left eye was 1.30 (0.15-2.28)/1.30 (0.15-2.28) in the logarithm of the minimum angle of resolution unit. Ten patients (10/38, 27.0%) showed confined macular dysfunction, and 27 (27/37, 73.7%) had generalized retinal dysfunction. Fifty-eight pathogenic/likely pathogenic <i>ABCA4</i> variants, including 14 novel variants, were identified. Eight patients (8/35, 22.8%) harbored multiple deleterious variants, and 17 (17/35, 48.6%) had a single deleterious variant. Significant associations were revealed between subjective functional, retinal imaging, and objective functional groups, identifying a significant genotype-phenotype association.</p> <p>Thirty-three affected subjects from 29 Japanese families with <i>ABCA4</i>-RD were recruited. The median age/age of onset was 29.0/9.0 years (range, 7.0-85.0/2.0-70.0). The best corrected median visual acuity in the logarithm of the minimum angle of resolution unit in the right/left eye was 0.7(0.0-2.28)/ 0.76 (-0.18-2.28). There were 23 patients with available fERG; 11 (11/23, 47.8%) in ERG group 1, 4 (4/23, 17.4%) in ERG group 2, and 8(8/23, 34.8%) in ERG group 3. 34 disease causing/associated variants were identified, including 7 novel variants. The three most prevalent variants are c.1760+2T>G (16.7%), c.6445C>T, p.Arg2149Ter (5.0%), and c.869G>A, p.Arg290Gln (5.0%). 24 probands with multiple pathogenic <i>ABCA4</i> variants were identified; 9 (9/24, 37.5%) in Genotype group A, 9 (9/24, 37.5%) in Genotype group B, and 6 (6/24, 25.0%) in Genotype group C. The distribution of Genotype Groups A/B/C of the European dominated and Chinese cohorts was 5.7%/44.4%/49.8% and 22.2%/47.2%/30.6%, which revealed a significant difference of genotype based on each ethnic group (P<0.001).</p>						

1. 研究概要(2)

5) 考察(Discussion)

a) This study is the first to comprehensively reveal the demographic, morphological, and functional features of patients with STGD1 in a large molecularly confirmed cohort, which enabled an elucidation of the genotype–phenotype association in the East Asian population.

b) The median onset in Chinese cohort (10.0 years) and Japanese cohort (9.0 years) was earlier than that in the large prospective international *ABCA4*–RD (STGD1) cohort (21.8 years for the retrospective cohort and 22.3 years for the prospective cohort in the ProgStar studies) or the other reports from Europe(5–8).

c) The three most prevalent variants detected in the two East Asian cohorts were completely different from the three most prevalent variants (c.5882G>A (p.Gly1961Glu); c.2588G>C (p.Gly863Ala); and c.5461–10T>C) in the ProgStar study(9).

d) There are several limitations in this study. First, selection bias at recruitment related to disease severity should be inherent since it is difficult to collect data from genetically affected subjects with good vision who do not visit clinics/hospitals. Second, this cross–sectional retrospective case series study did not include longitudinal data; thus, prospective natural history studies in a larger cohort could provide more accurate information on the disease severity and progression of *ABCA4*–RD. Third, the molecular mechanisms of disease causation for most variants have been unclear, and the clinical effects of variants are not perfectly understood. Further functional analysis is required to conclude the disease causation of each variant. Fourth, due to the limited number of subjects, statistical analysis to investigate correlations between the clinical parameters and the particular variants (or genotype groups) were not available in the current study. Last, the number of our patients was too small to draw conclusions about the genotype–phenotype associations in such a heterogeneous disease.

6) 参考文献(References)

1. Stargardt K. Über familiäre, progressive Degeneration in der Maculagegend des Auges. Graefe's Archive for Clinical and Experimental Ophthalmology. 1909;71(3):534–50.
2. Allikmets R, Singh N, Sun H, Shroyer NF, Hutchinson A, Chidambaram A, Gerrard B, Baird L, Stauffer D, Peiffer A. A photoreceptor cell–specific ATP–binding transporter gene (*ABCR*) is mutated in recessive Stargardt macular dystrophy. Nature genetics. 1997;15(3):236.
3. Tanna P, Strauss RW, Fujinami K, Michaelides M. Stargardt disease: clinical features, molecular genetics, animal models and therapeutic options. Br J Ophthalmol. 2017;101(1):25–30.
4. Fujinami–Yokokawa Y, Pontikos N, Yang L, Tsunoda K, Yoshitake K, Iwata T, Miyata H, Fujinami K, Japan Eye Genetics Consortium obo. Prediction of Causative Genes in Inherited Retinal Disorders from Spectral–Domain Optical Coherence Tomography Utilizing Deep Learning Techniques. Journal of Ophthalmology. 2019;2019:1691064.
5. Fujinami K, Zernant J, Chana RK, Wright GA, Tsunoda K, Ozawa Y, Tsubota K, Webster AR, Moore AT, Allikmets R. *ABCA4* gene screening by next–generation sequencing in a British cohort. Investigative ophthalmology & visual science. 2013;54(10):6662–74.
6. Zahid S, Jayasundera T, Rhoades W, Branham K, Khan N, Niziol LM, Musch DC, Heckenlively JR. Clinical phenotypes and prognostic full–field electroretinographic findings in Stargardt disease. Am J Ophthalmol. 2013;155(3):465–73 e3.
7. Fujinami K, Singh R, Carroll J, Zernant J, Allikmets R, Michaelides M, Moore AT. Fine central macular dots associated with childhood–onset Stargardt Disease. Acta ophthalmologica. 2014;92(2):e157.
8. Strauss RW, Ho A, Munoz B, Cideciyan AV, Sahel JA, Sunness JS, Birch DG, Bernstein PS, Michaelides M, Traboulsi EI, et al. The Natural History of the Progression of Atrophy Secondary to Stargardt Disease (ProgStar) Studies: Design and Baseline Characteristics: ProgStar Report No. 1. Ophthalmology. 2016;123(4):817–28.
9. Fujinami K, Strauss RW, Chiang JP, Audo IS, Bernstein PS, Birch DG, Bomotti SM, Cideciyan AV, Ervin AM, Marino MJ, et al. Detailed genetic characteristics of an international large cohort of patients with Stargardt disease: ProgStar study report 8. Br J Ophthalmol. 2019;103(3):390–7.

2. 執筆論文 Publication of thesis ※記載した論文を添付してください。Attach all of the papers listed below.

論文名 1 Title	Oguchi disease caused by a homozygous novel <i>SAG</i> splicing alteration associated with the multiple evanescent white dot syndrome: A 15-month follow-up					
掲載誌名 Published journal	Documenta Ophthalmologica					
	2020 年 4 月	141(3) 巻(号)	217 頁 ~ 226 頁	言語 Language	English	
第1著者名 First author	Xiao Liu,Lixia Gao	第2著者名 Second author	Gang Wang	第3著者名 Third author	Yanling Long	
その他著者名 Other authors	Jiayun Ren, Kaoru Fujinami, Xiaohong Meng, Shiyong Li					
論文名 2 Title	Clinical and Genetic Characteristics of 15 Affected Patients From 12 Japanese Families with <i>GUCY2D</i> -Associated Retinal Disorder					
掲載誌名 Published journal	Translational Vision Science & Technology					
	2020 年 5 月	9(6) 巻(号)	2:01 頁 ~ 2:19 頁	言語 Language	English	
第1著者名 First author	Xiao Liu, Kaoru Fujinami	第2著者名 Second author	Kazuki Kuniyoshi	第3著者名 Third author	Mineo Kondo	
その他著者名 Other authors	Shinji Ueno, Takaaki Hayashi, Kiyofumi Mochizuki, Shuhei Kameya, Lizhu Yang, Yu Fujinami-Yokokawa, Gavin Arno, Nikolas Pontikos,Hiroyuki Sakuramoto, Taro Kominami, Hiroko Terasaki, Satoshi Katagiri,Kei Mizobuchi, Natsuko Nakamura, Kazutoshi Yoshitake, Yoza Miyake1, Shiyong Li, Toshihide Kurihara, Kazuo Tsubota,Takeshi Iwata,Kazushige Tsunoda,Japan Eye Genetics Consortium Study Group					
論文名 3 Title	Clinical and genetic characteristics of Stargardt disease in a large Western China cohort: Report 1					
掲載誌名 Published journal	American Journal of Medical Genetics Part C Seminars in Medical Genetics					
	2020 年 8 月	184(3) 巻(号)	694 頁 ~ 707 頁	言語 Language	English	
第1著者名 First author	Xiao Liu	第2著者名 Second author	Xiaohong Meng	第3著者名 Third author	Lizhu Yang	
その他著者名 Other authors	Yanling Long,Yu Fujinami-Yokokawa,Jiayun Ren,Toshihide Kurihara,Kazuo Tsubota, Kazushige Tsunoda,Kaoru Fujinami,Shiyong Li					
論文名 4 Title	RP2-associated retinal disorder in a Japanese cohort: report of novel variants and a literature review, identifying a genotype-phenotype association					
掲載誌名 Published journal	American Journal of Medical Genetics Part C Seminars in Medical Genetics					
	2020 年 8 月	184(3) 巻(号)	675 頁 ~ 693 頁	言語 Language	English	
第1著者名 First author	Kaoru Fujinami,Xiao Liu	第2著者名 Second author	Shinji Ueno	第3著者名 Third author	Atsushi Mizota	
その他著者名 Other authors	Kei Shinoda, Kazuki Kuniyoshi, Yu Fujinami-Yokokawa, Lizhu Yang, Gavin Arno, Nikolas Pontikos Shuhei Kameya, Taro Kominami, Hiroko Terasaki, Hiroyuki Sakuramoto, Natsuko Nakamura, Toshihide Kurihara, Kazuo Tsubota, Yoza Miyake, Kazutoshi Yoshiake, Takeshi Iwata, Kazushige Tsunoda,Japan Eye Genetics Consortium Study Group					
論文名 5 Title	Long-term follow-up of a Chinese patient with <i>KCNV2</i> -retinopathy					
掲載誌名 Published journal	OPHTHALMIC GENETICS					
	2020 年 12 月	10(1080) 巻(号)	1 頁 ~ 6 頁	言語 Language	English	
第1著者名 First author	Hongxuan Lie,Gang Wang, Xiao Liu	第2著者名 Second author	Xiaohong Meng	第3著者名 Third author	Yanling Long	
その他著者名 Other authors	Yanling Long,Jiayun Ren,Lizhu Yang,Yu Fujinami-Yokokawa,Toshihide Kurihara,Kazuo Tsubota, Kaoru Fujinami,Shiyong Li					

3. 学会発表 Conference presentation ※筆頭演者として総会・国際学会を含む主な学会で発表したものを記載してください。

※Describe your presentation as the principal presenter in major academic meetings including general meetings or international meetings

学会名 Conference	The 58th Annual Symposium of the International Society for Clinical Electrophysiology of Vision (ISCEV)		
演題 Topic	Oguchi disease Licaused by a homozygous novel <i>SAG</i> splicing alteration associated with the multiple evanescent white dot syndrome: A 15-month follow-up		
開催日 date	2020 年 9 月 14 日	開催地 venue	Virtual. Les Iles-de-la-Madeleine, Québec, Canada
形式 method	<input type="checkbox"/> 口頭発表 Oral <input checked="" type="checkbox"/> ポスター発表 Poster	言語 Language	<input type="checkbox"/> 日本語 <input checked="" type="checkbox"/> 英語 <input type="checkbox"/> 中国語
共同演者名 Co-presenter	Lixia, Gao, Jiayun Ren, Xiaohong Meng, Yu Fujinami-Yokokawa, Lizhu Yang, Kaoru Fujinami, Shiyong Li		
学会名 Conference	第68回日本臨床視覚電気生理学学会		
演題 Topic	Electrophysiological characteristics of Stargardt disease in a large Western China cohort		
開催日 date	2020 年 9 月 20 日	開催地 venue	Virtual, Tokyo, Japan
形式 method	<input checked="" type="checkbox"/> 口頭発表 Oral <input type="checkbox"/> ポスター発表 Poster	言語 Language	<input type="checkbox"/> 日本語 <input checked="" type="checkbox"/> 英語 <input type="checkbox"/> 中国語
共同演者名 Co-presenter	Xiaohong Meng, Lizhu Yang, Yanling Long, Yu Fujinami-Yokokawa, Jiayun Ren, Toshihide Kurihara, Kazuo Tsubota, Kazushige Tsunoda, Kaoru Fujinami, Shiyong Li		
学会名 Conference	The 2nd Symposium of East Asia Inherited Retinal Disease Society (EAIRDs)		
演題 Topic	Clinical and genetic characteristics of Stargardt disease in a large Western China cohort: report 1		
開催日 date	2020 年 11 月 14 日	開催地 venue	Virtual, Tokyo, Japan
形式 method	<input checked="" type="checkbox"/> 口頭発表 Oral <input type="checkbox"/> ポスター発表 Poster	言語 Language	<input type="checkbox"/> 日本語 <input checked="" type="checkbox"/> 英語 <input type="checkbox"/> 中国語
共同演者名 Co-presenter	Xiaohong Meng, Lizhu Yang, Yanling Long, Yu Fujinami-Yokokawa, Jiayun Ren, Toshihide Kurihara, Kazuo Tsubota, Kazushige Tsunoda, Kaoru Fujinami, Shiyong Li		
学会名 Conference			
演題 Topic			
開催日 date	年 月 日	開催地 venue	
形式 method	<input type="checkbox"/> 口頭発表 Oral <input type="checkbox"/> ポスター発表 Poster	言語 Language	<input type="checkbox"/> 日本語 <input type="checkbox"/> 英語 <input type="checkbox"/> 中国語
共同演者名 Co-presenter			

4. 受賞(研究業績) Award (Research achievement)

名称 Award name	Best Yong Investigator Award (2nd East Asia Inherited Retinal Disease Society symposium)		
	国名 Country	Japan	受賞年 Year of
			2020 年 9 月
名称 Award name	2020 Keio Ophthalmology best graduate student		
	国名 Country	Japan	受賞年 Year of
			2020 年 10 月

5. 本研究テーマに関わる他の研究助成金受給 Other research grants concerned with your research theme

受給実績 Receipt record	<input type="checkbox"/> 有 <input checked="" type="checkbox"/> 無
助成機関名称 Funding agency	
助成金名称 Grant name	
受給期間 Supported period	年 月 ~ 年 月
受給額 Amount received	円
受給実績 Receipt record	<input type="checkbox"/> 有 <input checked="" type="checkbox"/> 無
助成機関名称 Funding agency	
助成金名称 Grant name	
受給期間 Supported period	年 月 ~ 年 月
受給額 Amount received	円

6. 他の奨学金受給 Another awarded scholarship

受給実績 Receipt record	<input checked="" type="checkbox"/> 有 <input type="checkbox"/> 無
助成機関名称 Funding agency	慶應義塾大学
奨学金名称 Scholarship name	慶應義塾大学院医学研究科博士課程奨学金
受給期間 Supported period	2019 年 6 月 ~ 2020 年 6 月
受給額 Amount received	1,000,000 円

7. 研究活動に関する報道発表 Press release concerned with your research activities

※記載した記事を添付してください。Attach a copy of the article described below

報道発表 Press release	<input type="checkbox"/> 有 <input checked="" type="checkbox"/> 無	発表年月日 Date of release	
発表機関 Released medium			
発表形式 Release method	・新聞 ・雑誌 ・Web site ・記者発表 ・その他()		
発表タイトル Released title			

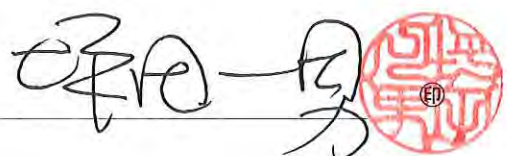
8. 本研究テーマに関する特許出願予定 Patent application concerned with your research theme

出願予定 Scheduled	<input type="checkbox"/> 有 <input checked="" type="checkbox"/> 無	出願国 Application	
出願内容(概要) Application contents			

9. その他 Others

--

指導責任者(署名)





Oguchi disease caused by a homozygous novel *SAG* splicing alteration associated with the multiple evanescent white dot syndrome: A 15-month follow-up

Xiao Liu · Lixia Gao · Gang Wang · Yanling Long · Jiayun Ren ·
Kaoru Fujinami · Xiaohong Meng · Shiyong Li

Received: 8 December 2019 / Accepted: 31 March 2020
© Springer-Verlag GmbH Germany, part of Springer Nature 2020

Abstract

Purpose We report a 15-month follow-up case on a Chinese patient with Oguchi disease associated with the multiple evanescent white dot syndrome (MEWDS).

Methods The patient's clinical presentation and follow-up visits were documented via decimal best-corrected visual acuity, fundus photography, fundus autofluorescence (FAF) imaging, near-infrared FAF, spectral domain optical coherence tomography,

Humphrey's visual fields, microperimetry, and multi-focal electroretinography. We also performed whole exome sequencing for screening variation in the patient and her relatives.

Results The patient had typical clinical characteristic of Oguchi disease, including night blindness, the Mizuo–Nakamura phenomenon (a golden yellow discoloration of the fundus that disappears in the prolonged dark adaptation [DA]) and typical full-field electroretinogram changes (nearly undetected b-wave in 0.01 and 0.03 ERGs that can partially recover only after prolonged DA). Aside from Oguchi disease, the

Co-first authors: Xiao Liu and Lixia Gao

X. Liu · L. Gao · G. Wang · Y. Long · J. Ren ·
X. Meng (✉) · S. Li (✉)
Southwest Hospital/Southwest Eye Hospital, Third
Military Medical University (Army Medical University),
No. 30 Gaotanyan Street Shapingba District, Chongqing,
China
e-mail: cqwmwm@163.com

S. Li
e-mail: shiyong_li@126.com

X. Liu · L. Gao · G. Wang · Y. Long · J. Ren ·
X. Meng · S. Li
Key Lab of Visual Damage and Regeneration &
Restoration of Chongqing, Chongqing, China

X. Liu
Laboratory of Visual Physiology, Division for Vision
Research, National Institute of Sensory Organs, National
Hospital Organization, Tokyo Medical Center, Tokyo,
Japan

X. Liu · K. Fujinami
Department of Ophthalmology, Keio University School of
Medicine, Tokyo, Japan

K. Fujinami
Department of Genetics, UCL Institute of Ophthalmology,
London, UK

K. Fujinami
Division of Inherited Eye Diseases, Moorfields Eye
Hospital, London, UK

patient was also diagnosed with the MEWDS based on clinical detections, including suddenly reduced visual acuity, appeared white dots, blurred ellipsoid zone and disrupted interdigitation zone, enlarged blind spot, and reduced macular sensitivity. A series of investigations revealed that along with the 15-month follow-up after onset, the visual acuity enhanced, the numerous white dots disappeared, and the macular structure returned to normal. Moreover, the novel homozygous splicing alteration c.181 + 1G > A was identified in the *SAG* gene.

Conclusions This work is the first long-term case study of a patient with Oguchi disease associated with the MEWDS. The recovery period of symptoms caused by the MEWDS was much longer than that in typical patients with MEWDS. Molecular genetics demonstrate that this is the first case of Oguchi disease caused by splicing alterations in the *SAG* gene.

Keywords Oguchi disease · MEWDS · Longitudinal follow-up · Electroretinogram · Optical coherence tomography

Introduction

Oguchi disease (MIM # 258100) is a rare autosomal recessive form of congenital stationary night blindness, first described in 1907 [1]. It is characterized by a tapetal-like fundus discoloration after dark adaptation (DA), called the Mizuo–Nakamura phenomenon, along with characteristic electroretinographic (ERG) abnormalities [2, 3]. Two genes, namely *SAG* (s-antigen; OMIM: 181031) and *GRK1* (G protein-coupled receptor kinase 1; OMIM: 180381), have been reported to be associated with Oguchi disease. *SAG* encodes arrestin, which forms a complex with phosphorylated rhodopsin, preventing the further interaction of the activated rhodopsin during transduction. *GRK1* encodes rhodopsin kinase that recognizes photoactivated rhodopsin and desensitizes rhodopsin to receive new light stimuli [4]. The multiple evanescent white dot syndrome (MEWDS) is a unilateral chorioretinitis that affects young women in the third and fourth decades of life; it is characterized with multiple small subretinal white dots, extending from the posterior pole to the midperiphery and associated with a self-healing capacity in a few

weeks or months [5, 6]. In this study, we report a 15-month follow-up case of Oguchi disease caused by novel *SAG* splicing alterations (novel variant) associated with MEWDS.

Methods

Patient recruitment

The patient and her relatives, who were also studied upon, gave informed consent for all procedures described here and the publication of this case study. The procedures used were approved by the local ethics committee of Southwest Eye Hospital, Third Military Medical University (Army Medical University), Chongqing, China (reference number: 73981486-2), and all procedures were performed in accordance with the Declaration of Helsinki.

Clinical investigation

Detailed history and comprehensive ophthalmological examinations were conducted, including decimal best-corrected visual acuity (BCVA), dilated ophthalmoscopy, color fundus photography, spectral domain optical coherence tomography (SD-OCT, Heidelberg and Zeiss), fundus autofluorescence imaging (FAF; excitation: 488 nm, Spectralis HRA + OCT; Heidelberg Engineering, Dossenheim, Germany), near-infrared fundus autofluorescence (NIR-FAF; excitation: 787 nm), Humphrey's visual fields (HVF, 30-2), and microperimetry (MP, MAIA, 4-2). We recorded full-field ERGs (ffERGs, Diagnosys LLC, Lowell, MA) in accordance with the standards of the International Society for Clinical Electrophysiology of Vision (ISCEV) [7]. We also recorded ffERGs after 3, 4, and 12 h DA. Multifocal ERGs (mf-ERGs) were recorded with a VERIS Science 6.3.2 imaging system (EDI, San Mateo, CA) in accordance with the ISCEV standard protocol [8]. We selected mf-ERGs with a stable fixation for further analysis.

Pathogenic variant detection

After obtaining informed consent, we collected blood samples in EDTA tubes from the proband and the unaffected father, mother, and son of the proband. The genomic DNA was subjected to whole exome

sequencing (WES) with an Illumina Genome Analyzer II platform in accordance with the manufacturer's (Illumina's) instructions. It covered 20,794 genes and 201,121 exons in the Consensus Coding Sequence (CCDS) Region database, and approximately 97.0% of CCDS exons or 96.5% of Reference Sequence (RefSeq) exons were captured, all called SNVs and INDELs of the 790 genes registered as retinal disease-causing genes on the RetNet database (<https://sph.uth.edu/retnet/home.htm>) were selected for further analysis in the public domain. The identified variants were filtered with allele frequency (less than 1%) of 1000 Genomes Project Database (1000 genome; <https://www.internationalgenome.org>). WES and annotation were done by Genesky Biotechnologies (Shanghai, China). Polyphen2, SIFT, and MutationTaster were used to predict the pathogenicity of candidate variants. PCR amplification and bidirectional sequencing were performed to confirm the variant.

Case description

Baseline

A 28-year-old female with a complaint of photopsia with periphery visual field loss of the right eye for 10 days was presented. The patient reported no flu-like symptoms, such as fever and headache. She denied allergies to medicine and foods. She declared a history of measles 7 years ago and additionally remarked night blindness since her childhood and did not see a doctor before. Comprehensive antibodies of autoimmune diseases and inflammation revealed negative responses. She reported no family history, and her parents were not consanguineous (Fig. 1). On the first examination, slit-lamp examination showed that the pupil, intraocular pressure, and motility were normal and had no evidence of intraocular inflammation. Her best-corrected LogMAR visual acuity was 0.05 OD and – 0.08 OS with a myopic refractive error of – 5.75 and – 5.00 diopters in her right and left eyes, respectively.

The fundus of both eyes revealed a widespread golden yellow discoloration throughout the posterior pole (Fig. 2a) and showed the normal appearance of the retina after 4 h DA (Fig. 2b). ffERGs were recorded after 30 min, 3 h, 4 h, and 12 h DA. The DA with 30 min was recorded at the first visit time,

and DA with 3 h, 4 h, and 12 h was recorded at the 2-day interval following the first time. The results showed that rod photoreceptor ERG amplitudes were nonrecordable under 30 min, 3 h, and 4 h DA, and the a-wave and b-wave responses partly recovered in the initial single flash after 12 h DA of both eyes. The combined cone-rod ERGs of the right eye were absent after 12 h DA, and her left eye showed a slight recovery. The mixed cone-rod ERGs were severely reduced due to the second combined flash, which is compatible with previous reports [9]. The cone responses were normal at all recordings (Fig. 2c).

FAF images of the right eye showed the presence of several hyperfluorescent dots in the posterior pole, which fuse in a flake-like manner in the area surrounding the optic disc (Fig. 3a). The hypofluorescent areas showed in the NIF were associated with the demarcated dark region without golden yellow reflexes of both eyes in the fundus images (Fig. 3a).

The SD-OCT showed that the hyperreflective bands corresponding to the outer segments were densely packed in the temporal and nasal sides of the left eye and the temporal side of the right eye outside the fovea. This packed structure of the parafovea is thought to be a specific feature in patients with Oguchi disease. The fovea area and nasal side of the right eye showed a blurred ellipsoid zone (EZ) and disrupted outer segments. Hyperreflective materials accumulated over the retinal pigment epithelium (RPE) to the interdigitation zone (IZ) and EZ. The fovea structure of the left eye was perfectly preserved (Fig. 3a).

The HFV demonstrated a blind spot enlargement breaking out to the temporal periphery in the right eye at the first examination (Fig. 4a). The MP examinations demonstrated the abnormality of the macular integrity of the right eye (Fig. 4a). The average of the macular sensitivity dropped to 25.6 dB at the presentation compared with the normal reference (27–36 dB).

The mfERGs revealed lower amplitudes of N1- and P1- in rings 1–2 compared with the normal. Moreover, the right eye showed severer reduction than the left eye and severely attenuated responses along the nasal region of the fovea (Fig. 5a).

Pathogenic variants screening

WES was performed in the patient and three relatives (parents and son). After processing the annotation, a

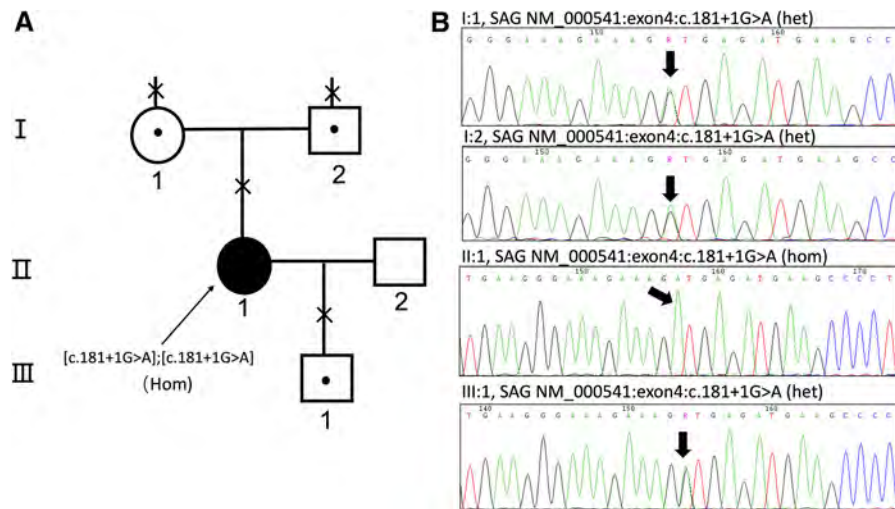


Fig. 1 Family pedigree of the patient. **a** Filled shape with an arrow indicates the affected proband with a homozygous c.181 + 1G > A splicing alteration. (●) indicates a heterozygous state in her parents and her son. (×) indicates the family members who got whole exome sequencing detection.

b Sequence chromatogram of SAG c.181 + 1G > A variant. Sequence trace of part of exon 4 of SAG in proband and relatives carrying the homozygous and heterozygous c.181 + 1G > A pathogenic variant which are indicated by black arrows, respectively

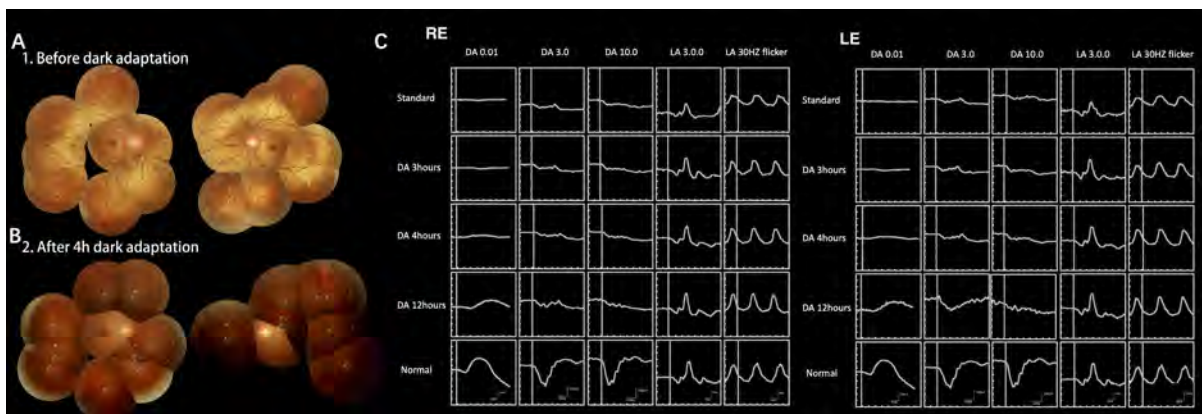


Fig. 2 Fundus photographs and full-field ERG before and after DA of the patient. **a** Fundus images before and after 4 h dark adaptation (DA). The golden discoloration of fundus appearance disappeared after 4 h DA. **b** ffERGs of both eyes after DA at different time points and the normal reference for comparison.

Rod ERGs were undetectable after 30 min, 3 h, and 4 h DA. Rod response had a partial recovery after the DA time prolonged to 12 h. Light-adapted ERGs reveal the normal function of a generalized cone system of both eyes

total 143,052 coding and splice sites variants, including 4114 variants with $MAF \leq 1\%$ in genes unrelated to retinopathies and 16 variants with $MAF \leq 1\%$ in genes related to retinopathies, were identified. The average sequencing coverage of the targeted exons was 86.53%. The coverage of targeted exons for > 10 reads was 96.57% and > 20 reads was 85.19%. A splicing alteration of c.181 + 1G > A was identified in the SAG gene (NM_000541) with a homozygous status in this patient. All other three relatives had a

heterozygous status (Fig. 1). No variants in *GRK1* were found. The splicing alteration of the SAG gene is first reported in this study.

Overall, we diagnosed the patient with Oguchi disease associated with the MEWDS in accordance with her characteristic clinical appearance and genetic molecular test results.

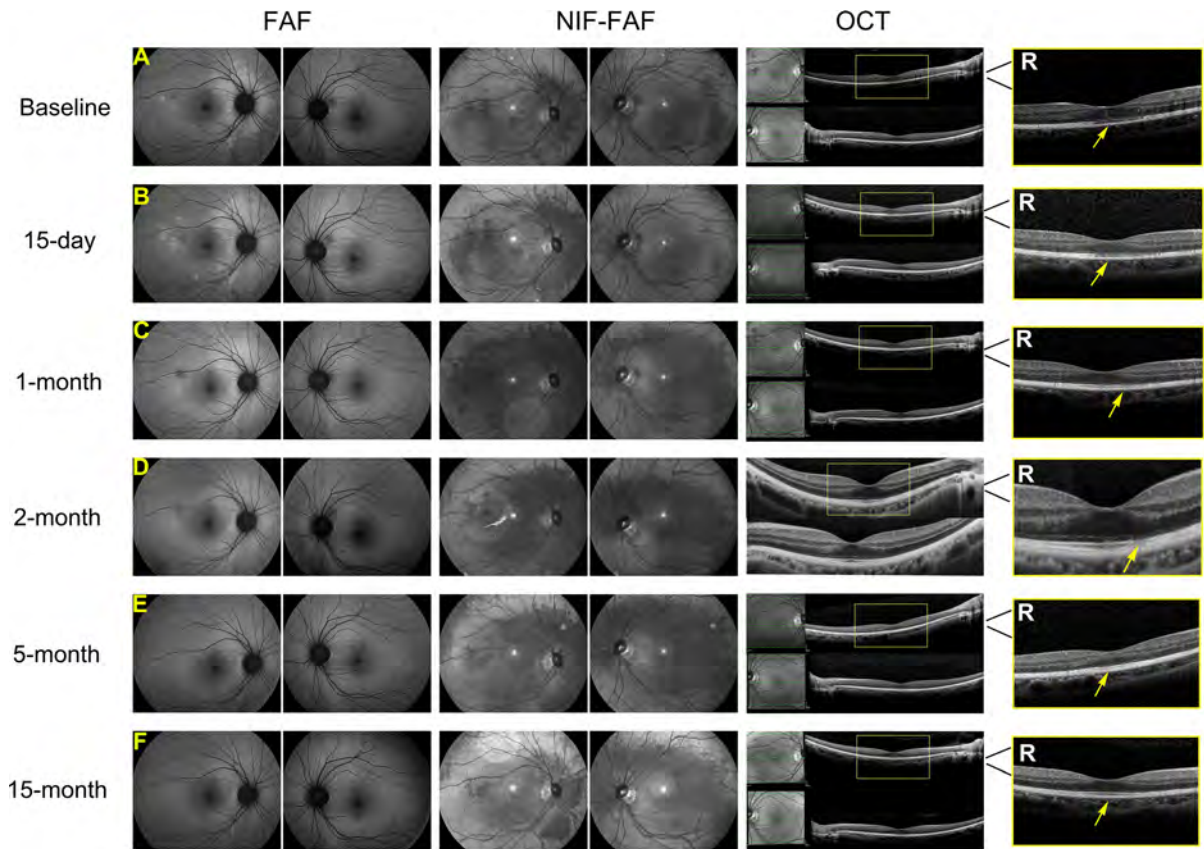


Fig. 3 Serial changes of autofluorescence, near-infrared, and SD-OCT with 15-month follow-up. FAF, NIR, and SD-OCT images of both eyes at baseline (a), 15-day (b), 1-month (c), 2-month (d), 5-month (e), and 15-month (f) follow-up. FAF detected several hyperfluorescent lesions at posterior at the initial presentation of the right eye, which showed consecutive disappearance during follow-up. NIR images showed a

corresponding golden discoloration area with fundus images. SD-OCT demonstrated the recovery of disrupted EZ and IZ at the macula with a maintained RPE over the followings. The fovea of the right eye is framed by a yellow rectangular box and enlarged (right). Atrophic fovea area marked by single-head yellow arrow is given

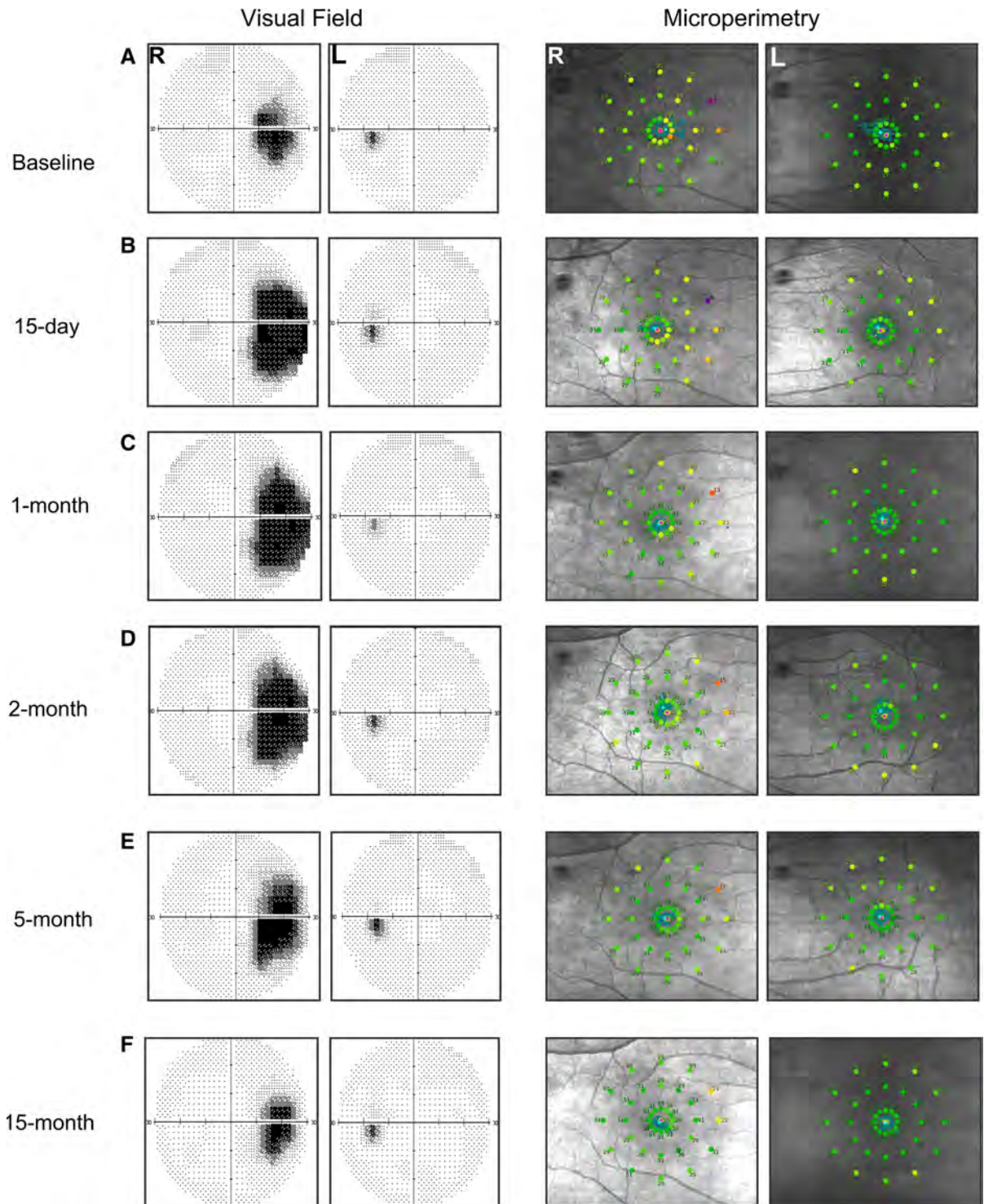
Follow-up

We observed the patient through a 15-month follow-up. The LogMAR BCVA of the right eye dropped to 0.4 in a 1-month time, which lasted until the 5-month follow-up time. The BCVA improved to 0.22 at the 15-month follow-up time, which was still lower than the first time she came to see a doctor.

Numerous hyperfluorescent white dots in the posterior pole were increased to the peak, and the hyperfluorescent area surrounding the optic disc became larger at the 15-day follow-up. Then, all the symptoms gradually reduced starting from the 1-month follow-up, with a 1/4 PD hypofluorescent

area showing at the vessel arcade and kept almost stable until the 2-month follow-up. These phenomena almost disappeared from the 5-month and 15-month follow-up (Fig. 3b–e). Only a tiny hyperfluorescent area was found at the temporal side of the optic disc border at the last examination (Fig. 3f).

The fovea region of the blurred EZ and disrupted IS/OS junction line obviously spreads, and the granularity deposit increased at the 15-day follow-up (Fig. 3b). Over time, these changes tended to disappear with a partial restoration from the 1-month to 2-month follow-up time (Fig. 3c, d). A slight patchy change of the IS/OS junction line can be observed at



◀ **Fig. 4** Serial changes of visual field and MP with a 15-month follow-up. Visual field and MP images at baseline (a), 15-day (b), 1-month (c), 2-month (d), 5-month (e), and 15-month (f) follow-up. Visual field images note the progress of an enlarged blind spot (black color) of the right eye that started to get smaller at the 2-month follow-up. The improvement is evidenced by the average intensity of macular measured by MP from 25.6, 26.4, 27.7, 27.5, 28.8, and 30 dB at presentation, 15-day, 1-month, 2-month, 5-month, and 15-month follow-up

the 5-month follow-up (Fig. 3e), with a normal retinal appearance at the 15-month follow-up (Fig. 3f).

The blind spot enlarged to the summit at the 15-day follow-up time and kept almost the same size when detected at the 2-month follow-up (Fig. 4b–d). The enlarged blind spot area had partial recovery at the 5-month follow-up and reverted to a similar size to baseline at the 15-month follow-up (Fig. 4e, f). In terms of the MP results, the average intensity consequently had an increment from 26.4 dB at the 15-day follow-up to 30 dB at the 15-month follow-up. The average intensity was 27.7, 27.5, and 28.8 at the 1-month, 2-month, and 5-month follow-up, respectively (Fig. 4b–f).

The mfERG records in the central and nasal regions of the fovea eventually enhanced from the 1-month to the 5-month follow-up but were still smaller than the control (Fig. 5b–d). The left eye served as a control.

Discussion

Oguchi disease is characterized by nyctalopia with the Mizuo–Nakamura phenomenon, golden retinal exhibition, abnormal rod responses in electroretinography,

and no obvious subjective changes in other symptoms, such as visual acuity reduction, achromatopsia, or visual field loss [1]. It is an unusual form of congenital stationary night blindness. However, Nishiguchi et al. [10] recently reported Oguchi disease shows a progressive degeneration to retinitis pigmentosa after a long-term follow-up. Our patient was suffering night blindness since her childhood and presented with a golden discoloration of the fundus; the SD-OCT findings of the well-structured fovea accompany complex packed highly reflective bands at parafovea, which are compatible to reported Oguchi cases [9, 11–17]. Hayashi et al. reported mfERG findings in one Oguchi case with homozygous 1147delA in the *SAG* gene. The patient showed preserved central (ring 1) and paracentral (ring 2) responses with normal latencies but attenuated and prolonged responses in the periphery macular (rings 3–5) [18]. On the contrary, our patient showed a severe response reduction in the central and paracentral macular along with the relatively preserved responses at the outer macular of both eyes.

For the DA 3.0 ERG, after 12 h of dark adaptation, the amplitude of the right eye was smaller than that of the left eye. The right eye was at the inflammatory stage of MEWDS which temporarily influenced the function of photoreceptors. Most reports revealed that a longer DA time can produce the b-wave of rods. The DA time varies from “longer than 30 min” to “overnight” [2, 9, 19]. No exact DA time was available for reference. We first conducted a series of DA time points to determine the optimal time. We found a single flash and combined cone-rod responses, which can be recorded after 12 h (overnight) DA, which is compatible with previous papers [9]. Our

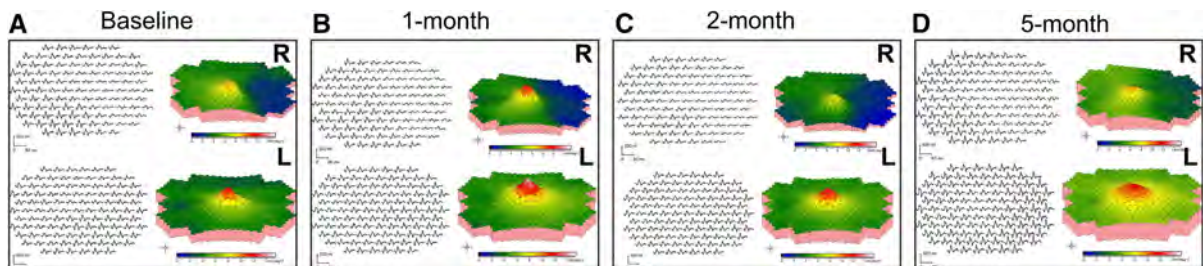


Fig. 5 Serial recordings of multifocal electroretinography with the 5-month follow-up. Trace and 3D-plot waveform of mfERGs at baseline (a), 1-month (b), 2-month (c), and 5-month (d) follow-up shows the reductive central region of both eyes and severely attenuated responses along the nasal region of the

fovea of the right eye. Responses of the right eye eventually recovered from the 1-month to 5-month follow-up: Responses of the central and nasal regions of the fovea enhanced along the time but were still smaller than the control. The left eye served as a control

results also indicate that although the Mizuo–Nakamura phenomenon can occur after 4 h DA through fundus images, the occurrence of b-wave in fFERGs needs longer DA.

The typical characteristics of the MEWDS have been known since its first description by Jampol et al. in 1984 [20]. The condition predominantly affects young women with myopia. The symptoms usually start with vaccination, allergy, and flulike episode complaints, followed by photopsia, enlarged blind spot, and unilateral blurred vision, which can totally recover within 10 weeks. The multimodal ophthalmology examinations are crucial to distinct MEWDS cases from other white dot syndromes: Fundus images show white patches scattered over the posterior macular area to the optic. The AF and fluorescein angiography (FA) show hyperfluorescent wreath-like dots corresponding to the hypofluorescent spots on the indocyanine green angiography (ICGA) images; the NIR reveals small areas of hypo-NIR-AF; the EZ and IZ disruptions can be seen in majority of patients and some cases showed focal choroidal excavation via OCT; and the VF test shows the enlarged blind spot [6, 21–23]. The expressions of this case were mostly consistent with the typical MEWDS, except that no lesions can be observed in the fundus images. It may be due to the dots that overlapped with tapetal-like fundus changes caused by Oguchi disease. The clinical course of typical MEWDS patients is short, the period of completed visual acuity recovery can be within three to 10 weeks, and the period of recovery of enlarged blind spots may last longer than 1 year [24–27]. In prospective studies, Marcela et al. reported 34 MEWDS patients experienced visual acuity recovery in 10 weeks [28]. Li et al. reported visual acuity, OCT, and FAF findings of seven MEWDS patients, which show full recovery within 3 months, and the visual field returned to normal in five patients within 6 months [29]. In the present patient, the visual acuity, OCT structure, FAF images, and visual field were still abnormal at the 5-month follow-up. These parameters returned to normal at the 15-month follow-up. The extension of the recovery time of her Oguchi disease was mainly caused by the photoreceptor dysfunction. The precise pathogenesis of MEWDS was unknown although it has been reckoned as an immune-mediated process [30].

This patient suffered Oguchi disease caused by *SAG* gene which is critical for recovery to normal

vision by deactivating phosphorylated opsins. Autoimmune affections or viral infections are thought to be the main causes of MEWDS, and the presence of antibodies could be detected in certain patients in the process of the infections as reported [31]. Although our patient had negative results for the antibody test, the time point of the presence of inflammatory antibodies is variable. We cannot exclude the possibility that this patient is susceptible to be affected by the MEWDS caused by inflammation antibodies.

SAG variations are mostly discovered in the Japanese population, and one specific homozygous frameshift alteration (c.924delA, previously named 1147delA) has been reported in majority of Japanese patients [10, 18, 32–34]. To date, in total 17 different pathogenic variants have been reported in the *SAG* gene (HGMD database) including eight missense, four nonsense, and five frameshift alterations [9, 16, 35]. A Chinese patient with a compound heterozygosity of a nonsense pathogenic variants and a heterozygous deletion of 3224 bp encompassing exon 2 has been reported by Huang et al. in 2012 [14]. Our patient's screening results showed a novel homozygous splicing alteration in the *SAG* gene (c.181 + 1G > A). It is the first time to report a splicing variant associated with Oguchi disease.

Conclusion

We first determine the exact time point of DA to induce b-wave in the rod response in fFERGs. This is the first case of Oguchi disease associated with the MEWDS and the first case of Oguchi disease caused by a *SAG* homozygous splicing alteration.

Acknowledgements Kaoru Fujinami is a paid consultant of Astellas Pharma Inc, Kubota Pharmaceutical Holdings Co., Ltd, and Acucela Inc. Kaoru Fujinami reports personal fees from Astellas Pharma Inc, personal fees from Kubota Pharmaceutical Holdings Co., Ltd., personal fees from Acucela Inc., personal fees from SANTEN Company Limited, personal fees from Foundation Fighting Blindness, personal fees from Foundation Fighting Blindness Clinical Research Institute, personal fees from Japanese Ophthalmology Society, personal fees from Japan Retinitis Pigmentosa Society. Kaoru Fujinami reports grants from Astellas Pharma Inc (NCT03281005), outside the submitted work.

Funding Shiyong Li is supported by grants from the National Nature Science Foundation of China (81974138), Third Military Medical University (Army Medical University) research grant

(2017XYY02), and National Basic Research Program of China (2018YFA0107301). Gang Wang is supported by grants from the Third Military Medical University, Southwest Hospital Innovation Grant (SWH2015LC15). Kaoru Fujinami is supported by grants from Grant-in-Aid for Young Scientists (A) of the Ministry of Education, Culture, Sports, Science and Technology, Japan (16H06269), grants from Grant-in-Aid for Scientists to support international collaborative studies of the Ministry of Education, Culture, Sports, Science and Technology, Japan (16KK01930002), grants from National Hospital Organization Network Research Fund (H30-NHO-2-12), grants from the Foundation for Fighting Blindness–Alan Lattes Career Development Program (CF-CL-0416-0696-UCL), grants from Health Labor Sciences Research Grant, The Ministry of Health, Labor and Welfare (201711107A), and grants from the Great Britain Sasakawa Foundation Butterfly Awards.

Compliance with ethical standards

Conflict of interest All authors have completed the COI Form for Disclosure of Potential Conflicts of Interest. Individual investigators who participate in the sponsored project(s) are not directly compensated by the sponsor but may receive a salary or other support from the institution to support their effort on the project(s).

Statements of human rights The procedures used were approved by the local ethics committee of Southwest Eye Hospital, Third Military Medical University (Army Medical University), Chongqing, China (reference number: 73981486-2), and all procedures were performed in accordance with the Declaration of Helsinki.

Informed consent The patient and her relatives, who were also studied upon, gave informed consent for all procedures described involved in the study.

Statement on the welfare of animals All the experimental procedures were performed in accordance with institutional animal welfare guidelines, were approved by the Third Military Medical University Animal Care and Use Committee

References

- Fuchs S, Nakazawa M, Maw M, Tamai M, Oguchi Y, Gal A (1995) A homozygous 1-base pair deletion in the arrestin gene is a frequent cause of Oguchi disease in Japanese. *Nat Genet* 10(3):360
- Miyake Y, Horiguchi M, Suzuki S, Kondo M, Tanikawa A (1996) Electrophysiological findings in patients with Oguchi's disease. *Jpn J Ophthalmol* 40(4):511–519
- Godara P, Cooper RF, Sergouniotis PI, Diederichs MA, Streb MR, Genead MA et al (2012) Assessing retinal structure in complete congenital stationary night blindness and Oguchi disease. *Am J Ophthalmol* 154(6):987–1001.e1
- Yamamoto S, Sippel KC, Berson EL, Dryja TP (1997) Defects in the rhodopsin kinase gene in the Oguchi form of stationary night blindness. *Nat Genet* 15(2):175
- dell'Omo R, Pavesio CE (2012) Multiple evanescent white dot syndrome (MEWDS). *Int Ophthalmol Clin* 52(4):221–228
- Brydak-Godowska J, Golebiewska J, Turczynska M, Moneta-Wielgos J, Samsel A, Borkowski PK et al (2017) Observation and clinical pattern in patients with white dot syndromes: the role of color photography in monitoring ocular changes in long-term observation. *Med Sci Monit: Int Med J Exp Clin Res* 23:1106–1115
- McCulloch DL, Marmor MF, Brigell MG, Hamilton R, Holder GE, Tzekov R et al (2015) ISCEV Standard for full-field clinical electroretinography (2015 update). *Doc Ophthalmol* 130(1):1–12
- Hood DC, Bach M, Brigell M, Keating D, Kondo M, Lyons JS et al (2012) ISCEV standard for clinical multifocal electroretinography (mfERG) (2011 edition). *Doc Ophthalmol* 124(1):1–13
- Sergouniotis PI, Davidson AE, Sehmi K, Webster AR, Robson AG, Moore AT (2011) Mizuo–Nakamura phenomenon in Oguchi disease due to a homozygous nonsense mutation in the SAG gene. *Eye (London, England)*. 25(8):1098–1101
- Nishiguchi KM, Ikeda Y, Fujita K, Kunikata H, Akiho M, Hashimoto K et al (2019) Phenotypic features of Oguchi disease and retinitis pigmentosa in patients with S-antigen mutations: a long-term follow-up study. *Ophthalmology* 126:1557–1566
- Yuan A, Nusinowitz S, Sarraf D (2011) Mizuo–Nakamura phenomenon with a negative waveform ERG. *Br J Ophthalmol* 95(1):147–148
- Agarwal R, Tripathy K, Bandyopadhyay G, Basu K (2019) Mizuo–Nakamura phenomenon in an Indian male. *Clin Case Rep* 7(2):401–403
- Colombo L, Abeshi A, Maltese PE, Frecer V, Miertus J, Cerra D et al (2018) Oguchi type I caused by a homozygous missense variation in the SAG gene. *Eur J Med Genet* 62:103548
- Huang L, Li W, Tang W, Zhu X, Ou-Yang P, Lu G (2012) A Chinese family with Oguchi's disease due to compound heterozygosity including a novel deletion in the arrestin gene. *Mol Vis* 18:528–536
- Kuroda M, Hirami Y, Nishida A, Jin ZB, Ishigami C, Takahashi M et al (2011) A case of Oguchi disease with disappearance of golden tapetal-like fundus reflex after vitreous resection. *Nippon Ganka Gakkai Zasshi* 115(10):916–923
- Fujinami K, Tsunoda K, Nakamura M, Oguchi Y, Miyake Y (2011) Oguchi disease with unusual findings associated with a heterozygous mutation in the SAG gene. *Arch Ophthalmol (Chicago, IL: 1960)* 129(10):1375–1376
- Maw M, Kumaramanickavel G, Kar B, John S, Bridges R, Denton M (1998) Two Indian siblings with Oguchi disease are homozygous for an arrestin mutation encoding premature termination. *Hum Mutat* 50(Suppl 1):S317–S319
- Hayashi T, Tsuzuranuki S, Kozaki K, Urashima M, Tsuneoka H (2011) Macular dysfunction in Oguchi disease with the frequent mutation 1147delA in the SAG gene. *Ophthalmic Res* 46(4):175–180

19. Zhang Q, Zulfiqar F, Riazuddin SA, Xiao X, Yasmeen A, Rogan PK et al (2005) A variant form of Oguchi disease mapped to 13q34 associated with partial deletion of GRK1 gene. *Mol Vis* 11:977–985
20. Jampol LM, Sieving PA, Pugh D, Fishman GA, Gilbert H (1984) Multiple evanescent white dot syndrome: I. Clinical findings. *Arch Ophthalmol* 102(5):671–674
21. Cahuzac A, Wolff B, Mathis T, Errera MH, Sahel JA, Mauget-Faysse M (2017) Multimodal imaging findings in ‘hyper-early’ stage MEWDS. *Br J Ophthalmol* 101(10):1381–1385
22. Furino C, Boscia F, Cardascia N, Alessio G, Sborgia C (2009) Fundus autofluorescence and multiple evanescent white dot syndrome. *Retina* 29(1):60–63
23. Margolis R, Mukkamala SK, Jampol LM, Spaide RF, Ober MD, Sorenson JA et al (2011) The expanded spectrum of focal choroidal excavation. *Arch Ophthalmol* 129(10):1320–1325
24. Mantovani A, Invernizzi A, Staurenghi G, Herbort CP Jr (2019) Multiple evanescent white dot syndrome: a multimodal imaging study of foveal granularity. *Ocular Immunol Inflamm* 27(1):141–147
25. Hashimoto Y, Saito W, Hasegawa Y, Noda K, Ishida S (2019) Involvement of inner choroidal layer in choroidal thinning during regression of multiple evanescent white dot syndrome. *J Ophthalmol* 2019:6816925
26. Yang JS, Chen CL, Hu YZ, Zeng R (2018) Multiple evanescent white dot syndrome following rabies vaccination: a case report. *BMC Ophthalmol* 18(1):312
27. Yang CS, Wang AG, Lin YH, Huang YM, Lee FL, Lee SM (2012) Optical coherence tomography in resolution of photoreceptor damage in multiple evanescent white dot syndrome. *J Chin Med Assoc: JCMS* 75(12):663–666
28. Marsiglia M, Gallego-Pinazo R, De Souza EC, Munk MR, Yu S, Mrejen S et al (2016) Expanded clinical spectrum of multiple evanescent white dot syndrome with multimodal imaging. *Retina* 36(1):64–74
29. Li D, Kishi S (2009) Restored photoreceptor outer segment damage in multiple evanescent white dot syndrome. *Ophthalmology* 116(4):762–770
30. Jampol LM, Becker KG (2003) White spot syndromes of the retina: a hypothesis based on the common genetic hypothesis of autoimmune/inflammatory disease. *Am J Ophthalmol* 135(3):376–379
31. Gass JD (2003) Are acute zonal occult outer retinopathy and the white spot syndromes (AZOOR complex) specific autoimmune diseases? *Am J Ophthalmol* 135:380–381
32. Yamada T, Matsumoto M, Kadoi C, Nagaki Y, Hayasaka Y, Hayasaka S, Hayasaka S (1999) 1147 del A mutation in the arrestin gene in Japanese patients with Oguchi disease. *Ophthalmic Genet* 20(2):117–120
33. Nakamachi Y, Nakamura M, Fujii S, Yamamoto M, Okubo K (1998) Oguchi disease with sectoral retinitis pigmentosa harboring adenine deletion at position 1147 in the arrestin gene. *Am J Ophthalmol* 125(2):249–251
34. Nakazawa M, Wada Y, Fuchs S, Gal A, Tamai M (1997) Oguchi disease: phenotypic characteristics of patients with the frequent 1147delA mutation in the arrestin gene. *Retina (Philadelphia, PA)* 17(1):17–22
35. Waheed NK, Qavi AH, Malik SN, Maria M, Riaz M, Cremers FP et al (2012) A nonsense mutation in S-antigen (p.Glu306*) causes Oguchi disease. *Mol Vis* 18:1253–1259

Publisher’s Note Springer Nature remains neutral with regard to jurisdictional claims in published maps and institutional affiliations.

Clinical and Genetic Characteristics of 15 Affected Patients From 12 Japanese Families with *GUCY2D*-Associated Retinal Disorder

Xiao Liu^{1-3,*}, Kaoru Fujinami^{1,2,4,5,*}, Kazuki Kuniyoshi⁶, Mineo Kondo⁷, Shinji Ueno⁸, Takaaki Hayashi⁹, Kiyofumi Mochizuki¹⁰, Shuhei Kameya¹¹, Lizhu Yang^{1,2}, Yu Fujinami-Yokokawa^{1,12,13}, Gavin Arno^{1,4,5,14}, Nikolas Pontikos^{4,5}, Hiroyuki Sakuramoto⁶, Taro Kominami⁸, Hiroko Terasaki⁸, Satoshi Katagiri⁹, Kei Mizobuchi⁹, Natsuko Nakamura^{1,15}, Kazutoshi Yoshitake¹⁶, Yoza Miyake^{1,17}, Shiyong Li³, Toshihide Kurihara², Kazuo Tsubota², Takeshi Iwata¹⁶, and Kazushige Tsunoda¹, Japan Eye Genetics Consortium

¹ Laboratory of Visual Physiology, Division of Vision Research, National Institute of Sensory Organs, National Hospital Organization Tokyo Medical Center, Meguro-ku, Tokyo, Japan

² Department of Ophthalmology, Keio University School of Medicine, Shinjuku-ku, Tokyo, Japan

³ Southwest Hospital/Southwest Eye Hospital, Third Military Medical University (Army Medical University), Chongqing, China

⁴ UCL Institute of Ophthalmology, London, UK

⁵ Moorfields Eye Hospital, London, UK

⁶ Department of Ophthalmology, Kindai University Faculty of Medicine, Osakasayama, Osaka, Japan

⁷ Department of Ophthalmology, Mie University Graduate School of Medicine, Tsu, Mie, Japan

⁸ Department of Ophthalmology, Nagoya University Graduate School of Medicine, Showa-ku, Nagoya, Japan

⁹ Department of Ophthalmology, The Jikei University School of Medicine, Minato-ku, Tokyo, Japan

¹⁰ Department of Ophthalmology, Gifu University Graduate School of Medicine, Gifu-shi, Gifu, Japan

¹¹ Department of Ophthalmology, Nippon Medical School Chiba Hokusoh Hospital, Inzai, Chiba, Japan

¹² Graduate School of Health Management, Keio University, Shinjuku-ku, Tokyo, Japan

¹³ Division of Public Health, Yokokawa Clinic, Suita, Osaka, Japan

¹⁴ North East Thames Regional Genetics Service, UCL Great Ormond Street Institute of Child Health, Great Ormond Street NHS Foundation Trust, London, UK

¹⁵ Department of Ophthalmology, The University of Tokyo, Bunkyo-ku, Tokyo, Japan

¹⁶ Division of Molecular and Cellular Biology, National Institute of Sensory Organs, National Hospital Organization National Tokyo Medical Center, Meguro-ku, Tokyo, Japan

¹⁷ Aichi Medical University, Nagakute, Aichi, Japan

Correspondence: Kaoru Fujinami, Laboratory of Visual Physiology, Division of Vision Research, National Institute of Sensory Organs, National Hospital Organization, Tokyo Medical Center, 2-5-1 Higashigaoka, Meguro-ku, Tokyo 152-8902, Japan. e-mail: k.fujinami@ucl.ac.uk

Received: March 21, 2019

Accepted: January 9, 2020

Published: May 11, 2020

Keywords: macular dystrophy; cone rod dystrophy; *GUCY2D*; autosomal dominant; Leber congenital amaurosis

Purpose: To determine the clinical and genetic characteristics of patients with *GUCY2D*-associated retinal disorder (*GUCY2D*-RD).

Methods: Fifteen patients from 12 families with inherited retinal disorder (IRD) and harboring *GUCY2D* variants were ascertained from 730 Japanese families with IRD. Comprehensive ophthalmological examinations, including visual acuity (VA) measurement, retinal imaging, and electrophysiological assessment were performed to classify patients into three phenotype subgroups; macular dystrophy (MD), cone-rod dystrophy (CORD), and Leber congenital amaurosis (LCA). In silico analysis was performed for the detected variants, and the molecularly confirmed inheritance pattern was determined (autosomal dominant/recessive [AD/AR]).

Results: The median age of onset/examination was 22.0/38.0 years (ranges, 0-55 and 1-73) with a median VA of 0.80/0.70 LogMAR units (ranges, 0.00-1.52 and 0.10-1.52) in the right/left eye, respectively. Macular atrophy was identified in seven patients (46.7%), and two had diffuse fundus disturbance (13.3%), and six had an essentially normal

Citation: Liu X, Fujinami K, Kuniyoshi K, Kondo M, Ueno S, Hayashi T, Mochizuki K, Kameya S, Yang L, Fujinami-Yokokawa Y, Arno G, Pontikos N, Sakuramoto H, Kominami T, Terasaki H, Katagiri S, Mizobuchi K, Nakamura N, Yoshitake K, Miyake Y, Li S, Kurihara T, Tsubota K, Iwata T, Tsunoda K, Japan Eye Genetics Consortium. Clinical and genetic characteristics of 15 affected patients from 12 Japanese families with *GUCY2D*-associated retinal disorder. *Trans Vis Sci Tech.* 2020;9(6):2. <https://doi.org/10.1167/tvst.9.6.2>

fundus (40.0%). There were 11 patients with generalized cone-rod dysfunction (78.6%), two with entire functional loss (14.3%), and one with confined macular dysfunction (7.1%). There were nine families with ADCORD, one with ARCORD, one with ADMD, and one with ARLCA. Ten *GUCY2D* variants were identified, including four novel variants (p.Val56GlyfsTer262, p.Met246Ile, p.Arg761Trp, p.Glu874Lys).

Conclusions: This large cohort study delineates the disease spectrum of *GUCY2D*-RD. Diverse clinical presentations with various severities of ADCORD and the early-onset severe phenotype of ARLCA are illustrated. A relatively lower prevalence of *GUCY2D*-RD for ADCORD and ARLCA in the Japanese population was revealed.

Translational Relevance: The obtained data help to monitor and counsel patients, especially in East Asia, as well as to design future therapeutic approaches.

Introduction

Inherited retinal disorder (IRD) is a leading cause of blindness,¹ and includes disorders such as retinitis pigmentosa (RP), cone/cone-rod dystrophy (CORD), macular dystrophy (MD), Stargardt disease (STGD), Leber congenital amaurosis (LCA) and others.^{1–6} IRD is characterized by heterogeneity both in the clinical and genetic aspects, with different inheritance patterns, including autosomal dominant (AD), autosomal recessive (AR), X-linked, and mitochondrial inheritance.^{7–9} Significant clinical and genetic overlap is well-known in the spectrum of IRD, and diverse clinical phenotypes, including CORD, MD, STGD, RP, and LCA, can manifest as a result of pathogenic variants in a single gene (e.g., *ABCA4*, *BEST1*, *PRPH2*, *RPGR*, *CRX*, *GUCY2D*, *RS1*, *POC1B*, *PROM1*, *CNGA3*, *CNGB3*).^{2,3,7,8,10–18}

GUCY2D, denoted as guanylate cyclase 2D (OMIM: 600179), is located on 17p13.1 and contains 20 exons and encodes one of the two retinal membrane guanylyl cyclase isozymes expressed in photoreceptors.^{19,20} Retinal membrane guanylyl cyclase isozymes synthesize the intracellular messenger of photoreceptor excitation, cyclic guanosine monophosphate, which is regulated by the intracellular Ca²⁺-sensor proteins of guanylate cyclase-activating proteins.^{19–26} RetGCs and guanylate cyclase-activating proteins are responsible for the Ca²⁺-sensitive restoration of cyclic guanosine monophosphate levels after the light activation of the phototransduction cascade.²⁶

A locus and gene for LCA was first mapped and identified as *GUCY2D* (LCA1) in 1995 and 1996.^{19,27} Since then, more than 200 variants in the

GUCY2D gene have been associated with a wide range of different phenotypes of IRDs.^{9,19,20,28–39} Sharon et al. reported that 88% of *GUCY2D*-associated retinal disorder (*GUCY2D*-RD) is AR-LCA, whereas pathogenic heterozygous missense *GUCY2D* variants cause AD-CORD.²⁰ In that, pathogenic *GUCY2D* variants are one of the major causes of LCA, as well as a major cause of AD-CORD.²⁰ Recently, Stunkel et al. identified five patients with AR congenital night blindness caused by biallelic *GUCY2D* variants, which may slowly progress to mild retinitis pigmentosa.⁴⁰ Thus, AR-LCA, AD-CORD, and AR congenital night blindness are the main clinical presentations of *GUCY2D*-RD.

Studies of *GUCY2D*-RD have been conducted separately for each phenotype, such as CORD or RP/LCA; thus, it has been hard to comprehensively understand the disorder with diverse clinical manifestations and different modes of inheritance. To grasp the whole picture of *GUCY2D*-RD, large cohort studies with standardized clinical and genetic investigations for IRD in total are required.

The purpose of this study was to characterize the clinical and molecular genetic features of *GUCY2D*-RD in a large nationwide cohort of Japanese subjects diagnosed with IRD.

Methods

The protocol of this study followed the tenets of the Declaration of Helsinki. Informed consent was obtained from all affected subjects and unaffected subjects after explanation of the nature and possible consequences of the study. This research was

approved by the Institutional Review Board of the National Institute of Sensory Organs, National Hospital Organization Tokyo Medical Center (Reference R18-029).

Participants from the Japan Eye Genetics Consortium Study

Participants with a clinical diagnosis of IRD and available genetic data by whole-exome sequencing (WES) were studied between 2008 and 2018 as part of the Japan Eye Genetics Consortium Study (JEGC studies; <http://www.jegc.org/>) conducted in collaboration of 38 institutes all over Japan.⁴¹ A total of 1294 subjects from 730 families were reviewed, including 30 families with AD-CORD/MD/STGD (defined as families with clear AD family history) and 41 families with AR or sporadic LCA.

Clinical Examinations

A detailed history was obtained in all affected subjects and unaffected family members (where available). The onset of disease was defined as the age when any visual symptom was first noted by patients or parents or when the subject was first diagnosed. The duration of disease was defined as the time between the onset of disease and the latest examination.

Comprehensive ophthalmological investigations were performed, including measurements of the best-corrected decimal visual acuity (BCVA) converted to the logarithm of the minimum angle of resolution (LogMAR) units, ophthalmoscopy, fundus photography, fundus autofluorescence (FAF) imaging, spectral-domain optical coherence tomography (SD-OCT), visual field testing, and electrophysiological assessments mainly according to the international standards of the International Society for Clinical Electrophysiology of Vision.^{42–45}

Phenotype Subgroup

For the purpose of this study, the phenotype subgroup was defined based on clinical findings such as disease onset, symptoms, natural course, affected part on retinal imaging, the pattern of retinal dysfunction, and the history and phenotype of affected family members, partially according to the previous report¹³: LCA (including early-onset RP), a severe retinal dystrophy with early onset (<10 years) and complete loss of retinal function; RP (including rod-cone dystro-

phy), a progressive retinal dystrophy initially often affecting the peripheral retina with generalized rod dysfunction; CORD, a progressive retinal dystrophy initially often affecting the macula with generalized cone dysfunction; MD, a progressive retinal dystrophy presenting macular atrophy with confined macular dysfunction despite no abnormal generalized retinal function; and SNB, a stationary night blindness presenting congenital or early-onset night blindness, often affecting generalized rod function despite essentially normal visual acuity (VA) and no atrophy.

GUCY2D Variant Detection

Genomic DNA was extracted from affected subjects and unaffected family members (where available for cosegregation analysis). WES with target analysis of 301 retinal disease-associated genes (RetNET) was performed based on the previously published method and through the Phenopolis platform.^{41,46} The identified variants were filtered with the allele frequency (less than 1%) of the Human Genetic Variation Database (HGVD), which provides the allele frequency of the general Japanese population. Depth and coverage for the target exons were examined with the integrative Genomics Viewer.

Disease-causing variants were determined from the detected variants in the 301 retinal-disease-associated genes, considering the clinical findings of the affected subjects, the pattern of inheritance in the pedigree, and the results of cosegregation analysis.

In Silico Molecular Genetic Analysis

Sequence variant nomenclature was performed according to the guidelines of the Human Genome Variation Society (HGVS). The allele frequency of all detected *GUCY2D* variants in the HGVD, Integrative Japanese Genome Variation (iJGVD 2k), the 1000 Genomes Project, and the genome Aggregation Database (gnomAD) was established according to the previous method.⁴¹

All detected *GUCY2D* variants were analyzed with the following prediction programs; MutationTaster, FATHMM, SIFT, PROVEAN, and PolyPhen-2. Evolutional conservation scores were calculated for all detected *GUCY2D* variants by the UCSC database. Pathogenicity classification of all detected *GUCY2D* variants was performed based on the guidelines of the American College of Medical Genetics and Genomics.⁴⁷

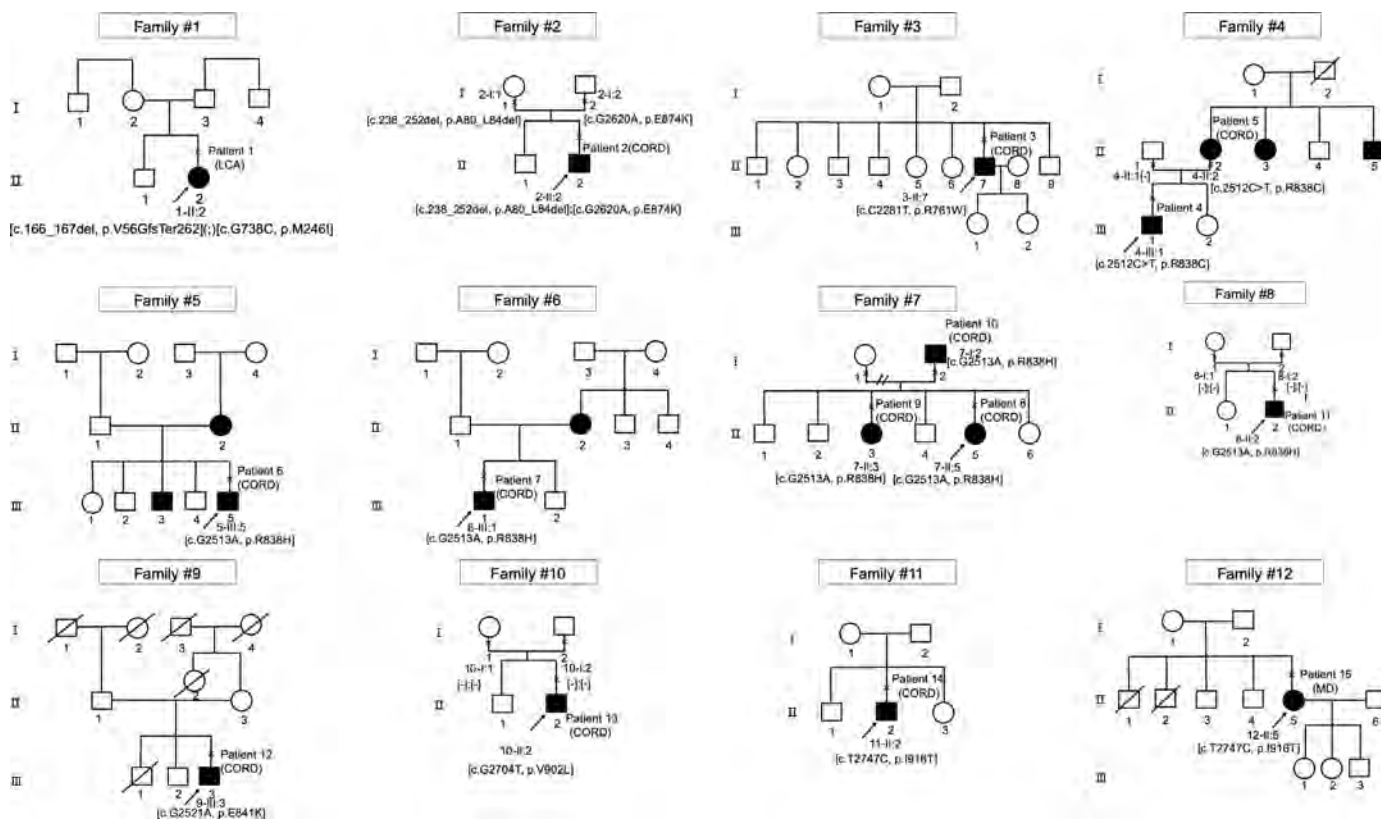


Figure 1. Pedigrees of 12 Japanese families with inherited retinal disorder harboring *GUCY2D* variants. The solid squares and circles (men and women, respectively) represent the affected subjects and the white icons represent the unaffected family members. The slash symbol indicates deceased individuals. The generation number is noted on the left. The proband is marked by an arrow; the clinically investigated individuals are indicated by a cross.

Results

Participants

Fifteen affected subjects from 12 families with a clinical diagnosis of IRD and harboring *GUCY2D* variants were ascertained. The detailed demographic features and summarized genetic results are provided in Table 1, and the pedigrees of 12 families are shown in Figure 1.

All affected and unaffected subjects were Japanese, and any mixture with other ethnicity was not reported. There were four families with clear AD family history (4/12, 33.3%; families 4–7), and eight sporadic families with no affected family members than the proband (8/12, 66.7%; families 1–3, 8–12). There were four families with unknown familial information (families 3, 9, 11, 12). Consanguineous marriage was not reported in any of the 12 families.

There were five affected females (5/15, 33.3%) and 10 affected males (10/15, 66.7%). The median age at

the latest examination of the 15 affected subjects was 38.0 years (range, 1–73).

Onset, Chief Complaint, and Visual Acuity

The median age of onset and duration of disease of the 12 affected subjects with available records was 22.0 years (range, 0–55), and 11.5 years (range, 1–40), respectively.

Four subjects had childhood-onset of 15 years or earlier (4/12, 33.3%; patients 1, 2, 7, 13). Later onset of disease (45 years or later) was reported in one subject (1/12, 8.3%; patient 15).

Reduced visual acuity/poor visual acuity was reported as a chief complaint at the initial visit in 12 of 14 affected subjects with available records (12/14, 85.7%; patients 1, 2, 4–9, 12–14, 15), one with photophobia (1/14, 7.1%; patient 11), and one with night blindness (1/14, 7.1%; patient 3).

The median BCVA in the right and left eyes of the 12 affected subjects with available records was 0.80 (range, 0.00–1.52) and 0.70 (range, 0.10–1.52) LogMAR units,

Table 1. Demographic Features of 15 Japanese Patients from 12 Families with *GUCY2D*-Associated Retinal Disorder (*GUCY2D*-RD)

Family No.	Patient No.	Inheritance	Sex	Age (at Latest Examination)	Onset	Chief Complaint	Other ocular symptoms	Refraction		LogMAR VA		Phenotype Subgroup	Inheritance Suggested by Molecular genetic diagnosis	Genotype
								RE	LE	RE	LE			
1 (MU01)	1-II:2 (Patient 1)	Sporadic	F	1	0	Reduced visual acuity/poor visual acuity	Nystagmus	NA	NA	NA	NA	LCA	AR	c.167_168delTG, p.Val56GlyfsTer262; c.738G>C, p.Met246Ile
2 (TMC01)	2-II:2 (Patient 2)	Sporadic	M	12	3	Reduced visual acuity/ poor visual acuity	Night blindness	-1	-1	0.22	0.22	CORD (moderate)	AR	c.238_252del, p.Ala80_Leu84del; c.2620G>A, p.Glu874Lys
3 (NU01)	3-II:7 (Patient 3)	Sporadic	M	73	NA	Night blindness	NA	+1.5	+3.5	1	1.52	CORD (severe)	AD	c.2281C>T, p.Arg761Trp
4 (KDU01)	4-III:1 (Patient 4)	AD	M	30	23	Reduced visual acuity/ poor visual acuity	NA	-2.5	2.5	0.82	0.82	CORD (moderate)	AD	c.2512C>T, p.Arg838Cys
4 (KDU01)	4-II:2 (Patient 5)	AD	F	61	21	Reduced visual acuity/ poor visual acuity	Photophobia	-1.5	-1.5	1.05	1.05	CORD (moderate)	AD	c.2512C>T, p.Arg838Cys
5 (GU01)	5-III:5 (Patient 6)	AD	F	31	18	Reduced visual acuity/ poor visual acuity	Photophobia	-7	-7	0	0.1	CORD (mild)	AD	c.2513G>A, p.Arg838His
6 (TMC02)	6-III:1 (Patient 7)	AD	M	38	7	Reduced visual acuity/ poor visual acuity	Photophobia	-5	-5	1.52	1.52	CORD (severe)	AD	c.2513G>A, p.Arg838His
7 (JU01)	7-II:5 (Patient 8)	AD	F	36	35	Reduced visual acuity/ poor visual acuity	NA	-6	-6.5	0.22	0.52	CORD (mild)	AD	c.2513G>A, p.Arg838His
7 (JU01)	7-II:3 (Patient 9)	AD	F	43	30	Reduced visual acuity/ poor visual acuity	NA	-6	-6.5	0.7	0.7	CORD (moderate)	AD	c.2513G>A, p.Arg838His
7 (JU01)	7-I:2 (Patient 10)	AD	M	68	NA	NA	NA	+1	-2	0.82	1	CORD (NA)	AD	c.2513G>A, p.Arg838His
8 (JU02)	8-II:2 (Patient 11)	Sporadic	M	23	23	Photophobia	Color vision abnormality	-11.5	-11.5	0.15	0.15	CORD (mild)	AD (de novo)	c.2513G>A, p.Arg838His
9 (KDU02)	9-III:3 (Patient 12)	Sporadic	M	64	41	Reduced visual acuity/ poor visual acuity	NA	NA	NA	NA	NA	CORD (NA)	AD	c.2521G>A, p.Glu841Lys
10 (TMC03)	10-II:2 (Patient 13)	Sporadic	M	10	0	Reduced visual acuity/ poor visual acuity	Photophobia	+1.5	+1.5	1	1	CORD (moderate)	AD (de novo)	c.2704G>T, p.Val902Leu
11 (NU02)	11-II:2 (Patient 14)	Sporadic	M	43	NA	Reduced visual acuity/ poor visual acuity	Central visual field loss	-10	-12	0.8	0.6	CORD (moderate)	AD	c.2747T>C, p.Ile916Thr
12 (MU02)	12-II:5 (Patient 15)	Sporadic	F	71	55	Reduced visual acuity/ poor visual acuity	Photophobia	0	0	0.52	0.52	MD	AD	c.2747T>C, p.Ile916Thr

AD, autosomal dominant; AR, autosomal recessive; CORD, cone rod dystrophy; F, female; LCA, Leber congenital amaurosis; LE, left eye; M, male; NA, not available; RE, right eye; LogMAR VA, best corrected logarithm of the minimum angle of resolution visual acuity; MD, macular dystrophy.

Autosomal dominant family history (at least having two affected subjects in two consecutive generations) was clearly reported in four families. Age described in the column was defined as the age when the latest examination was performed. The age of onset was defined as either the age at which visual loss was first noted by the patient or, in the "asymptomatic" patients, when an abnormal retinal finding was first detected. Patients 10 and 14 had cataract.

The phenotype subgroup was defined based on clinical findings, such as disease onset, symptoms, natural course, affected part on retinal imaging, the pattern of retinal dysfunction, and the history and phenotype of affected family members, partially according to the previous report: LCA (including early-onset RP), a severe retinal dystrophy with early-onset (< 10 years) and complete loss of retinal function; RP (including rod-cone dystrophy), a progressive retinal dystrophy initially often affecting the peripheral retina with generalized rod dysfunction; CORD, a progressive retinal dystrophy initially often affecting the macula with generalized cone dysfunction; MD, a progressive retinal dystrophy presenting macular atrophy with confined macular dysfunction despite no abnormal generalized retinal function; and SNB, a stationary night blindness presenting congenital or early-onset night blindness often affecting generalized rod function despite essentially normal visual acuity and no atrophy.

There were two severe CORD subjects with poor VA and severe retinal dysfunction (patients 3, 7), six moderate CORD subjects with intermediate severity of VA or retinal function (patients 2, 4, 5, 9, 13, 14), and three mild CORD subjects with relatively favorable VA and relatively preserved generalized rod function (patients 6, 8, 11). Two subjects with CORD were unavailable for severity assessment due to unavailable VA or electrophysiological data.

Sequence variant nomenclature was performed according to the guidelines of the Human Genome Variation Society.

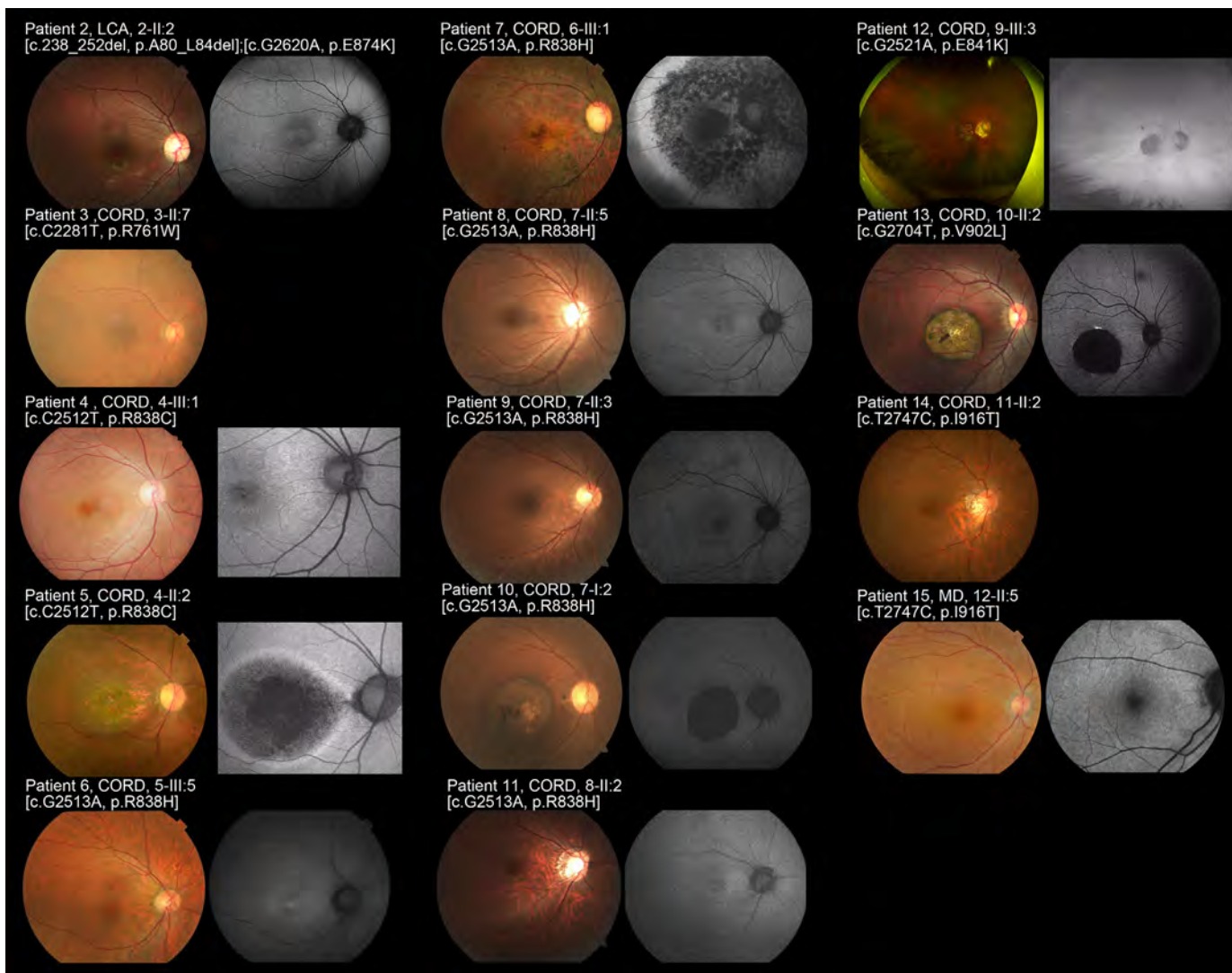


Figure 2. Fundus photographs and fundus autofluorescence images of 14 patients with *GUCY2D*-associated retinal disorder (*GUCY2D*-RD; patients 2–15). Fundus photographs and fundus autofluorescence (FAF) images of the right eyes demonstrated macular atrophy in seven affected subjects (patients 4, 5, 7, 9, 10, 12, 13) with intrachoroidal cavitation in three subjects (patients 5, left; 10, left; 13) and slight fine dots at the macula in two subjects (patients 4, 9). Atrophic change at the posterior pole extending to the periphery was observed in patient 7 and subtle diffuse disturbance at the posterior pole with vessel attenuation was found in patient 7. Normal fundus appearance was noted in five subjects (patients 1, 2, 6, 8, 14). Patient 11 had essentially normal retinal appearance except for optic disk cupping. The atrophic changes were more evident on FAF images. A loss of AF signal at the macula was identified in five subjects (patients 5, 7, 10, 12, 13). Increased AF signal at the macula was observed in five subjects (patients 2, 4, 6, 8, 11). A patchy area of decreased AF signal at the posterior pole extending to the periphery surrounded by a ring of increased AF signal was found in patient 7.

respectively. One of the two subjects with unavailable LogMAR VA testing had nystagmus (patient 1). Four subjects of 13 with available records had relatively favorable VA (4/13, 30.8%, patients 2, 6, 8, 11; 0.22 or better LogMAR units in the better eye), five subjects had intermediate VA (5/13, 38.5%, patients 4, 9, 10, 14, 15; between 0.22 and 1.0 LogMAR units in the better eye), and four subjects had poor VA (4/13, 30.8%; patients 3, 5, 7, 13; 1.0 or worse LogMAR units in the better eye).

Retinal Imaging and Morphological Findings

Fundus photographs were obtained in 14 affected subjects (patients 2–15), and FAF images were available in 12 affected subjects (patients 2, 4–13, 15). A description of funduscopy was available in one subject (patient 1). The representative images are presented in [Figure 2](#), and the detailed findings are described in [Table 2](#).

Macular atrophy was identified in seven affected subjects (7/15, 46.7%; patients 4, 5, 7, 9, 10, 12, 13), with

Table 2. Retinal Imaging and Morphological Findings of 15 Patients with *GUCY2D*-RD

Patient No.	Phenotype Subgroup	Fundus					FAF							SD-OCT						
		Macular Atrophy	Atrophy Along the Arcade	Peripheral Atrophy	Vessel Attenuation	Pigmentation	Comments	Area of Decreased Density at the Central Retina	Area of Increased Density at the Macula	Ring of Increased Density	Areas of Abnormal Density Along the Arcade	Areas of Abnormal Density in the Periphery	Foveal Sparing Surrounded by Decreased Density at the Parafovea	Comments	Outer Retinal Disruption at the Fovea	Outer Retinal Disruption at the Parafovea	Increased Signal of the Choroid	EZ Preservation at the fovea (RE)	EZ Preservation at the fovea (LE)	Comments
1 (MU01-01)	LCA	No	No	No	No	No	Funduscopy, normal	NA	NA	NA	NA	NA	NA		NA	NA	NA	NA	NA	
2 (TMC01-01)	CORD	No	No	No	No	No	Normal	No	Yes	No	No	No	No	Slightly increased AF at the fovea	No	No	No	Yes	Yes	Loss of IZ at the macula
3 (NU01-01)	CORD	No	No	No	Yes	No	Subtle diffuse disturbance at the posterior pole	NA	NA	NA	NA	NA	NA		No	Yes	No	Yes	Yes	Loss of IZ at the macula with ERM in the right eye
4 (KDU01-01)	CORD	Yes	No	No	No	No	Subtle fine dots at the macula	No	Yes	No	No	No	No		No	No	No	No	No	Loss of EZ/IZ at the fovea
5 (KDU01-02)	CORD	Yes	Yes	No	No	No	Intrachoroidal cavitation in the left eye	Yes	No	Yes	No	No	No		Yes	Yes	Yes	No	No	Thinned sensory retina and loss of EZ/IZ at the macula; Intrachoroidal cavitation at the left macula
6 (GU01-01)	CORD	No	No	No	No	No	Normal	No	Yes	No	No	No	No	Slightly increased AF at the fovea	No	No	No	Yes	Yes	Loss of IZ at the macula
7 (TMC02-01)	CORD	Yes	Yes	Yes	Yes	Yes	Atrophic changes with at the posterior pole extended to the periphery	Yes	No	Yes	Yes	Yes	No		Yes	Yes	Yes	No	No	
8 (JU01-01)	CORD	No	No	No	No	No	Normal	No	Yes	Yes	No	No	No	Slightly increased AF at the fovea of the right eye	No	No	No	Yes	Yes	Loss of IZ at the macula
9 (JU01-02)	CORD	Yes	No	No	No	No	Subtle fine dots at the macula	No	No	No	No	No	No	Slightly abnormal background	Yes	No	No	No	No	

Table 2. Continued

Patient No.	Phenotype Subgroup	Fundus					FAF							SD-OCT						
		Macular Atrophy	Atrophy Along the Arcade	Peripheral Atrophy	Vessel Attenuation	Pigmentation	Comments	Area of Decreased Density at the Central Retina	Area of Increased Density at the Macula	Ring of Increased Density	Areas of Abnormal Density Along the Arcade	Areas of Abnormal Density in the Periphery	Foveal Sparing Surrounded by Decreased Density at the Parafovea	Comments	Outer Retinal Disruption at the Fovea	Outer Retinal Disruption at the Parafovea	Increased Signal of the Choroid	EZ Preservation at the fovea (RE)	EZ Preservation at the fovea (LE)	Comments
10 (JU01-03)	CORD	Yes	No	No	No	Yes	Pigmentation at the macula in both eyes, intrachoroidal cavitation in the left eye	Yes	No	No	No	No	No	Loss of AF signal at the macula	Yes	Yes	Yes	No	No	Intrachoroidal cavitation at the left macula.
11 (JU02-01)	CORD	No	No	No	No	No	Essential normal except for optic disc cupping	No	Yes	No	No	No	Yes		No	No	No	Yes	Yes	Loss of IZ at the macula
12 (KDU02-01)	CORD	Yes	No	No	No	Yes		Yes	No	No	No	No	No	Artifact due to the medial condition	Yes	Yes	Yes	No	No	Thinned sensory retina and loss of EZ/IZ at the macula
13 (TMC03-01)	CORD	Yes	Yes	No	No	No	Intrachoroidal cavitation	Yes	No	No	No	No	No	Loss of AF signal at the macula	Yes	Yes	Yes	No	No	Thinned sensory retina/ intrachoroidal cavitation at the macula
14 (NU02-01)	CORD	No	No	No	No	No	Normal	NA	NA	NA	NA	NA	NA		No	No	No	No	No	Loss of EZ/IZ at the macula
15 (MU02-01)	MD	No	No	No	No	No	Subtle diffuse disturbance at the posterior pole	No	No	No	No	No	No	Slightly abnormal background	No	No	No	Yes	Yes	Loss of IZ at the macula

BE, both eyes; EZ, ellipsoid zone; FAF, fundus autofluorescence; FS, foveal sparing; LE, left eye; M male; NA not available; RE, right eye; SD-OCT, spectral domain optical coherence tomography. Foveal sparing was defined as remaining foveal AF signal surrounded by the area of decreased AF.

intrachoroidal cavitation in three subjects (patients 5, 10, 13) and slight fine dots at the macula in two subjects (patients 4, 9). Atrophic change at the posterior pole extending to the periphery was observed in one subject (1/15, 6.7%; patient 7). Subtle diffuse disturbance at the posterior pole with vessel attenuation was found in two subjects (2/15, 13.3%; patients 3, 15). Normal fundus appearance was noted in five subjects (5/15, 33.3%; patients 1, 2, 6, 8, 14). One subject had a normal retinal appearance except for optic disk cupping (1/15, 6.7%, patient 11).

The retinal atrophy at the macula was more evident on FAF images, and the loss of AF signal at the macula was identified in five subjects (5/12, 41.7%, patients 5, 7, 10, 12, 13). Increased AF signal at the macula was observed in five subjects (5/12, 41.7%; patients 2, 4, 6, 8, 11), one of whom showed subtle fine dots at the macula and the other four subjects had no abnormal findings at the macula on fundus photography. One subject showed patchy areas of decreased AF signal at the posterior pole extending to the periphery (1/12, 8.3%; patient 7).

SD-OCT images were obtained in 14 affected subjects (patients 2–15), and the representative images are presented in [Figure 3](#). One subject had an epiretinal membrane (patient 3, right). Outer retinal disruption at the fovea and/or parafovea was identified in six subjects (6/14, 42.9%; patients 5, 7, 9, 10, 12, 13), three of whom showed intrachoroidal cavitation (patients 5, left; 10, left; 13). A relatively preserved photoreceptor ellipsoid zone (EZ) line at the fovea was found in six subjects (6/14, 42.9%; patients 2, 3, 6, 8, 11, 15), one of whom showed outer retinal disruption at the parafovea (patient 3).

Visual Fields and Electrophysiological Findings

The detailed findings of visual fields and electrophysiological assessments are described in [Table 3](#). Visual field testing was performed in nine affected subjects (patients 2, 4–9, 12, 13), with Goldmann perimetry (seven subjects) and Humphrey visual field analyzer (four subjects). Central scotoma was detected in eight subjects (8/9, 88.9%; patients 4–9, 12, 13) and paracentral scotoma was observed in all nine subjects (9/9; 100%). Peripheral visual loss was found in four subjects (4/9, 44.4%; patients 2, 5–7).

Full-field electroretinograms were recorded in 14 affected subjects (patients 2–9, 11–15). Multifocal ERGs (mfERGs) were recorded in three subjects (patients 4, 6, 11), and focal macular ERGs (FMERGs) were obtained in one subject (patient 15).

Undetectable light-adapted (LA) responses were demonstrated in seven subjects (7/14, 50.0%; patients 1–3, 5, 7, 11, 13), with undetectable dark-adapted (DA) responses in two subjects (patients 1, 3), severely decreased DA responses in two subjects (patients 2, 7), moderately decreased DA responses in one subject (patient 13), and mildly decreased DA responses in two subjects (patients 5, 11). Severely decreased LA responses were identified in four subjects (4/14, 28.6%; patients 6, 8, 12, 14), with moderately decreased DA responses in one subject (patient 12) and mildly decreased DA responses in three subjects (patients 6, 8, 14). Moderately decreased LA responses with mildly decreased DA responses were shown in one subject (1/14, 7.1%; patient 9). Mildly decreased LA responses with normal DA responses were found in one subject (1/14, 7.1%; patient 4). Normal responses both in LA and DA conditions were noted in one subject (1/14, 7.1%; patient 15). A lower b-to-a ratio (ratio of b wave to a wave for dark-adapted bright flash responses was less than 0.9) was observed in three subjects (3/14, 21.4%; patients 5, 11, 14). Reduced central responses were detected by mfERG in three subjects (patients 4, 6, 11), and reduced central focal responses were demonstrated by FMERGs in one subject (patient 15).

Generalized entire loss of function was identified in two subjects (2/14, 14.3%; patients 1, 3), generalized cone rod dysfunction was found in 11 subjects (11/14, 78.6%; patients 2, 4, 5–9, 11–14), and confined macular dysfunction was noted in one subject (1/14, 7.1%; patient 15).

Phenotype Subgroups

Phenotype subgroup classification was performed in all 15 affected subjects. There were 13 subjects with CORD (13/15, 86.7%; patients 2–14), one with MD (1/15, 6.7%; patient 15), and one with LCA (1/15, 6.7%; patient 1). There were no subjects with RP or SNB.

The mean age of onset of the 13 subjects with CORD/one with MD/one with LCA was 20.0 (range, 0–41)/55/0 years, with the mean duration of disease of 14.7 (range, 0–40)/1.0/16.0 years, respectively. The mean VA for eyes with CORD/MD was 0.73 (range, 0.00–1.52)/0.52 in LogMAR units.

There were two severe CORD subjects with poor VA and severe retinal dysfunction (patients 3, 7), six moderate CORD subjects with intermediate severity of VA or retinal function (patients 2, 4, 5, 9, 13, 14), and three mild CORD subjects with relatively favorable VA and relatively preserved generalized rod function (patients 6, 8, 11). Two subjects with CORD were unavailable for severity assessment because of unavailable VA or electrophysiological data.

Table 3. Visual fields, and Electrophysiological Assessments of 15 Patients with GUCY2D-RD

Patient No.	Phenotype Subgroup	Method	Visual Fields			Comments	Electrophysiological Assessment			
			Central Scotoma	Paracentral Scotoma	Peripheral Visual Field Loss		Responses in Dark-adapted Condition	Responses in Light-adapted Condition	Lower b to a Ratio in Dark-adapted Bright Flash Responses	Comments
1 (MU01-01)	LCA	NA	NA	NA	NA		Undetectable	Undetectable	No	Skin electrodes
2 (TMC01-01)	CORD	GP	No	Yes	Yes	Paracentral relative scotoma	Severely decreased	Undetectable	No	
3 (NU01-01)	CORD	NA	NA	NA	NA		Undetectable	Undetectable	No	Recorded in the right eye
4 (KDU01-01)	CORD	GP/HFA	Yes	Yes	No		WNL	Mildly decreased	NA	Reduced central responses in mfERGs
5 (KDU01-02)	CORD	GP/HFA	Yes	Yes	Yes	Central and paracentral relative scotoma	Mildly decreased	Undetectable	Yes	
6 (GU01-01)	CORD	HFA	Yes	Yes	Yes		Mildly decreased	Severely decreased	No	Reduced central responses in mfERGs
7 (TMC02-01)	CORD	GP	Yes	Yes	Yes		Severely decreased	Undetectable	No	
8 (JU01-01)	CORD	GP	Yes	Yes	No		Mildly decreased	Severely decreased	No	
9 (JU01-02)	CORD	GP/HFA	Yes	Yes	No		Mildly decreased	Moderately decreased	No	
10 (JU01-03)	CORD	NA	NA	NA	NA		NA	NA	NA	
11 (JU02-01)	CORD	NA	NA	NA	NA		Mildly decreased	Undetectable	Yes	Reduced central responses in mfERGs
12 (KDU02-01)	CORD	GP	Yes	Yes	Yes		Moderately decreased	Severely decreased	No	
13 (TMC03-01)	CORD	GP	Yes	Yes	No		Moderately decreased	Undetectable	No	
14 (NU02-01)	CORD	NA	NA	NA	NA		Mildly decreased	Severely decreased	Yes	
15 (MU02-01)	MD	NA	NA	NA	NA		WNL	WNL	No	Reduced central responses in FMERG

FMERG, focal macular electroretinogram; GP, Goldmann kinetic perimetry; HFA, Humphry field analyzer; mfERG, multifocal electroretinogram; WNL, within normal limit.

Lower b to a ratio in dark-adapted bright flash responses was defined as less than 0.9.

Severity of electrophysiological responses were defined as follows; undetectable, more than 90% amplitude reduction compared to the normal reference; severely decreased response, between 90% and 75% amplitude reduction; moderately decreased response, between 75% and 50% amplitude reduction; mildly decreased responses, less than 50% amplitude reduction.

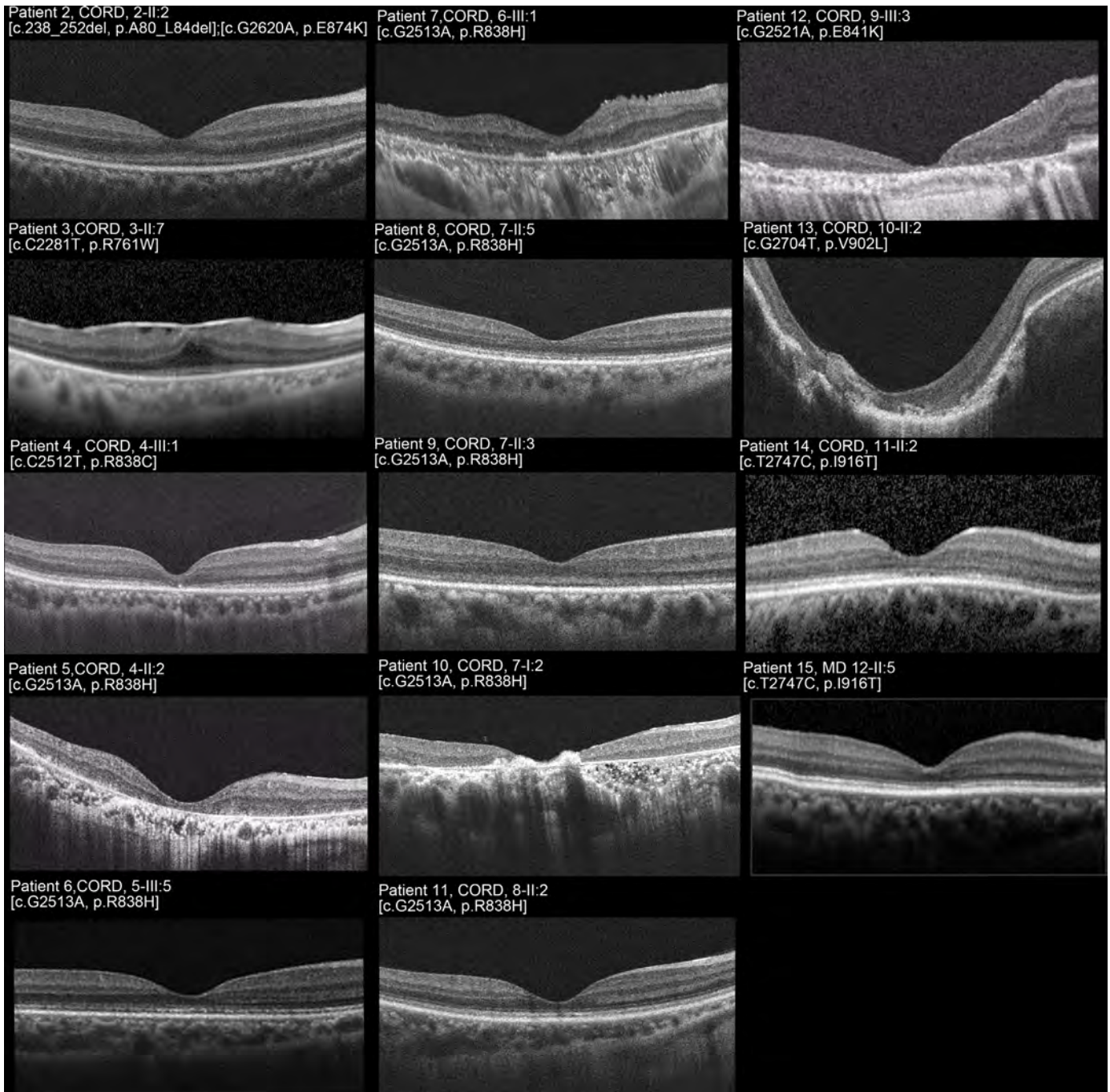


Figure 3. Spectral-domain optical coherence tomographic images of 11 patients with *GUCY2D*-RD (patients 2, 3, 6–11, 13–15). Spectral-domain optical coherence tomography of the right eye demonstrated outer retinal disruption at the fovea in six subjects (patients 5, 7, 9, 10, 12, 13) and at the parafovea in six subjects (patients 3, 5, 7, 10, 12, 13) with intrachoroidal cavitation in one subject (patient 13, right). A relatively preserved photoreceptor ellipsoid zone (EZ) line at the fovea was found in six subjects (patients 2, 3, 6, 8, 11, 15), one of whom showed outer retinal disruption at the parafovea (patient 3). One subject had an epiretinal membrane (patient 3).

GUCY2D Variants

The variant data of 15 affected and seven unaffected subjects from 12 families are summarized in [Table 4](#). Ten *GUCY2D* variants were identi-

fied in the heterozygous state: c.167_168delTG, p.Val56GlyfsTer262; c.238_252del, p.Ala80_Leu84del; c.738G>C, p.Met246Ile; c.2281C>T, p.Arg761Trp; c.2513G>A, p.Arg838His; c.2512C>T, p.Arg838Cys; c.2521G>A, p.Glu841Lys; c.2620G>A, p.Glu874Lys;

Table 4. Summary of Detected Variants of 15 Affected and 7 Unaffected Subjects from 12 Families with *GUCY2D*-RD

Family ID	Subject ID	Affected/ Unaffected	Exon	Nucleotide and Amino Acid Changes	State		
1 (MU01)	1-II:2 (patient 1)	Affected	2	<i>c.167_168delTG, p.Val56GlyfsTer262</i>	Heterozygous		
			3	<i>c.738G>C, p.Met246Ile</i>	Heterozygous		
2 (TMC01)	2-II:2 (patient 2)	Affected	2	<i>c.238_252del, p.Ala80_Leu84del</i>	Compound heterozygous		
			14	<i>c.2620G>A, p.Glu874Lys</i>			
			14	<i>c.2620G>A, p.Glu874Lys</i>	Heterozygous		
3 (NU01)	2-I:2	Unaffected	2	<i>c.226_240del, p.Ala76_Ala80del</i>	Heterozygous		
			3-II:7 (patient 3)	Affected	12	<i>c.2281C>T, p.Arg761Trp</i>	Heterozygous
4 (KDU01)	4-III:1 (patient 4)	Affected	13	<i>c.2512C>T, p.Arg838Cys</i>	Heterozygous		
			4-II:2 (patient 5)	Affected	13	<i>c.2512C>T, p.Arg838Cys</i>	Heterozygous
5 (GU01)	4-II:1	Unaffected	13	<i>c.2512C>T, p.Arg838Cys</i>	ND		
			5-III:5 (patient 6)	Affected	13	<i>c.2513G>A, p.Arg838His</i>	Heterozygous
6 (TMC02)	6-III:1 (patient 7)	Affected	13	<i>c.2513G>A, p.Arg838His</i>	Heterozygous		
7 (JU01)	7-II:5 (patient 8)	Affected	13	<i>c.2513G>A, p.Arg838His</i>	Heterozygous		
			7-II:3 (patient 9)	Affected	13	<i>c.2513G>A, p.Arg838His</i>	Heterozygous
			7-I:2 (patient 10)	Affected	13	<i>c.2513G>A, p.Arg838His</i>	Heterozygous
8 (JU02)	8-II:2 (patient 11)	Affected	13	<i>c.2513G>A, p.Arg838His</i>	Heterozygous (de novo)		
			8-I:2	Unaffected	13	<i>c.2513G>A, p.Arg838His</i>	ND
			8-I:1	Unaffected	13	<i>c.2513G>A, p.Arg838His</i>	ND
9 (KDU02)	9-III:3 (patient 12)	Affected	13	<i>c.2521G>A, p.Glu841Lys</i>	Heterozygous		
10 (TMC03)	10-II:2 (patient 13)	Affected	14	<i>c.2704G>T, p.Val902Leu</i>	Heterozygous (de novo)		
			10-I:2	Unaffected	14	<i>c.2704G>T, p.Val902Leu</i>	ND
			10-I:1	Unaffected	14	<i>c.2704G>T, p.Val902Leu</i>	ND
11 (NU02)	11-II:2 (patient 14)	Affected	14	<i>c.2747T>C, p.Ile916Thr</i>	Heterozygous		
12 (MU02)	12-II:5 (patient 15)	Affected	14	<i>c.2747T>C, p.Ile916Thr</i>	Heterozygous		

GUCY2D transcript ID: NM_000180.3

ND, not detected

Novel variants are shown in italic.

Whole-exome sequencing with targeted analysis for retinal disease-causing genes on RetNET (<https://sph.uth.edu/retnet/>) was performed in 15 affected and 7 unaffected subjects from 12 families.

c.2704G>T, p.Val902Leu; and *c.2747T>C, p.Ile916Thr* (NM_000180.3).

There were eight missense variants, one with a 2-bp deletion leading to a frame shift, and one with an in-frame deletion. Three variants were identified in multiple families: *p.Arg838Cys* (families 4, 5), *p.Arg838His* (families 6–8), and *p.Ile916Thr* (families 11, 12). Intrafamilial cosegregation analysis was performed in five families (families 2, 4, 7, 8, 10), and the de novo (patient 11, *p.Arg838His*; patient 10, *p.Val902Leu*), compound heterozygous (patient 2; *p.Ala80_Leu84del, p.Glu874Lys*), and heterozygous (patient 4, *p.Arg838Cys*; patient 8, *p.Arg838His*; patient 11, *p.Arg838His*) states were confirmed.

GUCY2D-RD caused by six detected variants has been reported before: CORD for *p.Ala80_Leu84del*⁹; ADCORD for *p.Arg838His*;^{34,38} ADCORD for *p.Arg838Cys*;^{29,34} ADCORD for *p.Glu841Lys*;³⁰ ADCORD for *p.Val902Leu*;³¹ ADCORD for *p.Ile916Thr*.³² Four variants have never been reported; *p.Val56GlyfsTer262, p.Met246Ile, p.Arg761Trp,* and *p.Glu874Lys*.

In Silico Molecular Genetic Analysis

The detailed results of in silico molecular genetic analyses for the 10 detected *GUCY2D* variants are

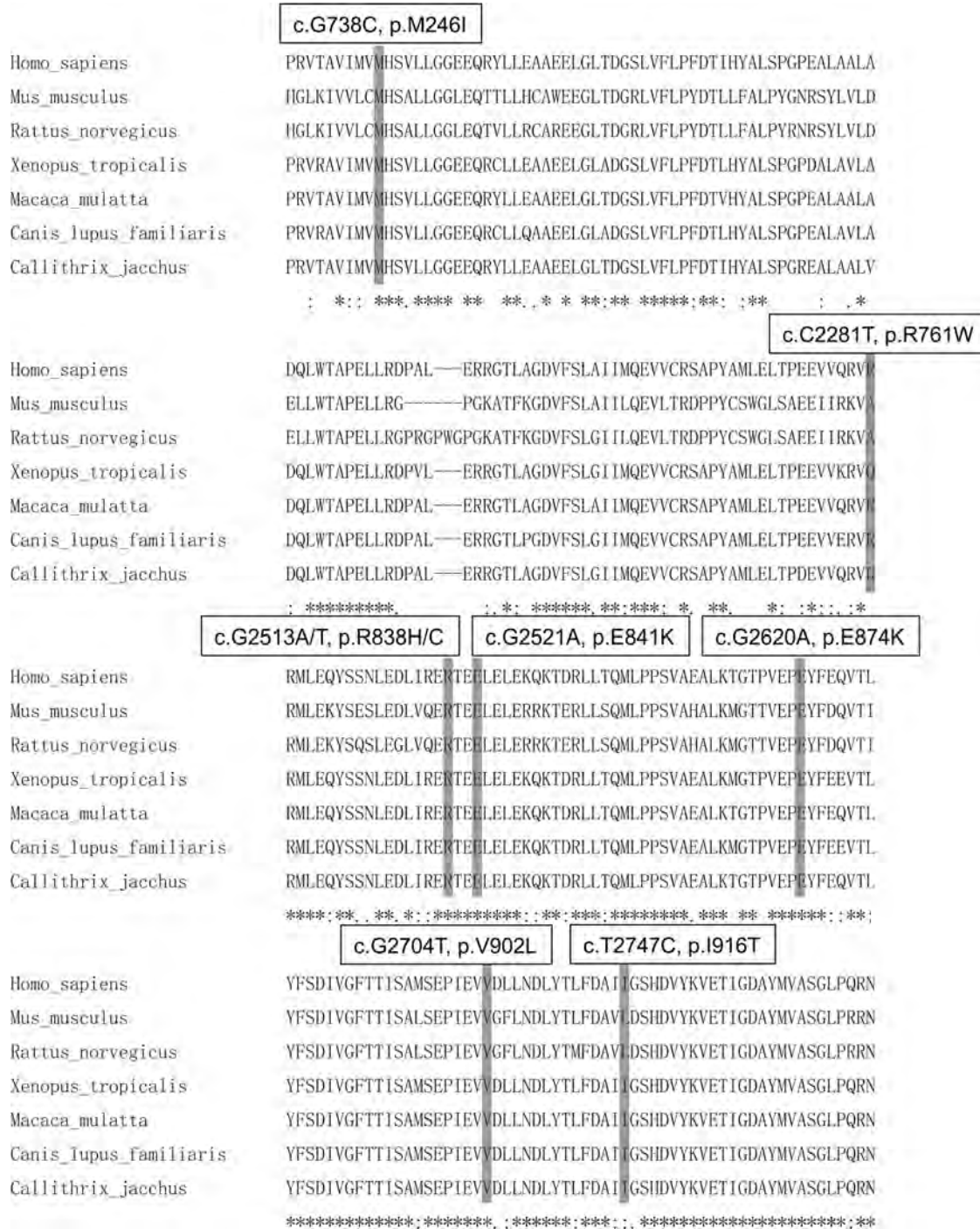


Figure 4. Multiple alignment of eight species of *GUCY2D*. The alignment was performed with the Clustal Omega program (<https://www.ebi.ac.uk/Tools/msa/clustalo/>) and the amino-acid-sequence alignment was numbered in accordance with the Homo sapiens *GUCY2D* sequence (ENST00000254854.4). *Complete conservation across the eight species. The positions of eight missense variant residues are highlighted with gray background: p.Met246Ile, p.Arg761Trp, p.Arg838His, p.Arg838Cys, p.Glu841Lys, p.Glu874Lys, p.Val902Leu, and p.Ile916.

presented in Supplementary Tables S1 and S2. A schematic genetic and protein structure of *GUCY2D* and multiple alignments of eight species of *GUCY2D* are shown in Figures 4 and 5.

Seven variants are located in exons 12-14 (p.Arg761Trp, p.Arg838His, p.Arg838Cys, p.Glu841Lys, p.Glu874Lys, p.Val902Leu, p.Ile916Thr), which are presumably associated

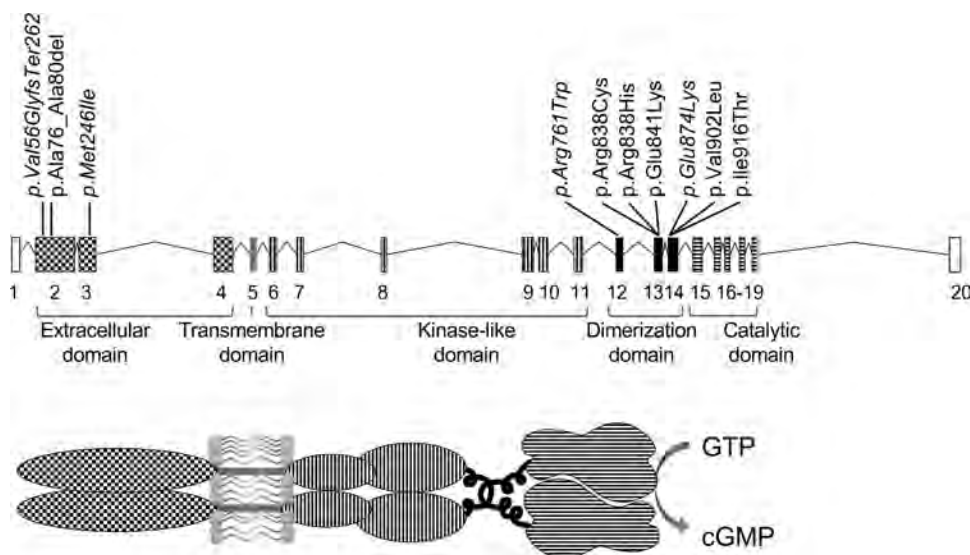


Figure 5. A schematic genetic and protein structure of *GUCY2D* and the location of the detected variants. The *GUCY2D* gene (ENST00000254854.4) contains 20 exons that encode a protein containing an extracellular domain, transmembrane domain, kinase-like domain, dimerization domain, catalytic domain, and others (Lazar et al., 2014). The 10 variants detected in this study are presented. The four novel variants are shown: p.Val56GlyfsTer262, p.Met246Ile, p.Arg761Trp, and p.Glu874Lys.

with the dimerization domain in the *GUCY2D* protein, and the other missense variant was in exon 3, which is associated with the extracellular domain (Fig. 4). Complete evolutionary conservation was confirmed in six missense variants (p.Met246Ile, p.Arg838His, p.Arg838Cys, p.Glu841Lys, p.Glu874Lys, p.Val902Leu) and relatively high conservation was found in two variants (p.Arg761Trp, p.Ile916Thr) (Fig. 5).

The allele frequency available for three *GUCY2D* variants (p.Ala80_Leu84del, p.Arg761Trp, and p.Arg838Cys) in the East Asian/South Asian/African/European (non-Finnish) general population was 0.0%/0.000055%/0.00085%/0.0%, 0.0%/0.0%/0.0%/0.000045%, and 0.0%/0.0%/0.0%/0.0%, respectively. All detected *GUCY2D* variants were not found in the general Japanese population according to the HGVD and iJGVD databases.

General prediction, functional prediction, and conservation were assessed for the 10 *GUCY2D* variants, and the pathogenicity classification according to the American College of Medical Genetics and Genomics guidelines was pathogenic for the four missense variants (p.Arg838His, p.Arg838Cys, p.Glu841Lys, p.Val902Leu); likely pathogenic for the truncating variant, the in-frame deletion variant, and the missense variant (p.Val56GlyfsTer262, p.Ala80_Leu84del, p.Ile916Thr, respectively); and

uncertain significance for the three missense variants (p.Met246Ile, p.Arg761Trp, p.Glu874Lys).

Overall, 10 disease-causing variants in the *GUCY2D* gene were ascertained in nine families with ADCORD, one family with ARCORD, one family with MD, and one family with ARLCA. Together with the clinical features of the affected subjects and the models of inheritance in the pedigree, 10 disease-causing variants in the *GUCY2D* gene were determined.

Discussion

The detailed clinical and genetic characteristics of a cohort of 15 affected subjects from 12 families with *GUCY2D*-RD are illustrated in a nationwide cohort with IRD in Japan. Different clinical presentations were identified with different inheritance patterns, including ADCORD with various severities, severe ARLCA, severe ARCORD, and mild ADMD.

To our knowledge, this large cohort of *GUCY2D*-RD patients includes the highest number of ADCORD patients to date. Four of 30 families (13.3%) with ADCORD/MD/STGD in the JEGC IRD cohort were associated with AD*GUCY2D*-CORD. The proportion of *GUCY2D*-RD in molecularly confirmed ADCORD/MD/STGD in the JEGC cohort was 27.2% (6/22 families). In a previous report of a Chinese cohort, Jiang et al. reported nine unrelated probands

with *GUCY2D*-RD ascertained from 74 probands with COD (9/74, 12.2%) and seven of 15 ADCORD families had *GUCY2D*-RD (7/15, 46.7%).³⁷ The proportion of *GUCY2D*-RD in molecularly confirmed ADCORD was 34.6% in a UK cohort and 29.4% in a French cohort.^{5,48} Given these results, the prevalence of *GUCY2D*-RD for COD in Japan was not as high as that in other populations in Asia or Europe; however, *GUCY2D*-RD is a major cause of the ADCORD.

One family with ARLCA was ascertained from 41 families with AR or sporadic LCA in the JEGC cohort (1/41 families, 2.4%). The proportion of *GUCY2D*-RD for molecularly confirmed LCA in the JEGC cohort was 5.3% (1/19 families). Hosono et al. reported two families with ARLCA in 34 Japanese families with LCA (2/34, 5.9%).³⁶ In previous reports of Chinese cohorts, Wang et al. reported the prevalence of *GUCY2D*-RD as 10.7% (14/131 LCA families), and Xu et al. reported the prevalence as 10.7% (17/159 LCA families).^{49,50} In European cohorts, *GUCY2D*-RD accounts for approximately 10% to 20% of LCA.⁴ These findings imply the low prevalence of ARLCA in the Japanese population, although data from a larger cohort of ARGUCY2D-LCA patients are still to draw conclusions.

In the present study of Japanese *GUCY2D*-RD, there were no patients with SNB. There was one 12-year-old subject with night blindness, favorable VA, normal fundus, and compound heterozygous *GUCY2D* variants (patient 2). These findings were consistent with the spectrum of SNB; however, this subject demonstrated undetectable generalized cone function with severely decreased rod function, which is not compatible with the striking ERG features of SNB (undetectable rod responses with identical traces for a single cone and DA bright flash ERGs).⁴⁰

Thirteen affected subjects from nine families with molecularly confirmed *GUCY2D*-associated ADCORD demonstrated various findings, in terms of onset (0-41 years), the duration of disease (0-40 years), VA (0.0-1.52) in LogMAR units, fundus appearance (normal to extended atrophy, without/with intrachoroidal cavitation), and morphological finding (EZ preservation at the fovea to outer retinal disruption at the macula and paramacula); however, ocular symptoms such as reduced VA/poor VA, photophobia, and the pattern of dysfunction in electrophysiology with early involvement of generalized cone function were commonly shared.

Several reports have described patients with COD/CORD showing a coloboma-like macular atrophy caused by pathogenic variants in several genes, such as *NMNAT1*,^{51,52} *ADAM9*,⁵³ *GUCAIA*,⁵⁴ and

GUCY2D.⁵⁵ In the present study, an intrachoroidal cavitation resembling coloboma-like macular atrophy was presented in three subjects bilaterally or unilaterally. Poor visual acuity was observed in the eyes with intrachoroidal cavitation; thus, this striking finding implies severe central visual loss. The mechanism that causes the coloboma-like macular atrophy/intrachoroidal cavitation remains uncertain.

All eight subjects with normal or subtle changes demonstrated generalized retinal dysfunction (patients 2-4, 6, 8, 9, 11, 14), which is crucial to make a clinical diagnosis of *GUCY2D*-RD. Interestingly, a lower b-to-a ratio in dark-adapted bright flash responses was identified in three subjects (3/14, 21.4%). This electronegative finding is also observed in the early stage of other COD and may not be specific for *GUCY2D*-RD.^{11-13,16,56} These findings are consistent with previous reports of ADGUCY2D-CORD.^{20,34,37,38} Therefore, comprehensive clinical investigations, including electrophysiological assessments, are essential for the diagnosis and monitoring of *GUCY2D*-RD.

Ten *GUCY2D* variants were identified in our cohort, including six previously reported and four novel variants. Six pathogenic and three likely pathogenic variants have been previously reported, and the phenotype subgroups determined in our cohort were compatible with those of the previous reports, whereas the phenotype subgroup for p.Ile916Thr in our cohort was MD, and the phenotype subgroup for this variant in the previous report was COD. Two variants (p.Arg838His, p.Val902Leu) were found in the de novo state in our cohort (patients 11, 13), and these variants were also identified as de novo in the previous report.^{31,39} Because haplotype analysis around these variants was not performed, the possibility of the nonpaternity cannot be formally excluded in these families (families 8, 10). Therefore, it is more precise to describe these variants not found in parents as “most likely de novo.” A different inheritance pattern of ADCORD was described for p.Ala80_Leu84del in the previous report⁹; however, the detailed information of the parents of the proband was not shown. Thus, the disease causation by this variant, in our case with AR inheritance (patient 2), is still unclear.

Four novel *GUCY2D* variants were found in our cohort: one variant with likely pathogenic frameshift (p.Val56GlyfsTer262) and three variants of uncertain significance (p.Met246Ile, p.Arg761Trp, p.Glu874Lys). Two variants in the compound heterozygous state (p.Val56GlyfsTer262, p.Met246Ile) were found in a subject with ARLCA (Patient 1). Because there are no candidate variants for the other ARLCA-associated genes, the putative causation of these

two *GUCY2D* variants is predicted. One missense variant (p.Arg761Trp) was found in a subject with night blindness, normal fundus, relatively preserved foveal structure, and a loss of generalized retinal function. Although there were no candidate variants causative for *ARRP*, *ARCORD*, and *ARLCA*, further detailed analyses with more samples/information of the other family members are required to decide the conclusive genetic diagnosis. Another missense variant (p.Glu874Lys) was identified with the aforementioned in-frame deletion variant (p.Ala80_Leu84del) in a subject with *ARCORD* (patient 2). Given the clinically examined unaffected mother harboring this variant (p.Glu874Lys), the possibility that the disease was caused by this variant in an AR manner cannot be excluded.

This study has several limitations. The selection bias related to disease severity is inherent because it is uncommon for genetically affected subjects with good vision to visit clinics or hospitals. The resources of clinical information or genomic DNA from unaffected family members are limited in our cohort, and it was hard to conclusively determine the inheritance pattern in most families. Further information on clinical and genetic assessment both in affected and unaffected subjects could improve the accuracy of clinical inheritance, as well as molecularly confirmed inheritance.

The data of the current study were obtained from the JEGC IRD database. The clinical data from patients registered from multiple institutions were uploaded into the database and shared among the JEGC study group. However, the examination devices used at the different institutions could have been different because the diagnostic criteria and monitoring methods were shared. It is of note that the information was collected retrospectively, and that some of the interpatient variability may be due to differences in methods of testing patients in different institutions. Therefore, a detailed quantitative analysis could not be performed.

WES with targeted analysis applied in the current study could miss the disease-causing variants in the genes outside of the target (301 retinal disease-associated genes) and structural variants, including large deletions in the target region. More comprehensive gene screening and analysis by methods such as long-read whole-genome sequencing could help to determine the genetic aberrations, including structural and noncoding variants, in our cohort. The molecular mechanisms of some AD missense, AR missense, and AR in-frame deletion variants have not yet been clarified, and further functional investigation for each variant is required to draw conclusions on the disease causation.

In conclusion, this nationwide large cohort study delineates the clinical and genetic characteristics of *GUCY2D*-RD, including nine *ADCORD* families, one *ARCORD* family, one MD family, and one *ARLCA* family. Diverse clinical presentations with various severities were demonstrated in *ADCORD*, and an early-onset severe phenotype was shown in *ARLCA*. A relatively low prevalence of *GUCY2D*-RD for *ADCORD* and *ARLCA* in the Japanese population was identified compared to the other populations. This information helps to monitor and counsel patients, especially in East Asia, as well as to design future therapeutic approaches.

Acknowledgments

We thank Kazuki Yamazawa and Satomi Inoue, National Institute of Sensory Organs, National Tokyo Medical Center, Japan, for their help in the clinical genetic data analysis.

The laboratory of Visual Physiology, Division for Vision Research, National Institute of Sensory Organs, National Hospital Organization, Tokyo Medical Center, Tokyo, Japan is supported by grants from Astellas Pharma Inc. (NCT03281005), outside the submitted work. Supported by grants from Grant-in-Aid for Young Scientists (A) of the Ministry of Education, Culture, Sports, Science and Technology, Japan (16H06269); grants from Grant-in-Aid for Scientists to support international collaborative studies of the Ministry of Education, Culture, Sports, Science and Technology, Japan (16KK01930002); grants from the National Hospital Organization Network Research Fund (H30-NHO-Sensory Organs-03); grants from FOUNDATION FIGHTING BLINDNESS ALAN LATIES CAREER DEVELOPMENT PROGRAM (CF-CL-0416-0696-UCL); grants from Health Labour Sciences Research Grant, the Ministry of Health, Labour and Welfare (201711107A); and grants from the Great Britain Sasakawa Foundation Butterfield Awards (KF). Supported by grants from Grant-in-Aid for Young Scientists of the Ministry of Education, Culture, Sports, Science and Technology, Japan (18K16943) (YF-Y). Supported by a Fight for Sight (UK) early career investigator award, NIHR-BRC at Moorfields Eye Hospital and the UCL Institute of Ophthalmology, NIHR-BRC at Great Ormond Street Hospital and UCL Institute of Child Health, and Great Britain Sasakawa Foundation Butterfield Award, UK (GA). Funded by the NIHR-BRC at Moorfields Eye Hospital and the UCL Institute of Ophthalmology (NP). Supported by Tsubota Laboratory, Inc, Fuji

Xerox Co., Ltd, Kirin Company, Ltd, Kowa Company, Ltd, Novartis Pharmaceuticals, Santen Pharmaceutical Co. Ltd, and ROHTO Pharmaceutical Co.,Ltd. (TK). Supported by the Japan Agency for Medical Research and Development (AMED) (18ek0109282h0002) (TI). Supported by AMED; the Ministry of Health, Labor and Welfare, Japan (18ek0109282h0002); Grants-in-Aid for Scientific Research, Japan Society for the Promotion of Science, Japan (H26-26462674); grants from the National Hospital Organization Network Research Fund, Japan (H30-NHO-Sensory Organs-03) and Novartis Research Grant (2018) (KT). The funding sources had no role in the design and conduct of the study; the collection, management, analysis, and interpretation of the data; the preparation, review, and approval of the manuscript; or the decision to submit the manuscript for publication.

Kaoru Fujinami has full access to all the data in the study and takes responsibility for the integrity of the data and the accuracy of the data analysis. Research design: Xiao Liu, Kaoru Fujinami, Lizhu Yang, Yu Fujinami-Yokokawa, Kazushige Tsunoda. Data acquisition and/or research execution: All authors. Data analysis and/or interpretation: All authors. Manuscript preparation: Xiao Liu, Kaoru Fujinami, Lizhu Yang, Yu Fujinami-Yokokawa, Gavin Arno, Nikolas Pontikos, Kazushige Tsunoda.

Disclosure: **X. Liu**, None; **K. Fujinami**, Astellas Pharma Inc. (C, F), Kubota Pharmaceutical Holdings Co. Ltd (C, F), Acucela Inc. (C, F), Novartis AG (C), Janssen Pharmaceutical K.K. (C), NightStar (C, F), SANTEN Company Limited (F), Foundation Fighting Blindness (F), Foundation Fighting Blindness Clinical Research Institute (F), Japanese Ophthalmology Society (F), Japan Retinitis Pigmentosa Society (F); **K. Kuniyoshi**, None; **M. Kondo**, None; **S. Ueno**, None; **T. Hayashi**, None; **K. Mochizuki**, None; **S. Kameya**, None; **L. Yang**, None; **Y. Fujinami-Yokokawa**, None; **G. Arno**, None; **N. Pontikos**, None; **H. Sakuramoto**, None; **T. Kominami**, None; **H. Terasaki**, None; **S. Katagiri**, None; **K. Mizobuchi**, None; **N. Nakamura**, None; **K. Yoshitake**, None; **Y. Miyake**, None; **S. Li**, None; **T. Kurihara**, Tsubota Laboratory, Inc. (F), Fuji Xerox Co., Ltd. (F), Kirin Company, Ltd. (F), Kowa Company, Ltd. (F), Novartis Pharmaceuticals (F), Santen Pharmaceutical Co., Ltd. (F), ROHTO Pharmaceutical Co., Ltd. (F); **K. Tsubota**, None; **T. Iwata**, None; **K. Tsunoda**, None

* XL and KF are joint first authors.

References

1. Liew G, Michaelides M, Bunce C. A comparison of the causes of blindness certifications in England and Wales in working age adults (16-64 years), 1999-2000 with 2009-2010. *BMJ Open*. 2014;4:e004015.
2. Tee JJ, Smith AJ, Hardcastle AJ, Michaelides M. RPGR-associated retinopathy: clinical features, molecular genetics, animal models and therapeutic options. *Br J Ophthalmol*. 2016;100:1022-1027.
3. Hirji N, Aboshiha J, Georgiou M, Bainbridge J, Michaelides M. Achromatopsia: clinical features, molecular genetics, animal models and therapeutic options. *Ophthalmic Genet*. 2018;39:149-157.
4. Kumaran N, Pennesi ME, Yang P, et al. Leber congenital amaurosis/early-onset severe retinal dystrophy overview. In: Adam MP, Ardinger HH, Pagon RA, et al. (eds), *GeneReviews*(*(R)*). Seattle (WA); 2018.
5. Gill JS, Georgiou M, Kalitzeos A, Moore AT, Michaelides M. Progressive cone and cone-rod dystrophies: clinical features, molecular genetics and prospects for therapy. *Br J Ophthalmol*. 2019;103:711-720.
6. Tanna P, Strauss RW, Fujinami K, Michaelides M. Stargardt disease: clinical features, molecular genetics, animal models and therapeutic options. *Br J Ophthalmol*. 2017;101:25-30.
7. Neveling K, Collin RW, Gilissen C, et al. Next-generation genetic testing for retinitis pigmentosa. *Hum Mutat*. 2012;33:963-972.
8. Stone EM, Andorf JL, Whitmore SS, et al. Clinically focused molecular investigation of 1000 consecutive families with inherited retinal disease. *Ophthalmology*. 2017;124:1314-1331.
9. Carss KJ, Arno G, Erwood M, et al. Comprehensive rare variant analysis via whole-genome sequencing to determine the molecular pathology of inherited retinal disease. *Am J Hum Genet*. 2017;100:75-90.
10. Michaelides M, Hardcastle AJ, Hunt DM, Moore AT. Progressive cone and cone-rod dystrophies: phenotypes and underlying molecular genetic basis. *Surv Ophthalmol*. 2006;51:232-258.
11. Fujinami K, Lois N, Davidson AE, et al. A longitudinal study of Stargardt disease: clinical and electrophysiologic assessment, progression, and genotype correlations. *Am J Ophthalmol*. 2013;155:1075-1088 e1013.

12. Fujinami K, Sergouniotis PI, Davidson AE, et al. The clinical effect of homozygous ABCA4 alleles in 18 patients. *Ophthalmology*. 2013;120:2324–2331.
13. Hull S, Arno G, Plagnol V, et al. The phenotypic variability of retinal dystrophies associated with mutations in *CRX*, with report of a novel macular dystrophy phenotype. *Invest Ophthalmol Vis Sci*. 2014;55:6934–6944.
14. Oishi M, Oishi A, Gotoh N, et al. Comprehensive molecular diagnosis of a large cohort of Japanese retinitis pigmentosa and Usher syndrome patients by next-generation sequencing. *Invest Ophthalmol Vis Sci*. 2014;55:7369–7375.
15. Arai Y, Maeda A, Hirami Y, et al. Retinitis pigmentosa with *EYS* mutations is the most prevalent inherited retinal dystrophy in Japanese populations. *J Ophthalmol*. 2015;2015:819760.
16. Fujinami K, Zernant J, Chana RK, et al. Clinical and molecular characteristics of childhood-onset Stargardt disease. *Ophthalmology*. 2015;122:326–334.
17. Nakanishi A, Ueno S, Hayashi T, et al. Clinical and genetic findings of autosomal recessive bestrophinopathy in Japanese cohort. *Am J Ophthalmol*. 2016;168:86–94.
18. Oishi M, Oishi A, Gotoh N, et al. Next-generation sequencing-based comprehensive molecular analysis of 43 Japanese patients with cone and cone-rod dystrophies. *Mol Vis*. 2016;22:150–160.
19. Perrault I, Rozet JM, Calvas P, et al. Retinal-specific guanylate cyclase gene mutations in Leber's congenital amaurosis. *Nat Genet*. 1996;14:461–464.
20. Sharon D, Wimberg H, Kinarty Y, Koch KW. Genotype-functional-phenotype correlations in photoreceptor guanylate cyclase (GC-E) encoded by *GUCY2D*. *Prog Retin Eye Res*. 2018;63:69–91.
21. Goraczniak RM, Duda T, Sitaramayya A, Sharma RK. Structural and functional characterization of the rod outer segment membrane guanylate cyclase. *Biochem J*. 1994;302(Pt 2):455–461.
22. Yang RB, Foster DC, Garbers DL, Fulle HJ. Two membrane forms of guanylyl cyclase found in the eye. *Proc Natl Acad Sci USA*. 1995;92:602–606.
23. Goraczniak R, Duda T, Sharma RK. Structural and functional characterization of a second subfamily member of the calcium-modulated bovine rod outer segment membrane guanylate cyclase, ROS-GC2. *Biochem Biophys Res Commun*. 1997;234:666–670.
24. Pugh EN, Jr., Duda T, Sitaramayya A, Sharma RK. Photoreceptor guanylate cyclases: a review. *Biosci Rep*. 1997;17:429–473.
25. Dizhoor AM, Hurley JB. Regulation of photoreceptor membrane guanylyl cyclases by guanylyl cyclase activator proteins. *Methods*. 1999;19:521–531.
26. Hunt DM, Buch P, Michaelides M. Guanylate cyclases and associated activator proteins in retinal disease. *Mol Cell Biochem*. 2010;334:157–168.
27. Camuzat A, Dollfus H, Rozet JM, et al. A gene for Leber's congenital amaurosis maps to chromosome 17p. *Hum Mol Genet*. 1995;4:1447–1452.
28. Downes SM, Payne AM, Kelsell RE, et al. Autosomal dominant cone-rod dystrophy with mutations in the guanylate cyclase 2D gene encoding retinal guanylate cyclase-1. *Arch Ophthalmol*. 2001;119:1667–1673.
29. Kelsell RE, Gregory-Evans K, Payne AM, et al. Mutations in the retinal guanylate cyclase (*RETGC-1*) gene in dominant cone-rod dystrophy. *Hum Mol Genet*. 1998;7:1179–1184.
30. Lazar CH, Mutsuddi M, Kimchi A, et al. Whole exome sequencing reveals *GUCY2D* as a major gene associated with cone and cone-rod dystrophy in Israel. *Invest Ophthalmol Vis Sci*. 2014;56:420–430.
31. Wimberg H, Lev D, Yosovich K, et al. Photoreceptor guanylate cyclase (*GUCY2D*) mutations cause retinal dystrophies by severe malfunction of Ca(2+)-dependent cyclic GMP synthesis. *Front Mol Neurosci*. 2018;11:348.
32. de Castro-Miro M, Pomares E, Lores-Motta L, et al. Combined genetic and high-throughput strategies for molecular diagnosis of inherited retinal dystrophies. *PLoS One*. 2014;9:e88410.
33. Ito S, Nakamura M, Nuno Y, Ohnishi Y, Nishida T, Miyake Y. Novel complex *GUCY2D* mutation in Japanese family with cone-rod dystrophy. *Invest Ophthalmol Vis Sci*. 2004;45:1480–1485.
34. Ito S, Nakamura M, Ohnishi Y, Miyake Y. Autosomal dominant cone-rod dystrophy with R838H and R838C mutations in the *GUCY2D* gene in Japanese patients. *Jpn J Ophthalmol*. 2004;48:228–235.
35. Hosono K, Harada Y, Kurata K, et al. Novel *GUCY2D* gene mutations in Japanese male twins with Leber congenital amaurosis. *J Ophthalmol*. 2015;2015:693468.
36. Hosono K, Nishina S, Yokoi T, et al. Molecular diagnosis of 34 Japanese families with Leber congenital amaurosis using targeted next generation sequencing. *Sci Rep*. 2018;8:8279.
37. Jiang F, Xu K, Zhang X, Xie Y, Bai F, Li Y. *GUCY2D* mutations in a Chinese cohort with autosomal dominant cone or cone-rod dystrophies. *Doc Ophthalmol*. 2015;131:105–114.
38. Payne AM, Morris AG, Downes SM, et al. Clustering and frequency of mutations in the retinal

- guanylate cyclase (*GUCY2D*) gene in patients with dominant cone-rod dystrophies. *J Med Genet.* 2001;38:611–614.
39. Mukherjee R, Robson AG, Holder GE, et al. A detailed phenotypic description of autosomal dominant cone dystrophy due to a de novo mutation in the *GUCY2D* gene. *Eye (Lond).* 2014;28:481–487.
 40. Stunkel ML, Brodie SE, Cideciyan AV, et al. Expanded retinal disease spectrum associated with autosomal recessive mutations in *GUCY2D*. *Am J Ophthalmol.* 2018;190:58–68.
 41. Fujinami K, Kameya S, Kikuchi S, et al. Novel *RP1L1* variants and genotype-photoreceptor microstructural phenotype associations in cohort of Japanese patients with occult macular dystrophy. *Invest Ophthalmol Vis Sci.* 2016;57:4837–4846.
 42. Hood DC, Bach M, Brigell M, et al. ISCEV standard for clinical multifocal electroretinography (mfERG) (2011 edition). *Doc Ophthalmol.* 2012;124:1–13.
 43. McCulloch DL, Marmor MF, Brigell MG, et al. Erratum to: ISCEV Standard for full-field clinical electroretinography (2015 update). *Doc Ophthalmol.* 2015;131:81–83.
 44. McCulloch DL, Marmor MF, Brigell MG, et al. ISCEV Standard for full-field clinical electroretinography (2015 update). *Doc Ophthalmol.* 2015;130:1–12.
 45. Terasaki H, Miyake Y, Nomura R, et al. Focal macular ERGs in eyes after removal of macular ILM during macular hole surgery. *Invest Ophthalmol Vis Sci.* 2001;42:229–234.
 46. Pontikos N, Yu J, Moghul I, et al. Phenopolis: an open platform for harmonization and analysis of genetic and phenotypic data. *Bioinformatics.* 2017;33:2421–2423.
 47. Richards S, Aziz N, Bale S, et al. Standards and guidelines for the interpretation of sequence variants: a joint consensus recommendation of the American College of Medical Genetics and Genomics and the Association for Molecular Pathology. *Genet Med.* 2015;17:405–424.
 48. Boulanger-Scemama E, El Shamieh S, Demontant V, et al. Next-generation sequencing applied to a large French cone and cone-rod dystrophy cohort: mutation spectrum and new genotype-phenotype correlation. *Orphanet J Rare Dis.* 2015;10:85.
 49. Wang H, Wang X, Zou X, et al. Comprehensive molecular diagnosis of a large Chinese Leber congenital amaurosis cohort. *Invest Ophthalmol Vis Sci.* 2015;56:3642–3655.
 50. Xu Y, Xiao X, Li S, et al. Molecular genetics of Leber congenital amaurosis in Chinese: new data from 66 probands and mutation overview of 159 probands. *Exp Eye Res.* 2016;149:93–99.
 51. Falk MJ, Zhang Q, Nakamaru-Ogiso E, et al. *NMNAT1* mutations cause Leber congenital amaurosis. *Nat Genet.* 2012;44:1040–1045.
 52. Nash BM, Symes R, Goel H, et al. *NMNAT1* variants cause cone and cone-rod dystrophy. *Eur J Hum Genet.* 2018;26:428–433.
 53. El-Haig WM, Jakobsson C, Favez T, Schorderet DF, Abouzeid H. Novel *ADAM9* homozygous mutation in a consanguineous Egyptian family with severe cone-rod dystrophy and cataract. *Br J Ophthalmol.* 2014;98:1718–1723.
 54. Kamenarova K, Corton M, Garcia-Sandoval B, et al. Novel *GUCA1A* mutations suggesting possible mechanisms of pathogenesis in cone, cone-rod, and macular dystrophy patients. *Biomed Res Int.* 2013;2013:517570.
 55. Xu F, Dong F, Li H, Li X, Jiang R, Sui R. Phenotypic characterization of a Chinese family with autosomal dominant cone-rod dystrophy related to *GUCY2D*. *Doc Ophthalmol.* 2013;126:233–240.
 56. Khan KN, Kasilian M, Mahroo OAR, et al. Early patterns of macular degeneration in *ABCA4*-associated retinopathy. *Ophthalmology.* 2018;125:735–746.



RESEARCH ARTICLE

Clinical and genetic characteristics of Stargardt disease in a large Western China cohort: Report 1

Xiao Liu^{1,2,3} | Xiaohong Meng¹ | Lizhu Yang^{2,3} | Yanling Long¹ |
Yu Fujinami-Yokokawa^{2,4,5} | Jiayun Ren¹ | Toshihide Kurihara³ | Kazuo Tsubota³ |
Kazushige Tsunoda² | Kaoru Fujinami^{2,3,6,7} | Shiyong Li¹ | East Asia Inherited
Retinal Disease Society Study Group

¹Southwest Hospital/Southwest Eye Hospital, Third Military Medical University (Army Medical University), Chongqing, China

²Laboratory of Visual Physiology, Division of Vision Research, National Institute of Sensory Organs, National Hospital Organization Tokyo Medical Center, Tokyo, Japan

³Department of Ophthalmology, Keio University School of Medicine, Tokyo, Japan

⁴Department of Health Policy and Management, Keio University School of Medicine, Tokyo, Japan

⁵Department of Public Health Research, Yokokawa Clinic, Osaka, Japan

⁶UCL Institute of Ophthalmology, London, UK

⁷Moorfields Eye Hospital, London, UK

Correspondence

Kaoru Fujinami, 2-5-1, Higashigaoka, Meguro-ku, Laboratory of Visual Physiology, Division for Vision Research, National Institute of Sensory Organs, National Hospital Organization, Tokyo Medical Center, Tokyo 152-8902 Japan.
Email: k.fujinami@ucl.ac.uk

Shiyong Li, Southwest Hospital/Southwest Eye Hospital, Third Military Medical University (Army Medical University), No. 30 Gaotanyan Street, Shapingba District, Chongqing 400038, P.R. China.
Email: shiyong_li@126.com

Funding information

Chongqing Social and Livelihood Science Innovation grant, Grant/Award Number: cstc2017shmsA130100; Foundation for Fighting Blindness - Alan Lattes Career Development Program, Grant/Award Number: CF-CL-0416-0696-UCL; Grant-in-Aid for Scientists to support international collaborative studies of the Ministry of Education, Culture, Sports, Science and Technology, Japan, Grant/Award Number: 16KK01930002; Grant-in-Aid for Young Scientists (A) of the Ministry of Education, Culture, Sports, Science and

Abstract

Stargardt disease 1 (STGD1) is the most prevalent retinal dystrophy caused by pathogenic biallelic *ABCA4* variants. Forty-two unrelated patients mostly originating from Western China were recruited. Comprehensive ophthalmological examinations, including visual acuity measurements (subjective function), fundus autofluorescence (retinal imaging), and full-field electroretinography (objective function), were performed. Next-generation sequencing (target/whole exome) and direct sequencing were conducted. Genotype grouping was performed based on the presence of deleterious variants. The median age of onset/age was 10.0 (5–52)/29.5 (12–72) years, and the median visual acuity in the right/left eye was 1.30 (0.15–2.28)/1.30 (0.15–2.28) in the logarithm of the minimum angle of resolution unit. Ten patients (10/38, 27.0%) showed confined macular dysfunction, and 27 (27/37, 73.7%) had generalized retinal dysfunction. Fifty-eight pathogenic/likely pathogenic *ABCA4* variants, including 14 novel variants, were identified. Eight patients (8/35, 22.8%) harbored multiple deleterious variants, and 17 (17/35, 48.6%) had a single deleterious variant. Significant associations were revealed between subjective functional, retinal imaging, and objective functional groups, identifying a significant genotype–phenotype association. This study illustrates a large phenotypic/genotypic spectrum in a large well-characterized STGD1 cohort. A

This is an open access article under the terms of the Creative Commons Attribution-NonCommercial-NoDerivs License, which permits use and distribution in any medium, provided the original work is properly cited, the use is non-commercial and no modifications or adaptations are made.

© 2020 The Authors. *American Journal of Medical Genetics Part C: Seminars in Medical Genetics* published by Wiley Periodicals LLC.

Technology, Japan, Grant/Award Numbers: 16H06269, 18K16943; Health Labor Sciences Research Grant, The Ministry of Health, Labor and Welfare, Grant/Award Number: 201711107A; National Basic Research Program of China, Grant/Award Number: 2018YFA0107301; National Hospital Organization Network Research Fund, Grant/Award Number: H30-NHO-2-12; National Nature Science Foundation of China, Grant/Award Number: 81974138; The Great Britain Sasakawa Foundation Butterfield Awards

distinct genetic background of the Chinese population from the Caucasian population was identified; meanwhile, a genotype–phenotype association was similarly represented.

KEYWORDS

ABCA4, electroretinogram, multifocal electroretinogram, Stargardt disease

1 | INTRODUCTION

Stargardt disease (STGD1; MIM 248200), first described by Karl Stargardt, is an autosomal recessive retinal dystrophy caused by biallelic pathogenic variants in the *ABCA4* gene (ATP-binding cassette subfamily A member 4; MIM 601691) (Allikmets et al., 1997; K S, 1909). The *ABCA4* gene encodes a transmembrane rim protein (a member of the ABCA subfamily of ATP-binding cassette [ABC] transporters) in the outer segment discs of photoreceptors, which is involved in the active transport of retinoids from photoreceptors to retinal pigment epithelium (RPE) (Molday, 2015; Molday, Zhong, & Quazi, 2009; Quazi, Lenevich, & Molday, 2012). Failure of the transport results in accelerated deposition of a major lipofuscin fluorophore (N-retinylidene-N-retinylethanolamine; A2E) in the RPE, and A2E-associated cytotoxicity is believed to cause RPE dysfunction with subsequent photoreceptor cell loss over time (Chen et al., 2012; Maeda, Maeda, Golczak, & Palczewski, 2008; Molday, Rabin, & Molday, 2000; Tsybovsky, Molday, & Palczewski, 2010).

STGD1, with a prevalence of 1 in 8,000–10,000, is one of the most common inherited macular dystrophies with characteristic features, including macular atrophy and yellow–white flecks at the level of the RPE at the posterior pole (Gill, Georgiou, Kalitzeos, Moore, & Michaelides, 2019; Liu, Fujinami, Yang, Arno, & Fujinami, 2019; Rahman, Georgiou, Khan, & Michaelides, 2020; Tanna, Strauss, Fujinami, & Michaelides, 2017). Onset is most common in teens but variable, and a severe and progressive phenotype has been associated with childhood-onset and a mild phenotype with late-onset (Fujinami et al., 2011; Fujinami, Lois, Davidson, et al., 2013; Fujinami, Lois, Mukherjee, et al., 2013; Fujinami, Sergouniotis, Davidson, Mackay, et al., 2013; Fujinami, Sergouniotis, Davidson, Wright, et al., 2013; Fujinami et al., 2014; Fujinami et al., 2015; Fujinami-Yokokawa et al., 2019; Georgiou et al., 2020; Gill et al., 2019; Khan et al., 2018; Liu et al., 2019; Rahman et al., 2020; Singh, Fujinami, Chen, Michaelides, & Moore, 2014; Tanna et al., 2017, 2019). The vast phenotypic heterogeneity and variable severity of *ABCA4*-associated retinopathy are well-known and encompass macular atrophy without flecks, bull's-eye maculopathy, fundus flavimaculatus (retinal flecks without macular atrophy), a foveal sparing phenotype, cone-rod dystrophy, and “retinitis pigmentosa”; genotype–phenotype associations have been reported based on clinical severity and the presence of deleterious variants (Fujinami et al., 2011, 2014, 2015; Fujinami, Lois, Davidson, et al., 2013; Fujinami, Lois, Mukherjee, et al., 2013;

Fujinami, Sergouniotis, Davidson, Mackay, et al., 2013; Fujinami, Sergouniotis, Davidson, Wright, et al., 2013; Georgiou et al., 2020; McBain, Townend, & Lois, 2012; Singh et al., 2014; Strauss et al., 2019; Tanna et al., 2017, 2019; Testa et al., 2014).

Cross-sectional and longitudinal studies in large cohorts focusing mainly on the European population have been widely performed (Fujinami, Zernant, et al., 2013; Fujinami et al., 2019; Kong et al., 2016, 2018; Schonbach et al., 2017; Schulz et al., 2017; Strauss et al., 2016; Strauss, Munoz, Ho, Jha, Michaelides, Cideciyan, et al., 2017; Strauss, Munoz, Ho, Jha, Michaelides, Mohand-Said, et al., 2017; Strauss et al., 2019). Clinical trials of treatments including visual cycle modification (ClinicalTrials.gov Identifier: NCT02402660), gene augmentation therapy (ClinicalTrials.gov Identifier: NCT01367444), and stem cell therapy (ClinicalTrials.gov Identifier: NCT01469832) are ongoing mainly in Europe/North America (Charbel Issa, Barnard, Herrmann, Washington, & MacLaren, 2015; Hussain, Ciulla, et al., 2018; Hussain, Gregori, Ciulla, & Lam, 2018; Kubota et al., 2012; Kubota, Calkins, Henry, & Linsenmeier, 2019; Mehat et al., 2018; Rosenfeld et al., 2018; Schwartz et al., 2012, 2015). However, large cohort studies based on standardized clinical and genetic diagnostic criteria in the Asian population are very limited.

Therefore, the purpose of this study was to characterize the comprehensive phenotypic and genotypic features of Chinese patients with STGD1 in a large cohort in preparation for therapeutic trials. A systematic review of *ABCA4* variants was performed to delineate the genetic spectrum in the Chinese population.

2 | METHODS

The procedures applied in this study were approved by the local ethics committee of Southwest Eye Hospital, Third Military Medical University (Army Medical University), Chongqing, China (reference number: 73981486-2), and all procedures were performed in accordance with the Declaration of Helsinki.

2.1 | Participants

Patients were recruited at the Southwest Eye Hospital, Third Military Medical University (Army Medical University), Chongqing, China, from 2013 to 2019 according to the following criteria mainly described in a

previous publication: (Strauss et al., 2016) patients with multiple disease-causing variants in the *ABCA4* gene or patients with one disease-causing variant and typical clinical findings (i.e., macular atrophy with flecks) for STGD1. Clinical and molecular genetic diagnoses were confirmed by three senior doctors (XM, KF, SL). Patients who had other ocular diseases, such as choroidal neovascularization, glaucoma, and diabetic retinopathy, or were undergoing treatments/therapeutic trials were excluded.

2.2 | Clinical investigations

Detailed history and comprehensive ophthalmological examinations were conducted, including best-corrected decimal visual acuity (BCVA), dilated ophthalmoscopy, color fundus photography (non-myd WX 3D, Kowa, Tokyo, Japan), fundus autofluorescence imaging (FAF; excitation light: 488 nm, barrier filter: 500 nm, field of view: 30° × 30°, 55° × 55°; Spectralis, Heidelberg Engineering, Heidelberg, Germany), optical coherence tomography (OCT; Spectralis, Heidelberg Engineering; and ZEISS CIRRUS, Carl Zeiss Meditec AG, Oberkochen, Germany), and microperimetry (MP, MAIA, Padoba, Italy). BCVA was converted to the equivalent value in the logarithm of the minimum angle of resolution (LogMAR) unit, and low visual categories, including counting finger (CF) and hand movement (HM), were valued at 1.98 and 2.28, as reported previously (Fujinami, Lois, Mukherjee, et al., 2013; Lange, Feltgen, Junker, Schulze-Bonsel, & Bach, 2009).

Full-field electroretinograms (ffERGs; Diagnosys LLC, Lowell, MA) were recorded in accordance with the international standards of the International Society for Clinical Electrophysiology of Vision (ISCEV) (McCulloch et al., 2015a; McCulloch et al., 2015b) Multifocal ERGs (mfERGs) were recorded with a VERIS imaging system (EDI, San Mateo, CA) in accordance with the ISCEV standard protocol, and eyes with stable fixation during the mfERG recording were selected for further analyses (Hood et al., 2012).

Fundus appearance, FAF findings, OCT findings, and ffERG findings were classified based on specific features according to previous publications (Table 1) (Fujinami, Lois, Davidson, et al., 2013; Fujinami, Lois, Mukherjee, et al., 2013; Lois, Holder, Bunce, Fitzke, & Bird, 2001; Testa et al., 2014).

Fundus appearance was classified into four grades (grade 3 has three subgroups) based on the presence and location of central (macular), RPE atrophy and yellowish-white flecks. Grade 1: normal fundus; grade 2: macular and/or peripheral flecks without central atrophy; grade 3a: central atrophy without flecks; grade 3b: central atrophy with macular and/or peripheral flecks; grade 3c: paracentral atrophy with macular and/or peripheral flecks, without central atrophy; grade 4: multiple extensive atrophic changes of the RPE, extending beyond the vascular arcades.

Patterns of AF signal of the central retina and background was classified into three types. Type 1: localized low AF signal at the fovea surrounded by a homogeneous background, with/without perifoveal foci of high or low AF signal; Type 2: localized low AF signal at the

TABLE 1 Classification for fundus appearance, fundus autofluorescence images, optical coherence tomographic images, and full-field electroretinograms in Stargardt disease (STGD1)

Grade	Fundus grade	AF pattern	OCT category	FFERG group
Grade 1	Normal fundus	Pattern 1 Localized low AF signal at the fovea surrounded by a homogeneous background with/without perifoveal foci of high or low signal	Category I EZ preservation in the fovea	Group 1 Macular dysfunction (normal full-field ERG)
Grade 2	Macular and/or peripheral flecks without central atrophy	Pattern 2 Localized low AF signal at the macula surrounded by a heterogeneous background and widespread foci of high or low AF signal extending anterior to the vascular arcades	Category II EZ loss in the foveal area	Group 2 Macular dysfunction with generalized cone dysfunction
Grade 3a	Central atrophy without flecks	Pattern 3 Multiple areas of low AF signal at posterior pole with a heterogeneous background and/or foci of high or low signal	Category III Extensive loss of EZ line	Group 3 Macular dysfunction with generalized cone and rod dysfunction
Grade 3b	Central atrophy with macular and/or peripheral flecks			
Grade 3c	Para-central atrophy with macular and/or peripheral flecks, without a central atrophy			

Abbreviations: AF, autofluorescence; ERG, electroretinogram; EZ, photoreceptor ellipsoid zone; RPE, retinal pigment epithelium.

macula surrounded by a heterogeneous background, and widespread foci of high or low AF signal extending anterior to the vascular arcades; Type 3: multiple areas of low AF signal at the posterior pole with a heterogeneous background, with/without foci of high or low AF signal.

Morphological changes of photoreceptor ellipsoid zone (EZ) in the central retina detected by OCT were classified into three categories. Category I: preserved EZ in the fovea; category II: loss of EZ in the fovea; category III: extensive loss of EZ.

Based on the ffERGs findings, patients were assigned to three ffERG groups. Group 1: normal ffERG responses; group 2: generalized cone ERG abnormality with normal rod responses; group 3: generalized cone and rod ERG abnormality.

The median P1 amplitude decline rates [(medical value of normative range – P1 value)/medical value of normative range] of mfERG rings 1 and 2, rings 3 and 4, and rings 5 and 6 were calculated for the analyses.

One eye was randomly selected using random.org software (<https://www.random.org/>) for the classification and analysis of fundus appearance, FAF images, OCT images, and ffERGs.

2.3 | Classification of phenotypic severity

The overall classification of phenotypic severity was performed based on the following clinical parameters mainly according to a previous publication: (Fujinami, Sergouniotis, Davidson, Mackay, et al., 2013) age of onset, BCVA (LogMAR), fundus grade, AF pattern, OCT category, and ffERG grouping (group 1: mild phenotype; group 2: moderate phenotype; and group 3: severe phenotype) (Table 2).

2.4 | Variant detection

After obtaining informed consent, peripheral venous blood samples were collected from all subjects and unaffected family members (if available) for co-segregation analysis. Genomic DNA was isolated by a standard procedure. Either eye gene-enriched (from 36 to

450 target genes) panel-based next-generation sequencing (NGS) or whole exome sequencing (WES) was performed. Sanger bi-directional sequencing was conducted to confirm the rare candidate variants (allele frequency: less than 1.0% of the general population) and to perform the co-segregation analysis. Disease-causing variants were determined from the detected variants while considering the clinical findings of the affected subjects, the pattern of inheritance in the pedigree, and the results of the co-segregation analysis.

2.5 | *In silico* molecular genetic analyses

Sequence variant nomenclature was performed according to the guidelines of the Human Genome Variation Society (HGVS; <https://varnomen.hgvs.org>) with Mutalyzer (<https://mutalyzer.nl/>). All variants were analyzed using the following databases and prediction software: GnomAD (<http://gnomad.broadinstitute.org/>), 1,000 Genome (<https://www.internationalgenome.org/>), MutationTaster (<http://www.mutationtaster.org/>), FATHMM (<http://fathmm.biocompute.org.uk/9>), SIFT (<https://www.sift.co.uk/>), PROVEAN (<http://provean.jcvi.org/index.php>), Polyphen2 (<http://genetics.bwh.harvard.edu/pph2/>) PhyloP and Phastcons from the University of California Santa Cruz database (<https://genome.ucsc.edu/index.html>), Human Splicing Finder (HSF, <http://www.umd.be/HSF3/>), Database Splicing Consensus Single Nucleotide Variant (dbSNV, <http://sites.google.com/site/jpopgen/dbSNV>), and Ensembl Variant Effect Predictor (VEP, <http://grch37.ensembl.org/info/docs/tools/vep/index.html>). Missense variants with predicted splice site alterations were treated as deleterious variants.

In accordance with the American College of Medical Genetics (ACMG) guidelines, variants were classified as pathogenic, likely pathogenic, uncertain significance (VUS), likely benign, or benign (Richards et al., 2015).

2.6 | Genotype group classification

The patients harboring multiple pathogenic or likely pathogenic variants were classified into three genotype groups based on the

TABLE 2 Classification of phenotypic severity

	Onset of disease (years)	BCVA (logMAR) in the better eye	Fundus grade	AF type	OCT category	FfERG group
Mild phenotype (group 1)	Later onset (≥ 40)	<0.78	1	1	1	1
Moderate phenotype (group 2)	Patients who did not meet at least two criteria of either mild phenotype or severe phenotype were classified into the moderate phenotype subgroup.					
Severe phenotype (group 3)	Early onset (<10)	>1.0	4	3	3	3

Note: For the purpose of this study, patients who met at least three criteria of mild phenotype were classified into the mild phenotype subgroup and those who had at least three features of severe phenotype were classified into the severe phenotype subgroup. Patients who met both at least three features of mild phenotype and at least three features of severe phenotype were classified into group 2 (moderate phenotype).

Abbreviation: BCVA, best-corrected visual acuity in the LogMAR VA in the logarithm of the minimum angle of resolution (logMAR) unit.

number/presence of deleterious variants according to previous reports: (Fujinami et al., 2015; Fujinami et al., 2019; Fujinami, Lois, Mukherjee, et al., 2013; Kong et al., 2018) Sequence variants which presumably lead loss-of-function (frameshift, stop-gained, splice site alteration) are defined as null variants. Variants that are not likely to have null-effects such as missense variants or in-frame alteration were defined as non-null variants. Group A: patients with multiple definite or likely null variants; group B: patients with one null variant and one or more non-null variant(s); and group C: patients with multiple non-null variants.

2.7 | A systematic review of ABCA4 variants

A literature review of ABCA4-associated retinal disease in the Chinese population was performed. Peer-reviewed published papers were searched with the terms Chinese, ABCA4, and Stargardt disease; articles reporting at least 10 patients were surveyed.

In silico molecular genetic analyses were performed, and assessment of pathogenicity was performed with the same method applied in the current study cohort. Prevalent variants based on allele frequency in the affected group cohort were calculated for each study and the total study.

2.8 | Statistical analysis

Data analyses were performed using SPSS version 23.0 (IBM Corp, Armonk, NY). The age at baseline examination, age of onset, BCVA (in the LogMAR unit), MP threshold (4-2), and amplitude of P1 of mfERG were compared between fundus, FAF, OCT, fERG, and genotype groups with Mann-Whitney *U* tests. An association between phenotypic severity classification and genotype group classification was investigated by Fisher's exact test. *p* values <.05 were considered statistically significant.

3 | RESULTS

3.1 | Demographics

A total of 42 unrelated patients (28 men and 14 women) were included in this study. Two patients (A002 and A035) were from consanguineous families (Figure 1). The detailed clinical findings are presented in Data S1.

The patients mostly originated from the western part of China (32/42, 76.2%). The median age at baseline examination was 29.5 years (range, 12-72), and the median age of onset was 10 years (range, 5-52). The median BCVA, available in 40 patients, was 1.30 (range, 0.15-2.28) for the right eye and 1.30 (range, 0.15-2.28) for the left eye.

3.2 | Retinal images

The fundus photographs, autofluorescence images, and OCT images for three representative patients are shown in Figure 2.

Fundus photographs were obtained in 41 patients (Data S1). All these patients were classified into grades 3b and 4 according to their fundus appearance. No asymmetric grades were observed. There were 22 patients (22/41, 53.7%) in grade 3b and 19 (19/31, 61.3%) in grade 4 (Figure S1). There was a significant difference in BCVA between grades 3b and 4 ($p = .0004$; Data S1 and Figure S2). FAF images were obtained in 41 patients (Data S1). There were 10 patients (10/41, 24.4%) with a type 1 AF pattern, 18 (18/41, 43.9%) with a type 2 AF pattern, and 13 (13/41, 31.7%) with a type 1 AF pattern (Figure S1). No asymmetric types were observed. There were significant differences in age and BCVA between patients with AF type 1 and type 3 patterns ($p = .0111$, $p = .0167$; Data S1, Figure S2). OCT images were obtained in 39 patients (Data S1). There were eight patients (8/39, 20.5%) with category II OCT findings and 31 (31/39, 79.5%) with category III OCT findings (Figure S1). One patient (A013) showed an asymmetric classification with category II of the right eye and category III of the left eye. There was a significant difference in BCVA between patients with OCT category II and category III ($p = .000086$; Data S1, Figure S2).

3.3 | Retinal function and microperimetry

The traces of fFERGs and mfERGs and MP results for three representative patients are presented in Figure 3.

fFERGs were recorded in 37 patients (Data S1). There were 10 patients (10/37, 27.0%) in fFERG group 1, four patients (4/37, 10.8%) in group 2, and 23 patients (23/37, 62.2%) in group 3 (Figure S1). No asymmetric fFERG groups were observed. There were significant differences in age between patients in group 1 and group 2 as well as in BCVA between patients in fFERG group 1 and group 3 ($p = .034$, $p = .002$; Data S1 and Figure S2).

MfERGs were obtained in 30 patients, and 40 eyes from 24 patients with stable fixation were analyzed (Data S1). There were 15 eyes in fFERG group 1, seven eyes in fFERG group 2, and 18 eyes in fFERG group 3. The median P1 amplitude decline rates of mfERG rings 1 and 2, 3 and 4, and 5 and 6 in the fFERG groups are summarized in Table S2. There were significant differences in terms of the P1 amplitude decline rate of rings 1 and 2, rings 3 and 4, and rings 5 and 6 between fFERG group 1 and group 3 ($p = .0033$, $p = .000005$, $p = .0000009$). Significant differences were found in terms of the P1 amplitude decline rate for rings 3 and 4 and rings 5 and 6 between fFERG group 2 and group 3 ($p = .0012$, $p = .0004$). Significant differences in terms of the P1 amplitude decline rate of rings 5 and 6 were observed between fFERG group 1 and group 2 as well ($p = .059$, Figure S3).

MP was performed in 23 patients. All 23 patients showed preferred retinal locus (PRL)-fixation changes. There were 12 eyes in fFERG group 1, eight eyes in fFERG group 2, and 25 eyes in fFERG

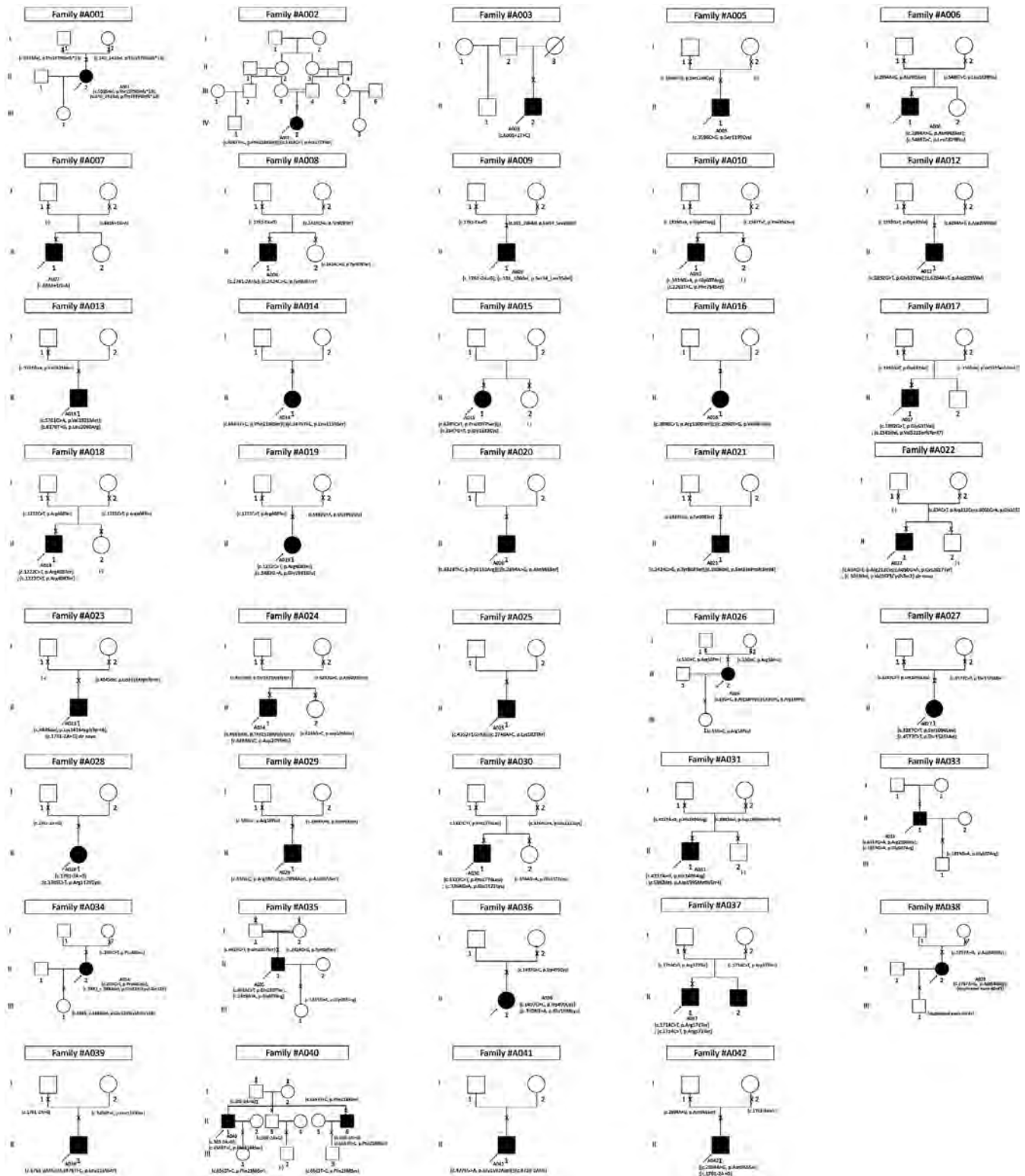


FIGURE 1 Pedigree charts of 42 families with Stargardt disease. An arrow (→) indicates the proband. A filled shape indicates the affected individual, and a cross (x) indicates the family members who underwent genetic testing. Square, male; circle, female. The generation number is shown on the left

group 3. The median average sensitivity threshold of the macula was 19.8 dB (range, 0.0–29.2), 15.1 dB (range, 0.0–25.8), and 0.0 dB (range, 0.0–18.9) in ffERG group 1, group 2, and group 3, respectively.

There was a significant difference between ffERG group 1 and group 3 as well as between ffERG group 2 and group 3 ($p = .000003$, $p = .076$; Figure S4).

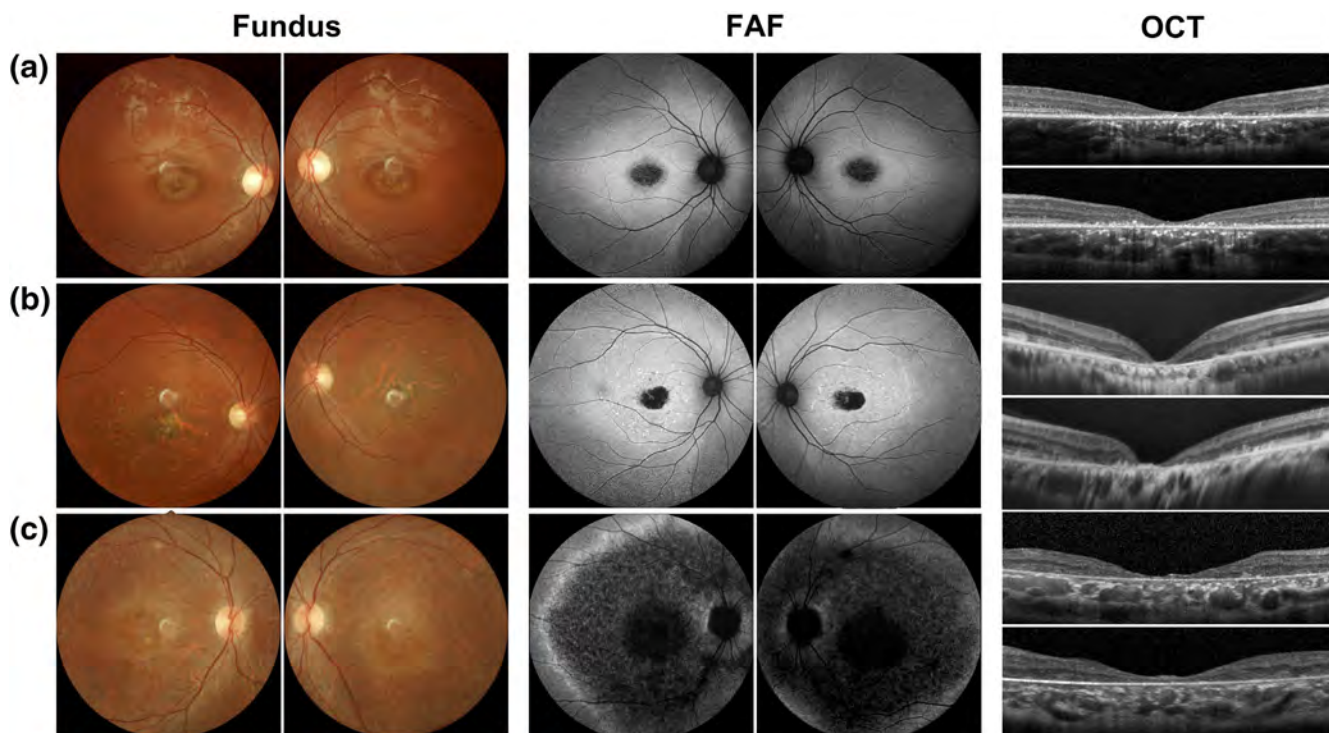


FIGURE 2 Color fundus photographs, fundus autofluorescence images, and optical coherence tomographic images from three representative patients with Stargardt disease (STGD1). (a) A002 (15-year-old female; onset at 9 years; best-corrected visual acuity of 0.82/0.82 in the logMAR unit for the right/left eye; [c.6563T>C (p.Phe2188Ser) and c.5318C>T (p.Ala1773Val)]; genotype group C). Fundus photographs show a central atrophy without flecks at the posterior. Fundus autofluorescence (FAF) images identify an area of low AF signal located at the fovea with homogenous background. Optical coherence tomographic (OCT) images demonstrate outer retinal disruption at the macula. (b) A040 (34-year-old male; onset at 10 years; best-corrected visual acuity of 1.00/1.00 in the logMAR unit for the right/left eye; [c.6563T>C (p.Phe2188Ser)] and [c.303-2A>G]; genotype group B). Fundus photographs show a central atrophy surrounded by flecks at the posterior pole; FAF images identify an area of low AF signal located at the macula with numerous foci of high AF density at the posterior pole; OCT images demonstrate outer retinal disruption at the macula. (c) A008 (22-year-old male; onset at 10 years; best-corrected visual acuity of 2.28/1.98 in the logMAR unit for the right/left eye; [c.1761-2A>G] and [c.2424C>G (p.Tyr808ter)]; genotype group A). Fundus photographs show multiple extensive atrophic changes in the retinal pigment epithelium (RPE), extending beyond the vascular arcades. FAF images identify multiple areas of low AF signal at posterior pole with a heterogeneous background. OCT images demonstrate widespread outer retinal disruption

3.4 | Phenotypic severity

Phenotype severity classification was available in 42 patients (Data S1). There was no patient (0/42, 0.0%) with a mild phenotype, 16 patients (16/42, 38.1%) with a moderate phenotype and 26 (26/42, 61.9%) with a severe phenotype.

3.5 | ABCA4 variants

Genetic results were obtained in all 42 unrelated patients: 34 patients underwent panel-based NGS, and eight patients underwent WES. Two ABCA4 variants were detected in 39 patients, while two patients (A003 and A005) had a single variant and one (A022) had three variants. Co-segregation analyses were available in 32 families: 26 probands with confirmed biallelic variants with genetic results of parents or certain family members; six probands with partially segregated results of a single parent or relatives; and 10 probands with no available data (Data S1 and Figure 1).

The detailed molecular genetic results are provided in Table S3. In total, 60 ABCA4 variants were identified in this study, including 36 missense variants (36/60, 60.0%), nine frameshift alterations (9/60, 15.0%), eight splice site alterations (13.3%), five nonsense variants (5/60, 8.3%), one in-frame deletion (1/60, 1.7%) and one duplication of exons 40–41 (1/60, 1.7%) (Figure 4). Two missense variants (c.6284A>T (p.Asp2095Val) and c.6283G>C (p.Asp2095His)) located around the end of exon 46 was predicted to cause splice site alterations. Fourteen novel ABCA4 variants were first reported in this study (Table S3). Two de novo ABCA4 variants were identified in two families: c.5019del (p.Val1673CysfsTer2) (A022) and c.1761-2A>G (A023) (Figure 1). There are three variants identified in the homozygous status: c.1222C>T (p.Arg408Ter) (A020); c.53G>C (p.Arg18Pro) (A030); and c.1714C>T (p.Arg572Ter) (A045).

The most prevalent six variants were c.1761-2A>G (6/80 alleles, 8%); c.2894A>G (p.Asn965Ser) (5/80 alleles, 6%); c.1222C>T (p.Arg408Ter) (4/80 alleles, 5%); c.2424C>G (p.Tyr808Ter) (3/80 alleles, 4%); c.53G>C (p.Arg18Pro) (3/80 alleles, 4%); and c.6563T>C (p.Phe2188Ser) (3/80 alleles, 4%) (Figure 4).

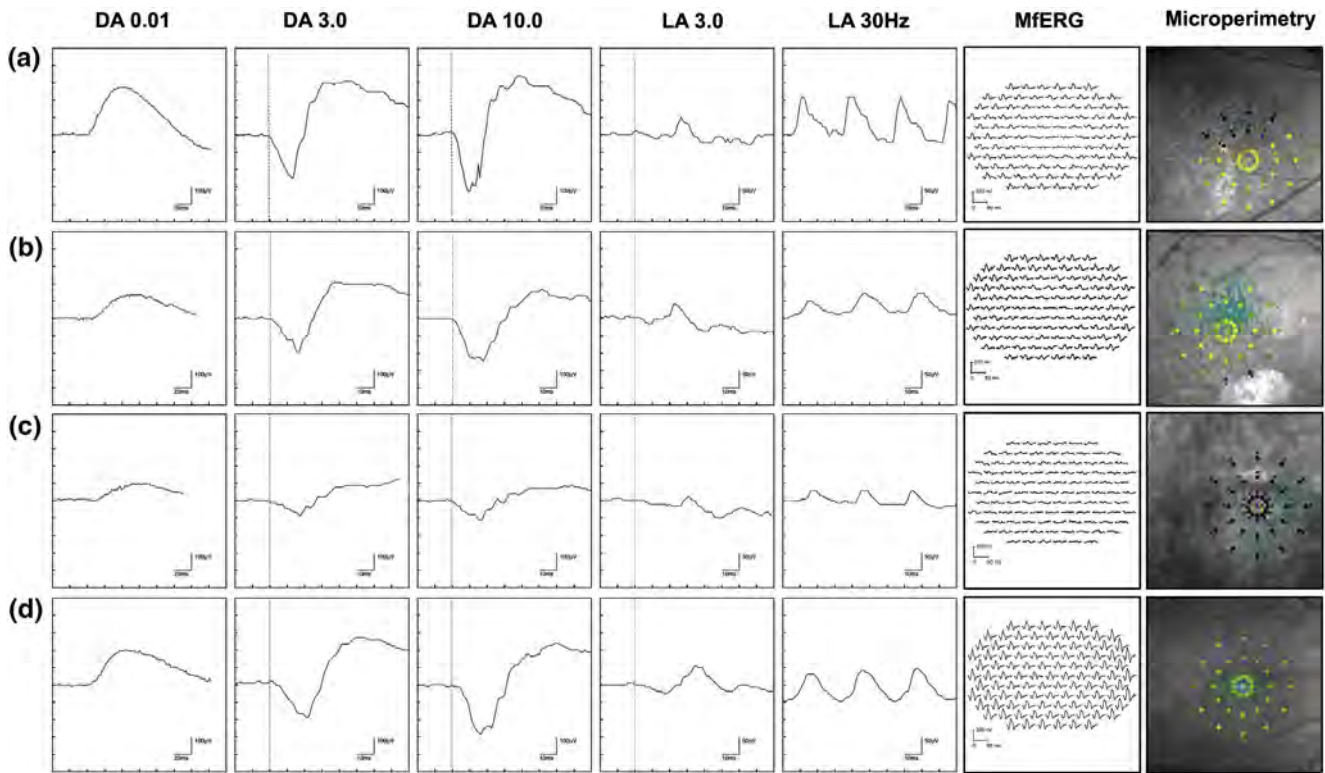


FIGURE 3 Full-field electroretinograms (ffERGs), multifocal ERGs (mfERGs), and microperimetry from three representative patients with STGD1. (a) A002 (full-field electroretinogram group 1; ffERG group 1). FfERGs demonstrate normal dark-adapted (DA) responses (DA 0.01, DA 3.0, DA 10.0) and normal light-adapted (LA) responses (LA 3.0, LA 3.0 30 Hz flicker). Multifocal ERGs (mfERGs) detect severely decreased responses in the central area (rings 1–2) and mildly decreased responses in rings 3–6. Microperimetry (MP) presents a preferred retinal locus (PRL) located at the nasal fovea, and the average threshold at the macula is 26.4 dB. (b) A040 (ffERG group 2). FfERGs demonstrate normal DA responses and mildly decreased LA responses. MfERGs detect severely decreased responses in rings 1–4 and mildly decreased responses in rings 5–6. MP present a PRL located at the superior fovea, and the average threshold at the macula is 25.8 dB. (c) A008 (ffERG group 3). FfERGs demonstrate moderately decreased DA responses and moderately decreased LA responses. MfERGs detect severely decreased responses over the recorded area. MP presents the average threshold of 0 dB. (d) Normal reference. Data from a normal subject are shown for reference

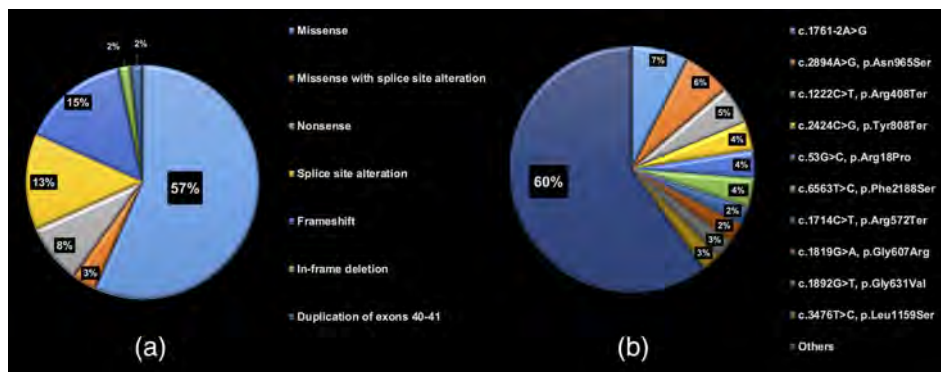


FIGURE 4 Distribution of detected *ABCA4* variants in a Western China cohort. (a) Type of detected variants. There were 36 missense variants (36/60, 60.0%), nine frameshift alterations (9/60, 15.0%), eight splice site alterations (13.3%), five nonsense variants (5/60, 8.3%), one in-frame deletion (1/60, 1.7%), and one duplication of exons 40–41 (1/60, 1.7%) identified in this study. Two missense variants (c.6284A>T (p.Asp2095Val) and c.6283G>C (p.Asp2095His)) are predicted to cause splice site alterations. (b) Allele frequency of detected variants. The distribution of 10 relatively prevalent variants identified in at least two families is demonstrated. The variants with allele frequencies less than 2% are summarized into others

The allele frequency provided by gnomAD in the total/East Asian general population for these six prevalent variants was 0.0004092%/0% for c.1761-2A>G; 0.013%/0% for p.Asn965Ser;

0.001625%/0.005% for p.Arg408Ter; 0%/0% for p.Tyr808Ter; 0%/0% for p.Arg18Pro; and 0.0008122%/0.005% for p.Phe2188Ser. The allele frequency provided by gnomAD in the total/East Asian

general population and this study for each variant was performed (Table S4).

Pathogenicity classification based on the ACMG guidelines was available for 60 detected variants. There were 24 variants classified as pathogenic, 34 as likely pathogenic, one as a variant of uncertain significance (VUS) (c.4577C>T (p.Thr152Met); A027), and one as a likely benign variant (c.3547G>T (p.Gly1183Cys); A015) (Table S3).

3.6 | Genotype classification

Genotype group classification was performed in 36 patients harboring multiple pathogenic or likely pathogenic variants. There were eight patients (8/36, 22.2%) with genotype A, 17 patients (47.2%) with genotype B, and 11 patients (30.5%) with genotype C (Figure S1).

The median age, age of onset, and BCVA in genotype A was 29.0 years (range, 18–52), 10.0 years (range, 8–14), and 1.64 in the LogMAR unit (range, 1.00–2.28), respectively. The median age, age of onset, and BCVA in genotype B was 34.0 years (range, 12–72), 10.0 years (range, 5–49), and 1.30 in the LogMAR unit (range, 0.15–1.98), respectively. The median age, age of onset, and BCVA in genotype C was 28.0 years (range, 15–46), 10.0 years (range, 8–20), and 1.00 in the LogMAR unit (range, 0.40–1.30), respectively. There was a significant difference in BCVA between genotype group A and genotype group C ($p = .0052$, Table S5).

3.7 | Genotype–phenotype association

An association between phenotypic severity and genotype group was investigated in 36 patients. The number of phenotypically moderate patients in genotype groups A, B, and C was zero, five, and seven, respectively (0%, 29.4%, 63.6%). The number of phenotypically severe patients in genotype groups A, B, and C was eight, twelve, and four, respectively (100%, 70.6%, 36.4%). A statistically significant association between phenotypic severity and genotype group was revealed ($p < .05$) ($p = .01$, Table 3 and Figure 5).

3.8 | A systematic review of ABCA4 variants

Four articles were selected for the analysis of Chinese ABCA4 variants (Table S6). A total of 212 ABCA4 variants were identified in these four

studies, including 114 missense, 36 splice site alterations, 31 nonsense variants, 25 frameshift variants, 3 synonymous variants, and 3 others (Table S7). Out of 212 ABCA4 variants, 150 were classified as pathogenic or likely pathogenic according to the ACMG guidelines. Prevalent variants in total were c.101_106del (p.Ser34_Leu35del) (allele frequency of 6%); c.2894A>G (p.Asn965Ser) (allele frequency of 4%); c.6563T>G (p.Phe2188Ser) (allele frequency of 4%); and c.2424C>G (p.Tyr808Ter) (allele frequency of 3%) (Figure S5).

Prevalent variants in each study were c.101_106del (p.Ser34_Leu35del); c.4773+1G>T; c.5646G>A (p.Met1882Ile); and c.1804C>T (p.Arg602Trp) in study 1 (Xin et al., 2015; $N = 33$). c.2424C>G (p.Tyr808Ter); c.6563T>G (p.Phe2188Ser); c.101_106del (p.Ser34_Leu35del); and c.2894A>G (p.Asn965Ser) in study 2 (Jiang, Pan, Xu, Tian, & Li, 2016; $N = 161$). c.101_106del (p.Ser34_Leu35del); c.2894A>G (p.Asn965Ser); c.6563T>G (p.Phe2188Ser); and c.1819G > A (p.Gly607Arg) in study 3 (Hu, J-k, Gao, Qi, & Wu, 2019; $N = 153$) and c.2894A>G (p.Asn965Ser); and c.101_106del (p.Ser34_Leu35del) in study 4 (Dan, Huang, Xing, & Shen, 2019; $N = 12$) (Table S6). Basically, those articles mainly focused on genotype analysis. There were little phenotypic data such as retinal image and electrophysiology was available and the correlation between phenotype and genotype was not analyzed.

4 | DISCUSSION

Detailed clinical and genetic characteristics are illustrated in a Western China cohort of 42 probands with STGD1. A wide disease spectrum both in phenotype and genotype was determined in a large Chinese cohort, identifying no patient with a mild phenotype, 38.1% with a moderate phenotype, and 61.9% with a severe phenotype associated with genetic severity.

To the best of the authors' knowledge, this study is the first to comprehensively reveal the demographic, morphological, and functional features of patients with STGD1 in a large molecularly confirmed cohort, which enabled an elucidation of the genotype–phenotype association in the Chinese population.

The median onset in our cohort (10.0 years) was earlier than that in the large prospective international STGD1 cohort (21.8 years for the retrospective cohort and 22.3 years for the prospective cohort in the ProgStar studies) or other reports from Europe (approximately 20 years) (Fujinami, Lois, Davidson, et al., 2013; Fujinami, Lois,

TABLE 3 Association between genotype group and phenotypic severity

		Phenotypic severity		
		Group 1 (mild)	Group 2 (moderate)	Group 3 (severe)
Genotype group	Group A (multiple deleterious)	0	0	8
	Group B (one deleterious)	0	5	12
	Group C (multiple missense)	0	7	4

Note: A statistically significant association was revealed between genotype group classification and phenotypic severity classification ($p = .014$; $p < .05$, Fisher exact test).

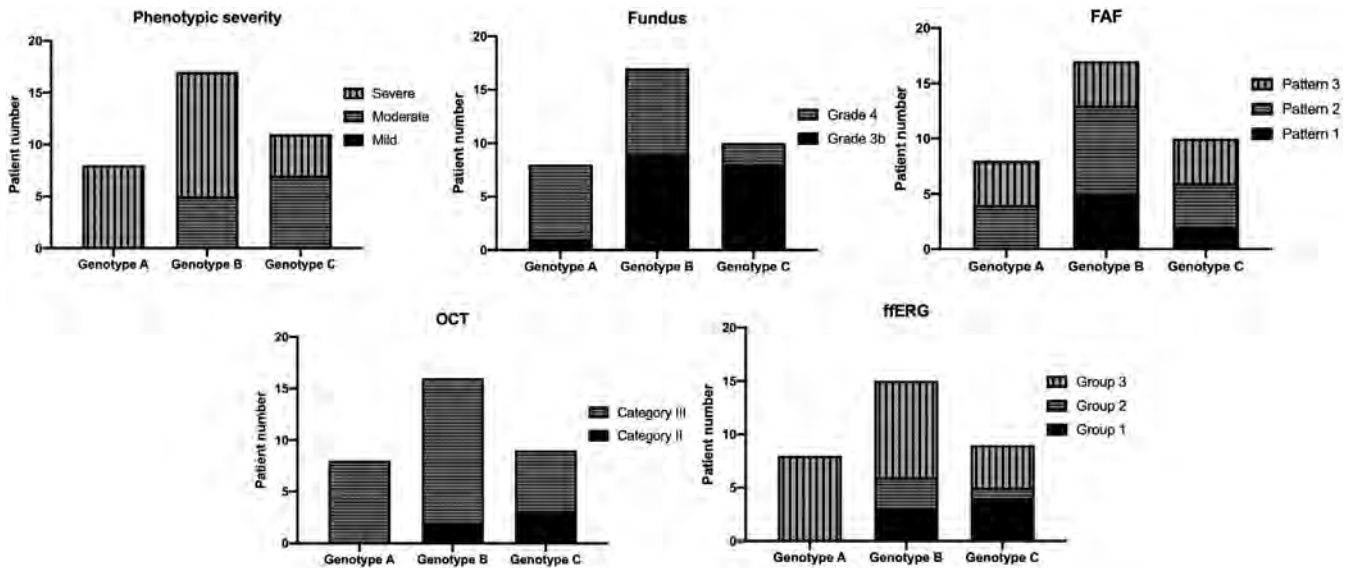


FIGURE 5 Clinical classification for each genotype group. Clinical classifications of phenotypic severity, fundus grades, FAF types, ffERG groups, and OCT categories for each genotype group are shown in bar graphs. There was a significant association between phenotypic severity and genotype group classification

Mukherjee, et al., 2013; Fujinami, Zernant, et al., 2013; Strauss et al., 2016). These findings were associated with a high proportion of severe phenotype in our cohort. The higher proportion of genotype group A with multiple deleterious variants (22%) in our cohort than in the other cohort (ProgStar cohort; 6%) supports this important fact (Fujinami et al., 2019; Kong et al., 2018). A similar proportion of genotype group A to our cohort was also found in the childhood-onset Stargardt disease cohort in the United Kingdom (Fujinami et al., 2015; Georgiou et al., 2020; Tanna et al., 2019).

Functional assessment is crucial in STGD1, since it provides not only distribution of the affected retinal area and affected systems (cone or rod) but also a prognostic value (Fujinami, Lois, Davidson, et al., 2013; Lois et al., 2001). The most severe functional phenotype (ffERG group 3: generalized cone and rod dysfunction) showed significant progression (over 50% loss of function) during the 10-year follow-up; (Fujinami, Lois, Davidson, et al., 2013) thus, careful observation and constructive intervention (if possible) are needed during the course in approximately 60% of our cohort. Spatial functional assessment with mfERGs detected a trend of an extended reduction in P1 amplitude according to the severity of ffERGs. This new approach could provide more detailed assessment/monitoring of retinal function in patients with STGD1 in natural history studies and therapeutic trials.

The combination of subjective and objective functional assessments provided useful information in our study. MP, a procedure to assess retinal sensitivity by monitoring the fundus, detected a lack of fixation stability with lower sensitivity thresholds, in keeping with previous reports (Sasso et al., 2017; Schonbach et al., 2017, 2020; Tanna et al., 2018, 2019). In addition, the severity of retinal sensitivity loss was associated with the severity of generalized retinal functional loss detected by ffERG, which suggests that the combination of subjective

and objective functional assessments could explain the key symptom of poor fixation and blurred central vision often associated with peripheral functional impairment.

Fourteen detected *ABCA4* variants (14/60, 23.3%) identified in our cohort have never been reported. This fact implies that the genetic background of the Chinese population was distinct from that of other populations. In addition, the three most prevalent variants (c.1761-2A>G; c.2894A>G (p.Asn965Ser); and c.1222C>T (p.Arg408Ter)) detected in our cohort were completely different from the three most prevalent variants (c.5882G>A (p.Gly1961Glu); c.2588G>C (p.Gly863Ala); and c.5461-10T>C) in the ProgStar study (Fujinami et al., 2019). In contrast to this regional/ethnic variation, genotype–phenotype associations were similarly identified in our cohort compared with cohorts from other populations, which supports the fact that the same approach to interpret/assess disease severity and the same concept of therapeutic window of opportunity can be applicable to the Chinese population.

There are four major reports describing *ABCA4*-associated retinal disease. The four prevalent variants (c.101_106del (p.Ser34-Leu35del); c.2894A>G (p.Asn965Ser); c.6563T>C (p.Phe2188Ser); and c.2424C>G (p.Tyr808Ter)) were different from those of the European population. In addition, the proportions of the types of detected variants were also different; a higher proportion of deleterious variants (43.4%; 92/212) was identified in the Chinese population compared to the ProgStar cohort (29.0%; 71/245), although the recruitment criteria can differ. In our study, three null variants: c.1761-2A>G (6/80 alleles, 8%), c.1222C>T (p.Arg408Ter) (4/80 alleles, 5%), and c.2424C>G (p.Tyr808Ter) (3/80 alleles, 4%) account for 16.3% (13/80 alleles) in total, and the association between genotype and phenotype has been revealed. The prevalence of null variants in this cohort is much higher than the European population, which can be considered as founder

alleles; although further genetic analysis utilizing haplotype data is required to conclude this hypothesis. Interestingly, four previous Chinese studies showed some regional differences, although similar features were observed. Three prevalent variants (c.2894A>G (p. Asn965Ser); c.6563T>G (p.Phe2188Ser); and c.101_106del (p. Ser34_Leu35del)) are shared among three out of the four Chinese cohorts, and the first two variants were prevalent in our cohort. On the other hand, the most prevalent variant (c.1761-2A>G) associated with a severe phenotype in our cohort was not listed as a frequently found variant in the other four Chinese cohorts. In most large Chinese cohort studies, patients were recruited without providing any clinical and genetic criteria of STGD1. This recruitment bias should include or exclude severe phenotypes, such as “retinitis pigmentosa.”

Three out of the most prevalent six variants in this study were only reported in the Chinese population: c.1761-2A>G; c.2424C>G (p.Tyr808Ter); and c.53G>C (p.Arg18Pro). Founder effects of these three variants can be considered. It is still difficult to conclude the enriched variants in Western China because the allele frequency data of the general population is only available as a cohort of the Western Chinese population.

In the current study, panel-based NGS targeting 36–450 genes have been applied that enables to detect 3–29% in patients with inherited retinal diseases. The advanced screening methods specifically designed for ABCA4 have been developed with a detection rate of 80% or more elsewhere (Cremers, Lee, Collin, & Allikmets, 2020; Jana et al., 2014). However, it is still not perfect for diagnosing patients only by genetic results. The vast phenotypic heterogeneity confounds the phenotypic diagnosis, especially in patients with generalized retinal dysfunction, thus the phenotypic criterion is focusing on the patients with macular atrophy that misses patients with generalized retinal dysfunction. The ProgStar criteria can miss patients with generalized retinal dysfunction with one pathogenic ABCA4 variant; however, we believe the present criteria are most suitable at this moment for a comprehensive diagnosis aiming for treatment.

There are several limitations in this study. First, selection bias at recruitment related to disease severity should be inherent since it is difficult to collect data from genetically affected subjects with good vision who do not visit clinics/hospitals. Second, this cross-sectional retrospective case series study did not include longitudinal data; thus, prospective natural history studies in a larger cohort could provide more accurate information on the disease severity and progression of STGD1. Third, the molecular mechanisms of disease causation for most variants have been unclear, and the clinical effects of variants are not perfectly understood. Further functional analysis is required to conclude the disease causation of each variant. Forth, due to the limited number of subjects, statistical analysis to investigate correlations between the clinical parameters and the particular variants (or genotype groups) were not available in the current study. Fifth, in our cohort, two patients harbor a VUS or likely benign variants for whom genotype grouping was unavailable. The further genetic analysis would help to determine their genotypes with identifying/excluding other candidate variants. Last, the number of our patients was too

small to draw conclusions about the genotype–phenotype associations/correlations in such a heterogeneous disease; therefore, larger cohort studies are required for further detailed analyses.

In conclusion, this study, for the first time, illustrated a spectrum of morphological and functional phenotypes and genotypes in a molecularly confirmed large STGD1 cohort in the Chinese population. A different genetic background underlying STGD1 from the Caucasian population was revealed in this study; meanwhile, shared features based on genotype–phenotype associations were determined. These findings delineate the clinical and genetic characteristics of STGD1.

ACKNOWLEDGEMENTS

The East Asia Inherited Retinal Disease Society (EAIRDs) Study Group: The East Asia Stargardt disease (EASTAR) study is supported by a contract from the EAIRDs. The EAIRDs Study Group members are as follows: Chair's Office: National Institute of Sensory Organs, Kaoru Fujinami, Se Joon Woo, Ruifang Sui, Shiyong Li, Hyeong Gon Yu, Bo Lei, Qingjiong Zhang, Chan Choi Mun, Fred Chen, Mineo Kondo, Takeshi Iwata, Kazushige Tsunoda, Yozo Miyake, Kunihiko Akiyama, Gen Hanazono, Masaki Fukui, Yu Fujinami-Yokokawa, Tatsuo Matsunaga, Satomi Inoue, Kazuki Yamazawa, Takayuki Kinoshita, Yasuhiro Yamada, Michel Michaelides, Gavin Arno, Nikolas Pontikos, Alice Davidson, Yasutaka Suzuki, Asako Ihama, Reina Akita, Jun Ohashi, Izumi Naka, Kazutoshi Yoshitake, Daisuke Mori, Toshihide Kurihara, Kazuo Tsubota, Hiroaki Miyata, Kei Shinoda, Atsushi Mizota, Natsuko Nakamura, Takaaki Hayashi, Kazuki Kuniyoshi, Shuheji Kameya, Kwangsic Joo, Min Seok Kim, Kyu Hyung Park, Seong Joon Ahn, Dae Joong Ma, Baek-Lok Oh, Joo Yong Lee, Sang Jin Kim, Christopher Seungkyu Lee, Jinu Han, Hyewon Chung, Jeeyun Ahn, Min Sagong, Young-Hoon-Ohn, Dong Ho Park, You Na Kim, Jong Suk Lee, Sang Jun Park, Jun Young Park, Won Kyung Song, Tae Kwan Park, Lizhu Yang, Xuan Zou, Hui Li, Zhengqin Yin, Yong Liu, Xiaohong Meng, Xiao Liu, Yanling Long, Jiayun Ren, Hongxuan Lie, Gang Wang, Anthony G. Robson, Xuemin Jin, Kunpeng Xie, Ya Li, Chonglin Chen, Qingge Guo, Lin Yang, Ya You, Tin Aung, Graham E. Holder, John N De Roach.

CONFLICT OF INTEREST

All authors have completed and submitted the ICMJE Form for Disclosure of Potential Conflicts of Interest. Individual investigators who participate in the sponsored project(s) are not directly compensated by the sponsor but may receive salary or other support from the institution to support their effort on the project(s).

Toshihide Kurihara is an investor in Tsubota Laboratory, Inc and RestoreVision, Inc. Toshihide Kurihara reports grants and personal fees from ROHTO Pharmaceutical Co., Ltd, Tsubota Laboratory, Inc, Fuji Xerox Co., Ltd, Kowa Company, Ltd, Santen Pharmaceutical Co. Ltd., outside the submitted work.

Kazuo Tsubota reports grants and personal fees from Santen Pharmaceutical Co., Ltd., grants and personal fees from Otsuka Pharmaceutical Co., Ltd., grants and personal fees from Wakamoto Pharmaceutical Co., Ltd., grants from Rohto Pharmaceutical Co., Ltd., grants from R-Tech Ueno, personal fees from Laboratoires Thea,

grants from Alcon Japan, investor of Tear Solutions, grants and investor of Tsubota Laboratory, Inc., outside the submitted work.

Kaoru Fujinami: Paid consultant—Astellas Pharma Inc., Kubota Pharmaceutical Holdings Co., Ltd, Acucela Inc., Novartis AG, Janssen Pharmaceutica, Sanofi Genzyme, NightstaRx Limited; Personal fees—Astellas Pharma Inc., Kubota Pharmaceutical Holdings Co., Ltd., Acucela Inc., Novartis AG, Santen Company Limited, Foundation Fighting Blindness, Foundation Fighting Blindness Clinical Research Institute, Japanese Ophthalmology Society, Japan Retinitis Pigmentosa Society; Grants—Astellas Pharma Inc. (NCT03281005), outside the submitted work.

DATA AVAILABILITY STATEMENT

Data available on request from the authors.

ORCID

Kaoru Fujinami  <https://orcid.org/0000-0003-4248-0033>

Shiyang Li  <https://orcid.org/0000-0001-9783-9520>

REFERENCES

- Allikmets, R., Singh, N., Sun, H., Shroyer, N. F., Hutchinson, A., Chidambaram, A., ... Lupski, J. R. (1997). A photoreceptor cell-specific ATP-binding transporter gene (ABCR) is mutated in recessive Stargardt macular dystrophy. *Nature Genetics*, 15(3), 236–246.
- Charbel Issa, P., Barnard, A. R., Herrmann, P., Washington, I., & MacLaren, R. E. (2015). Rescue of the Stargardt phenotype in Abca4 knockout mice through inhibition of vitamin A dimerization. *Proceedings of the National Academy of Sciences of the United States of America*, 112(27), 8415–8420.
- Chen, Y., Okano, K., Maeda, T., Chauhan, V., Golczak, M., Maeda, A., & Palczewski, K. (2012). Mechanism of all-trans-retinal toxicity with implications for stargardt disease and age-related macular degeneration. *The Journal of Biological Chemistry*, 287(7), 5059–5069.
- Cremers, F. P. M., Lee, W., Collin, R. W. J., & Allikmets, R. (2020). Clinical spectrum, genetic complexity and therapeutic approaches for retinal disease caused by ABCA4 mutations. *Progress in Retinal and Eye Research*, 100861. <https://doi.org/10.1016/j.preteyeres.2020.100861>.
- Dan, H., Huang, X., Xing, Y., & Shen, Y. (2019). Application of targeted exome and whole-exome sequencing for Chinese families with Stargardt disease. *Annals of Human Genetics*, 84(2), 177–184.
- Fujinami, K., Akahori, M., Fukui, M., Tsunoda, K., Iwata, T., & Miyake, Y. (2011). Stargardt disease with preserved central vision: Identification of a putative novel mutation in ATP-binding cassette transporter gene. *Acta Ophthalmologica*, 89(3), e297–e298.
- Fujinami, K., Lois, N., Davidson, A. E., Mackay, D. S., Hogg, C. R., Stone, E. M., ... Michaelides, M. (2013). A longitudinal study of stargardt disease: Clinical and electrophysiologic assessment, progression, and genotype correlations. *American Journal of Ophthalmology*, 155(6), 1075–1088 e1013.
- Fujinami, K., Lois, N., Mukherjee, R., McBain, V. A., Tsunoda, K., Tsubota, K., ... Michaelides, M. (2013). A longitudinal study of Stargardt disease: Quantitative assessment of fundus autofluorescence, progression, and genotype correlations. *Investigative Ophthalmology & Visual Science*, 54(13), 8181–8190.
- Fujinami, K., Sergouniotis, P. I., Davidson, A. E., Mackay, D. S., Tsunoda, K., Tsubota, K., ... Webster, A. R. (2013). The clinical effect of homozygous ABCA4 alleles in 18 patients. *Ophthalmology*, 120(11), 2324–2331.
- Fujinami, K., Sergouniotis, P. I., Davidson, A. E., Wright, G., Chana, R. K., Tsunoda, K., ... Webster, A. R. (2013). Clinical and molecular analysis of Stargardt disease with preserved foveal structure and function. *American Journal of Ophthalmology*, 156(3), 487–501 e481.
- Fujinami, K., Singh, R., Carroll, J., Zernant, J., Allikmets, R., Michaelides, M., & Moore, A. T. (2014). Fine central macular dots associated with childhood-onset Stargardt disease. *Acta Ophthalmologica*, 92(2), e157–e159.
- Fujinami, K., Strauss, R. W., Chiang, J. P., Audo, I. S., Bernstein, P. S., Birch, D. G., ... ProgStar Study, G. (2019). Detailed genetic characteristics of an international large cohort of patients with Stargardt disease: ProgStar study report 8. *The British Journal of Ophthalmology*, 103(3), 390–397.
- Fujinami, K., Zernant, J., Chana, R. K., Wright, G. A., Tsunoda, K., Ozawa, Y., ... Moore, A. T. (2015). Clinical and molecular characteristics of childhood-onset Stargardt disease. *Ophthalmology*, 122(2), 326–334.
- Fujinami, K., Zernant, J., Chana, R. K., Wright, G. A., Tsunoda, K., Ozawa, Y., ... Michaelides, M. (2013). ABCA4 gene screening by next-generation sequencing in a British cohort. *Investigative Ophthalmology & Visual Science*, 54(10), 6662–6674.
- Fujinami-Yokokawa, Y., Pontikos, N., Yang, L., Tsunoda, K., Yoshitake, K., Iwata, T., ... Fujinami, K. (2019). Japan eye genetics consortium OBO. 2019. Prediction of causative genes in inherited retinal disorders from spectral-domain optical coherence tomography utilizing deep learning techniques. *Journal of Ophthalmology*, 2019, 1691064.
- Georgiou, M., Kane, T., Tanna, P., Bouzia, Z., Singh, N., Kalitzeos, A., ... Michaelides, M. (2020). Prospective cohort Study of childhood-onset Stargardt disease: Fundus autofluorescence imaging, progression, comparison with adult-onset disease, and disease symmetry. *American Journal of Ophthalmology*, 211, 159–175.
- Gill, J. S., Georgiou, M., Kalitzeos, A., Moore, A. T., & Michaelides, M. (2019). Progressive cone and cone-rod dystrophies: Clinical features, molecular genetics and prospects for therapy. *The British Journal of Ophthalmology*, 103, 711–720.
- Hood, D. C., Bach, M., Brigell, M., Keating, D., Kondo, M., Lyons, J. S., ... International Society For Clinical Electrophysiology of V. (2012). ISCEV standard for clinical multifocal electroretinography (mfERG) (2011 edition). *Documenta Ophthalmologica*, 124(1), 1–13.
- Hu, F.-Y., J-k, L., Gao, F.-J., Qi, Y.-H., & Wu, J.-H. (2019). ABCA4 gene screening in a Chinese cohort with Stargardt disease: Identification of 37 novel variants. *Frontiers in Genetics*, 10, 773–773.
- Hussain, R. M., Ciulla, T. A., Berrocal, A. M., Gregori, N. Z., Flynn, H. W., Jr., & Lam, B. L. (2018). Stargardt macular dystrophy and evolving therapies. *Expert Opinion on Biological Therapy*, 18(10), 1049–1059.
- Hussain, R. M., Gregori, N. Z., Ciulla, T. A., & Lam, B. L. (2018). Pharmacotherapy of retinal disease with visual cycle modulators. *Expert Opinion on Pharmacotherapy*, 19(5), 471–481.
- Jana, Z., Xie, Y., Carmen, A., Rosa, R. A., Miguel-Angel, L. M., Francesca, S., ... Mette, B. (2014). Analysis of the ABCA4 genomic locus in Stargardt disease. *Human Molecular Genetics*, 23(25), 6797.
- Jiang, F., Pan, Z., Xu, K., Tian, L., & Li, Y. (2016). Screening of ABCA4 gene in a Chinese cohort with Stargardt disease or cone-rod dystrophy with a report on 85 novel mutations. *Investigative Ophthalmology & Visual Science*, 57(1), 145–152.
- K S. (1909). Über familiäre, progressive Degeneration in der Maculagegend des Auges. *Graefe's Archive for Clinical and Experimental Ophthalmology*, 71, 534–550.
- Khan, K. N., Kasilian, M., Mahroo, O. A. R., Tanna, P., Kalitzeos, A., Robson, A. G., ... Michaelides, M. (2018). Early patterns of macular degeneration in ABCA4-associated retinopathy. *Ophthalmology*, 125(5), 735–746.
- Kong, X., Fujinami, K., Strauss, R. W., Munoz, B., West, S. K., Cideciyan, A. V., ... ProgStar Study, G. (2018). Visual acuity change over 24 months and its association with foveal phenotype and genotype in individuals with Stargardt disease: ProgStar Study report no. 10. *JAMA Ophthalmology*, 136(8), 920–928.

- Kong, X., Strauss, R. W., Michaelides, M., Cideciyan, A. V., Sahel, J. A., Munoz, B., ... ProgStar, S. G. (2016). Visual acuity loss and associated risk factors in the retrospective progression of Stargardt disease Study (ProgStar report no. 2). *Ophthalmology*, 123(9), 1887–1897.
- Kubota, R., Boman, N. L., David, R., Mallikarjun, S., Patil, S., & Birch, D. (2012). Safety and effect on rod function of ACU-4429, a novel small-molecule visual cycle modulator. *Retina*, 32(1), 183–188.
- Kubota, R., Calkins, D. J., Henry, S. H., & Linsenmeier, R. A. (2019). Emixustat reduces metabolic demand of dark activity in the retina. *Investigative Ophthalmology & Visual Science*, 60(14), 4924–4930.
- Lange, C., Feltgen, N., Junker, B., Schulze-Bonsel, K., & Bach, M. (2009). Resolving the clinical acuity categories "hand motion" and "counting fingers" using the Freiburg visual acuity test (FrACT). *Graefes Archive for Clinical and Experimental Ophthalmology*, 247(1), 137–142.
- Liu, X., Fujinami, Y. Y., Yang, L., Arno, G., & Fujinami, K. (2019). Stargardt disease in Asian population. In *Advances in vision research* (Vol. II, pp. 279–295). Singapore: Springer.
- Lois, N., Holder, G. E., Bunce, C., Fitzke, F. W., & Bird, A. C. (2001). Phenotypic subtypes of Stargardt macular dystrophy-fundus flavimaculatus. *Archives of Ophthalmology*, 119(3), 359–369.
- Maeda, A., Maeda, T., Golczak, M., & Palczewski, K. (2008). Retinopathy in mice induced by disrupted all-trans-retinal clearance. *The Journal of Biological Chemistry*, 283(39), 26684–26693.
- McBain, V. A., Townend, J., & Lois, N. (2012). Progression of retinal pigment epithelial atrophy in stargardt disease. *American Journal of Ophthalmology*, 154(1), 146–154.
- McCulloch, D. L., Marmor, M. F., Brigell, M. G., Hamilton, R., Holder, G. E., Tzekov, R., & Bach, M. (2015a). Erratum to: ISCEV standard for full-field clinical electroretinography (2015 update). *Documenta Ophthalmologica*, 131(1), 81–83.
- McCulloch, D. L., Marmor, M. F., Brigell, M. G., Hamilton, R., Holder, G. E., Tzekov, R., & Bach, M. (2015b). ISCEV standard for full-field clinical electroretinography (2015 update). *Documenta Ophthalmologica*, 130(1), 1–12.
- Mehat, M. S., Sundaram, V., Ripamonti, C., Robson, A. G., Smith, A. J., Borooah, S., ... Bainbridge, J. W. B. (2018). Transplantation of human embryonic stem cell-derived retinal pigment epithelial cells in macular degeneration. *Ophthalmology*, 125(11), 1765–1775.
- Molday, L. L., Rabin, A. R., & Molday, R. S. (2000). ABCR expression in foveal cone photoreceptors and its role in Stargardt macular dystrophy. *Nature Genetics*, 25(3), 257–258.
- Molday, R. S. (2015). Insights into the molecular properties of ABCA4 and its role in the visual cycle and Stargardt disease. *Progress in Molecular Biology and Translational Science*, 134, 415–431.
- Molday, R. S., Zhong, M., & Quazi, F. (2009). The role of the photoreceptor ABC transporter ABCA4 in lipid transport and Stargardt macular degeneration. *Biochimica et Biophysica Acta*, 1791(7), 573–583.
- Quazi, F., Lenevich, S., & Molday, R. S. (2012). ABCA4 is an N-retinylidene-phosphatidylethanolamine and phosphatidylethanolamine importer. *Nature Communications*, 3, 925.
- Rahman, N., Georgiou, M., Khan, K. N., & Michaelides, M. (2020). Macular dystrophies: Clinical and imaging features, molecular genetics and therapeutic options. *The British Journal of Ophthalmology*, 104(4), 451–460.
- Richards, S., Aziz, N., Bale, S., Bick, D., Das, S., Gastier-Foster, J., ... Committee, A. L. Q. A. (2015). Standards and guidelines for the interpretation of sequence variants: A joint consensus recommendation of the American College of Medical Genetics and Genomics and the Association for Molecular Pathology. *Genetics in Medicine*, 17(5), 405–424.
- Rosenfeld, P. J., Dugel, P. U., Holz, F. G., Heier, J. S., Pearlman, J. A., Novack, R. L., ... Kubota, R. (2018). Emixustat hydrochloride for geographic atrophy secondary to age-related macular degeneration: A randomized clinical trial. *Ophthalmology*, 125(10), 1556–1567.
- Sasso, P., Scupola, A., Silvestri, V., Amore, F. M., Abed, E., Calandriello, L., ... Caporossi, A. (2017). Morpho-functional analysis of Stargardt disease for reading. *Canadian Journal of Ophthalmology*, 52(3), 287–294.
- Schonbach, E. M., Strauss, R. W., Ibrahim, M. A., Janes, J. L., Birch, D. G., Cideciyan, A. V., ... ProgStar study g. (2020). Faster sensitivity loss around dense scotomas than for overall macular sensitivity in Stargardt disease: ProgStar report no. 14. *American Journal of Ophthalmology*, 216, 219–225.
- Schonbach, E. M., Wolfson, Y., Strauss, R. W., Ibrahim, M. A., Kong, X., Munoz, B., ... ProgStar Study, G. (2017). Macular sensitivity measured with microperimetry in Stargardt disease in the progression of atrophy secondary to Stargardt disease (ProgStar) study: Report no. 7. *JAMA Ophthalmology*, 135(7), 696–703.
- Schulz, H. L., Grassmann, F., Kellner, U., Spital, G., Ruther, K., Jagle, H., ... Stohr, H. (2017). Mutation spectrum of the ABCA4 gene in 335 Stargardt disease patients from a multicenter German cohort-impact of selected deep intronic variants and common SNPs. *Investigative Ophthalmology & Visual Science*, 58(1), 394–403.
- Schwartz, S. D., Hubschman, J. P., Heilwell, G., Franco-Cardenas, V., Pan, C. K., Ostrick, R. M., ... Lanza, R. (2012). Embryonic stem cell trials for macular degeneration: A preliminary report. *Lancet*, 379(9817), 713–720.
- Schwartz, S. D., Regillo, C. D., Lam, B. L., Elliott, D., Rosenfeld, P. J., Gregori, N. Z., ... Lanza, R. (2015). Human embryonic stem cell-derived retinal pigment epithelium in patients with age-related macular degeneration and Stargardt's macular dystrophy: Follow-up of two open-label phase 1/2 studies. *Lancet*, 385(9967), 509–516.
- Singh, R., Fujinami, K., Chen, L. L., Michaelides, M., & Moore, A. T. (2014). Longitudinal follow-up of siblings with a discordant Stargardt disease phenotype. *Acta Ophthalmologica*, 92(4), e331–e332.
- Strauss, R. W., Ho, A., Munoz, B., Cideciyan, A. V., Sahel, J. A., Sunness, J. S., ... Progression of Stargardt Disease Study G. (2016). The natural history of the progression of atrophy secondary to Stargardt disease (ProgStar) studies: Design and baseline characteristics: ProgStar report no. 1. *Ophthalmology*, 123(4), 817–828.
- Strauss, R. W., Kong, X., Ho, A., Jha, A., West, S., Ip, M., ... ProgStar Study, G. (2019). Progression of Stargardt disease as determined by fundus autofluorescence over a 12-month period: ProgStar report no. 11. *JAMA Ophthalmology*, 137, 1134.
- Strauss, R. W., Munoz, B., Ho, A., Jha, A., Michaelides, M., Cideciyan, A. V., ... ProgStar Study, G. (2017a). Progression of Stargardt disease as determined by fundus autofluorescence in the retrospective progression of Stargardt disease Study (ProgStar report no. 9). *JAMA Ophthalmology*, 135(11), 1232–1241.
- Strauss, R. W., Munoz, B., Ho, A., Jha, A., Michaelides, M., Mohand-Said, S., ... ProgStar Study, G. (2017b). Incidence of atrophic lesions in Stargardt disease in the progression of atrophy secondary to Stargardt disease (ProgStar) study: Report no. 5. *JAMA Ophthalmology*, 135(7), 687–695.
- Tanna, P., Georgiou, M., Aboshiha, J., Strauss, R. W., Kumaran, N., Kalitzeos, A., ... Michaelides, M. (2018). Cross-sectional and longitudinal assessment of retinal sensitivity in patients with childhood-onset Stargardt disease. *Translational Vision Science & Technology*, 7(6), 10.
- Tanna, P., Georgiou, M., Strauss, R. W., Ali, N., Kumaran, N., Kalitzeos, A., ... Michaelides, M. (2019). Cross-sectional and longitudinal assessment of the ellipsoid zone in childhood-onset Stargardt disease. *Translational Vision Science & Technology*, 8(2), 1.
- Tanna, P., Strauss, R. W., Fujinami, K., & Michaelides, M. (2017). Stargardt disease: Clinical features, molecular genetics, animal models and therapeutic options. *The British Journal of Ophthalmology*, 101(1), 25–30.

- Testa, F., Melillo, P., Di Iorio, V., Orrico, A., Attanasio, M., Rossi, S., & Simonelli, F. (2014). Macular function and morphologic features in juvenile stargardt disease: Longitudinal study. *Ophthalmology*, *121*(12), 2399–2405.
- Tsybovsky, Y., Molday, R. S., & Palczewski, K. (2010). The ATP-binding cassette transporter ABCA4: Structural and functional properties and role in retinal disease. *Advances in Experimental Medicine and Biology*, *703*, 105–125.
- Xin, W., Xiao, X., Li, S., Jia, X., Guo, X., & Zhang, Q. (2015). Identification of genetic defects in 33 Proband with Stargardt disease by WES-based bioinformatics gene panel analysis. *PLoS One*, *10*, e0132635.

SUPPORTING INFORMATION

Additional supporting information may be found online in the Supporting Information section at the end of this article.

How to cite this article: Liu X, Meng X, Yang L, et al. Clinical and genetic characteristics of Stargardt disease in a large Western China cohort: Report 1. *Am J Med Genet Part C*. 2020;184C:694–707. <https://doi.org/10.1002/ajmg.c.31838>



RESEARCH ARTICLE

RP2-associated retinal disorder in a Japanese cohort: Report of novel variants and a literature review, identifying a genotype–phenotype association

Kaoru Fujinami^{1,2,3,4} | Xiao Liu^{1,2,5} | Shinji Ueno⁶ | Atsushi Mizota⁷ | Kei Shinoda^{7,8} | Kazuki Kuniyoshi⁹ | Yu Fujinami-Yokokawa^{1,3,10,11} | Lizhu Yang^{1,2} | Gavin Arno^{1,3,4,12} | Nikolas Pontikos^{1,3,4} | Shuhei Kameya¹³ | Taro Kominami⁶ | Hiroko Terasaki⁶ | Hiroyuki Sakuramoto⁹ | Natsuko Nakamura^{1,7,14} | Toshihide Kurihara² | Kazuo Tsubota² | Yozo Miyake^{1,15,16} | Kazutoshi Yoshiake¹⁷ | Takeshi Iwata¹⁷ | Kazushige Tsunoda¹ | Japan Eye Genetics Consortium Study Group

¹Laboratory of Visual Physiology, Division of Vision Research, National Institute of Sensory Organs, National Hospital Organization Tokyo Medical Center, Tokyo, Japan

²Department of Ophthalmology, Keio University School of Medicine, Tokyo, Japan

³UCL Institute of Ophthalmology, London, UK

⁴Moorfields Eye Hospital, London, UK

⁵Southwest Hospital/Southwest Eye Hospital, Third Military Medical University (Army Medical University), Chongqing, China

⁶Department of Ophthalmology, Nagoya University Graduate School of Medicine, Nagoya, Japan

⁷Department of Ophthalmology, Teikyo University, Tokyo, Japan

⁸Department of Ophthalmology, Saitama Medical University, Moroyama Campus, Saitama, Japan

⁹Department of Ophthalmology, Kindai University Faculty of Medicine, Osaka-Sayama, Japan

¹⁰Department of Health Policy and Management, Keio University School of Medicine, Tokyo, Japan

¹¹Division of Public Health, Yokokawa Clinic, Suita, Japan

¹²North East Thames Regional Genetics Service, UCL Great Ormond Street Institute of Child Health, NHS Foundation Trust, London, UK

¹³Department of Ophthalmology, Nippon Medical School Chiba Hokusoh Hospital, Inzai, Japan

¹⁴Department of Ophthalmology, The University of Tokyo, Tokyo, Japan

¹⁵Aichi Medical University, Nagakute, Japan

¹⁶Next vision, Kobe Eye Center, Kobe, Japan

¹⁷Division of Molecular and Cellular Biology, National Institute of Sensory Organs, National Hospital Organization Tokyo Medical Center, Tokyo, Japan

Correspondence

Kaoru Fujinami, Laboratory of Visual Physiology, Division for Vision Research, National Institute of Sensory Organs, National Hospital Organization Tokyo Medical Center, No. 2-5-1, Higashigaoka, Meguro-ku, Tokyo

Abstract

The retinitis pigmentosa 2 (*RP2*) gene is one of the causative genes for X-linked inherited retinal disorder. We characterized the clinical/genetic features of four patients with *RP2*-associated retinal disorder (*RP2*-RD) from four Japanese families in

Kaoru Fujinami and Xiao Liu are joint first authors of this study.

This is an open access article under the terms of the Creative Commons Attribution-NonCommercial-NoDerivs License, which permits use and distribution in any medium, provided the original work is properly cited, the use is non-commercial and no modifications or adaptations are made.

© 2020 The Authors. *American Journal of Medical Genetics Part C: Seminars in Medical Genetics* published by Wiley Periodicals LLC.

152-8902 Japan.
Email: k.fujinami@ucl.ac.uk

Funding information

FOUNDATION FIGHTING BLINDNESS ALAN LATIES CAREER DEVELOPMENT PROGRAM, Grant/Award Number: CF-CL-0416-0696-UCL; Grant-in-Aid for Scientists to support international collaborative studies of the Ministry of Education, Culture, Sports, Science and Technology, Japan, Grant/Award Number: 16KK01930002; Grant-in-Aid for Young Scientists (A) of the Ministry of Education, Culture, Sports, Science and Technology, Japan, Grant/Award Number: 16H06269; Great Britain Sasakawa Foundation Butterfield Awards; Health Labour Sciences Research Grant, The Ministry of Health Labour and Welfare, Grant/Award Number: 201711107A; National Hospital Organization Network Research Fund, Grant/Award Number: H30-NHO-Sensory Organs-03; Novartis Research Grant; Grants-in-Aid for Scientific Research, Japan Society for the Promotion of Science, Japan, Grant/Award Number: H26-26462674; Ministry of Health, Labor and Welfare, Grant/Award Number: 18ek0109282h0002; Japan Agency for Medical Research and Development (AMED); ROHTO Pharmaceutical Co., Ltd.; Santen Pharmaceutical Co. Ltd.; Novartis Pharmaceuticals; Kowa Company, Ltd.; Kirin Company, Ltd.; Fuji Xerox Co., Ltd.; Tsubota Laboratory, Inc.; UCL Institute of Ophthalmology; Great Britain Sasakawa Foundation Butterfield Award; UCL Institute of Child Health; Great Ormond Street Hospital; Moorfields Eye Hospital; Ministry of Education, Culture, Sports, Science and Technology, Grant/Award Number: 18K16943

a nationwide cohort. A systematic review of *RP2*-RD in the Japanese population was also performed. All four patients were clinically diagnosed with retinitis pigmentosa (RP). The mean age at examination was 36.5 (10–47) years, and the mean visual acuity in the right/left eye was 1.40 (0.52–2.0)/1.10 (0.52–1.7) in the logarithm of the minimum angle of resolution unit, respectively. Three patients showed extensive retinal atrophy with macular involvement, and one had central retinal atrophy. Four *RP2* variants were identified, including two novel missense (p.Ser6Phe, p.Leu189Pro) and two previously reported truncating variants (p.Arg120Ter, p.Glu269CysfsTer3). The phenotypes of two patients with truncating variants were more severe than the phenotypes of two patients with missense variants. A systematic review revealed additional 11 variants, including three missense and eight deleterious (null) variants, and a statistically significant association between phenotype severity and genotype severity was revealed. The clinical and genetic spectrum of *RP2*-RD was illustrated in the Japanese population, identifying the characteristic features of a severe form of RP with early macular involvement.

KEYWORDS

inherited retinal disorder, retinitis pigmentosa, *RP2* gene, X-linked recessive

1 | INTRODUCTION

Inherited retinal disorder (IRD) is one of the major causes of blindness in developed countries in both children and the working population (Liew, Michaelides, & Bunce, 2014; Sohocki et al., 2001; Solebo, Teoh, & Rahi, 2017). Retinitis pigmentosa (RP) represents a heterogeneous group of RDs characterized by progressive bilateral degeneration of rod and cone photoreceptors, which affects approximately 1:3000 individuals (Boughman, Conneally, & Nance, 1980; Chizzolini et al., 2011; Lyraki, Megaw, & Hurd, 2016; Prokisch, Hartig, Hellinger, Meitinger, & Rosenberg, 2007). Various inheritance patterns have been identified in RP and allied disorders, including autosomal dominant, autosomal recessive (AR), X-linked recessive (XL), mitochondrial inheritance, and others (Wright, Chakarova, Abd El-Aziz, & Bhattacharya, 2010).

XLRP is observed in approximately 10 to 20% of RP cases (Breuer et al., 2002; Fishman, 1978; Haim, 1992; Prokisch et al., 2007; Wright et al., 2010) and is associated with the most severe form of the disease (Fishman, 1978). Three causative genes for XLRP are the RP GTPase regulator (*RPGR*; OMIM: 312610), the retinitis pigmentosa

2 (*RP2*; OMIM: 312600), and orofacioidigital syndrome 1 (*OFD1*; OMIM: 300170) genes. *RGPR* and *RP2* account for 70–90% and 7–18% of XLRP cases, respectively (Hardcastle et al., 1999; Neidhardt et al., 2008; Pelletier et al., 2007; Sahel, Marazova, & Audo, 2014; Vervoort et al., 2000).

RP2 was first identified by linkage analysis and encodes the *RP2* protein, which consists of 350 residues (Schwahn et al., 1998). The *RP2* protein is localized to the plasma membrane of rod/cone photoreceptors, the retinal pigment epithelium (RPE), and other retinal cells in human (Grayson et al., 2002), as well as in the Golgi complex, the primary cilia, and the basal body of the connecting cilium in mice (Evans et al., 2010; T. Hurd et al., 2010; T. W. Hurd, Fan, & Margolis, 2011; Lyraki et al., 2016). *RP2* goes through dual acylation at the extreme N-terminus, and this modification is crucial for plasma membrane localization and connecting cilium targeting (Chapple et al., 2000; Chapple, Hardcastle, Grayson, Willison, & Cheetham, 2002; Evans et al., 2010; T. Hurd et al., 2010; Lyraki et al., 2016). Cone-dominated retinal degeneration was reported in mouse models (Li et al., 2013; Li, Rao, & Khanna, 2019; H. Zhang et al., 2015).

Since the discovery of *RP2* as a causative gene for RP, 133 disease-associated variants have been identified, including 43 missense variants, 14 nonsense variants, 15 splice site alterations, 50 small insertions/deletions, nine gross deletions, one gross insertion, and others (HGMD; <https://portal.biobase-international.com>; Supporting Information), and patients with *RP2*-associated retinal disorder (*RP2*-RD) often present a severe and "atypical" form for RP, with early macular involvement causing central visual loss (Andreasson et al., 2003; Carss et al., 2017; Dandekar et al., 2004; Hosono et al., 2018; Jayasundera et al., 2010; Ji et al., 2010; Jin, Liu, Hayakawa, Murakami, & Nao-i, 2006; Maeda et al., 2018; Mashima et al., 2000; Mashima, Saga, Akeo, & Oguchi, 2001; Mears et al., 1999; Miano et al., 2001; Prokisch et al., 2007; Sharon et al., 2000; Sharon et al., 2003; Vorster et al., 2004; Wada, Nakazawa, Abe, & Tamai, 2000; Wang et al., 2014; Yang et al., 2014). A number of studies have been published about *RP2*-RD, especially in the European population; however, only a limited number of case reports/series have described the clinical and genetic features of *RP2*-RD in the East Asian population (Dan, Huang, Xing, & Shen, 2020; Hosono et al., 2018; Ji et al., 2010; Jiang et al., 2017; Jin et al., 2006; Kim et al., 2019; Koyanagi et al., 2019; Kurata et al., 2019; Lim, Park, Lee, & Taek Lim, 2016; Maeda et al., 2018; Mashima et al., 2001; Mashima et al., 2000; Pan et al., 2014; Wada et al., 2000; Xu et al., 2019; J. Zhang et al., 2019).

Therefore, the purpose of this study was to characterize the clinical and genetic features of patients with *RP2*-RD in a large nationwide Japanese cohort. A systematic review of *RP2*-RD in the Japanese population was also performed to clarify the genetic background and establish a genotype–phenotype association.

2 | METHODS

The protocol of this study adhered to the tenets of the Declaration of Helsinki and was approved by the Ethics Committee of the participating institutions of the Japan Eye Genetics Consortium (JEGC; <http://www.jegc.org/>). The principal institute is National Institute of Sensory Organs (NISO), National Hospital Organization Tokyo Medical Center (Reference: R18-029) (World Medical Association, 2013).

2.1 | Participants

Patients with a clinical diagnosis of IRD and available whole-exome sequencing (WES) genetic data were studied between 2008 and 2018. A total of 1,294 subjects from 730 families for whom genotype–phenotype association studies were completed, were surveyed, including 47 families with XLRP and 141 families with sporadic RP (Fujinami et al., 2016; Fujinami et al., 2019; Fujinami-Yokokawa et al., 2019; Fujinami-Yokokawa et al., 2020; Kameya et al., 2019; Katagiri et al., 2020; Kondo et al., 2019; Maeda-Katahira et al., 2019; Mawatari et al., 2019; Mizobuchi et al., 2019; Nakamura et al., 2019; Nakanishi et al., 2016; Pontikos et al., 2020; Xiao Liu et al., 2020; Yang et al., 2020).

2.2 | Clinical examinations

Clinical information is available in the NISO online database, including ethnicity, medical and family history, chief complaints of visual symptoms, onset of disease (of when the visual loss was first noted by the patient or when an abnormal retinal finding was first detected), measurement of refractive errors, best-corrected decimal visual acuity (BCVA) converted to the logarithm of the minimum angle of resolution (LogMAR) unit, fundus photographs, fundus autofluorescence (FAF) images, spectral-domain optical coherence tomographic (SD-OCT) images, kinetic visual fields, and electrophysiological responses recorded in accordance with the international standards of the International Society for Clinical Electrophysiology of Vision (ISCEV) (McCulloch et al., 2015a, 2015b).

2.3 | Variant detection

Genomic DNA was extracted from all affected subjects and unaffected family members (where available) for co-segregation analysis. WES with target sequence analysis of 301 retinal disease-associated genes mainly listed in a public database (RetNet <https://sph.uth.edu/retnet/home.htm>) was performed (Fujinami et al., 2016; Xiao Liu et al., 2020). The called variants were filtered based on the allele frequencies in the general Japanese population (less than 1%) of the Human Genetic Variation Database (HGVD; <http://www.hgvd.genome.med.kyoto-u.ac.jp/>). Hypomorphic variants with high allele frequencies (>1%) were analyzed for three particular genes (*EYS*, *ABCA4*, *USH2A*) (Yang et al., 2020). Depth and coverage for the target areas were assessed using the integrative Genomics Viewer (<http://www.broadinstitute.org/igv/>). Sanger bi-direct sequencing was performed to confirm the detected *RP2* variants and to conduct co-segregation analysis. Primer sequences are provided in Table S1.

Together with the clinical features (phenotype categorization) and the patterns of inheritance, disease-causing variants were determined from the detected/filtered variants in the retinal disease-associated genes (Fujinami-Yokokawa et al., 2020; Xiao Liu et al., 2020).

2.4 | In silico molecular genetic analysis

The allele frequencies of all called variants for the Japanese, East Asian, South Asian, European, and African populations were established based on the HGVD (Japanese), Integrative Japanese Genome Variation (iJGVD 3.5k, 4.7k; <https://jmorp.megabank.tohoku.ac.jp/ijgvd/>; Japanese), 1,000 Genomes (<http://www.internationalgenome.org/>; total), and the Genome Aggregation Database (gnomAD; <http://gnomad.broadinstitute.org/>; East Asian, South Asian, European [non-Finish], and African).

All detected variants in the *RP2* gene were analyzed with general and functional prediction programs: MutationTaster (<http://www.mutationtaster.org/>), FATHMM (<http://fathmm.biocompute.org.uk/9/>), Combined Annotation Dependent Depletion (CADD; <https://cadd.gs.washington.edu/>), SIFT (<https://www.sift.co.uk/>), PROVEAN ([-83-](http://</p>
</div>
<div data-bbox=)

provean.jcvi.org/index.php), Polyphen 2 (<http://genetics.bwh.harvard.edu/pph2/>), and Human Splicing Finder (<http://www.umd.be/HSF3/>). The evolutionary conservation scores were evaluated with the UCSC database (<https://genome.ucsc.edu/index.html>).

The location of the detected *RP2* variants was analyzed with a schematic genetic and protein structure of *RP2* (ENST00000218340.3), and multiple alignments of eight species of *RP2* were performed with the Clustal Omega program (<https://www.ebi.ac.uk/Tools/msa/clustalo/>). Molecular modeling of missense variants was performed with YASARA software (<http://www.yasara.org/>) based on a Swiss model (O75695; XRP2_HUMAN; <https://swissmodel.expasy.org/>).

The variant classification was performed for all detected variants, according to the guidelines of the American College of Medical Genetics and Genomics (ACMG) (Richards et al., 2015).

2.5 | A systematic review of *RP2*-RD

A systemic review of peer-reviewed articles that describe Japanese cases with *RP2*-RD was performed. A public search engine (PubMed; <https://www.ncbi.nlm.nih.gov/pubmed/>) was used to identify articles, and clinical and genetic information was collected. For the previously reported *RP2* variants, in silico molecular genetic analyses were performed in the same way as in the current study.

2.6 | Analysis of genotype–phenotype association

Patients in the current study and previously reported cases were classified into two genotype groups based on the presence of null *RP2* variants such as nonsense variants, frameshift variants, and splice site alterations: genotype group A with null variants and genotype group B with missense variants. For the purpose of this analysis, probands in the current cohort and previous publications were classified into two phenotype groups based on disease onset and BCVA: (a) a mild phenotype group showing both late-onset (≥ 10 years) and moderate or better VA (between 0.22 and 1.0 LogMAR unit in the better eye) and (b) a severe phenotype group with both early-onset (< 10 years) and severe VA (1.0 LogMAR unit or worse in the better eye). Patients who did not meet any of the two criteria were classified into an intermediate phenotype group. Probands with available data in families were selected for the further analyses and patients with unavailable data of either onset or VA were excluded.

An association between the genotype group classification and the phenotype severity group classification was investigated with Cochran-Armitage Test. A *p* value $< .05$ was considered statistically significant.

3 | RESULTS

3.1 | Demographics

Four affected males from four families who had a clinical diagnosis of IRD and were harboring *RP2* variants were identified. The detailed

demographics are described in Table 1. All four patients were clinically diagnosed with RP by attending doctors. The pedigrees of the four families are presented in Figure 1. All four families were originally from Japan and any mixture with other ethnicity was not reported. XL family history was clearly reported or possible in three families (Families #2, #3, and #4), and no affected subjects except for the proband were reported in one family (Family #1). One patient had a medical history of severe uveitis in the left eye (Patient 2), and retinal imaging, visual field testing and electrophysiological assessment were unavailable due to the dense corneal opacity. Cataracts were reported in two patients (Patients 2 and 4), and one patient underwent cataract surgery in the right eye (Patient 2). The mean age at the latest examination of four patients was 32.5 years (range, 10–47).

3.2 | Onset, chief complaint, refraction, and visual acuity

The mean age of onset was 11.3 (range, 3–28) years in the three patients with available records. Two of these three patients had early-onset of 3 years (Patients 1 and 2). Chief complaints at the initial visit of four patients with available records were night blindness in two patients (Patients 2 and 3), photophobia in one (Patient 1), and reduced visual acuity in one (Patient 4).

The mean spherical equivalent of the refractive errors of three phakic patients with available records was -2.17 diopter (-6.0 to 0.0) in the right eye and -2.33 diopter in the left eye (-6.0 to -0.50). Two patients had high myopia (Patients 2 and 4). One patient had an intraocular lens in the right eye (Patient 2). The median values of BCVA in the right and left eyes of the four patients with available records were 1.27 (0.52–2.00), and 1.12 (0.52–1.70) LogMAR units, respectively. There were three patients with severe VA (1.0 or worse LogMAR units in the better eye) (Patients 1, 2, and 4), and one with moderate VA (between 0.22 and 1.0 LogMAR unit in the better eye) (Patient 3).

3.3 | Retinal images and morphological findings

Fundus photographs were obtained in all four patients, and FAF images were available in one patient (Patient 1). The representative images are presented in Figure 2, and the detailed findings are described in Table 2. Extensive atrophic changes were observed in two patients (Patients 1 and 2). There was one patient with peripheral atrophy (Patient 3) and one with atrophic changes at the posterior pole (Patient 4). Preserved foveal appearance was shown in two patients (Patients 1 and 3), and preserved peripheral appearance was found in one patient (Patient 4). Bone spicule pigmentation at the periphery was identified in one patient (Patient 2), and macular pigmentation was detected in two patients (Patients 2 and 4). Retinal vessel attenuation was observed in three patients (Patients 1–3), and optic disc pallor was shown in two patients (Patients 2 and 3).

SD-OCT was obtained in four patients (Patients 1–4). Representative images are presented in Figure 3. Loss of photoreceptor layers

TABLE 1 Demographics and detected variants of four Japanese patients with RP2-associated retinal disorder (RP2-RD)

Family no	Patient no	Patient ID	Inheritance	Sex	Age (at latest examination)	Onset	Chief complaint/ other symptoms	Refractive errors		BCVA in the LogMAR unit		Phenotype severity group	Genotype group
								RE (diopter)	LE (diopter)	RE	LE		
1 (TMC-01)	1-II:1 (patient 1)	1-II:3	Sporadic	M	10	3	Photophobia/poor VA/ night blindness	0.0	-0.5	1.3	1.15	C.358C>T, p.Arg120Ter	A
2 (NU-01)	2-II:3 (patient 2)	2-II:3	XL	M	35	3	Night blindness/poor VA/ peripheral visual field defect	-6.0	NA	2	NLP	c.801_804del, p.Glu269CysfsTer3	A
3 (TU-01)	3-III:1 (patient 3)	3-III:1	XL	M	38	28	Night blindness	-0.5	-0.5	0.52	0.52	c.17C>T, p.Ser6Phe	B
4 (KDU-01)	4-II:1 (patient 4)	4-II:1	XL	M	47	NA	Reduced visual acuity	-6.0	-6.0	1.7	1.7	c.566T>C, p.Leu189Pro	B

Note: Age was defined the age when the latest examination was performed. The age of onset was defined as either the age at which visual loss was first noted by the patient or when an abnormal retinal finding was first detected. Severe post-uveitic changes with dense corneal opacity (invisible fundus) were found in the left eye of patient 2. Cataracts were reported in two patients (patients 2 and 4), and one patient underwent cataract surgery in the right eye (patient 2). RP2 transcript ID: NM_006915.2. Whole-exome sequencing with target analysis of 301 retinal disease-associated genes mainly listed on a public database (RetNet <https://sph.uth.edu/retnet/home.htm>) was performed. Genotype A: Null variants, severe group; genotype B: Missense variants, mild group. Abbreviations: AR, autosomal recessive; BCVA, best corrected deimal visual acuity converted to the logarithm of the minimum angle of resolution (LogMAR) unit; F, female; LE, left eye; M, male; NA, not available; NLP, no light perception; no. number; RE, right eye; XL, x-linked recessive.

was observed at the entire retina in three patients (Patients 1, 2, and 4) and at the peripheral retina in one patient (Patient 3). Relatively preserved foveal structure, including slight changes of fluid in the inner layers were identified in one patient (Patient 3).

3.4 | Visual fields and electrophysiological findings

Visual field testing was performed in four patients with Goldmann kinetic perimetry (Table 2). Peripheral visual field loss with central scotoma was observed in two patients (Patients 1 and 3). There was one patient with an entire visual field defect (Patient 2) and one with a large central scotoma and preserved peripheral field (Patient 4). Electrophysiological assessment was performed in four patients (Patients 1-4) (Table 2). Extinguished responses in both dark-adapted and light-adapted conditions were recorded in three patients (Patients 1-3). Relatively preserved responses in both dark-adapted and light-adapted conditions were observed in one patient (Patient 4).

3.5 | RP2 variants

Four affected probands (males) were tested with WES with target analysis of 301 retinal disease-associated genes: 1-II:1 (Patient 1), 2-II:3 (Patient 2), 3-III:1 (Patient 3), and 4-II:1 (Patient 4). In addition, two unaffected family members from Family 1 and two unaffected family members in Family 3 were examined for segregation: 1-I:1 (father of Patient 1), 1-I:2 (mother of Patient 1), 3-II:7 (father of Patient 3), and 3-II:8 (mother of Patient 3) (Figure 1, Table S2). Two mothers from two families (Families 1 and 3) were proved to be carriers: 1-I:2 (mother of Patient 1) and 3-II:8 (mother of Patient 3).

Variants data of four patients are summarized in Table 1 and Figure 1. Four hemizygous RP2 variants were identified: c.17C>T (p.Ser6Phe); c.358C>T (p.Arg120Ter); c.566T>C (p.Leu189Pro); and c.801_804del (p.Glu269CysfsTer3) (NM_006915.2). Two variants have been previously reported: p.Arg120Ter in eight articles (Carss et al., 2017; Hardcastle et al., 1999; Jin et al., 2006; Kurata et al., 2019; Mashima et al., 2001; Mears et al., 1999; Vorster et al., 2004; Wang et al., 2014) and p.Glu269CysfsTer3 in one article (Pelletier et al., 2007). The other two variants have never been reported: c.17C>T (p.Ser6Phe) and c.566T>C (p.Leu189Pro).

A schematic of the RP2 protein structure showing the positions of the four detected variants in the current study is presented in Figure 4. There was one missense variant located in exon 1 (p.Ser6Phe), one nonsense variant (p.Arg120Ter), and one missense variant (p.Leu189Pro) in exon 2, and one frameshift variant in exon 3 (p.Glu269CysfsTer3).

3.6 | In silico molecular genetic analysis

The detailed results of *in silico* molecular genetic analyses for the four detected RP2 variants in the current study are provided in Table 3.

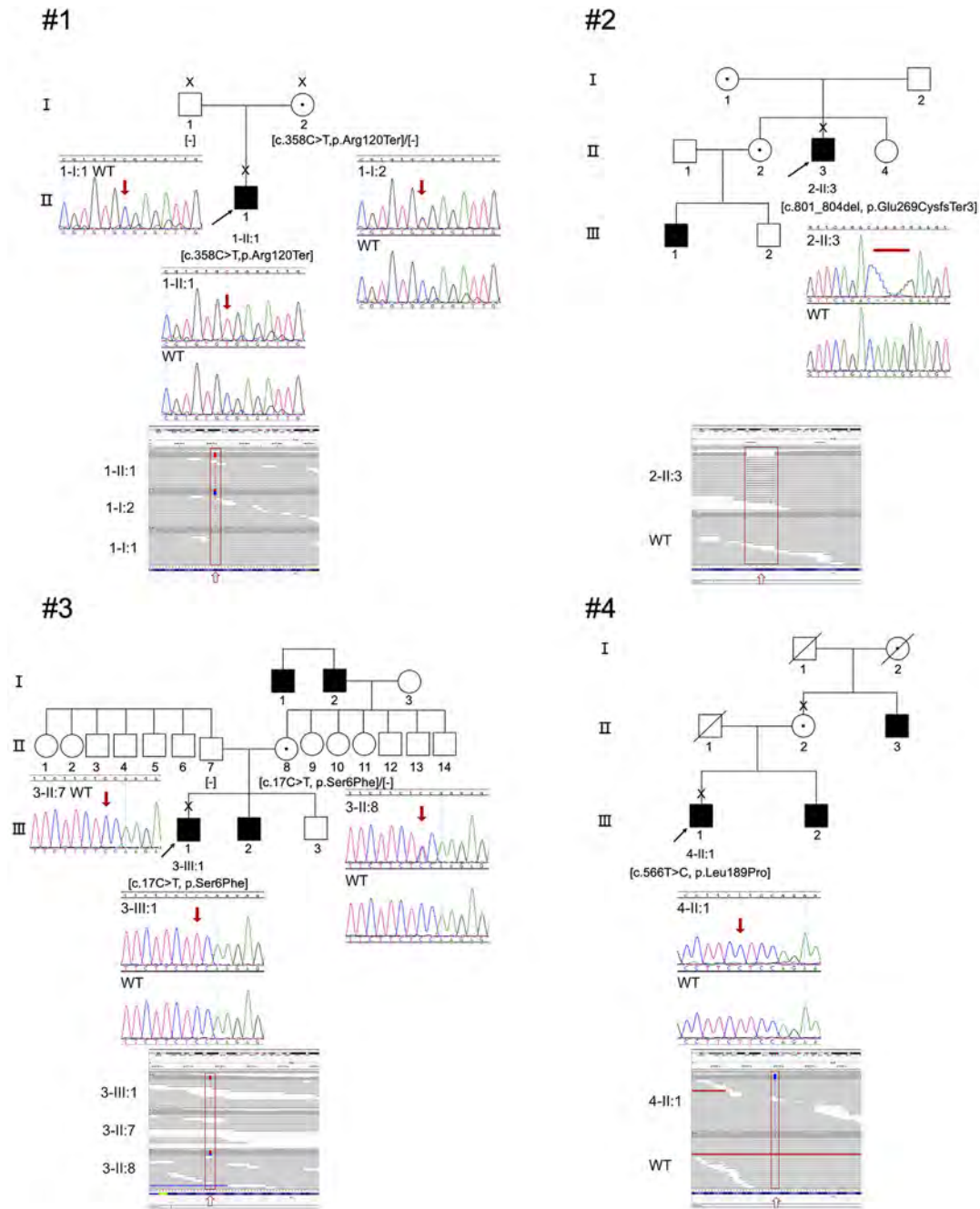


FIGURE 1 Pedigrees of four Japanese families with retinitis pigmentosa harboring hemizygous *RP2* variants. The affected males are represented by solid squares (men), and unaffected family members are represented by white icons. The slash symbol indicates deceased individuals. The generation is numbered on the left. The probands and the clinically examined individuals are marked by an arrow and a cross, respectively. Depth and coverage for the target areas by next-generation sequencing were assessed using the integrative Genomics Viewer (<http://www.broadinstitute.org/igv/>). Sanger bi-direct sequencing was also performed to confirm each variant

These four *RP2* variants were well-covered with WES, but no subjects in the general population had these variants, which confirmed the rarity of these detected variants (Table 3, Table S3).

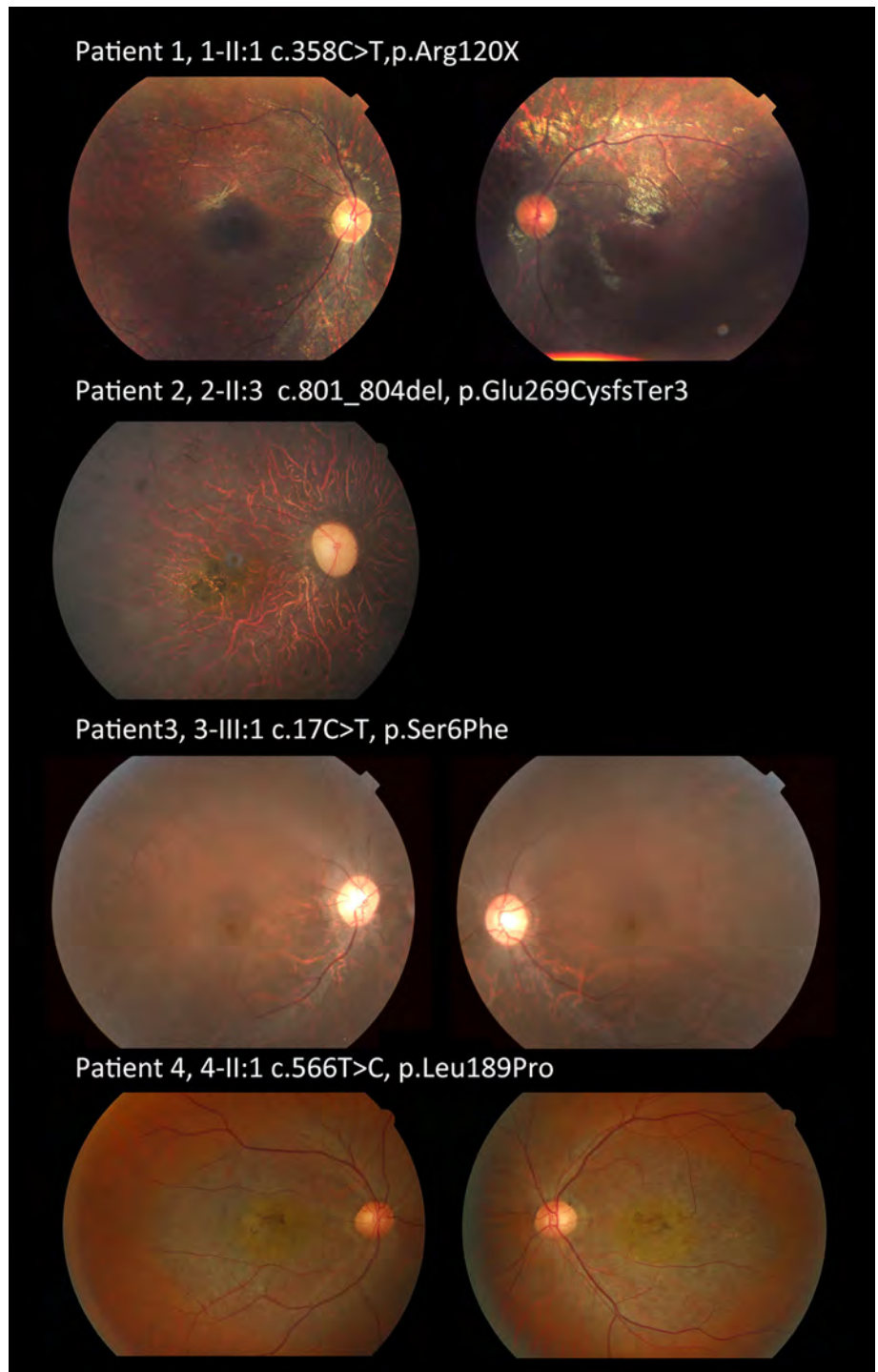
Three general (MutationTaster, FATHMM, CADD) and three functional (SIFT, PROVEAN, Polyphen2) prediction programs were applied for two missense variants (p.Ser6Phe, p.Leu189Pro), and all programs predicted disease-causing/damaging effects. The evolutionary conservation scores obtained with the UCSC database indicated high

conservation of the two missense variants (Figure 5). Molecular modeling of these missense variants is shown in Figure S1. Pathogenicity classifications, according to the ACMG guidelines, were pathogenic for the two truncating variants (p.Glu269CysfsTer3, p.Arg120Ter), likely pathogenic for the one missense variant (p.Ser6Phe), and uncertain significance for the one missense variant (p.Leu189Pro).

Overall, given the inheritance and the phenotype, two disease-causing variants (p.Glu269CysfsTer3, p.Arg120Ter) and two putative

FIGURE 2 Fundus photographs and fundus autofluorescence images of *RP2*-associated retinal disorder (*RP2*-RD).

Patient 1: Extensive retinal atrophic changes with relatively preserved foveal appearance and vessel attenuation.
Patient 2: Extensive retinal atrophic changes with bone spicule pigmentation at the periphery and patchy pigmentation at the macula, vessel attenuation, and disc pallor.
Patient 3: Atrophic changes at the peripheral retina with relatively preserved foveal appearance, vessel attenuation, and disc pallor.
Patient 4: Atrophic changes at the posterior pole with pigmentation at the macula



disease-causing variants (p.Ser6Phe, p.Leu189Pro) were determined in four families with XLRP.

3.7 | Nineteen cases from 14 Japanese families with *RP2*-RD in previous reports

There are eight previous reports of *RP2*-RD in the Japanese population (Hosono et al., 2018; Jin et al., 2006; Koyanagi et al., 2019;

Kurata et al., 2019; Maeda et al., 2018; Mashima et al., 2000; Mashima et al., 2001; Wada et al., 2000). The summarized data are presented in Table 4. Nineteen affected males from 14 families were reported in total. There were 17 patients with RP and two patients with Leber congenital amaurosis (LCA).

The mean age at the latest examination among the 16 patients with available data was 31.2 (16–61) years, and the mean age at onset of the eight patients with available data was 5.75 (3–11) years. Other descriptions about the age of onset were as follows: in the first

TABLE 2 Retinal, morphological, visual field, and electrophysiological findings of four Japanese patients with RP2-RD

Patient no	Fundus/FAF findings	SD-OCT findings	Visual field	Electrophysiological assessment
1	Extensive retinal atrophic changes with relatively preserved foveal appearance and vessel attenuation.	Loss of photoreceptor layers at the entire retina with relatively preserved other sensory retinal layers and RPE layer.	Peripheral visual field loss with central scotoma.	Extinguished responses in both dark-adapted and light-adapted conditions.
2	Extensive retinal atrophic changes with bone spicule pigmentation at the periphery and patchy pigmentation at the macula, vessel attenuation, and disc pallor.	Loss of photoreceptor layers at the entire retina with thinned RPE.	Entire visual field loss.	Extinguished responses in both dark-adapted and light-adapted conditions.
3	Atrophic changes at the peripheral retina with relatively preserved foveal appearance, vessel attenuation, and disc pallor.	Loss of photoreceptor layers at the peripheral retina with relatively preserved foveal structure including slight changes of fluid in the inner layers.	Peripheral visual field loss with central scotoma.	Extinguished responses in both dark-adapted and light-adapted conditions.
4	Atrophic changes at the posterior pole with pigmentation at the macula.	Loss of photoreceptor layers at the entire retina with thinned RPE.	Large central scotoma with preserved peripheral field.	Relatively preserved responses in both dark-adapted and light-adapted conditions.

Note: Retinal imaging, visual field testing, and electrophysiological assessment were unavailable due to the dense corneal opacity after severe uveitis in the left eye of Patient 2.

Abbreviations: FAF, fundus autofluorescence; LE, left eye; RE, right eye; RPE, retinal pigment epithelium; SD-OCT, spectral-domain optical coherence tomography.

decade (two patients), early teens (one patient), within 1 year (one patient), and childhood (one patient). Night blindness was noticed as the chief complaint in 10 out of the 12 patients (10/12, 83%) with available data. The mean spherical equivalent of refractive errors of 10 patients with available data was -6.6 diopter (-12.0 – 0.75) in the right eye and -6.1 diopter in the left eye (-10.0 – 0.50). The mean BCVA in the right and left eyes of 12 patients with available data was 1.14 (0.70–1.52) and 1.25 (0.52–1.70) LogMAR units, respectively. There were five eyes with hand motion, three eyes with light perception, and one eye with non-light perception. Electrophysiological responses were undetectable in 12 patients with available data.

The detailed results of *in silico* molecular genetic analyses for the 12 RP2 variants in the previous Japanese reports are provided in Table 3. There were four frameshift variants, three nonsense variants, two splice site alterations, and three missense variants: c.87G>A (p.Trp29Ter); c.102+1G>A; c.217delT (p.Tyr73IlefsTer18); c.353G>A (p.Arg118His); c.358C>T (p.Arg120Ter); c.413A>G (p.Glu138Gly); c.677delG (p.Gly226ValfsTer12); c.685C>T (p.Gln229Ter); c.758T>G (p.Leu253Arg); c.769-2A>G; c.882delA (p.Gly295ValfsTer14); and c.831_832dupTC (p.Gln278LeufsTer16). Eight variants are unique in the Japanese population. With regard to four variants, there are reports from other populations: c.102+1G>A; p.Arg118His; p.Arg120Ter; and p.Glu138Gly. One common variant (p.Arg120Ter) was identified in three Japanese families in the previous reports (Jin et al., 2006; Kurata et al., 2019; Mashima et al., 2001).

3.8 | Genotype–phenotype association

For the analysis, a total of 10 probands with available onset age and BCVA were studied: three from the current study and seven from previously reported cases. There were eight patients in genotype group A (null variants) and two in genotype group B (non-null variants) (Table S4). Seven patients had a severe phenotype with earlier onset of the disease and severe VA loss, and three had a mild phenotype with later onset and moderate VA loss. A statistically significant association between genotype group classification and phenotype severity classification was revealed ($p < .05$).

4 | DISCUSSION

The clinical and genetic spectrum of RP2-RD was documented in a nationwide cohort of the Japanese population, detecting four variants, two of which have never been reported. A severe RP phenotype with early macular involvement causing central visual loss was identified and a genotype–phenotype association based on the presence of null variants was illustrated.

In the present study, RP2-RD accounted for 6.4% of XLRP families (3/47 families with XLRP) and 0.7% of sporadic RP cases (1/141 families with sporadic RP) in the JEGC cohort with IRD. Koyanagi et al. reported genetic results of a large cohort of 1,209 patients with RP and revealed that three of 18 patients (3/18, 16.7%) with a family

FIGURE 3 Optical coherence tomographic images of RP2-RD. Patient 1: Loss of photoreceptor layers at the entire retina with relatively preserved other sensory retinal layers and retinal pigment epithelial (RPE) layer. Patient 2: Loss of photoreceptor layers at the entire retina with thinned RPE. Patient 3: Loss of photoreceptor layers at the peripheral retina with relatively preserved foveal structure, including slight changes of fluid in the inner layers. Patient 4: Loss of photoreceptor layers at the entire retina with thinned RPE

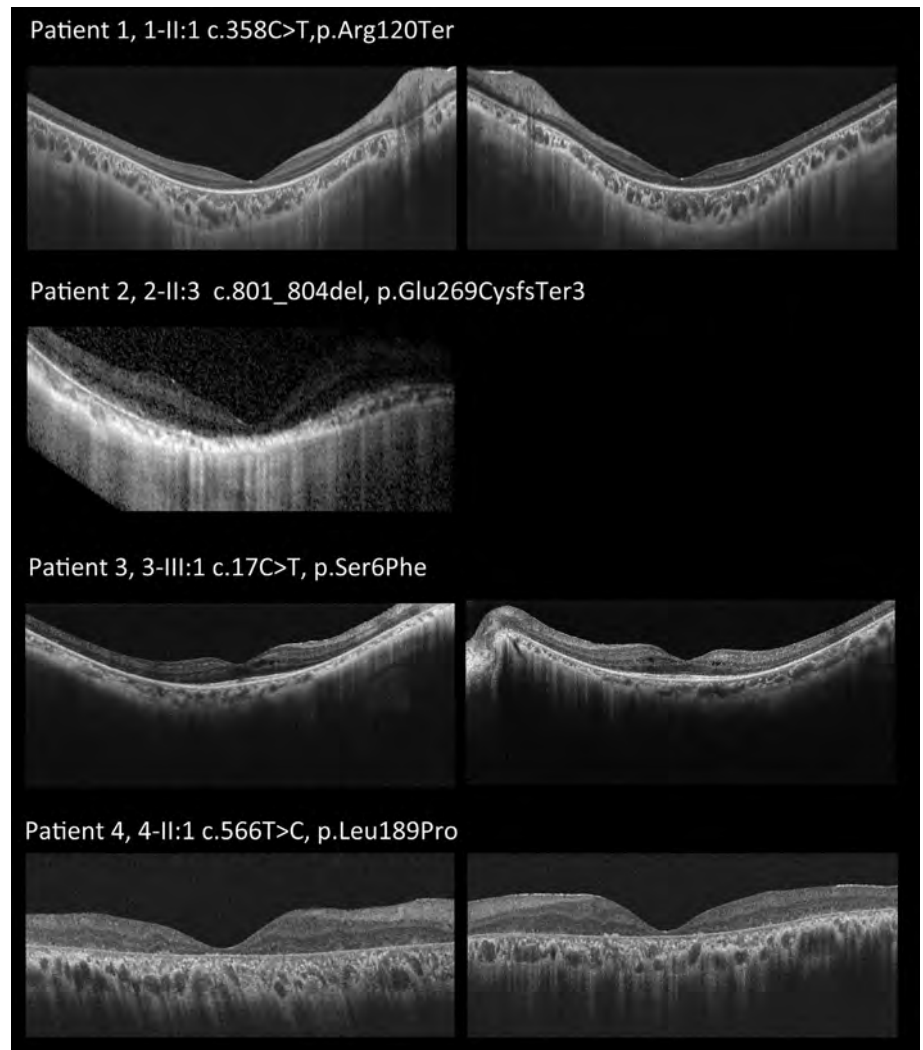


FIGURE 4 A schematic genetic and protein structure of RP2 and the location of the detected variants. The RP2 gene (ENST00000218340.3) contains five exons that encode a 350 amino acid protein containing a myristoylation part, a cofactor C (Arl3 binding) domain, and a ferredoxin-like domain (Jayasundera et al., 2010). Four variants detected in the current study are underlined (c.17C>T (p.Ser6Phe); c.358C>T (p.Arg120Ter); c.566T>C (p.Leu189Pro); and c.801_804del (p.Glu269CysfsTer3)), and previously reported variants in the Japanese populations are shown without an underline. Two detected variants (p.Ser6Phe, p.Leu189Pro), which have never been reported, are shown in *italic*

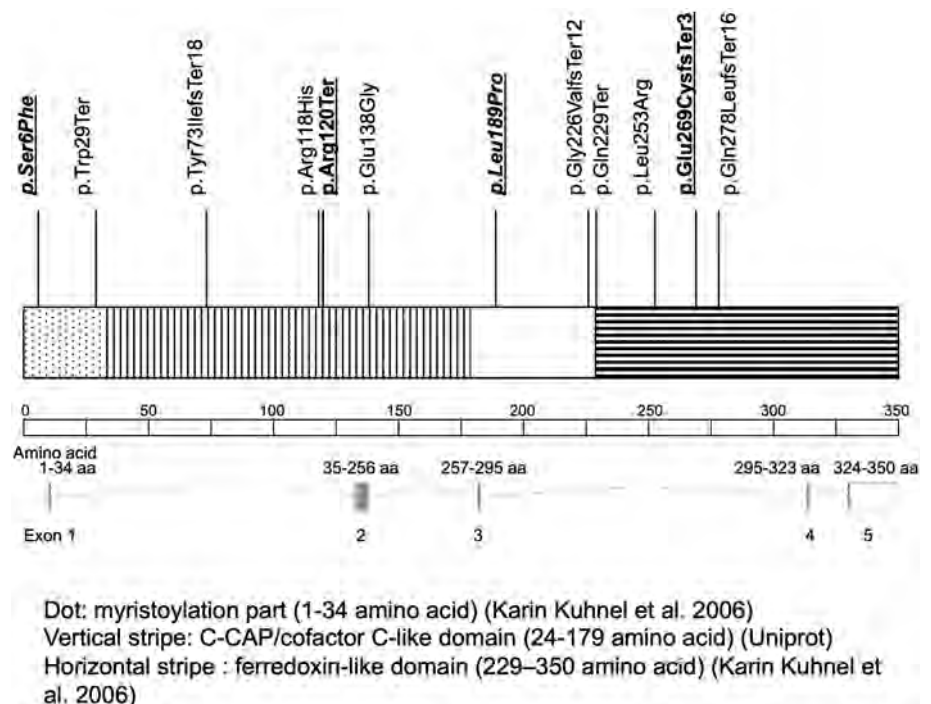


TABLE 3 *In silico* molecular genetic analysis results for four detected variants in the current study and 10 previously reported variants in Japanese patients with RP2-RD

Nucleotide change	Amino acid change/ effect	Position	Coding impact	Location	dbSNP ID	IJGVD					Allele frequency (genome)					
						HGVD	3.5K	4.7K	1000 genome	East Asian	South Asian	African	European (Non-Finnish)	Total	Male	
c.17C>T	p.Ser6Phe	46696552	Missense	Exon 1 of 5 position 75 of 160 (coding)	NA	NA	NA	NA	NA	NA	NA	NA	NA	NA	NA	NA
c.87G>A	p.Trp29Ter	46696622	Nonsense	Exon 1 of 5 position 145 of 160 (coding, NMD)	NA	NA	NA	NA	NA	NA	NA	NA	NA	NA	NA	NA
c.102+1G>A	Splice site alteration	46696638	Splice site alteration	Intron 1 of 4 position 1 of 16273 (splicing-ACMG, splicing, intronic)	NA	NA	NA	NA	NA	NA	NA	NA	NA	NA	NA	NA
c.217delT	p.Tyr73IlefsTer18	46713025	Frameshift	Exon 2 of 5 position 115 of 666 (coding, NMD)	NA	NA	NA	NA	NA	NA	NA	NA	NA	NA	NA	NA
c.353G>A	p.Arg118His	46713161	Missense	Exon 2 of 5 position 251 of 666 (coding)	rs28933687	NA	NA	NA	NA	NA	NA	NA	NA	NA	NA	NA
c.358C>T, p. Arg120Ter	p.Arg120Ter	46713166	Nonsense	Exon 2 of 5 position 256 of 666 (coding, NMD)	rs104894927	NA	NA	NA	NA	NA	NA	NA	NA	NA	NA	NA
c.413A>G	p.Glu138Gly	46713221	Missense	Exon 2 of 5 position 311 of 666 (coding)	NA	NA	NA	NA	NA	NA	NA	NA	NA	NA	NA	NA
c.566T>C	p.Leu189Pro	46713374	Missense	Exon 2 of 5 position 464 of 666 (coding)	NA	NA	NA	NA	NA	NA	NA	NA	NA	NA	NA	NA
c.677delG	p.Gly226ValfsTer12	46713485	Frameshift	Exon 2 of 5 position 575 of 666 (coding, NMD)	NA	NA	NA	NA	NA	NA	NA	NA	NA	NA	NA	NA
c.685C>T	p.Gln229Ter	46713493	Nonsense	Exon 2 of 5 position 583 of 666 (coding, NMD)	NA	NA	NA	NA	NA	NA	NA	NA	NA	NA	NA	NA
c.758T>G	p.Leu253Arg	46713566	Missense	Exon 2 of 5 position 656 of 666 (coding)	NA	NA	NA	NA	NA	NA	NA	NA	NA	NA	NA	NA
c.769-2A>G	Splice site alteration	46719421	Splice site alteration	Intron 2 of 4 position 5845 of 5846 (splicing-ACMG, splicing, intronic)	NA	NA	NA	NA	NA	NA	NA	NA	NA	NA	NA	NA
c.801_804delAAAG	p.Glu269CysfsTer3	46719455	Frameshift	Exon 3 of 5 position 33-36 of 115 (coding, NMD)	NA	NA	NA	NA	NA	NA	NA	NA	NA	NA	NA	NA

TABLE 3 (Continued)

Nucleotide change	Amino acid change/ effect	Position	Coding impact	Location	dbSNP ID	iGVGD				Allele frequency (genome)						
						HGVD	3.5K	4.7K	1000 genome	East Asian	South Asian	African	European (Non-Finnish)	Total	Male	
c.831_832dupTC	p.Gln278LeufsTer16	46719484	Frameshift	Exon 3 of 5 before position 65 of 115 (coding, NMD)	NA	NA	NA	NA	NA	NA	NA	NA	NA	NA	NA	
c.882delA	p.Gly295ValfsTer14	46719536	Frameshift	Exon 3 of 5 position 114 of 115 (splicing-ACMG, splicing, coding, NMD)	NA	NA	NA	NA	NA	NA	NA	NA	NA	NA	NA	
General prediction																
MutationTaster																
Functional prediction																
CADD																
SIFT																
Human Splice Finder 3.0																
Nucleotide change	Amino acid change/ effect	Prediction	Accuracy	Converted rankscore	Prediction	Score	Converted rankscore	Score	Prediction	Score	Converted rankscore	Score	Prediction	Score	Converted rankscore	Human Splice Finder 3.0
c.17C>T	p.Ser6Phe	Disease causing	0.9993	0.4646	Damaging	-2.81	0.9113	24	Damaging	-2.81	0.9113	24	Damaging	-2.81	0.9113	Probably no impact on splicing
c.87G>A	p.Trp29Ter	Disease causing automatic	1	0.81	Damaging	0.936	0.5866	37	NA	NA	NA	NA	NA	NA	NA	Potential alteration of splicing
c.102+1G>A	Splice site alteration	Disease causing	1	0.81	Damaging	0.9426	0.6059	33	NA	NA	NA	NA	NA	NA	NA	Most probably affecting splicing
c.217delT	p.Tyr73IlefsTer18	NA	NA	NA	NA	NA	NA	26.5	NA	NA	NA	NA	NA	NA	NA	Probably no impact on splicing
c.353G>A	p.Arg118His	Disease causing	1	0.81	Damaging	-2.73	0.9068	29.1	Damaging	-2.73	0.9068	29.1	Damaging	-2.73	0.9068	Potential alteration of splicing
c.358C>T, p. Arg120Ter	p.Arg120Ter	Disease causing automatic	1	0.81	Damaging	0.7834	0.3863	34	NA	NA	NA	NA	NA	NA	NA	Potential alteration of splicing
c.413A>G	p.Glu138Gly	Disease causing	1	0.81	Damaging	-2.81	0.9113	27.8	Damaging	-2.81	0.9113	27.8	Damaging	-2.81	0.9113	Potential alteration of splicing
c.566T>C	p.Leu189Pro	Disease causing	1	0.81	Damaging	-3.01	0.9221	27.1	Damaging	-3.01	0.9221	27.1	Damaging	-3.01	0.9221	Potential alteration of splicing
c.677delG	p.Gly226ValfsTer12	NA	NA	NA	NA	NA	NA	27.5	NA	NA	NA	27.5	NA	NA	NA	Potential alteration of splicing.
c.685C>T	p.Gln229Ter	Disease causing automatic	1	0.81	Damaging	0.947	0.6204	36	Damaging	0.947	0.6204	36	NA	NA	NA	Potential alteration of splicing
c.758T>G	p.Leu253Arg	Disease causing	0.9998	0.4908	Tolerated	-1.12	0.7759	24.7	Damaging	-1.12	0.7759	24.7	Damaging	-1.12	0.7759	This mutation has probably no impact on splicing.
c.769-2A>G	Splice site alteration	NA	NA	NA	NA	NA	NA	34	NA	NA	NA	34	NA	NA	NA	Most probably affecting splicing
c.801_804delAAAAG	p.Glu269CysfsTer3	NA	NA	NA	NA	NA	NA	11.53	NA	NA	NA	11.53	NA	NA	NA	Potential alteration of splicing
c.831_832dupTC	p.Gln278LeufsTer16	NA	NA	NA	NA	NA	NA	NA	NA	NA	NA	NA	NA	NA	NA	NA
c.882delA	p.Gly295ValfsTer14	NA	NA	NA	NA	NA	NA	NA	NA	NA	NA	NA	NA	NA	NA	Potential alteration of splicing

(Continues)

Nucleotide change	Conservation				Conservation				ACMG Classification					References in the Japanese population	References in other population		
	PhyloP46way		PhastCons46way		PhyloP100way		PhastCons100way		Identified classification rules								
	Mammalian rankscore	Mammalian rankscore	Mammalian rankscore	Mammalian rankscore	vertebrate rankscore	vertebrate rankscore	vertebrate rankscore	vertebrate rankscore	Verdict	Factor1	Factor2	Factor3	Factor4			Factor5	
c.17C>T	2.072	NA	1	NA	2.226	0.4261	1	0.7164	Likely pathogenic	PM2	PP1	PP2	PP3	PP3	This study	NA	NA
c.87G>A	2.134	NA	1	NA	4.5009	0.6011	1	0.7164	Pathogenic	PV51	PM2	PP3	PP3	PP3	Koyanagi et al., 2019	NA	NA
c.102+1G>A	2.134	NA	0.994	NA	4.5009	0.6011	1	0.7164	Pathogenic	PV51	PP1	PM2	PP3	PP3	Kurata et al., 2019	Sharon et al., 2000	NA
c.217delT	4.494	NA	1	NA	NA	NA	NA	NA	Pathogenic	PV51	PP1	PM2	PP3	PP3	Kurata et al., 2019	NA	NA
c.353G>A	5.5	NA	1	NA	9.4499	0.9677	1	0.7164	Likely Pathogenic	PM2	PM5	PP2	PP3	PP5	Koyanagi et al., 2019	Schwahn et al., 1998	and others
c.358C>T	NA	NA	NA	NA	0.8289	0.271	0.8659	0.3072	Pathogenic	PV51	PP1	PM2	PP3	PP5	This study, Mashima et al., 1999	Mears et al., 2001; Jin et al., 2006; Kurata et al., 2019	and others
c.413A>G	2.134	NA	0.994	NA	8.805	0.9154	1	0.7164	Likely pathogenic	PM2	PP1	PP2	PP3	PP5	Kurata et al., 2019	Miano et al., 2001	NA
c.566T>C	4.5	NA	1	NA	7.5549	0.8117	1	0.7164	Uncertain Significance	PM2	PP3	PP3	PP3	PP3	This study	NA	NA
c.677delG	5.506	NA	1	NA	NA	NA	NA	NA	Pathogenic	PV51	PM2	PP3	PP3	PP3	Koyanagi et al., 2019	NA	NA
c.685C>T	3.8	NA	1	NA	4.504	0.6014	1	0.7164	Pathogenic	PV51	PP1	PM2	PP3	PP3	Kurata et al., 2019	NA	NA
c.758T>G	4.542	NA	1	NA	7.5549	0.8117	1	0.7164	Likely pathogenic	PS3	PM2	PP1	PP3	PP5	Wada et al., 2000	NA	NA
c.769-2A>G	4.319	NA	1	NA	8.211	0.8971	1	0.7164	Pathogenic	PV51	PM2	PP1	PP3	PP3	Hosono et al., 2018	NA	NA
c.801_804delAAAG	4.319	NA	1	NA	NA	NA	NA	NA	Pathogenic	PV51	PM2	PP3	PP3	PP3	This study	Pelletier et al., 2007	NA
c.831_832dupTC	NA	NA	NA	NA	NA	NA	NA	NA	Pathogenic	PV51	PM2	PP1	PP3	PP3	Mashima et al., 2000	NA	NA
c.882delA	NA	NA	NA	NA	NA	NA	NA	NA	Pathogenic	PV51	PM2	PP3	PP3	PP3	Maeda et al., 2018	NA	NA

Note: Chr—chromosome; Het—heterozygous; ND—not detected. Reference: NM_006915.2, ENST00000218340.3, GRCh37.p13. The allele frequency of all called variants for Japanese, East Asian, South Asian, European, and African was established based on the HGVD (Japanese), Integrative Japanese Genome Variation (IJGV) 3.5k, 4.7k; <https://jmorp.megabank.tohoku.ac.jp/ijgv/>; Japanese), 1000 genome (<http://www.internationalgenome.org/>; total), and the genome aggregation database (gnomAD); <http://gnomad.broadinstitute.org/>; East Asian, South Asian, European (non-Finish), and African). All detected variants in

the *RP2* gene were analyzed with general and functional prediction programs; MutationTaster (<http://www.mutationtaster.org>), FATHMM (<http://fathmm.biocompute.org.uk/>), Combined Annotation Dependent Depletion (CADD; <https://cadd.gs.washington.edu/>), SIFT (<https://www.sift.co.uk/>), PROVEAN (<http://provean.jcvi.org/index.php>), Polyphen 2 (<http://genetics.bwh.harvard.edu/pph2/>), and Human Splicing Finder (<http://www.umd.be/HSF3/>). Evolutionary conservation score was evaluated with the UCSC database (<https://genome.ucsc.edu/index.html>). Classification of predictions by the American College of Medical Genetics and Genomics (ACMG) was also applied for all detected variants; PVS1 (Null variant (nonsense, frameshift, canonical ± 1 or 2 splice sites, initiation codon, single or multiexon deletion) in a gene where loss of function is a known mechanism of disease); PS3 (Well-established in vitro or in vivo functional studies supportive of a damaging effect on the gene or gene product); PM2 (pathogenicity moderate 2; absent from controls in Exome Sequencing Project, 1000 Genomes Project, or Exome Aggregation Consortium); PM5 (Novel missense change at an amino acid residue where a different missense change determined to be pathogenic has been seen before); PP1 (Cosegregation with disease in multiple affected family members in a gene definitively known to cause the disease.); PP3 (Multiple lines of computational evidence support a deleterious effect on the gene or gene product (conservation, evolutionary, splicing impact, etc.); PP4 (Patient's phenotype or family history is highly specific for a disease with a single genetic etiology); PP5 (pathogenicity supporting 5; reputable source recently reports variant as pathogenic, but the evidence is not available to the laboratory to perform an independent evaluation).

history of XL harbored pathogenic *RP2* variants (Koyanagi et al., 2019). The prevalence of *RP2*-RD in Japan can be slightly lower than that in Europe (21.6% in Denmark; 15.9% in France) (Pelletier et al., 2007; Prokisch et al., 2007). In total, four out of 287 families with RP with any inheritance (4/287, 1.4%) were diagnosed with *RP2*-RD in the JEGC cohort, and this proportion was lower than that in the United States (18/611, 2.9%) (Jayasundera et al., 2010).

In the current study, three patients presented extensive/peripheral retinal atrophy with macular involvement, and one had constricted retinal atrophic changes at the posterior pole. Thus, the characteristic clinical findings of an "atypical" form of early macular involvement were identified, as reported previously (Dandekar et al., 2004; Jayasundera et al., 2010). High myopia (≤ -6.0 diopters) was identified in a half (50%) of our four Japanese patients and its prevalence is similar to that of *RP2*-RD in a different cohort (12/25, 48.0%) (Jayasundera et al., 2010). This prevalence of high myopia in *RP2*-RD was much higher than that of the general Japanese population (5.8–11.8%) reported in previous reports (Ueda et al., 2019; Yotsukura et al., 2019). Central visual loss was also found in all four patients, which was likely caused by macular dysfunction in *RP2*-RD. Although the onset of disease was variable, it is notable that the presence of macular involvement is crucial for the impairment of visual acuity in *RP2*-RD.

Two novel and two previously reported variants were identified in four Japanese families in the current study. Two truncating variants (p.Arg120Ter, p.Glu269CysfsTer3) are located in exons 2 and 3, and functional loss of the *RP2* protein was predicted. One missense variant (p.Leu189Pro) was located in the ARL3 binding domain, and the other missense variant (p.Ser6Phe) was located in the myristoylation region of the *RP2* protein (Figure 4) (Jayasundera et al., 2010; Pelletier et al., 2007; Schwahn et al., 1998). Although functional analysis has not been performed, the clinical findings and the suggested inheritance highly support the disease causation with the XL recessive inheritance.

Mashima et al. reported detailed clinical findings of a patient with p.Arg120Ter: a 24-year-old Japanese male presented a severe form of RP with early macular involvement (Mashima et al., 2001). Similar clinical findings were observed in our patient with p.Arg120Ter (Patient 1). Likewise, Kurata et al. reported the severe phenotype of a patient with this variant. Although there are four reports from other populations, a founder effect should be considered for this allele in the Japanese population, given the high prevalence of this allele (4/18 families; 22.2%) in patients with *RP2*-RD.

The current study and literature search of *RP2*-RD in the Japanese population revealed a high proportion of null variants (11/15; 73.3%), which is in keeping with the findings among the European and North American populations (9/13; 69.2% in France; 11/17; 64.8% in the United States). This finding supports that the complete loss of function is the main mechanism of *RP2*-RD shared between the Japanese and European populations.

Ten unique *RP2* variants in the Japanese population were analyzed: two variants detected in the current study and eight previously reported variants. This high proportion (10/15, 66.7%) of unique



FIGURE 5 Multiple alignments of eight species of *RP2*. The alignment was performed with the Clustal Omega program (<https://www.ebi.ac.uk/Tools/msa/clustalo/>), and the amino acid sequence alignment is numbered in accordance with the *Homo sapiens* *RP2* sequence (ENST00000218340.3). An asterisk indicates complete conservation across the eight species. The positions of variant residues are highlighted with a gray background; c.17C>T (p.Ser6Phe) and c.566T>C (p.Leu189Pro) detected in the current study and c.353G>A (p.Arg118His); c.566T.C (p.Leu189Pro); and c.758T>G (p.Leu253Arg) from previous reports

variants suggests the distinct genetic background of the Japanese population with regard to the *RP2* gene.

A genotype–phenotype association based on the presence of null variants was revealed in the current study. A more severe phenotype with early-onset disease was associated with a severe genotype with null variants, while a milder phenotype with relatively preserved visual acuity was associated with a mild genotype with missense variants. This genotype–phenotype association is in keeping with that reported in the previous literature, and such information should be useful in predicting disease prognosis (Jayasundera et al., 2010; Pelletier et al., 2007).

There are limitations in the current study. First, the clinical assessments of mothers (carriers) of the probands were unavailable and cosegregation analysis was not performed in two families. Additional analysis of mothers of the proband both in regard to clinical and genetic aspects could further validate the clinical and molecular

genetic diagnosis of *RP2*-RD. Second, the molecular disease-causing mechanisms of the novel two variants are not yet known; therefore, further functional analysis is needed to elucidate the nature of novel variants. Third, the data obtained by the literature search were not standardized, and it could be difficult to compare the data with each other. Last, the sample size for genotype–phenotype association analysis in the current study was still small, so further studies in larger cohorts could help to elucidate the disease mechanism.

In conclusion, phenotypic and genotypic characteristics of *RP2*-RD were illustrated in the Japanese population. A distinct genetic background in the Japanese population was identified; however, a significant genotype–phenotype association was confirmed, as in other populations. This information should be helpful to monitor and counsel patients, as well as to selecting patients for future therapeutic trials.

TABLE 4 Clinical information of 19 patients from 14 Japanese families with RP2-RD

Patient ID in the original article	RP2 variants	Phenotype	Inheritance	Sex	Age (at latest examination)	Onset	Chief complaint	Refractive errors			BCVA in the LogMAR unit			Electrophysiological assessment			Phenotype severity group	Genotype group	References
								RE (dioptor)	LE (dioptor)	LE	RE	LE	LE	Dark-adapted condition	Light-adapted condition	Dark-adapted condition			
c.87G>A,p.Trp29Ter	YWC-116	RP	XL	M	24	NA	NA	NA	NA	NA	NA	NA	NA	NA	NA	NA	A	Koyanagi et al., 2019	
c.102+1G>A, splice site alteration	F8-P8	RP	XL	M	16	11	Night blindness	-8.5	-4.5	0.82	0.52	0.52	Non-recordable	NA	NA	Mild	A	Kurata et al., 2019	
c.217delT, p.Tyr73IlefsTer18	F9-P9	RP	XL	M	30	9	Night blindness	-7	-6.5	1.52	1.7	1.7	Non-recordable	Non-recordable	Severe	A	Kurata et al., 2019		
c.359G>A,p.Arg118His	N-212	RP	XL	M	61	NA	NA	NA	NA	NA	NA	NA	NA	NA	NA	B	Koyanagi et al., 2019		
c.358C>T, p.Arg120Ter	I-III-1	RP	XL	M	24	5	Night blindness	-3	-3	1.15	1.15	1.15	NA	NA	Severe	A	Mashima et al., 2001		
c.358C>T, p.Arg120Ter	I-II-2	RP	XL	M	48	<10 years	Night blindness	NA	NA	LP	LP	LP	NA	NA	Severe	A	Mashima et al., 2001		
C.358C>T, p.Arg120Ter	I-II-3	RP	XL	M	44	<10 years	Night blindness/ poor vision	NA	NA	LP	HM	HM	NA	NA	Severe	A	Mashima et al., 2001		
c.358C>T, p.Arg120Ter	E-3	RP	XL	M	NA	Childhood	Night blindness	NA	NA	NA	NA	NA	Non-recordable	Non-recordable	NA	A	Jin et al., 2006		
0.358C>T, p.Arg120Ter	F10-P10	RP	XL	M	17	6	Visual loss	0.75	0.5	1.1	1.3	1.3	Non-recordable	Non-recordable	Severe	A	Kurata et al., 2019		
c.413A>G,p.Glu138Gly	F11-P11	RP	XL	M	41	NA	Night blindness/ poor visual acuity	-12	-10	HM	HM	HM	Non-recordable	NA	NA	B	Kurata et al., 2019		
c.413A>G,p.Glu138Gly	F11-P12	RP	XL	M	38	NA	NA	-10	-8.5	1.15	1.15	1.15	Non-recordable	NA	NA	B	Kurata et al., 2019		
c.677delG, p.Gly226ValfsTer12	OPH-619	RP	XL	M	36	NA	NA	NA	NA	NA	NA	NA	NA	NA	NA	A	Koyanagi et al., 2019		
c.685C>T,p.Gln229Ter	F12-P13	RP	XL	M	30	3	Visual loss	-5.25	-5.75	1.52	1.7	1.7	Non-recordable	Non-recordable	Severe	A	Kurata et al., 2019		
c.758T>G,p.Leu253Arg	III-4	RP	XL	M	29	6	Night blindness/ poor visual acuity	NA	NA	NA	NA	NA	NA	NA	NA	B	Wada et al., 2000		
c.758T>G,p.Leu253Arg	III-1	RP	XL	M	NA	Early teens	NA	-6.5	-9	0.7	1.22	1.22	Non-recordable	Non-recordable	Mild	B	Koyanagi et al., 2019		
c.769-2A>G	NA	LCA	NA	M	NA	<1 year	NA	NA	NA	Severe visual impairment	Severe visual impairment	Severely reduced or non-detectable ERG	Severely reduced or non-detectable ERG	Severely reduced or non-detectable ERG	Severe	A	Hosono et al., 2018		
c.882delA, p.Gly295ValfsTer14	40	RP	XL	M	25	NA	NA	NA	NA	NA	NA	NA	NA	NA	NA	A	Maeda et al., 2018		
c.831_832dupTC, p.Gln278LeufsTer16	IV-1	RP	XL	M	19	3	Night blindness/ photophobia	-6.75	-7.0	HM	HM	HM	NA	NA	Severe	A	Mashima et al., 2000		
c.831_832dupTC, p.Gln278LeufsTer16	IV-2	LCA	XL	M	17	3	Night blindness/ photophobia	-8	-8	1.15	1.3	1.3	NA	NA	Severe	A	Mashima et al., 2000		

Note: A systematic review of peer-reviewed articles which describe Japanese cases with RP2-RD was performed.

Abbreviations: ERG, electroretinogram; ID, identification; LCA, Leber congenital amaurosis; RP, retinitis pigmentosa.

English proofreading: English proofreading has been conducted by the Springer Nature Author Services (<https://authorservices.springernature.com/>).

ACKNOWLEDGMENTS

The authors would like to thank The Japan Eye Genetics Study (JEGC) Group. The JEGC Study Group members are as follows: Chair's Office: National Institute of Sensory Organs, Takeshi Iwata, Kazushige Tsunoda, Kaoru Fujinami, Shinji Ueno, Kazuki Kuniyoshi, Takaaki Hayashi, Mineo Kondo, Atsushi Mizota, Nobuhisa Naoi, Kei Shinoda, Shuhei Kameya, Hiroyuki Kondo, Taro Kominami, Hiroko Terasaki, Hiroyuki Sakuramoto, Satoshi Katagiri, Kei Mizobuchi, Natsuko Nakamura, Go Mawatari, Toshihide Kurihara, Kazuo Tsubota, Yoza Miyake, Kazutoshi Yoshitake, Toshihide Nishimura, Yoshihide Hayashizaki, Nobuhiro Shimozawa, Masayuki Horiguchi, Shuichi Yamamoto, Manami Kuze, Shigeki Machida, Yoshiaki Shimada, Makoto Nakamura, Takashi Fujikado, Yoshihiro Hotta, Masayo Takahashi, Kiyofumi Mochizuki, Akira Murakami, Hiroyuki Kondo, Susumu Ishida, Mitsuru Nakazawa, Tetsuhisa Hatase, Tatsuo Matsunaga, Akiko Maeda, Kosuke Noda, Atsuhiko Tanikawa, Syuji Yamamoto, Hiroyuki Yamamoto, Makoto Araie, Makoto Aihara, Toru Nakazawa, Tetsuju Sekiryu, Kenji Kashiwagi, Kenjiro Kosaki, Carninci Piero, Takeo Fukuchi, Atsushi Hayashi, Katsuhiko Hosono, Keisuke Mori, Kouji Tanaka, Koichi Furuya, Keiichiro Suzuki, Ryo Kohata, Yasuo Yanagi, Yuriko Minegishi, Daisuke Iejima, Akiko Suga, Brian P. Rossmiller, Yang Pan, Tomoko Oshima, Mao Nakayama, Megumi Yamamoto, Naoko Minematsu, Daisuke Mori, Yusuke Kijima, Kentaro Kurata, Norihiro Yamada, Masayoshi Itoh, Hideya Kawaji, Yasuhiro Murakawa, Ryo Ando, Wataru Saito, Yusuke Murakami, Hiroaki Miyata, Lizhu Yang, Yu Fujinami-Yokokawa, Xiao Liu, Gavin Arno, Nikolas Pontikos, Kazuki Yamazawa, Satomi Inoue, and Takayuki Kinoshita.

Kaoru Fujinami is supported by grants from Grant-in-Aid for Young Scientists (A) of the Ministry of Education, Culture, Sports, Science and Technology, Japan (16H06269), grants from Grant-in-Aid for Scientists to support international collaborative studies of the Ministry of Education, Culture, Sports, Science and Technology, Japan (16KK01930002), grants from National Hospital Organization Research Fund (H30-NHO-Sensory Organs-03), grants from Foundation Fighting Blindness Alan Lattes Career Development Program (CF-CL-0416-0696-UCL), grants from Health Labour Sciences Research Grant, The Ministry of Health Labour and Welfare (201711107A), and grants from Great Britain Sasakawa Foundation Butterfield Awards.

Yu Fujinami-Yokokawa is supported by grants from Grant-in-Aid for Young Scientists of the Ministry of Education, Culture, Sports, Science and Technology, Japan (18K16943).

Gavin Arno is supported by a Fight for Sight (UK) Early Career Investigator Award, NIHR-BRC at Moorfields Eye Hospital and the UCL Institute of Ophthalmology, NIHR-BRC at Great Ormond Street Hospital and UCL Institute of Child Health, and Great Britain Sasakawa Foundation Butterfield Award, UK.

Nikolas Pontikos is funded by a Moorfields Eye Charity Career Development Award (R190031A), the NIHR-BRC at Moorfields Eye Hospital and the UCL Institute of Ophthalmology.

Toshihide Kurihara is supported by Tsubota Laboratory, Inc., Fuji Xerox Co., Ltd., Kirin Company, Ltd., Kowa Company, Ltd., Novartis Pharmaceuticals, Santen Pharmaceutical Co. Ltd., and ROHTO Pharmaceutical Co., Ltd.

Takeshi Iwata is supported by Japan Agency for Medical Research and Development (AMED) (18ek0109282h0002).

Kazushige Tsunoda is supported by AMED, the Ministry of Health, Labor and Welfare, Japan (18ek0109282h0002), Grants-in-Aid for Scientific Research, Japan Society for the Promotion of Science, Japan (H26-26462674), grants from National Hospital Organization Network Research Fund, Japan (H30-NHO-Sensory Organs-03), and Novartis Research Grant (2018).

The funding sources had no role in the design and conduct of the study; collection, management, analysis, and interpretation of the data; preparation, review, or approval of the manuscript; and decision to submit the manuscript for publication.

CONFLICT OF INTEREST

All authors have completed and submitted the ICMJE Form for disclosure of potential conflicts of interest. Individual investigators who participate in the sponsored project(s) are not directly compensated by the sponsor but may receive a salary or other support from the institution to support their effort on the project(s).

Kaoru Fujinami is a paid Consultant for Astellas Pharma Inc., Kubota Pharmaceutical Holdings Co., Ltd., Acucela Inc., Novartis AG, Janssen Pharmaceutica, Sanofi Genzyme, NightstaRx Limited; reports personal fees from Astellas Pharma Inc., Kubota Pharmaceutical Holdings Co., Ltd., Acucela Inc., Novartis AG, Santen Company Limited, Foundation Fighting Blindness, Foundation Fighting Blindness Clinical Research Institute, Japanese Ophthalmology Society, Japan Retinitis Pigmentosa Society; reports grants from Astellas Pharma Inc. (NCT03281005), outside the submitted work.

Toshihide Kurihara is an investor in Tsubota Laboratory, Inc. and RestoreVision, Inc. Toshihide Kurihara reports grants and personal fees from ROHTO Pharmaceutical Co., Ltd., Tsubota Laboratory, Inc., Fuji Xerox Co., Ltd., Kowa Company, Ltd., Santen Pharmaceutical Co. Ltd., outside the submitted work.

Kazuo Tsubota reports grants and personal fees from Santen Pharmaceutical Co., Ltd., grants and personal fees from Otsuka Pharmaceutical Co., Ltd., grants and personal fees from Wakamoto Pharmaceutical Co., Ltd., grants from ROHTO Pharmaceutical Co., Ltd., grants from R-Tech Ueno, personal fees from Laboratoires Thea, grants from Alcon Japan, investor of Tear Solutions, grants and investor of Tsubota Laboratory, Inc., outside the submitted work.

ORCID

Kaoru Fujinami  <https://orcid.org/0000-0003-4248-0033>

Gavin Arno  <https://orcid.org/0000-0002-6165-7888>

Nikolas Pontikos  <https://orcid.org/0000-0003-1782-4711>

REFERENCES

Andreasson, S., Breuer, D. K., Eksandh, L., Ponjavic, V., Frennesson, C., Hiriyan, S., ... Swaroop, A. (2003). Clinical studies of X-linked

- retinitis pigmentosa in three Swedish families with newly identified mutations in the RP2 and RPGR-ORF15 genes. *Ophthalmic Genetics*, 24(4), 215–223. <https://doi.org/10.1076/opge.24.4.215.17228>
- Boughman, J. A., Conneally, P. M., & Nance, W. E. (1980). Population genetic studies of retinitis pigmentosa. *American Journal of Human Genetics*, 32(2), 223–235.
- Breuer, D. K., Yashar, B. M., Filippova, E., Hiriyanna, S., Lyons, R. H., Mears, A. J., ... Swaroop, A. (2002). A comprehensive mutation analysis of RP2 and RPGR in a north American cohort of families with X-linked retinitis pigmentosa. *American Journal of Human Genetics*, 70(6), 1545–1554. <https://doi.org/10.1086/340848>
- Carss, K. J., Arno, G., Erwood, M., Stephens, J., Sanchis-Juan, A., Hull, S., ... Raymond, F. L. (2017). Comprehensive rare variant analysis via whole-genome sequencing to determine the molecular pathology of inherited retinal disease. *American Journal of Human Genetics*, 100(1), 75–90. <https://doi.org/10.1016/j.ajhg.2016.12.003>
- Chapple, J. P., Hardcastle, A. J., Grayson, C., Spackman, L. A., Willison, K. R., & Cheetham, M. E. (2000). Mutations in the N-terminus of the X-linked retinitis pigmentosa protein RP2 interfere with the normal targeting of the protein to the plasma membrane. *Human Molecular Genetics*, 9(13), 1919–1926.
- Chapple, J. P., Hardcastle, A. J., Grayson, C., Willison, K. R., & Cheetham, M. E. (2002). Delineation of the plasma membrane targeting domain of the X-linked retinitis pigmentosa protein RP2. *Investigative Ophthalmology & Visual Science*, 43(6), 2015–2020.
- Chizzolini, M., Galan, A., Milan, E., Sebastiani, A., Costagliola, C., & Parmeggiani, F. (2011). Good epidemiologic practice in retinitis pigmentosa: From phenotyping to biobanking. *Current Genomics*, 12(4), 260–266. <https://doi.org/10.2174/138920211795860071>
- Dan, H., Huang, X., Xing, Y., & Shen, Y. (2020). Application of targeted panel sequencing and whole exome sequencing for 76 Chinese families with retinitis pigmentosa. *Molecular Genetics & Genomic Medicine*, 8(3), e1131. <https://doi.org/10.1002/mgg3.1131>
- Dandekar, S. S., Ebenezer, N. D., Grayson, C., Chapple, J. P., Egan, C. A., Holder, G. E., ... Hardcastle, A. J. (2004). An atypical phenotype of macular and peripapillary retinal atrophy caused by a mutation in the RP2 gene. *The British Journal of Ophthalmology*, 88(4), 528–532. <https://doi.org/10.1136/bjo.2003.027979>
- Evans, R. J., Schwarz, N., Nagel-Wolfrum, K., Wolfrum, U., Hardcastle, A. J., & Cheetham, M. E. (2010). The retinitis pigmentosa protein RP2 links pericentriolar vesicle transport between the Golgi and the primary cilium. *Human Molecular Genetics*, 19(7), 1358–1367. <https://doi.org/10.1093/hmg/ddq012>
- Fishman, G. A. (1978). Retinitis pigmentosa. Genetic percentages. *Archives of Ophthalmology*, 96(5), 822–826.
- Fujinami-Yokokawa, Y., Pontikos, N., Yang, L., Tsunoda, K., Yoshitake, K., Iwata, T., ... Japan Eye Genetics Consortium. (2019). Prediction of causative genes in Inherited Retinal disorders from spectral-domain optical coherence tomography utilizing deep learning techniques. *Journal of Ophthalmology*, 2019, 1691064. <https://doi.org/10.1155/2019/1691064>
- Fujinami-Yokokawa, Y., Kuniyoshi, K., Hayashi, T., Ueno, S., Mizota, A., Shinoda, K., ... Japan Eye Genetics Consortium. (2020). Clinical and genetic characteristics of 18 patients from 13 Japanese families with CRX-associated Retinal disorder: Identification of genotype-phenotype associations. *Scientific Reports*, in press, 10, 9531.
- Fujinami, K., Kameya, S., Kikuchi, S., Ueno, S., Kondo, M., Hayashi, T., ... Tsunoda, K. (2016). Novel RP1L1 variants and genotype-phenotype microstructural phenotype associations in cohort of Japanese patients with occult macular dystrophy. *Investigative Ophthalmology & Visual Science*, 57(11), 4837–4846. <https://doi.org/10.1167/iovs.16-19670>
- Fujinami, K., Yang, L., Joo, K., Tsunoda, K., Kameya, S., Hanazono, G., ... East Asia Inherited Retinal Disease Society Study Group. (2019). Clinical and genetic characteristics of east Asian patients with occult macular dystrophy (Miyake disease): East Asia occult macular dystrophy studies report number 1. *Ophthalmology*, 126(10), 1432–1444. <https://doi.org/10.1016/j.ophtha.2019.04.032>
- Grayson, C., Bartolini, F., Chapple, J. P., Willison, K. R., Bhamidipati, A., Lewis, S. A., ... Cheetham, M. E. (2002). Localization in the human retina of the X-linked retinitis pigmentosa protein RP2, its homologue cofactor C and the RP2 interacting protein Arl3. *Human Molecular Genetics*, 11(24), 3065–3074.
- Haim, M. (1992). Prevalence of retinitis pigmentosa and allied disorders in Denmark. III. Hereditary pattern. *Acta Ophthalmologica*, 70(5), 615–624.
- Hardcastle, A. J., Thiselton, D. L., Van Maldergem, L., Saha, B. K., Jay, M., Plant, C., ... Bhattacharya, S. (1999). Mutations in the RP2 gene cause disease in 10% of families with familial X-linked retinitis pigmentosa assessed in this study. *American Journal of Human Genetics*, 64(4), 1210–1215.
- Hosono, K., Nishina, S., Yokoi, T., Katagiri, S., Saito, H., Kurata, K., ... Hotta, Y. (2018). Molecular diagnosis of 34 Japanese families with Leber congenital Amaurosis using targeted next generation sequencing. *Scientific Reports*, 8(1), 8279. <https://doi.org/10.1038/s41598-018-26524-z>
- Hurd, T., Zhou, W., Jenkins, P., Liu, C. J., Swaroop, A., Khanna, H., ... Margolis, B. (2010). The retinitis pigmentosa protein RP2 interacts with polycystin 2 and regulates cilia-mediated vertebrate development. *Human Molecular Genetics*, 19(22), 4330–4344. <https://doi.org/10.1093/hmg/ddq355>
- Hurd, T. W., Fan, S., & Margolis, B. L. (2011). Localization of retinitis pigmentosa 2 to cilia is regulated by importin beta2. *Journal of Cell Science*, 124(Pt 5), 718–726. <https://doi.org/10.1242/jcs.070839>
- Jayasundera, T., Branham, K. E., Othman, M., Rhoades, W. R., Karoukis, A. J., Khanna, H., ... Heckenlively, J. R. (2010). RP2 phenotype and pathogenetic correlations in X-linked retinitis pigmentosa. *Archives of Ophthalmology*, 128(7), 915–923. <https://doi.org/10.1001/archophthol.128.7.915>
- Ji, Y., Wang, J., Xiao, X., Li, S., Guo, X., & Zhang, Q. (2010). Mutations in RPGR and RP2 of Chinese patients with X-linked retinitis pigmentosa. *Current Eye Research*, 35(1), 73–79. <https://doi.org/10.3109/02713680903395299>
- Jiang, J., Wu, X., Shen, D., Dong, L., Jiao, X., Hejtmancik, J. F., & Li, N. (2017). Analysis of RP2 and RPGR mutations in five X-linked Chinese families with retinitis pigmentosa. *Scientific Reports*, 7, 44465. <https://doi.org/10.1038/srep44465>
- Jin, Z. B., Liu, X. Q., Hayakawa, M., Murakami, A., & Nao-i, N. (2006). Mutational analysis of RPGR and RP2 genes in Japanese patients with retinitis pigmentosa: Identification of four mutations. *Molecular Vision*, 12, 1167–1174.
- Kameya, S., Fujinami, K., Ueno, S., Hayashi, T., Kuniyoshi, K., Ideta, R., ... Japan Eye Genetics, C. (2019). Phenotypical characteristics of POC1B-associated retinopathy in Japanese cohort: Cone dystrophy with normal funduscopy appearance. *Investigative Ophthalmology & Visual Science*, 60(10), 3432–3446. <https://doi.org/10.1167/iovs.19-26650>
- Katagiri, S., Hayashi, T., Nakamura, M., Mizobuchi, K., Gekka, T., Komori, S., ... Nakano, T. (2020). RDH5-related fundus Albipunctatus in a large Japanese cohort. *Investigative Ophthalmology & Visual Science*, 61(3), 53. <https://doi.org/10.1167/iovs.61.3.53>
- Kim, M. S., Joo, K., Seong, M. W., Kim, M. J., Park, K. H., Park, S. S., & Woo, S. J. (2019). Genetic mutation profiles in Korean patients with Inherited Retinal diseases. *Journal of Korean Medical Science*, 34(21), e161. <https://doi.org/10.3346/jkms.2019.34.e161>
- Kondo, H., Oku, K., Katagiri, S., Hayashi, T., Nakano, T., Iwata, A., ... Iwata, T. (2019). Novel mutations in the RS1 gene in Japanese patients with X-linked congenital retinoschisis. *Human Genome Variation*, 6, 3. <https://doi.org/10.1038/s41439-018-0034-6>
- Koyanagi, Y., Akiyama, M., Nishiguchi, K. M., Momozawa, Y., Kamatani, Y., Takata, S., ... Sonoda, K. H. (2019). Genetic characteristics of retinitis

- pigmentosa in 1204 Japanese patients. *Journal of Medical Genetics*, 56(10), 662–670. <https://doi.org/10.1136/jmedgenet-2018-105691>
- Kurata, K., Hosono, K., Hayashi, T., Mizobuchi, K., Katagiri, S., Miyamichi, D., ... Hotta, Y. (2019). X-linked retinitis pigmentosa in Japan: Clinical and genetic findings in male patients and female carriers. *International Journal of Molecular Sciences*, 20(6), 1518–1518. <https://doi.org/10.3390/ijms20061518>
- Li, L., Khan, N., Hurd, T., Ghosh, A. K., Cheng, C., Molday, R., ... Khanna, H. (2013). Ablation of the X-linked retinitis pigmentosa 2 (Rp2) gene in mice results in opsin mislocalization and photoreceptor degeneration. *Investigative Ophthalmology & Visual Science*, 54(7), 4503–4511. <https://doi.org/10.1167/iovs.13-12140>
- Li, L., Rao, K. N., & Khanna, H. (2019). Structural but not functional alterations in cones in the absence of the Retinal disease protein retinitis Pigmentosa 2 (RP2) in a cone-only retina. *Frontiers in Genetics*, 10, 323. <https://doi.org/10.3389/fgene.2019.00323>
- Liew, G., Michaelides, M., & Bunce, C. (2014). A comparison of the causes of blindness certifications in England and Wales in working age adults (16–64 years), 1999–2000 with 2009–2010. *BMJ Open*, 4(2), e004015. <https://doi.org/10.1136/bmjopen-2013-004015>
- Lim, H., Park, Y. M., Lee, J. K., & Taek Lim, H. (2016). Single-exome sequencing identified a novel RP2 mutation in a child with X-linked retinitis pigmentosa. *Canadian Journal of Ophthalmology*, 51(5), 326–330. <https://doi.org/10.1016/j.cjco.2016.03.017>
- Lyraki, R., Megaw, R., & Hurd, T. (2016). Disease mechanisms of X-linked retinitis pigmentosa due to RP2 and RPGR mutations. *Biochemical Society Transactions*, 44(5), 1235–1244. <https://doi.org/10.1042/BST20160148>
- Maeda-Katahira, A., Nakamura, N., Hayashi, T., Katagiri, S., Shimizu, S., Ohde, H., ... Tsunoda, K. (2019). Autosomal dominant optic atrophy with OPA1 gene mutations accompanied by auditory neuropathy and other systemic complications in a Japanese cohort. *Molecular Vision*, 25, 559–573.
- Maeda, A., Yoshida, A., Kawai, K., Arai, Y., Akiba, R., Inaba, A., ... Takahashi, M. (2018). Development of a molecular diagnostic test for retinitis Pigmentosa in the Japanese population. *Japanese Journal of Ophthalmology*, 62(4), 451–457. <https://doi.org/10.1007/s10384-018-0601-x>
- Mashima, Y., Saga, M., Akeo, K., & Oguchi, Y. (2001). Phenotype associated with an R120X nonsense mutation in the RP2 gene in a Japanese family with X-linked retinitis pigmentosa. *Ophthalmic Genetics*, 22(1), 43–47.
- Mashima, Y., Saga, M., Hiida, Y., Imamura, Y., Kudoh, J., & Shimizu, N. (2000). Novel mutation in RP2 gene in two brothers with X-linked retinitis pigmentosa and mtDNA mutation of leber hereditary optic neuropathy who showed marked differences in clinical severity. *American Journal of Ophthalmology*, 130(3), 357–359. [https://doi.org/10.1016/s0002-9394\(00\)00553-5](https://doi.org/10.1016/s0002-9394(00)00553-5)
- Mawatari, G., Fujinami, K., Liu, X., Yang, L., Yokokawa, Y. F., Komori, S., ... JEGC Study Group. (2019). Clinical and genetic characteristics of 14 patients from 13 Japanese families with RPGR-associated retinal disorder: Report of eight novel variants. *Human Genome Variation*, 6, 34. <https://doi.org/10.1038/s41439-019-0065-7>
- McCulloch, D. L., Marmor, M. F., Brigell, M. G., Hamilton, R., Holder, G. E., Tzekov, R., & Bach, M. (2015a). Erratum to: ISCEV standard for full-field clinical electroretinography (2015 update). *Documenta Ophthalmologica*, 131(1), 81–83. <https://doi.org/10.1007/s10633-015-9504-z>
- McCulloch, D. L., Marmor, M. F., Brigell, M. G., Hamilton, R., Holder, G. E., Tzekov, R., & Bach, M. (2015b). ISCEV standard for full-field clinical electroretinography (2015 update). *Documenta Ophthalmologica*, 130(1), 1–12. <https://doi.org/10.1007/s10633-014-9473-7>
- Mears, A. J., Gieser, L., Yan, D., Chen, C., Fahrner, S., Hirianna, S., ... Swaroop, A. (1999). Protein-truncation mutations in the RP2 gene in a north American cohort of families with X-linked retinitis pigmentosa. *American Journal of Human Genetics*, 64(3), 897–900. <https://doi.org/10.1086/302298>
- Miano, M. G., Testa, F., Filippini, F., Trujillo, M., Conte, I., Lanzara, C., ... Ciccodicola, A. (2001). Identification of novel RP2 mutations in a subset of X-linked retinitis pigmentosa families and prediction of new domains. *Human Mutation*, 18(2), 109–119. <https://doi.org/10.1002/humu.1160>
- Mizobuchi, K., Hayashi, T., Katagiri, S., Yoshitake, K., Fujinami, K., Yang, L., ... Nakano, T. (2019). Characterization of GUCA1A-associated dominant cone/cone-rod dystrophy: Low prevalence among Japanese patients with inherited retinal dystrophies. *Scientific Reports*, 9(1), 16851. <https://doi.org/10.1038/s41598-019-52660-1>
- Nakamura, N., Tsunoda, K., Mizuno, Y., Usui, T., Hatase, T., Ueno, S., ... Miyake, Y. (2019). Clinical stages of occult macular Dystrophy based on optical coherence tomographic findings. *Investigative Ophthalmology & Visual Science*, 60(14), 4691–4700. <https://doi.org/10.1167/iovs.19-27486>
- Nakanishi, A., Ueno, S., Hayashi, T., Katagiri, S., Kominami, T., Ito, Y., ... Terasaki, H. (2016). Clinical and genetic findings of autosomal recessive Bestrophinopathy in Japanese cohort. *American Journal of Ophthalmology*, 168, 86–94. <https://doi.org/10.1016/j.ajo.2016.04.023>
- Neidhardt, J., Glaus, E., Lorenz, B., Netzer, C., Li, Y., Schambeck, M., ... Berger, W. (2008). Identification of novel mutations in X-linked retinitis pigmentosa families and implications for diagnostic testing. *Molecular Vision*, 14, 1081–1093.
- Pan, X., Chen, X., Liu, X., Gao, X., Kang, X., Xu, Q., ... Zhao, C. (2014). Mutation analysis of pre-mRNA splicing genes in Chinese families with retinitis pigmentosa. *Molecular Vision*, 20, 770–779.
- Pelletier, V., Jambou, M., Delphin, N., Zinovieva, E., Stum, M., Gigarel, N., ... Rozet, J. M. (2007). Comprehensive survey of mutations in RP2 and RPGR in patients affected with distinct retinal dystrophies: Genotype-phenotype correlations and impact on genetic counseling. *Human Mutation*, 28(1), 81–91. <https://doi.org/10.1002/humu.20417>
- Pontikos, N., Murphy, C., Moghul, I., Arno, G., Fujinami, K., Fujinami, Y., ... UK Inherited Retinal Dystrophy Consortium, Phenopolis Consortium. (2020). Phenogenon: Gene to phenotype associations for rare genetic diseases. *PLoS One*, 15(4), e0230587. <https://doi.org/10.1371/journal.pone.0230587>
- Prokisch, H., Hartig, M., Hellinger, R., Meitinger, T., & Rosenberg, T. (2007). A population-based epidemiological and genetic study of X-linked retinitis pigmentosa. *Investigative Ophthalmology & Visual Science*, 48(9), 4012–4018. <https://doi.org/10.1167/iovs.07-0071>
- Richards, S., Aziz, N., Bale, S., Bick, D., Das, S., Gastier-Foster, J., ... Committee, A. L. Q. A. (2015). Standards and guidelines for the interpretation of sequence variants: A joint consensus recommendation of the American College of Medical Genetics and Genomics and the Association for Molecular Pathology. *Genetics in Medicine*, 17(5), 405–424. <https://doi.org/10.1038/gim.2015.30>
- Sahel, J. A., Marazova, K., & Audo, I. (2014). Clinical characteristics and current therapies for inherited retinal degenerations. *Cold Spring Harbor Perspectives in Medicine*, 5(2), a017111. <https://doi.org/10.1101/cshperspect.a017111>
- Schwahn, U., Lenzner, S., Dong, J., Feil, S., Hinzmann, B., van Duijnhoven, G., ... Berger, W. (1998). Positional cloning of the gene for X-linked retinitis pigmentosa 2. *Nature Genetics*, 19(4), 327–332. <https://doi.org/10.1038/1214>
- Sharon, D., Bruns, G. A., McGee, T. L., Sandberg, M. A., Berson, E. L., & Dryja, T. P. (2000). X-linked retinitis pigmentosa: Mutation spectrum of the RPGR and RP2 genes and correlation with visual function. *Investigative Ophthalmology & Visual Science*, 41(9), 2712–2721.
- Sharon, D., Sandberg, M. A., Rabe, V. W., Stillberger, M., Dryja, T. P., & Berson, E. L. (2003). RP2 and RPGR mutations and clinical correlations in patients with X-linked retinitis pigmentosa. *American Journal of Human Genetics*, 73(5), 1131–1146. <https://doi.org/10.1086/379379>
- Sohocki, M. M., Daiger, S. P., Bowne, S. J., Rodriguez, J. A., Northrup, H., Heckenlively, J. R., ... Sullivan, L. S. (2001). Prevalence of mutations

- causing retinitis pigmentosa and other inherited retinopathies. *Human Mutation*, 17(1), 42–51. [https://doi.org/10.1002/1098-1004\(2001\)17:1<42::AID-HUMU5>3.0.CO;2-K](https://doi.org/10.1002/1098-1004(2001)17:1<42::AID-HUMU5>3.0.CO;2-K)
- Solebo, A. L., Teoh, L., & Rahi, J. (2017). Epidemiology of blindness in children. *Archives of Disease in Childhood*, 102(9), 853–857. <https://doi.org/10.1136/archdischild-2016-310532>
- Ueda, E., Yasuda, M., Fujiwara, K., Hashimoto, S., Ohno-Matsui, K., Hata, J., ... Sonoda, K. H. (2019). Trends in the prevalence of myopia and myopic Maculopathy in a Japanese population: The Hisayama study. *Investigative Ophthalmology & Visual Science*, 60(8), 2781–2786. <https://doi.org/10.1167/iovs.19-26580>
- Vervoort, R., Lennon, A., Bird, A. C., Tulloch, B., Axton, R., Miano, M. G., ... Wright, A. F. (2000). Mutational hot spot within a new RPGR exon in X-linked retinitis pigmentosa. *Nature Genetics*, 25(4), 462–466. <https://doi.org/10.1038/78182>
- Vorster, A. A., Rebello, M. T., Coutts, N., Ehrenreich, L., Gama, A. D., Roberts, L. J., ... Greenberg, L. J. (2004). Arg120stop nonsense mutation in the RP2 gene: Mutational hotspot and germ line mosaicism? *Clinical Genetics*, 65(1), 7–10. <https://doi.org/10.1111/j.2004.00163.x>
- Wada, Y., Nakazawa, M., Abe, T., & Tamai, M. (2000). A new Leu253Arg mutation in the RP2 gene in a Japanese family with X-linked retinitis pigmentosa. *Investigative Ophthalmology & Visual Science*, 41(1), 290–293.
- Wang, J., Zhang, V. W., Feng, Y., Tian, X., Li, F. Y., Truong, C., ... Wong, L. J. (2014). Dependable and efficient clinical utility of target capture-based deep sequencing in molecular diagnosis of retinitis pigmentosa. *Investigative Ophthalmology & Visual Science*, 55(10), 6213–6223. <https://doi.org/10.1167/iovs.14-14936>
- World Medical Association. (2013). World medical association declaration of Helsinki: Ethical principles for medical research involving human subjects. *JAMA*, 310(20), 2191–2194. <https://doi.org/10.1001/jama.2013.281053>
- Wright, A. F., Chakarova, C. F., Abd El-Aziz, M. M., & Bhattacharya, S. S. (2010). Photoreceptor degeneration: Genetic and mechanistic dissection of a complex trait. *Nature Reviews. Genetics*, 11(4), 273–284. <https://doi.org/10.1038/nrg2717>
- Xiao Liu, K. F., Kuniyoshi, K., Kondo, M., Ueno, S., Hayashi, T., Mochizuki, K., ... Consortium, J. E. G. (2020). Clinical and genetic characteristics of 15 affected patients from 12 Japanese families with GUCY2D-associated retinal disorder. *Translational Vision Science & Technology*, 9(6), 2.
- Xu, K., Xie, Y., Sun, T., Zhang, X., Chen, C., & Li, Y. (2019). Genetic and clinical findings in a Chinese cohort with Leber congenital amaurosis and early onset severe retinal dystrophy. *The British Journal of Ophthalmology*, 104, 932–937. <https://doi.org/10.1136/bjophthalmol-2019-314281>
- Yang, L., Fujinami, K., Ueno, S., Kuniyoshi, K., Hayashi, T., Kondo, M., ... JEGC Study Group. (2020). Genetic Spectrum of EYS-associated Retinal disease in a large Japanese cohort: Identification of disease-associated variants with relatively high allele frequency. *Scientific Reports*, 10(1), 5497. <https://doi.org/10.1038/s41598-020-62119-3>
- Yang, L., Yin, X., Feng, L., You, D., Wu, L., Chen, N., ... Ma, Z. (2014). Novel mutations of RPGR in Chinese retinitis pigmentosa patients and the genotype-phenotype correlation. *PLoS One*, 9(1), e85752. <https://doi.org/10.1371/journal.pone.0085752>
- Yotsukura, E., Torii, H., Inokuchi, M., Tokumura, M., Uchino, M., Nakamura, K., ... Tsubota, K. (2019). Current prevalence of myopia and Association of Myopia with Environmental Factors among Schoolchildren in Japan. *JAMA Ophthalmology*, 137, 1233. <https://doi.org/10.1001/jamaophthalmol.2019.3103>
- Zhang, H., Hanke-Gogokhia, C., Jiang, L., Li, X., Wang, P., Gerstner, C. D., ... Baehr, W. (2015). Mistrafficking of prenylated proteins causes retinitis pigmentosa 2. *The FASEB Journal*, 29(3), 932–942. <https://doi.org/10.1096/fj.14-257915>
- Zhang, J., Gao, F., Du, C., Wang, J., Pi, X., Guo, W., ... Cui, X. (2019). A novel RP2 missense mutation Q158P identified in an X-linked retinitis pigmentosa family impaired RP2 protein stability. *Gene*, 707, 86–92. <https://doi.org/10.1016/j.gene.2019.05.006>

SUPPORTING INFORMATION

Additional supporting information may be found online in the Supporting Information section at the end of this article.

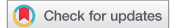
How to cite this article: Fujinami K, Liu X, Ueno S, et al. RP2-associated retinal disorder in a Japanese cohort:

Report of novel variants and a literature review, identifying a genotype-phenotype association. *Am J Med Genet Part C*.

2020;184C:675–693. <https://doi.org/10.1002/ajmg.c.31830>

RESEARCH REPORT

 OPEN ACCESS



Long-term follow-up of a Chinese patient with *KCNV2*-retinopathy

Hongxuan Lie^{a,b*}, Gang Wang^{a,b*}, Xiao Liu^{a,b,c,d*}, Xiaohong Meng^{a,b}, Yanling Long^{a,b}, Jiayun Ren^{a,b}, Lizhu Yang^{c,d}, Yu Fujinami-Yokokawa^{c,e,f,g}, Toshihide Kurihara^d, Kazuo Tsubota^d, Kaoru Fujinami^{c,d,f,g}, and Shiyong Li^{a,b}

^aOphthalmology Department, Southwest Hospital, Army Medical University (Third Military Medical University), Chongqing, China; ^bKey Lab of Visual Damage and Regeneration & Restoration of Chongqing, Chongqing, China; ^cLaboratory of Visual Physiology, Division for Vision Research, National Institute of Sensory Organs, National Hospital Organization, Tokyo Medical Center, Tokyo, Japan; ^dDepartment of Ophthalmology, Keio University School of Medicine, Tokyo, Japan; ^eGraduate School of Health Management, Keio University, Tokyo, Japan; ^fDepartment of Genetics, UCL Institute of Ophthalmology, London, UK; ^gDivision of Inherited Eye Diseases, Moorfields Eye Hospital, London, UK

ABSTRACT

Purpose: To characterize and monitor the clinical and electrophysiological features of a Chinese patient with *KCNV2* retinopathy.

Methods: A 17-year-old Chinese male with the diagnosis of cone dystrophy with supernormal rod response (CDSRR) was followed-up for 5 years, with full ophthalmological examinations, including decimal best corrected visual acuity (BCVA), fundus photography, fundus autofluorescence (FAF) imaging, spectral-domain optical coherence tomography (SD-OCT), and full-field electroretinogram (ERG). Genetic screening was performed to detect the sequence variations in the retinal dystrophy associated genes in the patient and his parents.

Results: The patient demonstrated the characteristic full-field electroretinography (ERG) features of CDSRR, namely a profound enlargement of the dark-adapted ERG b-wave amplitude with increasing flash strength and a broadened a-wave trough; this case also had undetectable light-adapted ERGs. A BCVA of 0.15 was maintained over 5 years in both eyes; while progressive macular atrophy was identified. Molecular genetic analyses revealed two novel disease-causing *KCNV2* variants in compound heterozygous state: c.1408 G > C (p.Gly470Arg) and c.1500 C > G (p.Tyr500Ter).

Conclusions: This is the first long-term case study of an East Asian patient with molecularly confirmed CDSRR. The progressive atrophy with maintained VA demonstrated in this case will be valuable for increasing the understanding of the natural course of *KCNV2* retinopathy and it will help in counselling patients with this disease.

ARTICLE HISTORY

Received November 06, 2019

Revised October 24, 2020

Accepted November 29, 2020

KEYWORDS

Cone dystrophy with supernormal rod responses; *KCNV2*; longitudinal follow-up; electroretinogram; optical coherence tomography

Introduction

Cone dystrophy with supernormal rod response (CDSRR) is an autosomal recessive disorder first described by Gouras et al. in 1983 (1). Affected individuals usually present within the first two decades of life, with visual decline, photophobia, and nyctalopia in approximately 50% of case (2–8). Some patients present with color vision deficits, myopia, central scotoma, and, particularly in younger patients, nystagmus. Fundus findings are usually unremarkable in children, but adults frequently exhibit distinct macular changes or retinal pigment epithelial (RPE) atrophy (2–10).

The term CDSRR refers to the unique characteristics observed with full-field electroretinogram (ERG) (1). The scotopic ERG to a dim light strength (≤ 0.01 cd·s/m²) is typically markedly delayed and of subnormal amplitude. Small increments in flash strength produce disproportionately large increments in the rod-mediated ERG b-wave amplitude, leading to high-normal or supernormal values

with a standard flash ERG (3.0 cd·s/m²) (3–7,11). At flash strengths ≥ 3.0 cd·s/m², a broadened trough of the rod-mediated ERG a-wave is seen, and cone-mediated ERGs are reduced and delayed.

CDSRR is caused by biallelic sequence variations in the potassium voltage-gated channel modifier subfamily V member 2 (*KCNV2*) gene (MIM# 607604), leading to a functional defect of the encoded voltage-gated potassium channel subunit, Kv8.2 (12). Over 100 different disease-associated variations in the *KCNV2* gene have been reported, but the number of publications focusing on patients in the East Asian population is very limited (5,13). Moreover, only a few reports have described the electrophysiological and morphological natural history of *KCNV2* retinopathy (3–9,11–20). Here, we report the long-term follow-up of a Chinese patient with CDSRR caused by biallelic pathogenic *KCNV2* variants. These findings are important for counselling patients and designing therapeutic trials, particularly in the East Asian population.

CONTACT Kaoru Fujinami  k.fujinami@ucl.ac.uk  Laboratory of Visual Physiology, Division for Vision Research, National Institute of Sensory Organs, National Hospital Organization, Tokyo Medical Center, 2-5-1, Higashigaoka, Meguro-ku, Tokyo 152-8902, Japan; Shiyong Li  shiyong_li@126.com  Southwest Hospital/ Southwest Eye Hospital, Third Military Medical University (Army Medical University), Chongqing 4000038, China.

*Co-first authors

 Supplemental data for this article can be accessed on the publisher's website.

© 2020 The Author(s). Published with license by Taylor & Francis Group, LLC.

This is an Open Access article distributed under the terms of the Creative Commons Attribution-NonCommercial-NoDerivatives License (<http://creativecommons.org/licenses/by-nc-nd/4.0/>), which permits non-commercial re-use, distribution, and reproduction in any medium, provided the original work is properly cited, and is not altered, transformed, or built upon in any way.

Methods

Patient recruitment

A Chinese patient with CDSRR was recruited from the Outpatient Department of Southwest Eye Hospital, Third Military Medical University (Army Medical University), Chongqing, China. Informed consent for all procedures described here was obtained from the patient and his relatives who were also assessed, and agreement for publishing this case study was obtained. The study procedures were approved by the local ethics committee (Reference number: 73981486–2), and all procedures were performed under the Declaration of Helsinki principles on human research.

Clinical investigation

A detailed medical history was obtained from the patient, and comprehensive ophthalmological examinations were performed, including decimal best corrected visual acuity (BCVA), dilated ophthalmoscopy, color fundus photography recorded with a nonmydriatic retinal camera (a Nonmyd WX-3D; Kowa, Tokyo, Japan), fundus autofluorescence (FAF) imaging with a confocal scanning laser ophthalmoscope (HRA 2; Heidelberg Engineering, Heidelberg, Germany; excitation light, 488 nm; barrier filter, 500 nm; field of view, $30 \times 30^\circ$), spectral-domain optical coherence tomography (SD-OCT) using a Spectralis OCT platform (Heidelberg Engineering), static visual field testing (Humphrey field analyzer, Model 750i, Zeiss, Germany), microperimetry (Maia, CenterVue, Padova, Italy), and electrophysiological recordings.

Electrophysiology

Full-field ERGs were recorded according to the standard International Society for Clinical Electrophysiology of Vision (ISCEV) protocol with a ColorDome Ganzfeld stimulator (Diagnosys LLC, Lowell, MA, USA) using the 'minimum' and 'extended' protocols.

The minimum protocol included the following: (i) dark-adapted dim flash $0.01 \text{ cd}\cdot\text{s}\cdot\text{m}^{-2}$ (DA 0.01), (ii) dark-adapted bright flash $3.0 \text{ cd}\cdot\text{s}\cdot\text{m}^{-2}$ (DA 3.0), (iii) light-adapted $3.0 \text{ cd}\cdot\text{s}\cdot\text{m}^{-2}$ at 2 Hz (LA 3.0), and (iv) light-adapted $3.0 \text{ cd}\cdot\text{s}\cdot\text{m}^{-2}$ 30 Hz flicker ERG (LA 3.0 30 Hz) (21).

The extended protocol included DA ERGs elicited by flash strengths of 0.001, 0.003, 0.01, 0.03, 0.1, 0.3, 1.0, 3.0, 10.0, 20.0, and $30.0 \text{ cd}\cdot\text{s}\cdot\text{m}^{-2}$, as described in previous reports (3,5,7). Moreover, multifocal ERGs (mfERGs) were recorded with a VERIS Science 6.3.2 imaging system (EDI, San Mateo, CA, USA) under careful monitoring of fixation, according to the ISCEV standard protocol (22). mfERGs with stable fixation were selected for further analysis.

Mutation detection

DNA was extracted from the blood of the proband and his parents using previously described protocols (23), and 21 genes associated with macular dystrophy were sequenced (Supplementary Table 1). Polymerase chain reaction (PCR) amplification and bidirectional sequencing with a genetic

analyzer (ABI PRISM 3100 \times I; Applied Biosystems, Foster City, CA, USA) were performed to confirm the variants, and the co-segregation analysis was conducted.

Molecular genetic analysis

Molecular genetic analyses were conducted for all the detected variants in the *KCNV2* gene, according to a published protocol; URLs for the software and databases are available in a previous report (15). The pathogenicity of each variant was predicted using three different software programs: PolyPhen2, PROVEAN, and Mutation Taster. The allele frequency of each variant was calculated using the GnomAD database. The evolutionary conservation of the affected amino acid residues was assessed using PhastCons, phyloP, and Clustal Omega.

Results

Clinical course

A 17-year-old Chinese male (of Han ancestry) presented to the ophthalmology clinic with a history of photophobia and abnormal color vision since childhood. Ophthalmological examinations were conducted at presentation and subsequently at the ages of 19 and 22. No family history of ocular diseases, general health problems, or consanguinity was reported (Figure 1).

Ocular examination and retinal imaging

At the first visit, the BCVA was 0.15 in both eyes, and this acuity was maintained for 5 years. Fundus photography revealed de-pigmented atrophic changes in both maculae, with optic disk cupping in the right eye. FAF imaging revealed a ring of hyperautofluorescence at the perifovea in both eyes (Figure 2). Serial investigations during the follow-up term demonstrated disappearance of the ring, but clear enlargement of the atrophic areas of low AF density, with well-demarcated macular atrophy being observed in fundus photography by the age of 22 (Figure 2).

On the initial visit, SD-OCT demonstrated loss of photoreceptor layers at the maculae, with a relatively well-maintained RPE. Over the 5-year follow-up period, thinning of the sensory retinal layers was observed, along with clear loss of outer retinal structures and RPE atrophy at the maculae, corresponding to the atrophic area seen on funduscopic/FAF imaging (Figure 2).

The significantly thinned foveal thickness indicated a minimal change over the 5-year period.

Electrophysiological findings

At the first presentation at age 17 (baseline), the b-wave in the DA0.01 condition was delayed in the peak time and reduced in the amplitude (Figure 3a). As the flash strength increased, there was a profound and abnormal increase in the amplitude of the rod-mediated DA ERG b-wave. To the strongest flashes, the DA ERG a-wave was abnormally broad and delayed, and it was similar to a square wave but with a late negative component

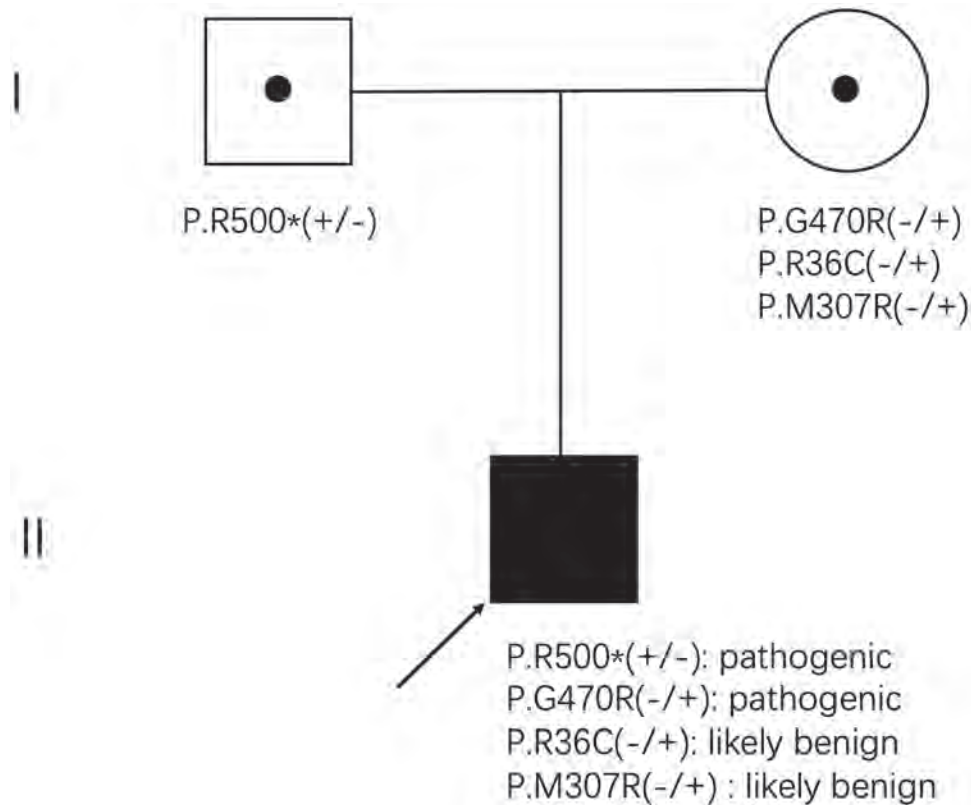


Figure 1. Pedigree and molecular status of a Chinese patient with CDSRR. Arrow indicates the proband. The filled shape indicates the affected individual and dots indicate carrier individuals. The codes indicate function-affecting sequence variations in KCNV2 versus the reference protein (p.) sequence. Amino acid substitutions are represented by one-letter amino acid codes, and an asterisk (*) is used to indicate a variation encoding a translation stopcodon. Square, male; circle, female. The generation number is shown on the left.

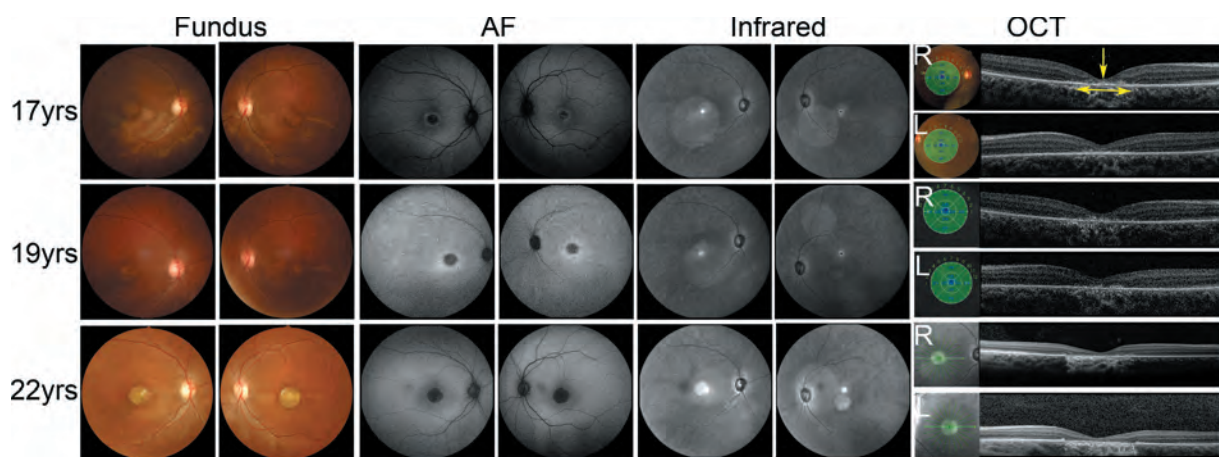


Figure 2. Retinal imaging of a Chinese patient with CDSRR. Serial fundus photographs, fundus autofluorescence (FAF) images, infrared (IR) images and spectral-domain optical coherence tomographic (SD-OCT) images of both eyes of the patient aged 17, 19, and 22 years. Fundus photography revealed a pronounced and well-demarcated area of atrophy which developed over 5 years. FAF imaging detected a corresponding hypo-autofluorescence (low-density) lesion at the initial presentation with a ring change of hyper-autofluorescence around, which developed into a pronounced well-demarcated area of low density. IR imaging revealed a corresponding lesion located at the fovea at the initial presentation, which progressed over the following years. SD-OCT at the initial presentation demonstrated loss of photoreceptor layers at the maculae with a maintained RPE. Over the 5-year follow-up, marked atrophy of the sensory retina and RPE at the macula were observed in a distribution corresponding to the atrophy detected in the other forms of imaging. Fovea is marked by a single-head yellow arrow, and atrophic macular areas are marked by a double-head yellow arrow.

(Figure 3a). No detectable ERG responses were observed in the LA conditions (LA 3.0 and LA 3.0 30 Hz; Figure 3a).

The DA stimulus-ERG response series of our patient were compared with those of age-matched healthy controls (Supplementary Table 2). The shapes of the DA stimulus-ERG

series for the a-waves and b-waves were abnormal at both baseline (age 17 years) and follow-up (19 and 22 years; Figure 3a). The baseline ERGs were undetectable to the dimmest flashes, but the b-waves exhibited abnormal enlargement as the stimulus strength increased (Figure 3a, b-e). In comparison to the control ERGs, the

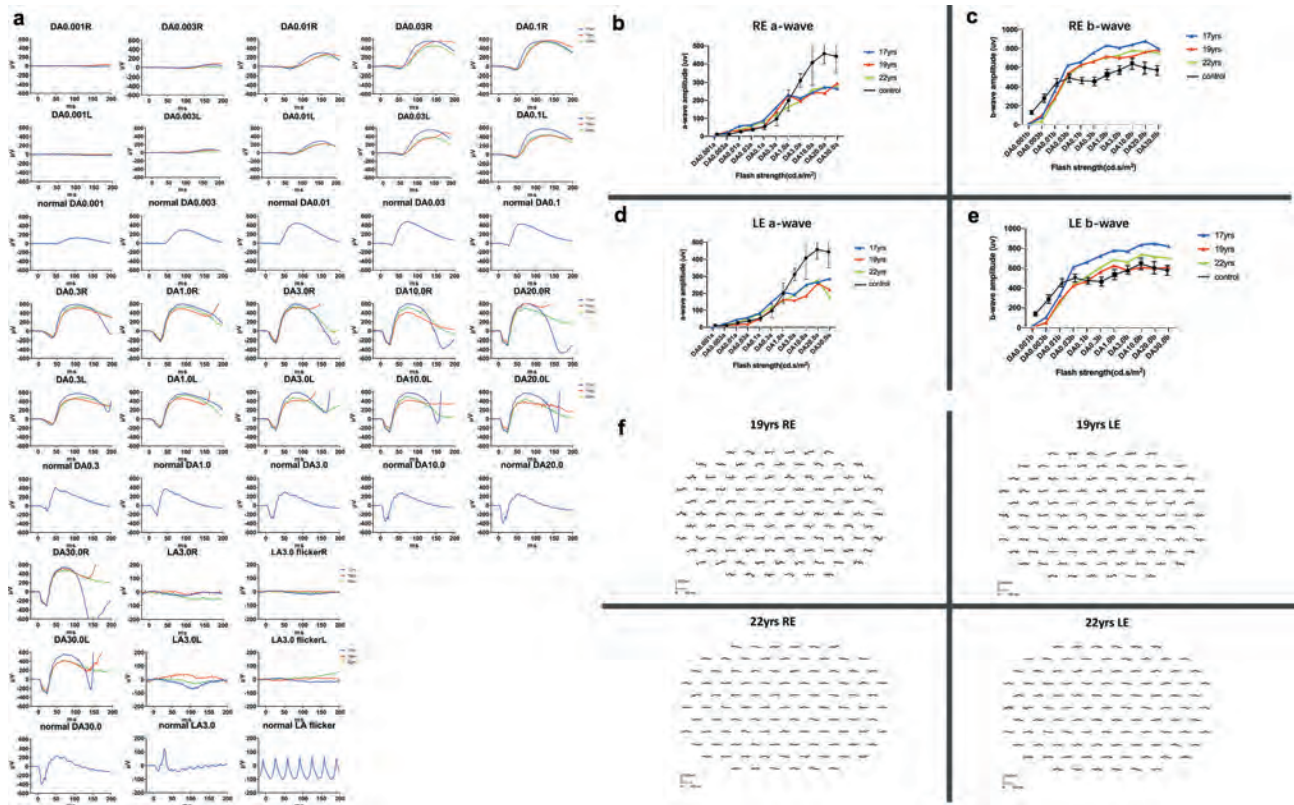


Figure 3. Full-field electroretinogram findings in a Chinese patient with CDSRR and comparison with healthy controls. A) Full-field electroretinograms (ERGs) to a range of flash strengths are shown for the right eye (R) and left eye (L) of the patient and are compared with control data from a representative age-matched individual without retinal disease (N; age 17 years). Patient traces obtained at the ages of 17, 19, and 22 years are shown in red, blue, and green, respectively. The corresponding DA ERG stimulus response series (B, C, D, and E) for the right eye (B, C) and the left eye (D, E). a- and b-waves are shown for each patient visit and compared with averaged control data from four healthy controls (age range 17–30 years); color coding of patient ages as in A); control data is presented in black. F) mfERG trace array for both eyes at the age of 19 and 22 years. mfERGs were undetectable or severely abnormal at both visits and at all eccentricities, consistent with severe widespread macular dysfunction.

baseline a-waves were smaller to flash strengths greater than 1.0 cd.s.m^{-2} (Figure 3 b,d) and showed relative stability at follow-up visits, and baseline b-waves were larger to flash strengths greater than 0.03 cd.s.m^{-2} (Figure 3 c, e). The follow-up ERG b-waves to the flashes $>0.03 \text{ cd.s.m}^{-2}$ were slightly smaller than those at baseline; the right eye b-waves were similar at the ages of 19 and 22 (Figure 3c), whereas the left eye b-waves were smallest at the last visit (Figure 3e).

The mfERGs demonstrated gross abnormality (i.e. a severe generalised reduction of the traces across all hexagons), consistent with severe cone system dysfunction across the posterior pole (Figure 3F). The mfERGs revealed no significant progression, whereas the FAF images indicated an enlargement of hypoauto-fluorescence at the maculae from 19 to 22 years of age.

Detected variants and pathogenicity analysis

In consideration of the recessive inheritance and phenotypic findings (Figure 1), four rare *KCNV2* variants were listed as candidates for the disease causation, none of which have been previously reported. Co-segregation analysis with the parental samples revealed three maternal missense alleles (c.106 C > T (p.Arg36Cys); c.920 T > G (p.Met307Arg); c.1408 G > C (p.Gly470Arg)) and one paternal nonsense (premature stop codon) allele (c.1500 C > G (p.Tyr500Ter)).

To determine the most likely disease-causing variant in the three maternal variants of the proband, *in silico* (software-based) molecular genetic analysis was performed (Table 1 and Supplementary Table 3), c.1408 G > C (p.Gly470Arg) was considered the pathogenic maternal variant. Evolutional conservation (Supplementary Figure 1) and predicted protein damage based on protein structure (Supplementary Figure 2) of the two pathogenic variants were performed.

Discussion

The clinical and genetic features of a male Chinese patient with CDSRR were described in detail; specifically, *KCNV2* retinopathy and detailed *in silico* molecular genetic analysis. Our results revealed two likely disease-causing variants that have not been previously described in the East Asian population. The progressive atrophy at the macula with maintained VA observed in our case will be valuable for increasing the understanding of the natural course of *KCNV2* retinopathy and help in patient counselling.

The BCVA was well-maintained over this 5-year period. This suggests that the decline in VA, corresponding to the loss of foveal function, occurs early in the disease, and that this is followed by further expansion of macular atrophy. These findings are corresponding to the previous literature that suggests a slow progress of *KCNV2* retinopathy (3,7,9,13). The subjective

Table 1. Results of *In silico* molecular genetic analysis of pathogenic variants in the *KCNV2* gene.

Exon	Nucleotide substitution	Amino acid change	Report	Polyphen 2		Mutation Taster	Proven(v1,1,3)		East Asian allele frequency observed by GnomAD	PhyloP	PhastCons	Reference
				Prediction	Hum var score (0–1)	Prediction	Prediction	Score				
2	c.1408 G > C	p.Gly470Arg	This study	PRD	1.000	DC	Deleterious	–7.526	ND	6.107	1	ND in dbSNP
2	c.1500 C > G	p. Tyr500Ter	This study	NA	NA	DC	NA	NA	0	3.411	1	ND in dbSNP

PRD = probably damaging; ND = not detected; Disease causing = DC; NA = not available

Polyphen2(vision 2.2.6) appraises mutations qualitatively as Benign, Possibly Damaging or Probably Damaging based on the model's false positive rate.

Mutation taster (<http://www.mutationtaster.org/>) were used to predict the probable damaging effects of the mutant allele at splicing level and protein expression levels.

GnomAD denotes variants in the Genome Aggregation Database, Cambridge, MA (URL: <http://gnomad.broadinstitute.org>).

Conservation in the positions of the identified variants was evaluated with primate PhyloP and phastCons scores provided by UCSC based on the human genome 19 coordinates (<http://genome.ucsc.edu/cgi-bin/hgTrackUi?db=hg19&g=cons46way>; accessed on August 7th, 2018).

visual reduction detected by the VA measurement is also consistent with the macular dysfunction objectively detected by mfERGs, which is in keeping with the findings reported in previous studies showing undetectable pattern ERG responses in all patients with this disorder irrespective of the macular appearance, the presence of macular atrophy, or age (3).

FAF and SD-OCT were particularly effective for monitoring the disease progression. A hypo-autofluorescence area seen at baseline developed over 5 years into a remarkably well-demarcated area of low density. The ring enhancement at the perifovea disappeared during the development of macular atrophy, which agrees with the previously reported findings (3,9,11). The lack of correlation between serial mfERGs and progressive macular atrophy on FAF imaging likely reflects the severity of macular dysfunction at baseline and the limited spatial resolution of the mfERG technique. Notably, in this case, the DA ERGs only revealed possible borderline reductions over the 5-year period, suggesting the relative stability of peripheral retinal function. Preservation of peripheral retinal function may be crucial for retaining peripheral visual function, which is essential in patients with severe central vision impairment.

The electrophysiological features demonstrated in our case were characteristic of the diagnosis of CDSRR. These unique abnormalities were similar to those previously reported for other cases with *KCNV2* retinopathy (3,5,13). Zobor et al. (24) demonstrated that in six patients with *KCNV2* retinopathy, the a-wave amplitude slowly and continuously increased in strength (from 10^{-3} cd*s/m² to 1.0 cd*s/m²); in contrast, the b-wave amplitude remained low until the flash strength reached 2.5 log cd*s/m² (–0.03 cd*s/m²). In our study, a strong flash (DA10.0) was required to define the characteristic broad and delayed a-wave trough, not clearly visible in the DA3.0 ERG. The amplitude of the b-wave at the strong flash was larger at baseline than at the follow-up visits. At the ages of 19 and 22, mild interocular asymmetries in response to stronger flash strengths were noted, with minimal differences between the follow-up visits on the right eye and mild reduction between visits on the left eye. These asymmetries are unlikely to be clinically significant and they may relate to technical factors and inter-session variability, such as due to small changes in the patient's compliance during testing. Generally, during the follow-up visits, the rod function was stable. In healthy subjects, the DA strong flash ERGs are mixed rod and cone responses. The undetectable LA ERGs at baseline (Figure 3a) suggest that, in this unusual case, DA strong flash ERGs are likely to reflect selective

activation of the rod system, therefore highlighting the relatively high degree of peripheral rod system stability in this disorder.

We demonstrated that our patient is a compound heterozygote for the two novel alleles, p.Gly470Arg and p.Tyr500Ter. The *KCNV2* gene encodes for a 545 amino acid protein, structurally composed of an N-terminal A and B box (NAB), six transmembrane domains (S1–S6), and a pore loop (between S5 and S6) (Supplementary Figure 2). In the East Asian population, a relatively high number of pathogenic variants have been seen around the P loop between S5 and S6. Further population-based studies are required to provide useful ethnicity-based genotype–phenotype correlations.

Further follow-up of this patient and an investigation of other East Asian patients with CDSRR will help us provide better advice to patients regarding useful clinical testing, disease prognosis, and potential treatment of this disease. The sequence variants occurring in the East Asian population are different from those found in the European population; thus, different genetic backgrounds are assumed to be underlying. Although related articles about this disorder involve Asian patients, longitudinal studies are still lacking. A longitudinal clinical and genetic study of a large sample of patients and relatives from multiple ethnicities will be required to confirm if there is a difference based on ethnicity, but such results are particularly important for ethnicity-based education and counseling of patients regarding the likelihood of their children being affected.

In conclusion, this study documented detailed findings over 5 years in a Chinese patient with CDSRR caused by biallelic novel pathogenic *KCNV2* variants. Progressive macular atrophy with maintained VA was observed, with relatively preserved peripheral rod function. This information in the natural course of *KCNV2* retinopathy could help in diagnosing, counselling, and monitoring patients; it could also be beneficial for designing potential therapeutic trials in the East Asian population.

Declaration of interest

The authors report no conflicts of interest. The authors alone are responsible for the content and writing of this article.

Role of the funder

The funding sources had no role in the design and conduct of the study; collection, management, analysis, and interpretation of the data;

preparation, review, or approval of the manuscript; or decision to submit the manuscript for publication.

Funding

Shiyang Li is supported by grants from the National Nature Science Foundation of China (81974138), National Basic Research Program of China (2018YFA0107301), Chongqing Social and Livelihood Science Innovation grant (cstc2017shmsA130100). Kaoru Fujinami is supported by grants from Grant-in-Aid for Young Scientists (A) of the Ministry of Education, Culture, Sports, Science and Technology, Japan (16H06269), grants from Grant-in-Aid for Scientists to support international collaborative studies of the Ministry of Education, Culture, Sports, Science and Technology, Japan (16KK01930002), grants from National Hospital Organization Network Research Fund (H30-NHO-2-12), grants from the Foundation for Fighting Blindness – Alan Lattes Career Development Program (CF-CL-0416-0696-UCL), grants from Health Labor Sciences Research Grant, The Ministry of Health, Labor and Welfare (201711107A), and grants from the Great Britain Sasakawa Foundation Butterfield Awards. Yu Fujinami–Yokokawa is supported by grants from Grant-in-Aid for Young Scientists of the Ministry of Education, Culture, Sports, Science and Technology, Japan (18K16943).

ORCID

Yanling Long  <http://orcid.org/0000-0003-3442-3311>
 Kaoru Fujinami  <http://orcid.org/0000-0003-4248-0033>
 Shiyang Li  <http://orcid.org/0000-0001-9783-9520>

References

- Alexander KR, Fishman GA. Supernormal scotopic ERG in cone dystrophy. *Br J Ophthalmol*. 1984;68(2):69–78. doi:10.1136/bjo.68.2.69.
- Michaelides M, Holder GE, Webster AR, Hunt DM, Moore AT. A detailed phenotypic study of “cone dystrophy with supernormal rod ERG”. *Digest World Latest Med Information*. 2005;89(3):332–39.
- Robson AG, Webster AR, Michaelides M, Downes SM, Cowing JA, Hunt DM, Moore AT, Holder GE. Cone dystrophy with supernormal rod electroretinogram”: A comprehensive genotype/phenotype study including fundus autofluorescence and extensive electrophysiology. *Retina*. 2010;30(1):51–62. doi:10.1097/IAE.0b013e3181bfe24e.
- Sergouniotis PI, Holder GE, Robson AG, Michaelides M, Webster AR, Moore AT. High-resolution optical coherence tomography imaging in KCNV2 retinopathy. *Br J Ophthalmol*. 2012;96(2):213–17. doi:10.1136/bjo.2011.203638.
- Fujinami K, Tsunoda K, Nakamura N, Yu K, Miyake Y. Molecular characteristics of four Japanese cases with KCNV2 retinopathy: report of novel disease-causing variants. *Mol Vis*. 2013;19(19):1580–90.
- Ajoy V, Anthony R, Graham H. Pathognomonic (diagnostic) ERGs. A review and update. *Retina*. 2013;33(1):5–12. doi:10.1097/IAE.0b013e31827e2306.
- Vincent A, Wright T, Garcia-Sanchez Y, Kisilak M, Campbell M, Westall C, Héon E. Phenotypic characteristics including in vivo cone photoreceptor mosaic in KCNV2-Related “Cone dystrophy with supernormal rod electroretinogram. *Investigative Ophthalmol Visual Sci*. 2013. doi:10.1167/iov.12-10971.
- Stockman A, Henning GB, Michaelides M, Moore AT, Webster AR, Cammack J, Ripamonti C. Cone dystrophy with “Supernormal” Rod ERG: psychophysical testing shows comparable rod and cone temporal sensitivity losses with no gain in rod function. *Invest Ophthalmol Vis Sci*. 2014;55(2):832. doi:10.1167/iov.13-12919.
- Friedburg C, Wissinger B, Schambeck M, Bonin M, Kohl S, Lorenz B. Long-term follow-up of the human phenotype in three siblings with cone dystrophy associated with a homozygous p. G461R mutation of KCNV2. *Invest Ophthalmol Vis Sci*. 2011;52(12):8621–29. doi:10.1167/iov.11-8187.
- Guimaraes TACD, Georgiou M, Robson AG, Michaelides M. KCNV2 retinopathy: clinical features, molecular genetics and directions for future therapy. *Ophthalmic Genet*. 2020;41(19):1–8. doi:10.1080/13816810.2020.1766087.
- Grigg JR, Holder GE, Billson FA, Korsakova M, Jamieson RV. The importance of electrophysiology in revealing a complete homozygous deletion of KCNV2. *J Am Asso Pediatric Ophthalmol Strabismus*. 2013;17(6):641–43. doi:10.1016/j.jaapos.2013.08.006.
- Wu H, Cowing JA, Michaelides M, Wilkie SE, Jeffery G, Jenkins SA, Mester V, Bird AC, Robson AG, Holder GE. Mutations in the gene KCNV2 encoding a voltage-gated potassium channel subunit cause “Cone dystrophy with supernormal rod electroretinogram” in humans. *Am J Hum Genet*. 2006;79(3):0–579. doi:10.1086/507568.
- Kutsuma T, Katagiri S, Hayashi T, Yoshitake K, Iejima D, Gekka T, Kohzaki K, Mizobuchi K, Baba Y, Terauchi R, et al. Novel biallelic loss-of-function KCNV2 variants in cone dystrophy with supernormal rod responses. *Doc Ophthalmol*. 2019;138(3):229–239. doi:10.1007/s10633-019-09679-6.
- Kaoru F, Shuhei K, Sachiko K, Shinji U, Mineo K. Novel RP11L variants and genotype-photoreceptor microstructural phenotype associations in cohort of Japanese patients with occult macular dystrophy. *Invest Ophthalmol Vis Sci*. 2016;57(11):4837–4846. doi:10.1167/iov.16-19670.
- Huang L, Xiao X, Li S, Jia X, Wang P, Sun W, Xu Y, Xin W, Guo X, Zhang Q, et al. Molecular genetics of cone-rod dystrophy in Chinese patients: new data from 61 probands and mutation overview of 163 probands. *Exp Eye Res*. 2016;146:252–58.
- Zelinger L, Wissinger B, Eli D, Kohl S, Banin E. Cone dystrophy with supernormal rod response: novel KCNV2 mutations in an underdiagnosed phenotype. *Ophthalmology*. 2013;120(11):2338–43. doi:10.1016/j.ophtha.2013.03.031.
- Ritter M, Vodopituz J, Lechner S, Moser E, Janecke AR. Coexistence of KCNV2 associated cone dystrophy with supernormal rod electroretinogram and MFRP related oculopathy in a Turkish family. *Br J Ophthalmol*. 2013;97(2):169–73. doi:10.1136/bjophthalmol-2012-302355.
- Wissinger B, Dangel S, Jaegle H, Hansen L, Baumann B, Rudolph G, Wolf C, Bonin M, Koeppen K, Ladewig T. Cone dystrophy with supernormal rod response is strictly associated with mutations in KCNV2. *Invest Ophthalmol Vis Sci*. 2008;49(2):751. doi:10.1167/iov.07-0471.
- Salah SB, Kamei S, Séné-Hal A, Lopez S, Bazalgette C, Bazalgette C, Eliaou CM, Zanlonghi X, Hamel CP. Novel KCNV2 mutations in cone dystrophy with supernormal rod electroretinogram. 2008;145(6):1099–106. doi:10.1016/j.ajo.2008.02.004.
- McCulloch DL, Marmor MF, Brigell MG, Hamilton R, Holder GE, Tzekov R, Bach M. ISCEV Standard for full-field clinical electroretinography (2015 update). *Documenta ophthalmologica*. 2015;130(1):1–12. doi:10.1007/s10633-011-9296-8.
- Hood DC, Bach M, Brigell M, Keating D, Kondo M, Lyons JS, Marmor MF, McCulloch DL, Palmowski-Wolfe AM, Vision FtiSFCEo. ISCEV standard for clinical multifocal electroretinography (mfERG) (2011 edition). *Documenta Ophthalmol*. 2012;124(1):1–13. doi:10.1007/s10633-011-9296-8.
- Nasiri H, Forouzandeh M, Rasae M, Rahbarizadeh F. Modified salting-out method: high-yield, high-quality genomic DNA extraction from whole blood using laundry detergent. *J Clin Lab Anal*. 2005;19(6):229–32. doi:10.1002/jcla.20083.
- Ditta Z, Susanne K, Bernd W, Eberhart Z, Herbert JG, Den HAI. Rod and Cone Function in Patients with KCNV2 Retinopathy. *Plos One*. 2012;7(10):e46762. doi:10.1371/journal.pone.0046762.
- Ottschytch N, Raes A, Van Hoorick D, Snyders DJ. Obligatory heterotetramerization of three previously uncharacterized Kv channel γ -subunits identified in the human genome. *Proc Natl Acad Sci U S A*. 2002;99(12):7986–91. doi:10.1073/pnas.122617999.

日中笹川医学奨学金制度(学位取得コース)中間評価書

課程博士：指導教官用



第 42 期 研究者番号： G4206

作成日：2021年3月10日

氏名	孟 華川	Meng Huachuan	性別	M	生年月日	1985. 02. 04
所属機関(役職)	中日友好医院院弁国際交流合作弁公室(通訳(日本プロジェクト担当))					
研究先(指導教官)	国際医療福祉大学大学院医療福祉経営専攻 医療経営管理分野(島崎 謙治教授) 国際医療福祉大学大学院医学研究科 医学専攻(桐生 茂教授)					
研究テーマ	ICTを活用した遠隔医療の導入効果及び推進方策 The introduction effects and promoting strategy of telemedicine by utilizing ICT					
専攻種別	<input type="checkbox"/> 論文博士			<input checked="" type="checkbox"/> 課程博士		

研究者評価(指導教官記入欄)

成績状況	優 良 可 不可	取得単位数
	学業成績係数=2.83(GPA) ※GPAは4.00(最高値)~0.00(最低値)	20(4)単位/12単位 ※()内は現状の取得すべき単位数
学生本人が行った 研究の概要	ICTの急速な進展や医療資源の地域格差の拡大等を背景に、近年、日中両国では遠隔診療の推進が図られてきたが、とりわけ新型コロナウイルス感染症の蔓延に伴い、大幅な規制緩和をはじめ様々な普及促進策が講じられている。孟氏は、政府の政策文書や審議会の報告書等の文献調査を丹念に行うことにより、日中の遠隔診療に関する規制緩和や経済的誘導策の動向や論点等を整理・分析した。また、対面診療に比べ遠隔診療は、患者の医療へのアクセスの改善、通院等の移動コストの低減などの有用性がある反面、誤診等のリスクもある。孟氏は、こうした点を含め遠隔診療の導入効果について、日中の先行研究のサーベイを行うとともに、遠隔診療を実施している医療機関を対象とするアンケート調査の設計に着手した。	
総合評価	【良かった点】 政府や学会のガイドラインの策定や規制緩和措置が講じられるなど、日中両国の遠隔診療をめぐる状況は大きく変化している。孟氏は新型コロナウイルス感染症の影響により来日が遅れたが、短期間で、日中の遠隔診療に関する規制緩和や経済的誘導策の動向・論点等を的確に整理・分析した。また、日中の先行研究の調査を行うとともに、アンケート調査の設計にも着手するなど、精力的に研究に取り組んでいる。	
	【改善すべき点】 特になし。	
	【今後の展望】 孟氏はこれまで順調に課題をこなしており、引き続き研究に精励することを期待している。なお、新型コロナウイルス感染症の蔓延状況によっては、アンケート調査や現地ヒアリング等に関する医療機関の協力が得られにくくなる可能性がある。このため、ゆとりのある研究計画を策定するとともに、できるだけ前倒しで研究を進める必要がある。助言・指導に当たっては、こうした点にも十分配慮してまいりたい。	

学位取得見込	孟氏は学位取得に向け精力的に研究に取り組んでいる。当方としても、孟氏が予定どおり学位取得できるよう、今後とも適切な助言・指導に努める所存である。
評価者（指導教官名） 島崎謙谷 	

日中笹川医学奨学金制度(学位取得コース)中間報告書 研究者用



第42期

研究者番号： G4206

作成日：2021年3月 2 日

氏名	Meng Huachuan	孟 華川	性別	M	生年月日	1985. 02. 04
所属機関(役職)	中日友好医院院弁国際交流合作弁公室(通訳(日本プロジェクト担当))					
研究先(指導教官)	国際医療福祉大学大学院医療福祉経営専攻 医療経営管理分野(島崎 謙治教授) 国際医療福祉大学大学院医学研究科 医学専攻(桐生 茂教授)					
研究テーマ	ICTを活用した遠隔医療の導入効果及び推進方策 The introduction effects and promotion strategy of telemedicine by utilizing ICT					
専攻種別	論文博士	<input type="checkbox"/>	課程博士	<input checked="" type="checkbox"/>		

1. 研究概要(1)

日本と中国における遠隔医療の社会的背景には、高齢化の急速な進行、医療資源の偏在(病床数や医師の偏在)、地域の医療格差による地方の医療ニーズ(総合病院の専門医への医療相談)などが挙げられる。日本と中国も高齢社会であり、高齢化の進行により、高齢者、とりわけ75歳以上の高齢者が今後も増える見込みである。地域医療連携と超高齢社会への対応として遠隔医療への期待が高まっている中、近年、ICT(情報通信技術)が日進月歩の進化を遂げてきたこともあり、オンライン診療(遠隔医療)は、アメリカや中国など国土が広く、医療の格差が大きく、また地域によって医療機関へのアクセスが難しい患者が多いところで発展してきた。日本の遠隔医療は主に離島や僻地において訪問診療を補うものとして北海道・香川県などから始まって、段階的に規制緩和されてきたが、なかなか普及ができなかった。新型コロナウイルス感染症(COVID-19)の対策の一環として、初診患者の遠隔診療が解禁され、これとともに、薬剤師による電話などでの服薬指導も解禁された。今までの医療は病院・医師という医療提供者を中心に展開してきたが、今回のコロナをきっかけに、患者中心のシステムに転換する貴重な機会になるのではないかと期待されている。

1) 目的(Goal)

本研究の目的は、ICTを活用した遠隔医療の導入について、質、アクセス、コストに着目し、分析・評価を行うとともに、遠隔医療の普及の阻害要因を分析したうえで遠隔医療の推進方策を提言することである。なお、本稿では、筆者が、中日友好病院において、日本と中国の協力体制の下、遠隔医療分野での協力体制の構築に携わっていることから、日本及び中国への政策提言を行う。

2) 戦略(Approach)

ステップ①：中国と日本における遠隔医療の経緯・現状を調査・分析し、多方面から問題を把握し、課題を洗い出す。
ステップ②：遠隔医療の普及の阻害要因(政策面・技術面・人的資源など)を明らかにする。
ステップ③：アンケート調査を通して、遠隔医療の導入効果を明確にしたうえで、課題解決の方策を提示する。

3) 材料と方法(Materials and methods)

当面は中国と日本で公開されている資料とデータをもとに情報収集して、先行研究も含め調査報告をまとめる。2016年、筆者が、日本全国の47都道府県、1,095自治体(市町村および特別区)に対する独自の遠隔医療の導入と実施状況に関するアンケート調査結果を利用しながら、情勢変化に合わせて、2021年に、遠隔医療の実施状況と導入効果について、遠隔医療を導入している医療機関に対してアンケート調査を行う予定である。(※当初の予定は2月に現地調査を行う予定であったが、コロナと緊急事態宣言の影響等により、協力医療機関との協議が遅れが出ている)

4) 実験結果(Results)

3月より、主論文に関するアンケート調査項目の検討および研究倫理委員会に対する申請書の作成し、4月中に提出する予定である。結果についてはコロナの情勢と協力医療機関との協議のこともあり、できるだけ早期(夏)にまとめることを考えている。

5) 考察(Discussion)

文献調査や公開データと情報をもとに、考察で以下のようなことが明らかになった。今までは、法整備(医師法)や診療報酬などの制度面の制約が、日本の遠隔医療普及の大きな阻害要因となっている。遠隔医療を導入している自治体病院の割合は未だ少ないが、導入している自治体では、画像診断と病理診断に遠隔医療が取り入れられている確率が高い。しかも、自治体が遠隔医療を必要としていると想定している患者数は多く、とりわけ、高齢者によるニーズは高いと考えられている。また、遠隔医療は中国で大きく普及した要因の一つに、政府主導の医療格差解消政策のための規制緩和と大都市圏の大型総合病院による地方(特に遠隔地)の遠隔医療支援、民間による設備投資の増大とオンライン診療を運営企業が多いことなどが考えられる。

6) 参考文献(References)

吉田晃敏・亀畑義彦(1998)『遠隔医療 どこに住んでも世界最高水準医療が享受できる』講談社
吉田晃敏(2007)『格差なき医療——日本中で世界最高水準の治療が受けられるようになる日』講談社
吉野清史(2012)「超高齢社会におけるICTを活用した単身高齢者見守り事業」国際CIO学会ジャーナル2012
印南一路(2020)「規制改革推進会議とデジタル医療」週刊社会保障 No. 3095(2020. 11. 9)
王琳華(2011)「遠隔医療が地域医療情報化の建設を如何に促進すべき」重慶医学 第35期
孟群・尹新(2016)「中国インターネット医療の発展現状と思考」中国衛生情報管理 2016年04期
陳芳(2020)「遠隔医療が高齢者管理における応用現状と示唆」中国継続医学教育 第12巻第1期
内閣府 https://www8.cao.go.jp/kourei/whitepaper/w-2019/html/zenbun/s1_1_1.html (2021年3月1日閲覧)
国家卫生健康委 <http://www.nhc.gov.cn/wjw/tia/202101/351df93c683340709885d381ec5dd16d.shtml> (2021年3月4日閲覧)

1. 研究概要 (2)

1) 研究の背景

近年、ICT（情報通信技術）の急速な進展を背景に、遠隔医療の技術的障壁が小さくなるとともに、医療資源の地域格差が拡大するなかで、遠隔診療に対する期待・関心が高まっている。遠隔医療が日本及び中国で注目されている理由としては、①人口当たり医師数は増加しているが、医師や医療機関の地域間格差はむしろ増大している。遠隔医療は医療資源の偏在の克服に寄与されることがきたされている。②日中とも高齢化が進展している。高齢者は糖尿病、高血圧など慢性疾患の罹患率が高い。遠隔医療はこうした患者の継続的診療に有用である。（参考）高齢化率 日本：28.1%（2018）→35.3%（2040年推計）中国：17.9%（2018）→約30%（2042推定）（※出典は参考文献をご参照）③近年のICT技術の飛躍的な進展により、遠隔診療の技術的基盤が整備・充実されてきた。

また、新型コロナウイルス感染症（COVID-19）の感染拡大の影響を受けて、日本と中国とも従来は様々な制約があったオンライン診療（遠隔診療）に関する規制緩和等は急速に進展している。2020年に、新型コロナウイルスの感染拡大に伴い、中央政府・中国国務院は、コロナウイルス感染症対策として、“インターネット+医療”の役割を十分に利用し、発熱を有する患者に対して、「呼吸器内科、感染科、救急医学科、重症医学科、精神衛生科および総合医を活かし、インターネットを通じて診療の相談サービスを提供するよう」と呼びかけていた。2020年2月6日、中国国家卫生健康委員会は「コロナウイルス感染症対策として、インターネットを活用した診療相談サービスを展開する通知」（国衛医発〔2020〕112号）を公表し、各レベル卫生健康行政部門が、インターネットを活用した遠隔診療相談サービスがコロナ感染症対策での役割を果たさせて、即時の健康評価と専門的な指導を受けさせ、患者の受診を円滑させ、病院の負担を減らし、外来受診による患者の集まりや、患者間や患者と医療従事者との間の感染リスクを減らすことを命じた形になった。中国は近年、地域医療格差の縮小のため、国務院（内閣に相当）の後押しもあって、遠隔医療に力を入れて速いスピードで実用化・拡大化されてきたが、まだまだ法整備などの課題がある。日本の厚生労働省は、これまでの診療の対面原則の規制を緩和し、過疎地、離島やへき地の遠隔診療を容認したのを皮切りに、2015年以降、遠隔診療の適用範囲を拡大するとともに、2018年度診療報酬改定において、糖尿病や認知症など継続治療が必要な慢性疾患に関する遠隔診療の診療報酬上の手当て（点数設定）を行った。さらに、新型コロナウイルスの感染拡大に伴い、厚生労働省は、2020年4月13日、臨時的・特例的に初診のオンライン診療（遠隔医療）も可能とした。菅総理がコロナ後もこの規制緩和を継続することを表明し、関係大臣合意により、かかりつけ医が関与することを条件に初診についても規制緩和を恒久化する方向が示されている。

このように遠隔診療に関する規制緩和等は急速に進展しているが、患者の医療へのアクセスの改善、通院や訪問診療の移動コストの削減、診療回数の増加による医療の質の向上等の点で、遠隔診療は大きなポテンシャルを有していると考えられる。したがって、遠隔医療の導入効果及び推進方策の検討することは、学術的にも政策的にも非常に重要なテーマである。なお、中国においても遠隔診療に関する規制緩和に関する政策が打ち出されているなど、日本と類似した状況にあり、日本の遠隔診療に関する研究は中国にとっても有用である。

※ 本研究の研究対象である「遠隔医療」の定義・範囲について

厚生労働省は、遠隔医療を「映像を含む患者情報の伝達に基づいて、遠隔地から診断、指示などの医療行為および医療に関連した行為を行うこと」と定義している。本研究も同様である。遠隔診療は、その主体・客体に着目すると、①専門医師が他の医師の診療を支援するDoctor to Doctor (D to D) と、②医師が遠隔地の患者を診療するDoctor to Patient (D to P) に分かれる。また、③遠隔の健康モニタリングなど在宅見守りの形態も遠隔医療に含まれる。本研究の対象は厚生労働省の定義と同様（上記①～③を対象）。※今後、研究のフィージビリティ等により、①と②に研究対象を絞る可能性あり。

2) 先行研究

日本の先行研究については、地方医療支援と地域格差の解消を手段とする遠隔医療の効果を中心に論じたものとして、吉田・亀畑（1998）、吉田（2007）などがあり、ICTを活用した単身高齢者見守り事業に関する研究を行ったものとして、吉野（2012）などがある。また、遠隔診療の実践例の紹介や規制緩和に関する論評は、印南（2020）など多数ある。中国の先行研究については、地域の医療の格差の是正や地方医療情報化の促進を論じた王（2011）、中国インターネット医療の発展現状を論じた孟・尹（2016）、遠隔医療を通して高齢者の健康管理に寄与する可能性を論じた陳（2020）などが挙げられる。

3) 本研究の位置づけ

これらの先行研究は、特定の遠隔診療の形態を取り上げ、地域の医療格差の是正や地方医療の支援などについて論じたもの多く、遠隔医療の導入効果と普及推進方策について体系的かつ総合的に分析・検討した研究は乏しい。また、今日、遠隔医療に関する技術的は日進月歩しているだけでなく、規制や診療報酬など遠隔医療の条件も大きく変化している。本研究の意義は、最新の情報等に基づき、遠隔医療の導入効果及び推進方策を体系的・総合的に分析・検討することにある。

4) 研究計画

2021年3月 主論文に関するアンケート調査項目の検討および研究倫理委員会に対する申請書の作成

2021年4月 主論文に関するアンケート調査項目の検討および研究倫理委員会に対する申請書の提出

倫理委員会の承認後、アンケート調査を行う。調査内容は、遠隔医療を導入した背景、導入後の実施状況、実績や評価指標、導入における利点及び問題点などを考えている。全国自治体病院協議会等の協力を求め対象病院数（サンプル数）を増やすことを検討している。アンケート調査対象の候補としては以下を含め遠隔医療を導入している病院を考えている。①旭川医科大学附属病院（北海道）：1999年に、旭川医科大学病院内に日本国内初の遠隔医療センターを設立。特徴としては地域医療格差の是正がメインで、D to DとD to P方式で行っている。②織田病院（佐賀県）：ICT活用で病院から在宅患者を見守る「在宅見守りシステム」を導入。必要に応じてオンライン診療を提供。③石川記念会HITO病院（愛媛県）：情報通信技術ICTを導入、2020年5月からオンライン診療を実施。

2021年5月～6月 アンケート調査の実施。

2021年6月～8月 アンケート調査結果の分析・考察。論文執筆開始。

2. 執筆論文 Publication of thesis ※記載した論文を添付してください。Attach all of the papers listed below.

論文名 1 Title						
掲載誌名 Published journal						
	年	月	巻(号)	頁 ~	頁	言語 Language
第1著者名 First author			第2著者名 Second author			第3著者名 Third author
その他著者名 Other authors						
論文名 2 Title						
掲載誌名 Published journal						
	年	月	巻(号)	頁 ~	頁	言語 Language
第1著者名 First author			第2著者名 Second author			第3著者名 Third author
その他著者名 Other authors						
論文名 3 Title						
掲載誌名 Published journal						
	年	月	巻(号)	頁 ~	頁	言語 Language
第1著者名 First author			第2著者名 Second author			第3著者名 Third author
その他著者名 Other authors						
論文名 4 Title						
掲載誌名 Published journal						
	年	月	巻(号)	頁 ~	頁	言語 Language
第1著者名 First author			第2著者名 Second author			第3著者名 Third author
その他著者名 Other authors						
論文名 5 Title						
掲載誌名 Published journal						
	年	月	巻(号)	頁 ~	頁	言語 Language
第1著者名 First author			第2著者名 Second author			第3著者名 Third author
その他著者名 Other authors						

3. 学会発表 Conference presentation ※筆頭演者として総会・国際学会を含む主な学会で発表したものを記載してください。

※Describe your presentation as the principal presenter in major academic meetings including general meetings or international meeting

学会名 Conference					
演題 Topic					
開催日 date	年	月	日	開催地 venue	
形式 method	<input type="checkbox"/> 口頭発表 Oral	<input type="checkbox"/> ポスター発表 Poster	言語 Language	<input type="checkbox"/> 日本語	<input type="checkbox"/> 英語 <input type="checkbox"/> 中国語
共同演者名 Co-presenter					
学会名 Conference					
演題 Topic					
開催日 date	年	月	日	開催地 venue	
形式 method	<input type="checkbox"/> 口頭発表 Oral	<input type="checkbox"/> ポスター発表 Poster	言語 Language	<input type="checkbox"/> 日本語	<input type="checkbox"/> 英語 <input type="checkbox"/> 中国語
共同演者名 Co-presenter					
学会名 Conference					
演題 Topic					
開催日 date	年	月	日	開催地 venue	
形式 method	<input type="checkbox"/> 口頭発表 Oral	<input type="checkbox"/> ポスター発表 Poster	言語 Language	<input type="checkbox"/> 日本語	<input type="checkbox"/> 英語 <input type="checkbox"/> 中国語
共同演者名 Co-presenter					
学会名 Conference					
演題 Topic					
開催日 date	年	月	日	開催地 venue	
形式 method	<input type="checkbox"/> 口頭発表 Oral	<input type="checkbox"/> ポスター発表 Poster	言語 Language	<input type="checkbox"/> 日本語	<input type="checkbox"/> 英語 <input type="checkbox"/> 中国語
共同演者名 Co-presenter					

4. 受賞(研究業績) Award (Research achievement)

名称 Award name	国名 Country		受賞年 Year of award	年	月
	国名 Country		受賞年 Year of award	年	月

5. 本研究テーマに関わる他の研究助成金受給 Other research grants concerned with your research theme

受給実績 Receipt record	<input type="checkbox"/> 有 <input checked="" type="checkbox"/> 無
助成機関名称 Funding agency	
助成金名称 Grant name	
受給期間 Supported period	年 月 ~ 年 月
受給額 Amount received	円
受給実績 Receipt record	<input type="checkbox"/> 有 <input checked="" type="checkbox"/> 無
助成機関名称 Funding agency	
助成金名称 Grant name	
受給期間 Supported period	年 月 ~ 年 月
受給額 Amount received	円

6. 他の奨学金受給 Another awarded scholarship

受給実績 Receipt record	<input type="checkbox"/> 有 <input checked="" type="checkbox"/> 無
助成機関名称 Funding agency	
奨学金名称 Scholarship name	
受給期間 Supported period	年 月 ~ 年 月
受給額 Amount received	円

7. 研究活動に関する報道発表 Press release concerned with your research activities

※記載した記事を添付してください。Attach a copy of the article described below

報道発表 Press release	<input type="checkbox"/> 有 <input checked="" type="checkbox"/> 無	発表年月日 Date of release	
発表機関 Released medium			
発表形式 Release method	・新聞 ・雑誌 ・Web site ・記者発表 ・その他()		
発表タイトル Released title			

8. 本研究テーマに関する特許出願予定 Patent application concerned with your research theme

出願予定 Scheduled	<input type="checkbox"/> 有 <input checked="" type="checkbox"/> 無	出願国 Application	
出願内容(概要) Application contents			

9. その他 Others

--

指導責任者(署名)

印

日中笹川医学奨学金制度 (学位取得コース) 中間評価書

課程博士：指導教官用



第 42 期

研究者番号： G4210

作成日： 2021 年 3 月 8 日

氏名	翟 達	Zhai Da	性別	F	生年月日	1992. 03. 12
所属機関 (役職)	長崎大学大学院医歯薬学総合研究科放射線医療科学専攻幹細胞生物学 (大学院生)					
研究先 (指導教官)	長崎大学原爆後障害医療研究所幹細胞生物学研究分野 (李 桃生教授)					
研究テーマ	メカノストレスが癌細胞に与える影響と機序					
専攻種別	<input type="checkbox"/> 論文博士			<input checked="" type="checkbox"/> 課程博士		

研究者評価 (指導教官記入欄)

成績状況	優	取得単位数
		取得単位数 / 取得すべき単位数総数
学生本人が行った研究の概要	<p>固形腫瘍内は静水圧の上昇など様々な生物力学変化(メカニカルストレス)が伴う。しかし、メカニカルストレスは癌細胞の生物学特性に与える影響が殆ど不明である。貴会の奨学生の Zhai さんは、圧力負荷装置を用いて、特に静水圧の上昇が癌細胞のエネルギー代謝や転移活性などの生物学特性に与える影響を調べ、その機序解明を研究テーマとしている。</p>	
総合評価	<p>【良かった点】 ものごとを真摯に取り組み、研究も順調に進んでいる。 一つ目の研究テーマは既に成果を出し、学会発表した。また、その成果を纏めた論文は学術誌に投稿し、現在修正して再投稿中である。</p>	
	<p>【改善すべき点】 特にない。敢えて言えば、新しい研究を挑戦する貪欲さがすこし足りない。</p>	
	<p>【今後の展望】 二つ目の研究テーマは現在進行中であり、少し面白い結果が得られている。順調に進めば、来年度中にその研究成果が公表できると見込んでいる。</p>	
学位取得見込	<p>現在博士課程 2 年生であるが、既に一定の研究成果を出している。学位取得見込みは予定通り、2023 年 3 月になる。</p>	
評価者 (指導教官名)		李 桃生



日中笹川医学奨学金制度(学位取得コース)中間報告書 研究者用



第42期

研究者番号: G4210

作成日: 2021年3月8日

氏名	Zhai Da	翟 達	性別	F	生年月日 1992. 03. 12
所属機関(役職)	長崎大学大学院医歯薬学総合研究科放射線医療科学専攻幹細胞生物学(大学院生)				
研究先(指導教官)	長崎大学原爆後障害医療研究所幹細胞生物学研究分野(李 桃生教授)				
研究テーマ	メカノストレスが癌細胞に与える影響と機序 Effects and mechanisms of mechanical stresses on cancer cells				
専攻種別	論文博士	<input type="checkbox"/>	課程博士	<input checked="" type="checkbox"/>	

1. 研究概要(1)

1) 目的(Goal)

- i. To investigate whether an elevated hydrostatic pressure in solid tumor promotes the metastasis of cancer cells.
- ii. To understand the relevant molecular mechanisms on tumor metastasis induced by elevated hydrostatic pressure.

2) 戦略(Approach)

Using a commercial device, we exposed Lewis lung cancer (LLC) cells to 50 mmHg for 24 hours, and then investigated the probable role of hydrostatic pressure on the metastatic property of LLC cells by in vitro and in vivo assessments.

3) 材料と方法(Materials and methods)

1. Lewis lung carcinoma (LLC) cells and hydrostatic pressure stimulation

Lewis lung carcinoma (LLC) cells was used for experiments. A pneumatic pressurizing system (Strex, Inc.) was used for inducing 50mmHg hydrostatic pressure to LLC cells for 24h (HP group). The cells without hydrostatic pressure exposure were used as control (CON group).

2. Adhesion assay

The freshly harvested cells (5 x10⁴ cells in 5 ml DMEM) were seeded on 25 cm² Collagen I-coated Flask. After 60 minutes incubation, unattached cells were gently removed by twice washing with PBS. The number of adherent cells were counted under a microscope with 200-fold magnification.

3. Detection of HIF-1 α and antioxidant enzymes expression

Use Western blot to detect the expression of HIF-1 α , SOD1, SOD2 in LLC cells after hydrostatic pressure stimulation.

4. Evaluation on oxidative stress resistance

Cells were stimulated with 50uM, 20uM H₂O₂ and without H₂O₂ for 2 h. Cells were then labeled with ANNEXIN V-FITC and propidium iodide (PI) to detect the apoptosis and dead cells. Quantitative flow cytometry analysis was performed using a FACSCalibur.

5. Experimental lung cancer metastasis model

LLC cells (5x10⁵) cultured at 50mmHg or without hydrostatic pressure were injected intravenously to C57BL/6 mice (10 to 12-week-old). Lung tissues were excised and weighted at 4 weeks later, and the number of tumor nodule in lungs were counted.

4) 実験結果(Results)

1. Hydrostatic pressure exposure enhanced the adhesion property of LLC cells.

There was not obvious difference in cell morphology and cell number after 24 hours exposure to 50mmHg hydrostatic pressure (Figure 1A). Adhesion property is critical for cancer cell metastasis. We found that the exposure to 50 mmHg hydrostatic pressure significantly increased the number of adherent cells on collagen I-coated flask (Figure 1B).

2. Hydrostatic pressure exposure increased the expression of HIF-1 α and antioxidant enzymes in LLC cells.

HIF-1 α is known to play critical roles in the metabolic reprogramming and metastasis of cancer cells. Western blotting showed that the expression of HIF-1 α was significantly increased in the HP group (Figure 2A). We further investigated the expression of antioxidant enzymes of SOD1 and SOD2, which belongs to HIF-1 α downstream signals. As expected, the exposure to 50 mmHg hydrostatic pressure for 24 hours also significantly upregulated the expression of SOD1 and SOD2 in LLC cells (Figure 2B, 2C).

1. 研究概要(2)

3. Hydrostatic pressure exposure induced the tolerance of LLC cells to oxidative stress.

As hydrostatic pressure showed to enhance the expression of SOD1 and SOD2, we evaluated the oxidative stress tolerance. The necrosis under 20 or 50 μM H_2O_2 stimulation were significantly reduced in these LLC cells pretreated with 50 mmHg hydrostatic pressure for 24 hours, although the apoptotic cells were not significantly different between groups (Figure 3).

4. Hydrostatic pressure exposure promoted the metastasis of LLC cells to lungs.

To evaluate the metastatic potency in vivo, we intravenously injected LLC cells into healthy adult mice. Compared with the mice that received LLC cells without hydrostatic pressure exposure, significantly worse survival was observed in the mice that received LLC cells pretreated with 50 mmHg (Figure 4A). All mice were killed at 4 weeks after cell injection and we found significantly more metastatic tumor lesions in lungs of mice in the HP group than in the CON group (Figure 4B, 4C). The weights of lung tissues were also significantly higher in the HP group than in the CON group (Figure 4D).

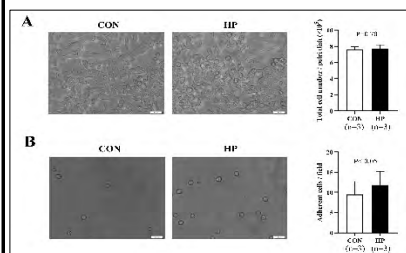


Figure 1

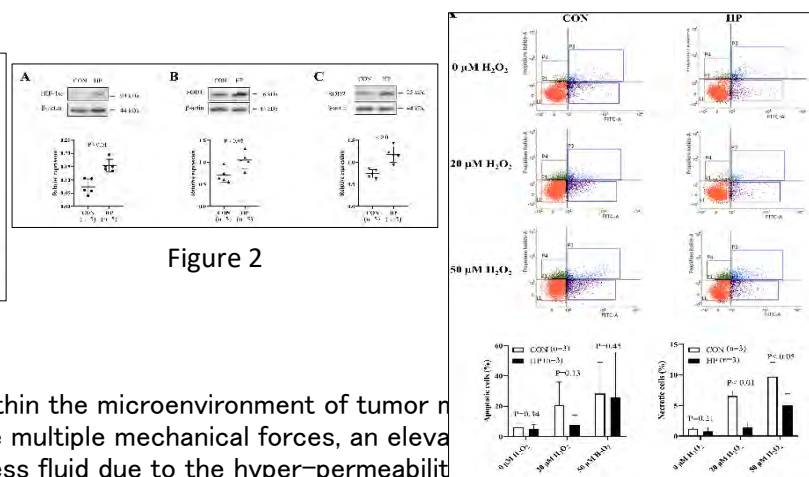


Figure 2

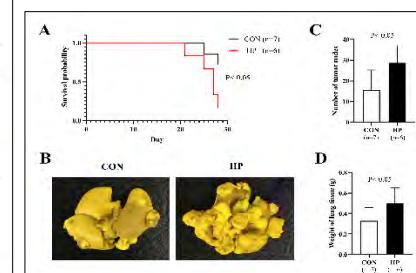


Figure 4

5) 考察(Discussion)

Various mechanical forces within the microenvironment of tumor malignant tumors [1]. Among the multiple mechanical forces, an elevated interstitial fluid hydrostatic pressure can be commonly induced by the presence of excess fluid due to the hyper-permeability of tumor blood vessels. Recent studies have reported that hydrostatic pressure may drive cancer cells toward metastasis [2]. However, the precise role and mechanism of mechanical forces in metastasis have poorly been addressed.

To investigate the role of hydrostatic pressure on metastatic property of cancer cells, we exposed LLC cells to 50 mmHg hydrostatic pressure by mimicking the in vivo tumor microenvironment. Using an experimental lung metastasis model, we further confirmed that the pretreatment of LLC cells with 50 mmHg hydrostatic pressure resulted in significantly higher number of tumor nodes in lungs of mice. These data suggested that an elevated interstitial fluid hydrostatic pressure in rapid growing malignant tumors might enhance the metastatic property of cancer cells.

We then tried to further understand how hydrostatic pressure enhanced the metastatic property of LLC cells. It is known that cancer cells have to enter the circulation system and expose to the hyperoxic arterial blood for hematogenous metastasis [4]. Accumulating evidences have suggested that oxidative stress kills the most of circulating cancer cells[4]. Therefore, oxidative stress tolerance is essential for the successful metastasis of cancer cells. HIF-1 α has been well recognized as an important mediator on the metabolism reprogramming of cancer cells by regulating the antioxidant enzymes and antioxidant properties. Very interestingly, it has been recently demonstrated that cyclic mechanical force stabilizes HIF-1 α by reducing protein degradation [5]. Consistently, our data exactly showed a significant increase of HIF-1 α in LLC cells with 24 hours exposure to 50 mmHg hydrostatic pressure. Hydrostatic pressure exposure also significantly enhanced the expressions of SOD1 and SOD2, and induced the oxidative stress tolerance of LLCs cells.

Based on the data of this study, an elevated hydrostatic pressure in malignant tumor environment may enhance the metastatic potency of cancer cells, through the stabilization of HIF-1 α to induce the expression of antioxidant enzymes for defending against oxidative damage during metastasis.

6) 参考文献(References)

[1] Bregenzler ME, Horst EN, Mehta P, Novak CM, Repetto T, Mehta G. The role of cancer stem cells and mechanical forces in ovarian cancer metastasis. *Cancers*. 11 (2019) 1008.
 [2] Jain RK, Martin JD, Stylianopoulos T. The role of mechanical forces in tumor growth and therapy. *Annu Rev Biomed Eng*. 16 (2014) 321-346.
 [3] Tse JM, Cheng G, Tyrrell JA, et al. Mechanical compression drives cancer cells toward invasive phenotype. *Proc Natl Acad Sci U S A*. 109 (2012) 911-916.
 [4] Piskounova E, Agathocleous M, Murphy MM, et al. Oxidative stress inhibits distant metastasis by human melanoma cells. *Nature*. 527 (2015) 186-191.
 [5] Solis AG, Bielecki P, Steach HR, et al. Mechanosensation of cyclical force by PIEZO1 is essential for innate immunity. *Nature*. 573 (2019) 69-74.

2. 執筆論文 Publication of thesis ※記載した論文を添付してください。Attach all of the papers listed below.

論文名 1 Title						
掲載誌名 Published journal						
	年	月	巻(号)	頁 ~	頁	言語 Language
第1著者名 First author			第2著者名 Second author			第3著者名 Third author
その他著者名 Other authors						
論文名 2 Title						
掲載誌名 Published journal						
	年	月	巻(号)	頁 ~	頁	言語 Language
第1著者名 First author			第2著者名 Second author			第3著者名 Third author
その他著者名 Other authors						
論文名 3 Title						
掲載誌名 Published journal						
	年	月	巻(号)	頁 ~	頁	言語 Language
第1著者名 First author			第2著者名 Second author			第3著者名 Third author
その他著者名 Other authors						
論文名 4 Title						
掲載誌名 Published journal						
	年	月	巻(号)	頁 ~	頁	言語 Language
第1著者名 First author			第2著者名 Second author			第3著者名 Third author
その他著者名 Other authors						
論文名 5 Title						
掲載誌名 Published journal						
	年	月	巻(号)	頁 ~	頁	言語 Language
第1著者名 First author			第2著者名 Second author			第3著者名 Third author
その他著者名 Other authors						

3. 学会発表 Conference presentation ※筆頭演者として総会・国際学会を含む主な学会で発表したものを記載してください。

※Describe your presentation as the principal presenter in major academic meetings including general meetings or international meeting

学会名 Conference	Japanese Cancer Association			
演題 Topic	Hydrostatic pressure stabilizes HIF-1 α of cancer cells to defense against oxidative damage during metastasis			
開催日 date	2020 年 10 月 1 日	開催地 venue	広島	
形式 method	<input checked="" type="checkbox"/> 口頭発表 Oral	<input type="checkbox"/> ポスター発表 Poster	言語 Language	<input type="checkbox"/> 日本語 <input checked="" type="checkbox"/> 英語 <input type="checkbox"/> 中国語
共同演者名 Co-presenter	Taosheng Li			
学会名 Conference				
演題 Topic				
開催日 date	年 月 日	開催地 venue		
形式 method	<input type="checkbox"/> 口頭発表 Oral	<input type="checkbox"/> ポスター発表 Poster	言語 Language	<input type="checkbox"/> 日本語 <input type="checkbox"/> 英語 <input type="checkbox"/> 中国語
共同演者名 Co-presenter				
学会名 Conference				
演題 Topic				
開催日 date	年 月 日	開催地 venue		
形式 method	<input type="checkbox"/> 口頭発表 Oral	<input type="checkbox"/> ポスター発表 Poster	言語 Language	<input type="checkbox"/> 日本語 <input type="checkbox"/> 英語 <input type="checkbox"/> 中国語
共同演者名 Co-presenter				
学会名 Conference				
演題 Topic				
開催日 date	年 月 日	開催地 venue		
形式 method	<input type="checkbox"/> 口頭発表 Oral	<input type="checkbox"/> ポスター発表 Poster	言語 Language	<input type="checkbox"/> 日本語 <input type="checkbox"/> 英語 <input type="checkbox"/> 中国語
共同演者名 Co-presenter				

4. 受賞(研究業績) Award (Research achievement)

名称 Award name	国名 Country		受賞年 Year of award	年 月
	国名 Country		受賞年 Year of award	年 月

5. 本研究テーマに関わる他の研究助成金受給 Other research grants concerned with your research

受給実績 Receipt record	<input type="checkbox"/> 有 <input checked="" type="checkbox"/> 無
助成機関名称 Funding agency	
助成金名称 Grant name	
受給期間 Supported period	年 月 ~ 年 月
受給額 Amount received	円
受給実績 Receipt record	<input type="checkbox"/> 有 <input type="checkbox"/> 無
助成機関名称 Funding agency	
助成金名称 Grant name	
受給期間 Supported period	年 月 ~ 年 月
受給額 Amount received	円

6. 他の奨学金受給 Another awarded scholarship

受給実績 Receipt record	<input type="checkbox"/> 有 <input checked="" type="checkbox"/> 無
助成機関名称 Funding agency	
奨学金名称 Scholarship name	
受給期間 Supported period	年 月 ~ 年 月
受給額 Amount received	円

7. 研究活動に関する報道発表 Press release concerned with your research activities

※記載した記事を添付してください。 Attach a copy of the article described below

報道発表 Press release	<input type="checkbox"/> 有 <input checked="" type="checkbox"/> 無	発表年月日 Date of release	
発表機関 Released medium			
発表形式 Release method	・新聞 ・雑誌 ・Web site ・記者発表 ・その他 ()		
発表タイトル Released title			

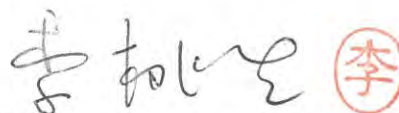
8. 本研究テーマに関する特許出願予定 Patent application concerned with your research theme

出願予定 Scheduled	<input type="checkbox"/> 有 <input checked="" type="checkbox"/> 無	出願国 Application	
出願内容(概要) Application contents			

9. その他 Others

--

指導責任者(署名)



公益財団法人日中医学協会
TEL 03-5829-9123
FAX 03-3866-9080
〒101-0032 東京都千代田区岩本町 1-4-3
住 泉 K M ビ ル 6 階
URL : <https://www.jpcnma.or.jp/>